

**Oscillatory activity in the basal ganglia: is it
relevant to movement disorders and their
therapy?**

Chiung Chu Chen

**Thesis submitted for the degree of
Doctors of Philosophy in Neurological studies
University London**

April 2008

**Sobell Department of Motor Neuroscience
and Movement Disorders
Institute of Neurology
University College London
Queen Square WC1N 3BG**

UMI Number: U593537

All rights reserved

INFORMATION TO ALL USERS

The quality of this reproduction is dependent upon the quality of the copy submitted.

In the unlikely event that the author did not send a complete manuscript and there are missing pages, these will be noted. Also, if material had to be removed, a note will indicate the deletion.



UMI U593537

Published by ProQuest LLC 2014. Copyright in the Dissertation held by the Author.
Microform Edition © ProQuest LLC.

All rights reserved. This work is protected against
unauthorized copying under Title 17, United States Code.



ProQuest LLC
789 East Eisenhower Parkway
P.O. Box 1346
Ann Arbor, MI 48106-1346

Abstract

Chronic high frequency stimulation of the basal ganglia can be a highly effective intervention for movement disorders in patients. In the past decade, therapeutic benefits have been seen with stimulation of the subthalamic nucleus and globus pallidus interna for Parkinson's disease (PD) and dystonia, respectively. These procedures have allowed direct recording of basal ganglia activity and have suggested that abnormal synchronisation of neurons in these nuclei may contribute to motor impairment.

This thesis explores the possible correlation between synchronised activity in the basal ganglia, as evidenced by oscillations in local field potentials, and movement disorders. In Chapter 3, we demonstrate the correlation between synchronization at frequencies under 10 Hz in the globus pallidus interna and dystonic EMG. This low frequency activity is shown to be locked to neuronal activity within GPi in patients with dystonia (Chapter 4).

Deep brain stimulation is thought to suppress spontaneous pathological activity in the basal ganglia. Equally, however, it must also suppress any residual physiological activity in these nuclei. In Chapter 5, we demonstrate that the basal ganglia are involved in the processing of simple limb movements in the human, by separating the effects of deep brain stimulation on pathological and physiological activities based on baseline task performance. An impairment of motor performance was seen during high frequency stimulation in those patients with the best task performance at baseline. This deleterious effect, however,

should be distinguished from the effect of direct stimulation at 20 Hz in Parkinson's disease. Oscillatory activity at around 20 Hz is thought to be a core feature in Parkinson's disease. In Chapter 6, we demonstrate that the excessive synchronization imposed by stimulation of the subthalamic nucleus at 20 Hz slows movement, in those patients with the best task performance at baseline. This supports the notion that synchronization around 20 Hz may be causally linked to bradykinesia. Last, the therapeutic effectiveness of DBS therapy for patients with PD partially relies on the accurate localisation of the motor region of the subthalamic nucleus. In Chapter 7, we propose an alternative method for the localization of this region using the spontaneous pathological 20 Hz activity to be found in this nucleus.

The findings of these studies provide evidence that basal ganglia oscillatory activities of differing frequencies contribute to movement disorders.

Acknowledgements

I would like to thank:

The patients, their caregivers and families who gave their time and support to this project, without whose generosity this work would not have been possible. I am grateful to them all, and hope that continuing interest in the themes discussed here may contribute to the better understanding of their disease and lead to future treatments.

My supervisor Prof. Peter Brown, for his unfailing enthusiasm, patient teaching, stimulating discussion and kind encouragement throughout the course of my PhD study.

Prof. Alim-Louise Benabid, my mentor whom I have the honor to work with prior to my PhD study. His enthusiasm toward researches, passion for new treatments and unselfish support to pupils have inspired me and led me to the start of my research carrier.

Andrea Kuhn, Louise Gaynor, Alek Pogosyan, Alexandros Androulidakis, Vladimir Litvak and Alex Eusebio for their contributions at different stages of the work.

Chang Gung Memorial Hospital, Taipei, Taiwan, and UCL for their financial support.

I am especially grateful to the functional neurosurgery unit of Prof. Marwan Hariz, Dr. Patricia Limousin, Stephen Tisch, Irene Martinez-Torres and Ms Ellie Borrell for taking care patients and the assistance they gave in support of my work.

I wish to express my special thanks to Prof. Ching-Song Lu – Department of Neurology, Chang Gung Memorial Hospital, Taiwan, for his unselfish support.

Many thanks to the following collaborative groups:

Prof. Andreas Kupsch and Dr. Thomas Trottenberg-Department of Neurology, Charite-University Medicine Berlin, CVK, Berlin, Germany

Prof. Bart Nuttin-Department of Neurology, University Hospitals Leuven, Leuven, Belgium

Prof. Chon-Haw Tsai, Department of Neurology, China Medical University, Tai-Chiung, Taiwan.

Last but not least, I am immensely grateful to my dear mother and Alexis, my husband, without whose endless patient during the ups and downs in the course of my research, I would not have completed the work.

Publications

Work incorporated in this thesis:

Chen CC, Kuhn AA, Hoffmann KT, Kupsch A, Schneider GH, Trottenberg T, Krauss JK, Wohrle JC, Bardinet E, Yelnik J and Brown P (2006) Oscillatory pallidal local field potential activity correlates with involuntary EMG in dystonia. *Neurology* 14: 66(3): 418-20

Chen CC, Kuhn A, Trottenberg T, Kupsch A, Schneider GH and Brown P (2006) Neuronal activity in globus pallidus interna can be synchronized to local field potential activity over 3-12 Hz in patients with dystonia. *Exp Neurol.* 202 (2) 480-6

Chen CC, Brucke C, Kempf F, Kupsch A, Lu CS, Lee ST, Tisch S, Limousin P, Hariz M and Brown P (2006) Deep brain stimulation of the subthalamic nucleus: A two-edged sword. *Curr Biol.* 21: 16(22): R952-3

Chen CC, Litvak V, Gilbertson T, Kuhn A, Lu CS, Lee ST, Tsai CH, Tisch S, Limousin P, Hariz M and Brown P (2007) Excessive synchronization of basal ganglia neurons at 20 Hz slows movement in Parkinson's disease. *Exp Neurol.* 205 (1): 214-21

Chen CC, Pogosyan A, Zrinzo LV, Tisch S, Limousin P, Ashkan K, Yousry T, Hariz M and Brown P (2006) Intra-operative recordings of local field potentials can help localize the subthalamic nucleus in Parkinson's disease surgery. *Exp Neurol.* 198(1): 214-21

Associated publications:

Androulidakis AG, Kuhn AA, Chen CC, Blomstedt P, Kempf F, Kupsch A, Schneider GH, Doyle L, Dowsey-Limousin P, Hariz M and Brown P (2007) Dopaminergic therapy promotes lateralized motor activity in the subthalamic area in Parkinson's disease. *Brain* 130 (2): 457-68

Brown P, Chen CC, Wang S, Kuhn A, Doyle L, Yarrow K, Nuttin B, Stein J and Aziz T (2006) Involvement of Human Basal Ganglia in offline feedback control of voluntary movement. *Curr Biol.* 7; 16(21): 2129-34

Kempf F, Brucke C, Kuhn A, Schneider GH, Kupsch A, Chen CC, Androulidakis A, Wang S, Vandenberghe W, Nuttin B, Aziz T and Brown P (2007) Involvement of human basal ganglia in off-line feed-back control of voluntary movement is modulated by dopamine. *Curr Biol.* In press.

Brucke C, Kupsch A, Schneider GH, Hariz MI, Nuttin B, Kopp U, Kempf F, Trottenberg T, Doyle L, Chen CC, Yarrow K, Brown P, Kuhn AA. The subthalamic region is activated during valence-related emotional processing in patients with Parkinson's disease. *Eur J Neurosci.* In press.

Table of contents

	Page
Title	1
Abstract	2
Acknowledgements	4
Publications	7
Table of contents	8
Index of figures	18
Index of tables	22
Abbreviations	23
 Chapter 1: Introduction	 20
<u>1.1</u> <u>Basal ganglia</u>	<u>26</u>
1.1.1 Anatomy of the basal ganglia	27
1.1.1.1 Striatum	27
1.1.1.2 STN	28
1.1.1.3 Globus pallidus and SNr	29
1.1.1.4 The substantia nigra pars compacta	30
1.1.2 Basal ganglia and movement control	31
1.1.2.1 Rate coding model	32
1.1.2.2 Center surround and dynamic model	35
1.1.2.3 Reinforcement learning model	37
1.1.2.4 Focused attention model	39
<u>1.2</u> <u>Oscillations in the basal ganglia</u>	<u>42</u>
1.2.1 Oscillation and synchrony	42

1.2.2	Oscillations in different frequency bands	43
1.2.3	What possibilities exist for direct recording from the BG?	44
1.2.3.1	Single unit recordings in basal ganglia	44
1.2.3.2	LFP recording in the basal ganglia	47
1.2.4	How does synchronous neuronal activity contribute to motor processing?	49
1.2.4.1	Single unit activity in the basal ganglia during movement	50
1.2.4.2	Local field potentials in the basal ganglia during movement	55
1.2.4.2.1	Synchronized oscillations in the healthy basal ganglia	56
1.2.4.2.2	Synchronized oscillations in the basal ganglia in movement disorders	57
1.2.4.3	What is the mechanism by which excessive synchrony might impair motor processing?	60
<u>1.3</u>	<u>Parkinson's disease</u>	<u>64</u>
1.3.1	Introduction of Parkinson's disease	64
1.3.2	Electrophysiology of PD	65
1.3.2.1	EMG, EEG and MEG in PD	65
1.3.2.2	BG electrophysiology in PD	67
1.3.2.2.1	Abnormal synchronization in PD	67
1.3.2.2.2	Relation to movement execution	69
1.3.2.3	PET studies of Parkinson's disease	70

1.3.3	Treatment for Parkinson's disease	71
1.3.3.1	Medical treatment	71
1.3.3.2	Surgical treatment for PD	75
<u>1.4</u>	<u>Dystonia</u>	<u>75</u>
1.4.1	Definition and classification of dystonia	76
1.4.2	The pathophysiology underlying dystonia –electrophysiology	78
1.4.2.1	EMG studies in dystonic movement	78
1.4.2.2	Spinal cord reflexes in dystonia	80
1.4.2.3.1	Brainstem motor function in dystonia	81
1.4.2.3.2	Other brainstem abnormalities in dystonia	81
1.4.2.4	Cortical function in dystonia	82
1.4.2.5	Sensory dysfunction in dystonia	84
1.4.3	Pathophysiology underling dystonia -imaging studies	85
1.4.3.1	Structural imaging	85
1.4.3.2	Functional imaging	86
1.4.4	Basal Ganglia dysfunction in dystonia	86
1.4.4.1	Disorganisation of sensory representation in pallidum	88
1.4.4.2	Disorganization of temporal patterning of pallidal activity	88
1.4.4.3	Spatio-temporal disorganization of pallidal neuronal activity	89
1.4.5	Treatment for dystonia	91

1.4.5.1	Medical treatment for dystonia	91
1.4.5.2	Botulinum toxin treatment for dystonia	92
1.4.5.3	Stereotactic functional neurosurgery for dystonia	92
<u>1.5</u>	<u>Deep brain stimulation</u>	<u>94</u>
1.5.1	Concept and history of DBS	94
1.5.2	Current indications for DBS	95
1.5.2.1	DBS for Parkinson's disease	95
1.5.2.2	DBS for Tremor	99
1.5.2.3	DBS for Dystonia	101
1.5.2.4	DBS Other disorders	101
1.5.3	Mechanisms of action of DBS for movement disorders	101
1.5.3.1	Suppression by DBS	103
1.5.3.2	Activation by DBS	104
1.5.3.3	Functional imaging studies	107
Chapter 2: Methods		110
<u>2.1</u>	<u>Patients and operative procedure</u>	<u>110</u>
<u>2.2</u>	<u>Clinical rating scales</u>	<u>112</u>
2.2.1	The Unified Parkinson's Disease Rating Scale (UPDRS)	112
2.2.2	The Toronto Western Spasmodic Torticollis scale (TWSTR)	113
2.2.3	BFMDRS (Burke-Fahn-Marsden Dystonia Rating Scale)	114

<u>2.3</u>	<u>Data collection</u>	<u>114</u>
2.3.1	LFP recording	114
2.3.2	Surface EMG recordings	115
2.3.3	Technical Basis of biological signal recording	116
2.3.3.1	Amplifiers	116
2.3.3.2	Filters of recorded bioelectric signals	117
2.3.3.3	Analog-digital conversion (ADC)	118
2.3.4	Tapping task	119
<u>2.4</u>	<u>Data analysis</u>	<u>120</u>
2.4.1	Time domain analysis	121
2.4.1.1	Correlation	121
2.4.1.2	Cross-correlation function	122
2.4.1.3	Spike triggered average (STA)	125
2.4.2	Frequency domain analysis	126
2.4.2.1	Fourier series	127
2.4.2.2	Fourier Transform	129
2.4.2.3	The power spectrum	132
<u>2.5</u>	<u>Statistical analysis</u>	<u>133</u>
2.5.1	Parametric tests	133
2.5.1.1	Correlation analysis	134
2.5.1.2	ANOVA	135
2.5.1.3	Z-score	135
2.5.1.4	The student's t-test	136
2.5.2.1	Non-parametric tests	136
2.5.2.2	Fisher's exact test	136

Chapter 3: Oscillatory pallidal local field potential activity correlates with

involuntary EMG in dystonia		138
<u>3.1</u>	<u>Introduction</u>	<u>138</u>
<u>3.2</u>	<u>Methods</u>	<u>139</u>
3.2.1	Patients and surgery	139
3.2.2	Post-operative radiological reconstruction of contact placement	144
3.2.3	Recordings and analysis	144
3.2.4	Statistical analysis	146
<u>3.3</u>	<u>Results</u>	<u>147</u>
3.3.1	Macroelectrode positioning	147
3.3.2	Spectral distribution of LFP power	149
3.3.3	Correlation between LFP and dystonic EMG	149
3.3.4	Distribution of correlations between pallidal LFP activities and dystonic EMG	157
<u>3.4</u>	<u>Discussion</u>	<u>158</u>
3.4.1	Experimental limitations	158
3.4.2	Correlations involving LFP activity in the 4-10 Hz band	159
3.4.3	Correlations involving LFP activity in the 11-30 Hz band	161
3.4.4	Correlations involving LFP activity in the 65-85 Hz band	162
3.4.5	Patients with insignificant correlations	163

<u>3.5</u>	<u>Summary</u>	<u>164</u>
------------	----------------	------------

**Chapter 4: Neuronal activity in globus pallidus interna can be
synchronized to local field potential activity over 3-12 Hz in patients with
dystonia**

<u>4.1</u>	<u>Introduction</u>	<u>166</u>
<u>4.2</u>	<u>Methods</u>	<u>167</u>
4.2.1	Patients and surgery	167
4.2.2	Intra-operative recordings	171
4.2.3	Off-line analyses	172
<u>4.3</u>	<u>Results</u>	<u>174</u>
4.3.1	Topographical distributions of LFP power over 3-12 Hz band	174
4.3.2	Relationship between multiunit spike and LFP	178
<u>4.4</u>	<u>Discussion</u>	<u>182</u>
4.4.1	Differences between recording techniques	183
4.4.2	Synchronization between LFPs and neuronal activity over 3-12 Hz	184
4.4.3	Topographical distributions of LFP power	185
<u>4.5</u>	<u>Summary</u>	<u>186</u>

**Chapter 5: Deep brain stimulation of the subthalamic nucleus: a two-edged
sword**

<u>5.1</u>	<u>Introduction</u>	<u>187</u>
<u>5.2</u>	<u>Methods</u>	<u>188</u>

5.2.1	Patients and surgery	188
5.2.2	Protocol	194
5.2.3	Statistical analysis	195
<u>5.3</u>	<u>Results</u>	<u>195</u>
5.3.1	Dependency of deep brain stimulation effects on baseline performance	195
5.3.2	Reproducibility of the results	197
<u>5.4</u>	<u>Discussion</u>	<u>198</u>
5.4.1	Differing effects of high frequency stimulation in basal ganglia	198
5.4.2	Clinical implications of the current findings	200
<u>5.5</u>	<u>Summary</u>	<u>201</u>

**Chapter 6: Excessive synchronization of basal ganglia neurons at 20 Hz
slows movement in Parkinson's disease** **202**

<u>6.1</u>	<u>Introduction</u>	<u>202</u>
<u>6.2</u>	<u>Methods</u>	<u>205</u>
6.2.1	Patients and surgery	205
6.2.2	Protocol	207
6.2.3	Task	207
6.2.4	Statistical analysis	208
<u>6.3</u>	<u>Results</u>	<u>209</u>
6.3.1	Dependency of stimulation effects on baseline performance	209
6.3.2	Correlation between change in tapping during	212

	DBS and baseline tapping performance	
<u>6.4</u>	<u>Discussion</u>	<u>215</u>
6.4.1	Frequency selective deleterious effects	215
6.4.2	Dual effects of 20 Hz stimulation	215
6.4.3	Limitations of the experiment	216
6.4.4	Differing mechanism underlies the deleterious effects induced by high and low frequency stimulation	217
<u>6.5</u>	<u>Summary</u>	<u>217</u>

**Chapter 7: Intraoperative recording of local field potential can help
localize the subthalamic nucleus in Parkinson's disease
surgery**

		219
<u>7.1</u>	<u>Introduction</u>	<u>219</u>
<u>7.2</u>	<u>Methods</u>	<u>220</u>
7.2.1	Patients and surgery	220
7.2.2	Recordings	222
7.2.3	Post-operative radiological reconstruction of contact placement	223
7.2.4	Analysis	226
<u>7.3</u>	<u>Results</u>	<u>227</u>
7.3.1	On-line recording of LFP activity in the 13-35 Hz band	227
7.3.2	Off-line analysis of the predictive value of	230

	LFP recordings	
7.3.3	Relationship between ‘ physiologically’ and ‘radiologically’ defined STN	236
<u>7.4</u>	<u>Discussion</u>	<u>236</u>
<u>7.5</u>	<u>Summary</u>	<u>239</u>
Chapter 8: Conclusion		240
<u>8.1</u>	<u>What is the pathophysiological role for synchronization of pallidal activity in hyperkinetic movement disorders?</u>	<u>243</u>
<u>8.2</u>	<u>Is the 4-10 Hz LFP in Globus Pallidus focally generated in dystonia?</u>	<u>246</u>
<u>8.3</u>	<u>The effect of high frequency deep brain stimulation: more or less?</u>	<u>247</u>
<u>8.4</u>	<u>The effect of beta band stimulation: amelioration and/or disruption?</u>	<u>249</u>
<u>8.5</u>	<u>Can local field potential recordings help localize the subthalamic nucleus in Parkinson’s disease surgery</u>	<u>251</u>
<u>8.6</u>	<u>Conclusion and future directions</u>	<u>252</u>

Index of figures

Figure 1.1	The ‘box and arrow’ models of BG circuitry	35
Figure 1.2	Introduction of ‘hyperdirect’ cortico-STN pathway	37
Figure 1.3	The reinforcement driven dimensionality reduction neural net	39
Figure 1.4	The akinetic and prokinetic effects of the different frequency bands of oscillations in the basal ganglia-cortical network	41
Figure 1.5	Biophysical basis of EEG and LFPs in the cerebral cortex	48
Figure 2.1	Schematic presentation of an EEG or LFP recording channel	116
Figure 2.2	Signal obtained by using different numbers of digitizing level	119
Figure 2.3	Introduces examples of autocorrelation	124
Figure 3.1	Positioning of macroelectrode contacts comprising the	148

bipolar electrodes

Figure 3.2	Example of simultaneous recordings of pallidal LFPs and rectified sEMG in case 1	150
Figure 3.3	Relationship between log pallidal LFP activity in the three frequency bands of interest and log rectified sEMG activity in case 1,5 and 8	151
Figure 3.4	Incidence of GP LFP-EMG correlations per pallidal contact pair in the 4-10 Hz, 13-30 Hz, 65-85 Hz band	152
Figure 3.5	Size of GP LFP-EMG correlations per pallidal contact pair in the 4-10Hz, 13-30Hz and 65-85 Hz bands	154
Figure 3.6	Incidence and size of GP LFP-SCM EMG correlations among the three contact pairs in the three frequency bands of interest	156
Figure 3.7	Distribution of significant GP LFP-SCM EMG correlations among the three contact pairs in the three frequency bands of interest	158
Figure 4.1	Example of raw data. Pallidal LFP, multiunit activity and corresponding discriminated multiunit activity from	175

the right side in case 6 at level of lower GPi.

Figure 4.2	Distribution of LFP power in the 3-12 Hz band along macroelectrode track in case 4	176
Figure 4.3	Distribution of LFP power in the 3-12 Hz band along microelectrode trajectory across cases	177
Figure 4.4	STAs and the corresponding STA spectra in the six patients	180
Figure 4.5	Eventual placement of deep brain stimulation (DBS) electrode. Representative post-operative MRI showing placement of DBS electrode in GPe (A) and GPi (B) in case 4	182
Figure 5.1	Dependency of deep brain stimulation effects on baseline performance	196
Figure 6.1	Dependence of stimulation effects on baseline performance	211
Figure 6.2	Correlation between change in tapping rate during DBS and baseline tapping performance	214

Figure 7.1	Localization of DBS electrode contacts on MRI	225
Figure 7.2	On-line displays of spectral change in LFP as DBS electrode descends through target, obtained intra-operatively. Recordings from case 9 right (A), 9 left (B), 5 right (C) and (8) left (D)	229
Figure 7.3	Off-line analysis of spectral change of LFP as DBS electrode descends through target	234

Index of tables

Table 3.1	Summary of patient details	140
Table 4.1	Clinical details of patients	169
Table 5.1	Clinical details of patients	190
Table 6.1	Clinical details of patients	206
Table 7.1	Core results of off-line analysis of the predictive value of LFP recordings	231

Abbreviations

AC	anterior commissure	MCP	mid-commissural point
ADC	Analog-digital conversion	ME	macroelectrode
ANOVA	analysis of variance	MEP	motor evoked potential
ATD	Amantadine hydrochloride	MPTP	1-methyl-4-phenyl-1,2,3,6-tetrahydropyridine
BFMRDS	Burke-Fahn-Marsden dystonia rating scale	MRI	magnetic resonance imaging
BoNT-A	botulinum toxin A	NMDA	N-methyl-D-aspartate
BP	bereitchaftspotential	OFF	off dopaminergic medication
CL	confidence limit	ON	on dopaminergic medication
CNV	contingent negative variation	PC	posterior commissure
COMT	catechol-O methyltransferase	PD	Parkinson's disease

CT	computerized tomography	PET	position emission tomography
DA	dopamine	PPN	pedunculopontine nucleus
DBS	deep brain stimulation	PRL	prelemniscal radiation
DRD	dopa-responsive dystonia	RT	reaction time
DTR	direct transfer function	SCM	sternocleidomastoid
EcoG	electrocorticography	SEM	standard error of mean
EEG	electroencephalogram	SGCE	epsilon sarcoglycan gene
EMG	electromyography	SICI	short interval intracortical inhibition
ENK	enkephalin	SMA	supplementary motor area
FS	Fourier series	SNe	substantia nigra pars compacta
GABA	gamma-amino butyric acid	SNr	substantial nigra pars nigra
GLU	glutamate	STA	spike triggered average

GP	globus pallidus	STN	subthalamic nucleus
GPe	globus pallidus externa	TMS	transcranial magnetic stimulation
GPI	globus pallidus interna	TWSTR	Toronto Western Spasmodic Torticollis Scale
GTPCH1	guanidine triphosphate cyclohydrolase 1	UPDRS	Unified Parkinson's Disease Rating Scale
LFP	local field potential	Vim	ventral intermedius nucleus
LID	levodopa induced dyskinesia	ZI	zona incerta

CHAPTER 1: Introduction

1. 1. Basal Ganglia

1.1.1 Anatomy of the basal ganglia

The basal ganglia (BG) comprise a group of sub-cortical nuclei that are highly interconnected and form complex loops between motor cortex and thalamus.

The main nuclei in the BG are the caudate nucleus and putamen (striatum), the globus pallidus interna and externa (GPi and GPe, respectively), the subthalamic nucleus (STN) and substantia nigra pars reticulata (SNr) and pars compacta (SNc) (Kandal and Shwarz 2000). Recently, the pedunculopontine nucleus (PPN) has been included in the basal ganglia group (Mena-Segovia et al., 2004). Similar architecture and connectivity are widely observed across different species, suggesting that the basal ganglia are fundamentally important to animal brain function.

Information flow within the BG is from cortical afferents to the striatum and STN, which in turn project to the GPe, GPi and SNr. The latter two, the output structures of the BG, then send efferents to the ventral nuclei of the thalamus, which in turn project back to areas of the cortex. Thalamic relay nuclei, however, also receive massive cortical input (Ray and Price, 1993; Siwek and Pandya, 1991). There are two components to this input, a reciprocal one, and a nonreciprocal one (Nikolaus et al., 2002). The nonreciprocal component provides a feedforward mechanism in which the thalamus influences higher

cortical areas (Sherman and Guillery, 1996; Jones, 1998). This highly complex chemo-architecture favors information processing at the level of synaptic interactions between nuclei rather than at the level of individual nuclei (Bar-Gad et al., 2003).

1.1.1.1. Striatum

The striatum is the main input nucleus of the BG as it receives glutamatergic cortical inputs from different areas of the cortex (Parent and Hazrati, 1995a; Parent and Hazrati, 1995b). Based on the functional specialization of these cortical afferents, the striatum is divided into anatomically defined sensorimotor, limbic and associative territories, a functional subdivision which also exists within other basal ganglia nuclei. The sensorimotor territory of the striatum receives afferents from the primary motor area, primary somatosensory cortex, premotor cortex and supplementary motor area. This organization allows processing of sensorimotor, associative and limbic information to be carried out in a segregated and reorganized manner at the level of the striatum (Parent 1995a). Persistent functional anatomical segregation at downstream nodes in cortico-basal ganglionic loops has led to the assumption that there is parallel processing of functionally discrete information throughout the basal ganglia (Alexander&Crutcher 1990a).

The majority of the striatal neurons are GABAergic projection neurons, the so-called medium spiny neurons (MSN) that provide the only striatal output. In the normal state, MSNs are at a hyperpolarized level and seldom fire. Action

potential discharge only occurs in response to synchronized activity in many converging cortico-striatal afferents. This has led to the suggestion that striatum shapes input-output relationships by filtering out uncorrelated synaptic cortical inputs. There are two subgroups of neurons within MSNs (Smith et al., 1998a; Smith et al., 1998b). One group, expressing the neuropeptides substance P and dynorphine and the D1 dopamine receptor, mainly projects to GPi and SNr. The other expresses the neuropeptide enkephalin and the D2 dopamine receptor, and projects to the GPe. The connection between cortex and striatum is highly topographically organized. The organization is preserved throughout the rest of BG, and is suggested to serve different motor and cognitive functions. The membrane potentials of striatal projection neurons are sensitive to dopaminergic modulation (Murer et al., 2002).

There are several populations of interneurons within the striatum, which comprise about 10% of this structure. The majority of interneurons are GABAergic, and are called tonically active neurons (TANs), (Apicella, 2002). Inhibitory interneurons send their feed forward or feed back to MSNs, thereby modulating the excitability of this projection neuron population.

1.1.1.2. STN

STN neurons are the only glutamatergic neurons in the basal ganglia and the only direct target of inputs from the frontal cortex. This “hyperdirect pathway”, from motor cortex, supplementary motor area (SMA), and premotor area (PMA) to STN, may be important in relaying sensory and motor input to the

basal ganglia (Hamada and DeLong, 1992; Hamani et al., 2004; Nambu et al., 2000). In contrast to striatum, STN is a homogenous nucleus and fires faithfully to cortical command. The afferents from cerebral cortex are highly topographically organized within STN. There are 3 main subdivisions within this small structure, somato-motor, associative and limbic (DeLong et al., 1985). Most of the STN neurons have intrinsic spontaneous activity and fire tonically at between 15-25 Hz, but also display spontaneous bursting activity (Wichmann et al., 1994a; Wichmann et al., 1994b). STN neurons provide an important source of excitatory drive onto GPe, GPi, SNr and the PPN.

1.1.1.3. Globus pallidus and SNr

Globus pallidus consists mainly of GABAergic projection neurons and is subdivided into external and internal segments that are separated by the internal medullary lamina. These two subdivisions, GPi and GPe, receive afferent input from both striatum and STN (Parent and Hazrati, 1995a; Parent and Hazrati, 1995b), as does SNr. SNr and GPi form the basal ganglia output nuclei. GPe neurons have reciprocal afferent projections to both the striatum and the STN (Parent and Hazrati, 1995a; Parent and Hazrati, 1995b). In the striatum, the majority of GPe inputs innervate interneurons (Bevan et al., 2002). Axons from the GPe form extensive synapses on the STN, creating a highly symmetrical arrangement of connections between the two structures (Parent and Hazrati, 1995a; Parent and Hazrati, 1995b). It has been proposed that GPe, GPi, STN and SNr neurons together form an extrastriatal network with interneurons (GPe and STN) and projection neurons (GPi and SNr) that integrate cortical

information already processed (direct and indirect pathways) or not (hyperdirect pathway) by the striatal network. The projection neurons project predominantly to the ventral anterior and ventral lateral nuclei of the thalamus, which in turn project back to the cerebral cortex, completing the basal ganglia loop. The thalamo-cortical projections can either be reciprocal regarding the origin of cortical input or project to other areas creating an “open loops” (Haber, 2003; Kelly et al., 2004). Recent studies have shown >80% of GPi neurons send axon collaterals to both the ventrolateral nucleus of the thalamus and the PPN in the primate (Harnois and Fillion, 1982; Pahapill 2000). The axon branches of GPi neurons projecting to the PPN in monkey are of larger diameter than the thalamic branches. This suggests that the PPN may be the principal target of pallidal outflow.

1.1.1.4. The substantia nigra pars compacta

The SNc contains dopaminergic neurons, is found in the mesencephalon, innervates the MSNs throughout the striatum and, to a lesser extent, innervates STN and pallidum, given observations of dopaminergic receptor in these nuclei (Freeman et al., 2001). The fact that MSNs receive both dopaminergic input from nigra and afferents from cortex has lead to the suggestion that dopaminergic input may modulate information sent from cortical to striatal levels.

The basal ganglia are connected with frontal cortex in a series of functional modules that maintain a relatively consistent anatomical and physiological

organization. Alexander et al (Alexander and Crutcher, 1990; Alexander et al., 1986) have proposed multiple channels, segregated circuits connecting various parts of cortical areas with the BG and projecting back to frontal areas. There are at least 5 segregated cortico-basal ganglia-thalamo-cortical circuits: motor, oculomotor, limbic, dorsolateral prefrontal and lateral-orbitofrontal. The processing of cortical information is through segregated and paralleled circuits.

Recent studies have suggested that regions within each of the BG nuclei are anatomically and physiologically associated with particular functions. Ventral BG are engaged with reward and reinforcement and play an important role in addictive behaviour and habit formation (Elliott et al., 2003; Everitt and Wolf, 2002; Hollerman and Schultz, 1998). Central BG areas are involved in cognitive functions such as procedural learning and working memory tasks (Jueptner et al., 1997; Levy et al., 1997). Finally, the dorsolateral portion of striatum is associated with the control of movement.

1.1.2 Basal Ganglia and movement control

In the 17th century, Thomas Willis was the first to draw attention to the basal ganglia, describing these structures as largely contributing to sensory integration. Later, the motoric importance of the BG was clarified by the clinical observation of a relationship between particular movement disorders and basal ganglia lesions, e.g. the hemiballism induced by subthalamic nucleus infarction and dystonia associated with lesions in the putamen. Recent theories of the functional role of the BG have been dominated by the view that the

function and dysfunction of the BG are determined by excitatory and inhibitory interactions between the different nuclei.

1.1.2.1 Rate coding model

The revolution in anatomical methods during the late 20th century led researchers to suggest a highly influential model of the BG (Albin et al., 1989; DeLong, 1990). The model proposed that the control of movement between motor cortex and BG is operated by two segregated systems within the motor circuit of the striatal-pallidal complex. First, there is the 'direct' putamino-GPi (GABA co-localized with substance P), and GPi-thalamic (GABA) system. This pathway from putamen also projects to substantia nigra reticulata (SNr), and thence to thalamus and brain stem. Second, there is the 'indirect pathway' involving putamino-lateral pallidal (GPe) (GABA co-localized with enkephalin), GPe-subthalamic (GABA), subthalamo-GPi (glutamate), and GPi-thalamic (GABA) relays. The projection striatal neurons in the direct pathway express D1 dopamine receptors, whereas those in the indirect pathway express D2 dopamine receptor. Stimulation of the direct pathway, either by glutamatergic cortico-striatal input from sensorimotor cerebral cortex, or by dopaminergic excitation from substantia nigra compacta (SNc), facilitates transmission and results in disinhibition of thalamic targets (in VA/VL) which project excitatory pathways onto motor cortical areas. The cortico-striatal stimulation of the 'indirect' pathway has the net effect of releasing the subthalamic drive to GPi, leading to increased GPi inhibition of thalamic targets and reduced thalamo-cortical input to motor cortex. Therefore, the net effects of

the 'direct pathway' and 'indirect pathway' are to facilitate and inhibit cortically initiated movement, respectively.

The model proposes that alterations in neuronal firing rates underlie the spectrum of movement disorders. Accordingly, the loss of striatal dopamine would induce a bias in the excitability of the two subpopulations of striatal projection neurons from which originate the direct and indirect striato-nigral pathways. This would result in changes in the discharge rate within the GPe, GPi (Filion and Tremblay, 1991; Filion et al., 1991) and STN (Bergman et al., 1994). Increased BG output reduces thalamocortical activity and leads to the development of parkinsonian motor signs, such as akinesia and bradykinesia. Conversely, dopamine-induced dyskinesia and dystonia have been postulated to result from decreased discharge rates. Reversed trends of pallidal and STN discharge rates in response to dopamine replacement therapy have been reported in both PD patients and MPTP-treated primates (Boraud 1998, 2001, Hutchinson 1997, Lozano 2000 apomorphine). Excessive firing of GPi neurons are brought down by at least 50% and even completely inhibited by systemic injection of L-Dopa or dopaminergic agonists, both in primates (Filion 1991, Boraud 1998, 2001, Papa 1999) and in patients with PD (Hutchinson 1997, Stefani 1997, Merello 1995, Lozano 2000). The decrease in firing frequency seems to be linked to clinical improvement (Filion 1991, Hutchinson 1997, Stefani 1997, Boraud 1998, 2001), and dyskinesias occur when frequency is excessively decreased. The crucial role of these rate changes in the pathophysiology of PD has successfully explained the hypokinetic and hyperkinetic movement disorders. This model has been verified by the

subsequent findings of improvement of motor symptoms in parkinsonian animals and PD patients by inactivation of GPi and STN.

The 'rate model' has influenced experimental and surgical interventions for movement disorders in the last decade. However, the model needs reappraisal in the light of recent studies and clinical findings. First, several studies have failed to find the expected significant changes of firing rates in the pallidum (Boraud et al., 2002), thalamus (Pessiglione et al., 2005) or motor cortical areas of MPTP monkeys (Goldberg et al., 2002). Electrophysiological recordings in GPe in MPTP monkeys provided controversial results. There is no consistent evidence showing a decrease of GPe activity in the parkinsonian state. Second, the 'box and arrows' model might have overlooked the complexity of the BG network. Most importantly, this essentially anatomical model of the BG fails to explain certain clinical findings and leaves a number of paradoxes.

The first paradox is that lesions in GPe do not worsen parkinsonism, while lesions in GPi do not induce hyperkinetic movements in PD. In contrast, therapeutic inactivation of the motor part of GPi (postero-ventral pallidus), whether by ablative surgery or high-frequency stimulation, improves parkinsonism, dyskinesia and dystonia. How GPi lesion/stimulation works on these discrepant movement disorders is still unclear. Another paradox observed by Obeso and Marsden (Marsden and Obeso, 1994) is that stereotaxic lesions in patients with PD directed at motor thalamus do not cause a prominent worsening of parkinsonian hypokinesia and bradykinesia; nor do they regularly cause dyskinesias.

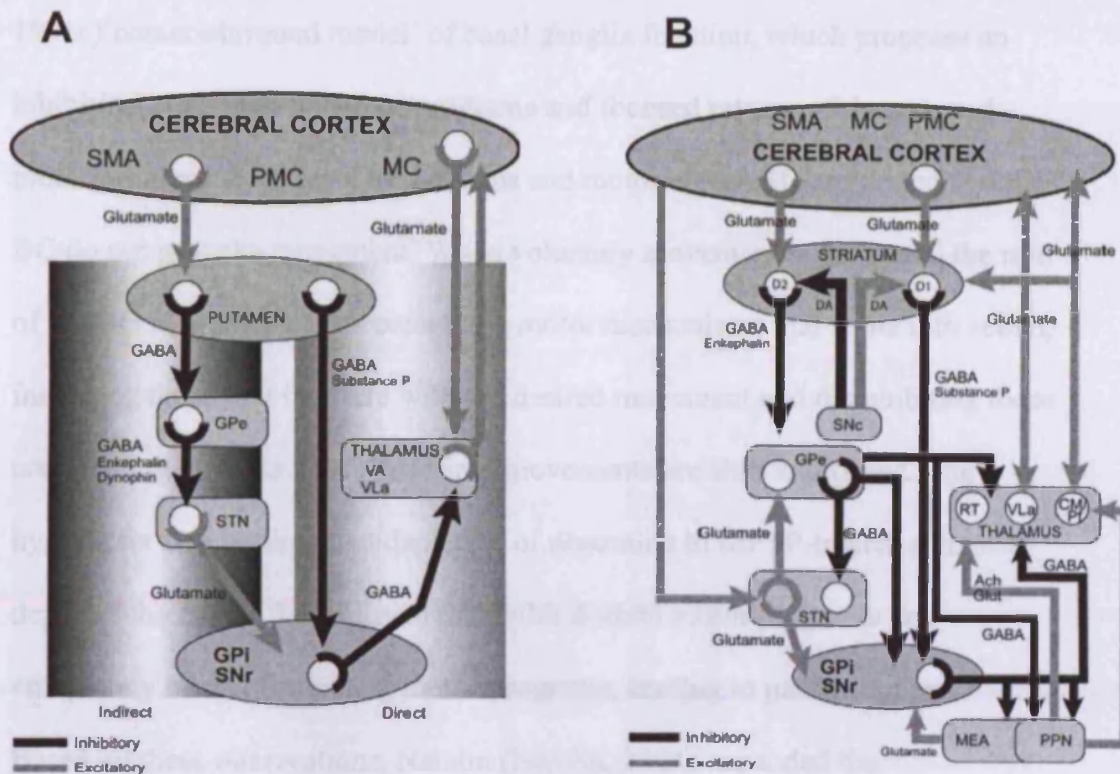


Figure 1.1. The ‘box and arrow’ models of BG circuitry. (A) The traditional model of direct and indirect pathways. The figure provides a schematic outline of the basic circuitry and the transmitters in the BG. Gray lines represent glutamatergic connections, black lines represent GABAergic connections. (B) The updated BG circuitry. PMC, premotor cortex; GPe, globus pallidus pars externa; GPi, globus pallidus pars interna; SNr, substantia nigra pars nigra; SNc, substantia nigra pars compacta; STN, subthalamic nucleus. PPN, pedunculopontine nucleus; RT, nucleus reticularis thalamic; CM/Pf, centromedian/parafascicularis thalamic nucleus; Ach, acetylcholine; DA, dopamine; glut, glutamate. (Adapted from Kopell, 2006).

1.1.2.2 ‘Center-surround’ and ‘dynamic’ model

Recent advances in the knowledge of BG circuits, the activity of BG neurons during movement and the effect of BG lesions have contributed to Mink’s (Mink and Thach, 1991a; Mink and Thach, 1991b; Mink and Thach,

1991c) 'center-surround model' of basal ganglia function, which proposes an inhibition of competing motor programs and focused release of the selected motor program at the level of thalamus and motor cortex. He suggested that the BG do not provoke movement. When voluntary movement is generated the role of the BG is to regulate the competing motor mechanisms that come into action, inhibiting those that interfere with the desired movement and disinhibiting those contributing to it. As a result, desired movements are able to proceed. The hypothesis also implied that depletion of dopamine in MPTP-treated primates deprives the BG of the ability to disinhibit desired motor programs and completely inhibit competing motor programs, leading to parkinsonism. Based on these observations, Nambu (Nambu, 2004) expanded the center-surround model into a 'dynamic model' in the temporal domain. This model included the cortico-STN-GPi/SNr 'hyperdirect' pathway. The conduction velocity of the latter is faster than that of the direct and indirect pathways. In essence, the selection of a motor program is mediated by sequential information processing: 1) GPi neurons are suppressed through the 'hyperdirect pathway' when the motor cortex commands the initiation of a voluntary movement. Thereby, the large areas of thalamus and cerebral cortex that are related to both the selected motor program and other competing programs are suppressed. 2) Thereafter, another inhibitory signal is transmitted through the 'direct pathway' to the GPi and results in the disinhibition of its targets and the release of the selected motor program. 3) In a final step, the signal reaches GPi through the 'indirect pathway' to activate neurons and inhibit target neurons. The dynamic control of the BG through the three

pathways, therefore, releases only the selected motor program at the selected timing.

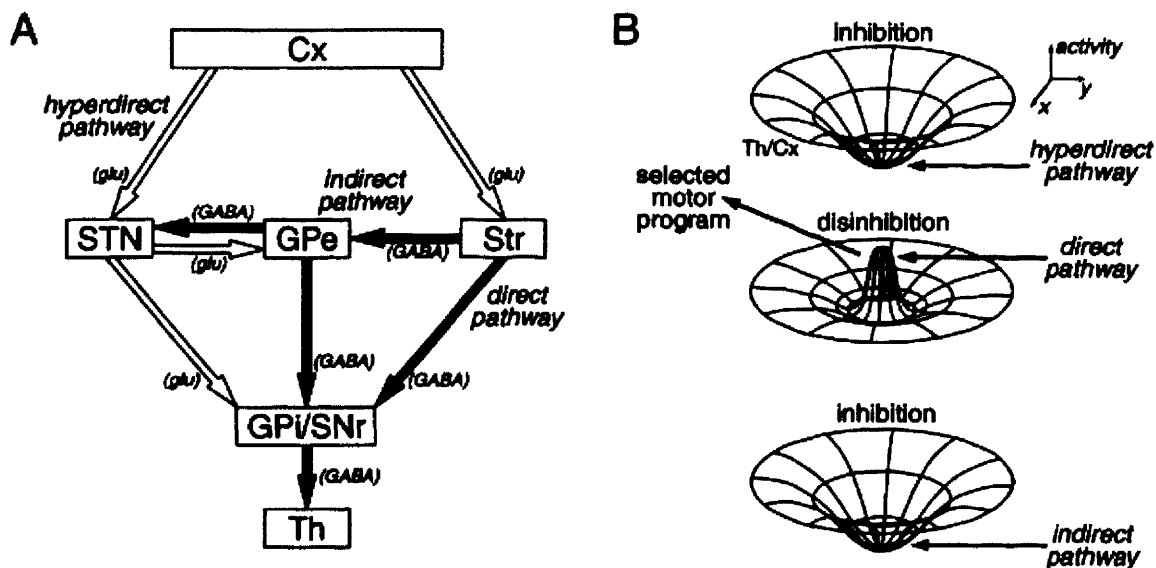


Figure 1.2. Introduction of “hyperdirect” cortico-STN pathway. (A) A schematic diagram of the cortico-STN-GPi/SNr “hyperdirect”, cortico-striato-GPi/SNr “direct” and cortico-striato-GPe-STN-GPi/SNr “indirect” pathways. Open and filled arrows represent excitatory glutamatergic (glu) and inhibitory GABAergic (GABA) projections, respectively. Cx, cerebral cortex; GPe, external segment of the globus pallidus; GPI, internal segment of the globus pallidus; SNr, substantia nigra pars reticulata; STN, subthalamic nucleus; Str, striatum; Th, thalamus. (B) The dynamic model of basal ganglia function explaining the activity changes in the thalamus and/or cortex (Th/Cx) caused by sequential inputs through the hyperdirect (top), direct (middle) and indirect (bottom) pathways. (Adapted from Nambu 2002).

1.1.2.3 ‘ Reinforcement learning models’

In agreement with most of the experimental data obtained from MPTP primates, Bergman and colleagues proposed a new concept of BG processing (Bar-Gad et

al., 2000; Bar-Gad et al., 2003). They suggest that the function of the BG loop is to perform efficient dimensionality reduction and decorrelation of complex forebrain activity. The computational goal of the BG networks is to maximize the representation of the cortical information by using decorrelation mechanisms controlled by dopamine reinforcement signals. Bergman and colleagues argue that the BG would not play any role in the initiation or control of movement but would simply provide relevant information to the cortical structure involved in the particular processing. In parkinsonism, the existence of synchronization of neuronal activity within the various basal ganglia nuclei would be associated with a failure to define relevant information. Deprived of feedback from the BG, the forebrain responsible for motor programming and execution would not be able to operate normally.

This theory proposes that the BG is not involved in movement encoding itself but simply in information processing. Therefore, the question would not be what is the exact nature of the parameter coded, but instead how this parameter is coded.

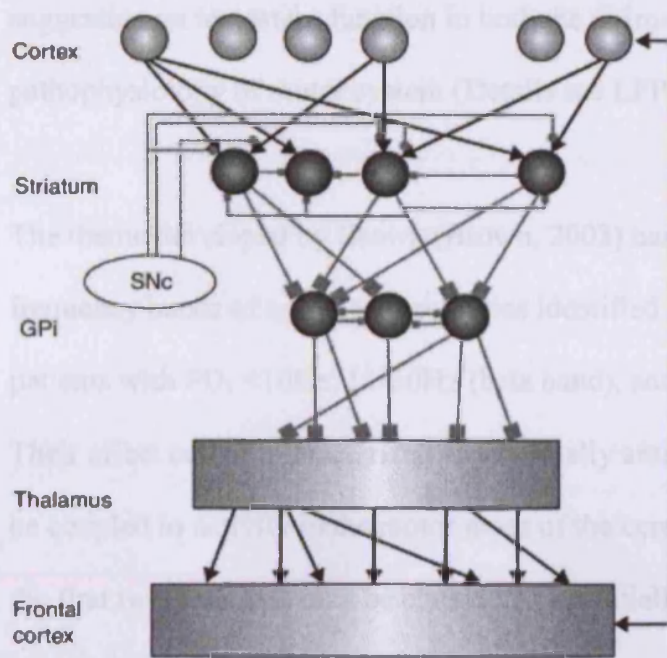


Figure 1.3. The reinforcement driven dimensionality reduction neural network model.

The model is composed of a three-layered feed-forward network simulating the cortico-striato-pallidal circuit with lateral inhibitory connections at the intermediate (striatum) and output (pallidum) layers. A reinforcement (dopaminergic) signal is provided at the intermediate (striatal) layer. Arrowhead black connections represent glutamatergic excitatory synapses, square-head gray connection represent GABAergic inhibitory synapse and round-head broken line connections represent dopaminergic modulatory synapses. (Adapted from Bar-Gad, 2001)

1.1.2.4 Focused attention model

Recent studies in animals and humans have revealed the existence of different modes of synchronized activities within various levels of the subthalamo-pallidal-thalamo-cortical circuit. The oscillations are dynamically and systematically modulated by task and dopaminergic stimulation, thereby

suggesting an important function in both the normal physiology and pathophysiology of motor system (Details see LFP section).

The theme developed by Brown (Brown, 2003) has emphasized three major frequency bands of oscillatory activities identified in the basal ganglia of patients with PD, <10Hz, 11-30Hz (beta band), and >60Hz (high gamma band). Their effect can be characterized as essentially anti- or prokinetic and each may be coupled to activity in the motor areas of the cerebral cortex. In this model, the first two activities may be considered essentially antikinetic. The high gamma band activity, related to attentional processes and favoring cortico-cortical interactions, is regarded as 'prokinetic'. Under the circumstance of dopaminergic denervation, coupling between basal ganglia and motor cortex is dominated by activity <30 Hz. The basal ganglia lead and lag cortex at <10 Hz and 11-30 Hz, respectively. These activities are reduced after reinstitution of levodopa, when strong coupling at >60 Hz appears. Activity in the BG leads cortex in the latter. In parkinsonism, the clamping of cortical activity in synchronous oscillations of low-frequency through low-frequency driving and the possible suppression of the high gamma band mode by the 11-30 Hz cortical input to the BG precludes cortico-cortical interaction in the gamma band thereby contributing to bradykinesia. On the other hand, BG oscillations at high gamma activity may be prokinetic by virtue of their facilitation of motor cortical interaction in the gamma band. Nevertheless, the assumption that <10 Hz activity is a characteristically anti-kinetic is challenged by some recent studies. Alonso-Frech et al (Alonso-Frech et al., 2006) have suggested that 4-10 Hz oscillatory activity could represent a specific signal that conveys a "code to

the thalamocortical motor projection, to release involuntary fragments of movement”. In line with this, Foffani and colleagues (Foffani et al., 2005) have reported enhanced coherence of low frequency between GPi and STN in a patient with PD while spontaneous unilateral choreiform dyskinesia was noted during simultaneous recording from GPi and STN through implanted electrodes. In order to establish whether the <10 Hz activity is anti- or pro-kinetic in nature would require the direct external stimulation at this frequency range of basal ganglia nuclei through implanted electrodes.

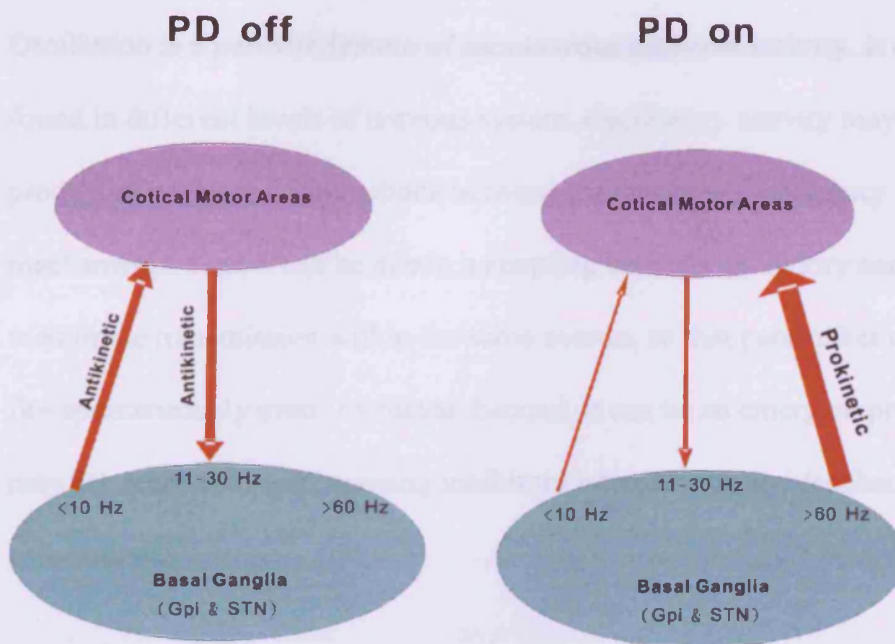


Figure1.4 . The akinetic and prokinetic effects of the different frequency bands of oscillations in the basal ganglia-cortical network. (Adapted and modified from Brown P 2003)

The existence of dynamic and different patterns of rhythmic activity in the BG also has clinical implications for the explanation of the paradoxes of functional

neurosurgery for PD, dyskinesia and dystonia. If hypokinetic disorders, such as parkinsonism, and hyperkinetic disorders, like dyskinesia and dystonia, are the products of oscillatory input to the thalamus, albeit at different frequencies, this may explain why deactivation of GPi through lesioning or high frequency stimulation is an effective therapy for hypokinesias and hyperkinesias in the human.

1.2 Oscillations in the basal ganglia

Oscillation is a periodic feature of spontaneous neuronal activity. It can be found in different levels of nervous system. Oscillatory activity may be the product of reciprocal interactions between excitatory and inhibitory mechanisms. First it can be due to a coupling between excitatory and inhibitory membrane transmission within the same neuron, so that pacemaker cells can fire spontaneously even if isolated. Second, it can be an emergent property of a network architecture comprising inhibitory interneurons and feedback connections.

1.2.1 Oscillations and synchrony

Oscillations can be recorded from striatum, Globus pallidus (GPi and GPe), STN and SNr. The oscillations of neurons between and within these nuclei can be synchronous or uncorrelated. For example, an oscillatory neuronal activity can be unsynchronized with other neurons. On the other hand, the failure to observe oscillatory activity does not necessarily infer there is no synchrony.

Currently, it is a widely accepted concept that synchrony plays an important role in brain.

1.2.2 Oscillations in different frequency bands

Oscillatory activities in different frequency ranges have been reported in neuronal networks in health and disease. They can be subdivided as ‘ultra slow’ frequencies (0.05-0.5 Hz) (Allers et al., 2002; Ruskin et al., 2003) and frequencies which are associated with sleep rhythms, such as ‘slow wave’ activities (~1 Hz) (Goto and O'Donnell, 2001a; Goto and O'Donnell, 2001b; Magill et al., 2000; Magill et al., 2001; Magill et al., 2004; Stern et al., 1998) and ‘spindles’ (5-12 Hz) (Berke et al., 2004; Magill et al., 2000; Magill et al., 2004; Magill et al., 2005). There is also ‘theta’ (4-10 Hz) activity, which is prominent in limbic structures such as the septum, the hippocampus, and the entorhinal cortex during states of attentive arousal. Oscillatory activity in the 8-15 Hz range, also known as ‘alpha’ or ‘mu’ activity, occurs during drowsiness or states of relaxation and is particularly pronounced over occipital cortical areas or sensorimotor cortex, respectively. Activities above this range are those in the ‘beta’ (15-30 Hz) and the ‘gamma’ (30-90 Hz) band. These frequency bands characterize a high level of arousal and attention. There is also a single report extending the gamut to ‘ultra fast’ frequencies at around 300 Hz (Foffani et al., 2003).

With respect to the BG several questions are raised. What possibilities exist for direct recording from BG? What's the nature of the activities in different

frequency band recorded from the BG? How do oscillatory neuronal activities at different neuronal levels attribute to motor processes? To which extent do the abnormal neuronal activities result in disorders of movement?

1.2.3 What possibilities exist for direct recording from the BG?

Early physiological studies of the BG relied on deep brain recording in healthy animals or animal models of disease in the rat or monkey. In the past decade, the renaissance in functional neurosurgery has provided a unique opportunity to record directly from the BG in the human. The most common recordings are from patients with PD or dystonia undergoing deep brain stimulation implantation. The most frequently visited targets are subthalamic nucleus (STN) and Globus Pallidus interna (GPi). Two different recordings exist: single unit recording made intraoperatively through microelectrode or local field potentials (LFPs). The LFPs can be recorded through microelectrodes intraoperatively or directly from the deep brain stimulation electrode (DBS-electrode) in the few days following implantation, while the DBS-electrode leads are externalized prior to connection to the subcutaneous stimulator.

1.2.3.1 Single unit recordings in basal ganglia

Ever since the pioneering work of Jasper in the early 1960(Jasper et al., 1960), the technique of recording units directly in the brains has been widely used in monkey studies. The recording of individual neuron spikes provides information of the brain at work. Albe-Fessard(Albe Fessard et al., 1963;

Albe-Fessard et al., 1967; Albe-Fessard et al., 1966) was the first person who used the single unit recording to map the thalamus before thalamotomy in patients. At present, many centers use microelectrode to map basal ganglia targets in the Vim, Globus Pallidus Interna (GPi), and more recently, the subthalamic nucleus (STN) during the procedure of stereotactic neurosurgery.

The single unit activity recorded from microelectrodes consists of extracellular potentials, resulting from action potentials generated by an individual neuron. The action potential (AP) is generated when the neuronal membrane potential reaches a certain threshold of depolarization, as a result of summation of excitatory postsynaptic potentials (EPSPs). The neuronal membrane thereafter becomes permeable to sodium (Na^+) and potassium (K^+) ions, which results in a brief reversal of the membrane potential. The change of potential comprises the action potential (AP).

The recordings of single units allow the determination of firing frequency, calculated from inter-spike interval (ISI) histograms (Vitek et al., 1996), and firing pattern. Apart from the striatum, in which the majority of projecting cells seldom fire, BG neurons are tonically active and present three different patterns of discharge: (1) irregular with random distribution, (2) regular, and (3) bursting. The bursting patterns appear to be correlated with certain physiological and pathological phenomena (Boraud et al., 2002; Boraud et al., 1998; Obeso et al., 2000).

More recently, attention has shifted to the interaction between pair of neurons at the intra- and inter-nuclei level. It can be assessed by recording neurons simultaneously. The statistical tool used to determine the degree of synchrony or coupling between units is the cross-correlogram (Abeles and Gerstein, 1988; Bergman et al., 1998). Cross-correlograms determine the temporal distribution of spikes of one neuron with respect to the spikes of another. If two neurons fire in synchrony, a peak at zero time appears in the cross-correlation. In contrast, a flat cross-correlogram indicates that there is no correlation between two neurons. If two neurons receive a common input, a symmetrical peak or a periodic cross-correlogram is observed. Cross-correlation studies are particularly appropriate in the analysis of spontaneous activity and can reveal anatomical connectivity. The auto-correlogram function of a single unit can also indicate oscillatory activity, characterized by repetitive, equally spaced peaks. Auto-correlograms and cross-correlogram may have distinct results and implications.

Single unit recordings provide excellent temporal and spatial resolution of neuronal activity. Nevertheless, there are several disadvantages to single unit recording. First, the recording ideally requires large samples of neurons, and, inevitably, shows a bias towards large units. Second, it may underestimate the significance of synchrony phenomena among neurons. Individual single units may be time-locked with oscillations of the local field potential, implying the neuronal discharge is synchronized to other neurons. However, there may be no oscillatory behaviour in auto- and cross- correlograms. This may be partly explained by non-stationary of the signals and sampling problems.

1.2.3.2 LFP recording in the basal ganglia

Recordings of single unit activity and LFPs from the basal ganglia are complementary. LFPs reflect a differing scale of synchronization. Recordable LFPs indicate that a large number of neurons must be engaged in synchronized rhythmic discharge at a given oscillation frequency (Singer, 1993a; Singer, 1993b). Accordingly, LFP activity can only be detected when neuronal activity exhibits some degree of synchrony. Entirely uncoordinated activity would not be detectable because the currents of synaptic events, which are the major source of the measured signal (Mitzdorf and Singer, 1979), would be cancelled out. Therefore, LFPs can be considered as a surrogate marker of the fluctuation of synchronized local neuronal activity.

LFPs are representative of the aggregate activity of local neuronal population in laminated structures, such as neocortex, hippocampus, olfactory bulb, and cerebellum. The generation of LFPs in these structures is due to the regimented apical dendrites of the principal neurons. The elongated morphology and asymmetric representation of synapses on cerebral cortical pyramidal neurons means that each may be considered a dipole, which their parallel orientation and the cortex's laminar architecture mean that currents tend to summate.

Oscillations in the cortical EEG therefore imply synchronous current changes in large numbers of pyramidal neurons.

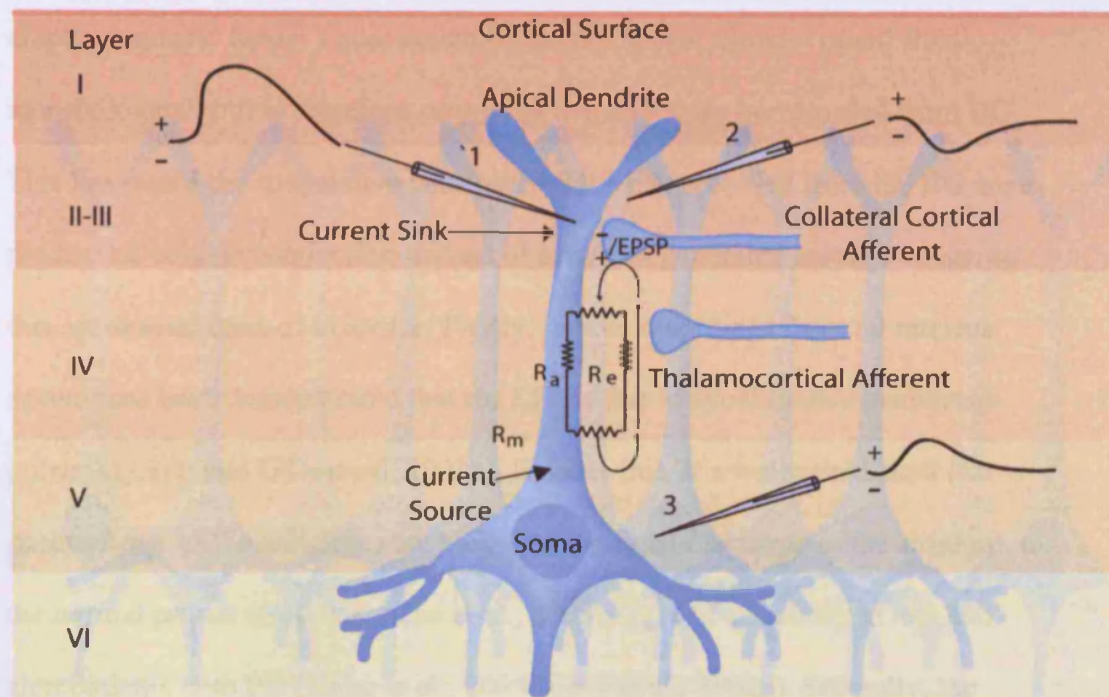


Figure 1.5. Biophysical Basis of EEG and LFPs in the Cerebral Cortex. The apical dendrites of pyramidal cells in the cerebral cortex are orientated perpendicular to the cortical surface and receive a variety of synaptic inputs. When an EPSP is elicited on the apical dendrite, current flows in to the dendrite creating a current sink. In turn, the flow of current along the dendrite and back across the membrane at other sites creates a current source. The electrical resistance of the cell membrane (R_m) greatly exceeds that of the extracellular fluid (R_e), leading to a larger voltage deflection at the intracellular electrode (1) than the extracellular electrodes (2,3). At the site of current generation, the flow of current away from the extracellular electrode (2) leads to a negative deflection in voltage. These changes in current flow across many neurons due to synaptic currents are the basis of both EEG and EcoG (adapted from Kandel and Schwarz, 2000).

In contrast, cytoarchitectural investigations of STN and GPi in the monkey and rat have shown that the nuclei contain tightly packed principal neurons with

elliptic dendritic fields. These structures do not appear clearly 'open' field morphologically. It is therefore surprising that LFPs can be recorded from BG. This has raised the speculative possibility that LFPs recorded from the BG are a product of volume conduction instead of activities generated locally. Against this are several lines of evidence. Firstly, in vivo recordings from rat nucleus accumbens have demonstrated that the LFP is due to synchronous membrane potential (Goto and O'Donnell, 2001b). Besides this, it's well established that spontaneous LFP oscillations are locked to neuronal discharge in the striatum of the normal primate (Courtemanche et al., 2003), STN of anesthetized rats and alert patients with PD (Kuhn et al., 2005; Levy et al., 2002a). Secondly, the coherence between distinct BG nuclei and between these and cortex have supported the notion that there is a close relationship between neuronal activity and the basal ganglia LFP. Thirdly, most groups have used a differential recording configuration, with bipolar recordings which would minimize contamination by volume conduction. Lastly, phase reversal has been observed in LFP recordings made in BG nuclei. This would not be explained by volume conduction. Proof of the principle that the LFP recorded from the human STN is focally generated from this structure would require the demonstration of a steep but focal increase of LFP activity during electrode descent. Chapter (IntraOP) will test the validity of intraoperative recordings of LFPs in localizing the STN in PD surgery, and investigate the focal increase of spontaneous LFPs when the recording electrode penetrates the border of STN nucleus.

1.2.4 How does synchronous neuronal activity contribute to motor processing?

1.2.4.1 Single unit activity in the basal ganglia during movement

Ever since the first recording made by DeLong of GP during movement almost 3 decades ago, single unit recording have been used to investigate the role played by the BG in motor control. The relationship between neuronal activity and the motor system is studied in two ways. One involves passive limb movement, in order to study sensory-motor fields, and the other involves voluntary movements to examine motor functions, such as planning and execution.

Striatum

The striatum is the main input nucleus of the BG and receives glutamatergic cortical inputs from motor cortex. Single unit recording have shown two populations of neurons, phasic activated neurons (PAN) and tonically active neurons (TANs). Early studies in normal primates (Kimura et al., 1996) have shown both populations responds to passive movement. PANs are correlated with movement preparation (Kimura et al., 1996). A recent cross-correlation analysis has shown that about half of TANs fire in a synchronized pattern without oscillation (Raz and Feingold 1996, Raz and Vaadia 2000).

There are few studies carried out in the striatum of the MPTP-treated monkey and the results are inconsistent. However, Raz (Raz et al., 1996; Raz et al., 2001) has reported a significant increase in the number of synchronized pairs of TANs, which became oscillatory over a frequency range of 10-15 Hz.

STN

The STN is the only glutamatergic structure in the BG. It receives glutamatergic excitatory input from the motor cortex through the hyperdirect pathway, GABAergic innervation from the striatum, and reciprocal afferents from the GP and PPN. Very little oscillatory activity has been detected in the normal monkey.

The STN is organized somatotopically with the lower limbs represented rostrally and the upper part of body represented caudally (DeLong et al., 1985; Matsumura et al., 1992). The majority of neurons within STN increase their firing rate during eye and limb movement. However, the temporal relation between the onset of movement and change of firing rate remain unclear.

The electrophysiological characteristics of STN have been widely investigated both in animal models and in patients with PD undergoing functional neurosurgery. In the MPTP-treated monkey, dopaminergic denervation induces an increase in STN discharge frequency. It is also associated with an increase in the number of bursting cells. Sensory-motor fields become impaired after MPTP treatment in the monkey. An increase in the magnitude and duration of neuronal response to passive movement has been reported in this situation (Bergman 1994).

Recordings from PD patients have shown the presence of bursting cells. There is one report showing a correlation between oscillation and tremor.

Rodriguez-Oroz et al (Rodriguez-Oroz et al., 2001) made single unit recording from PD patients undergoing bilateral STN implantation and demonstrated that the firing patterns were similar to those previously documented in MPTP-treated primates. Most cells (60%) fired irregularly. A quarter of cells fired tonically, while 15% fired in an oscillatory way. Movement-related firing was seen in the dorsolateral region of the STN and the authors argued that the latter firing pattern is influenced by projections from the primary motor cortex. The dorsolateral region of the STN may be the most appropriate site for placement of the stimulating electrode in DBS.

GPe

The vast majority of GPe neurons respond to passive movement of only one joint in normal animal. This structure is involved in motor behaviour similar to GPi (detail, see later). The change in activity in neurons in GPe with movement lags the onset of movement.

The firing pattern in GPe changes in MPTP-treated primates, with an increase in bursting cells and the probability of correlation between pairs of oscillatory cells. Sensori-motor fields became blurred and less selective to passive mobilization.

GPi

GPI is the main output structure of the BG and is GABAergic. Little oscillation or synchronized pairing has been observed in the GPI in normal animals.

Movement-related neurons are located in the caudal part of the GPI. In the normal animal, sensory-field responses to movement are rather selective to passive movement of single joints of the contralateral limb. Motor studies have demonstrated that the modification of GPI neuronal activity lags both motor cortex neurons and the onset of muscle activity. It is interesting to note that some data show that lesion and cooling of the GPI slows movement, without affecting reaction time.

Recent studies in monkeys and patients have revealed the predominance of the bursting pattern in GPI in parkinsonism. These also show phase locked oscillation in 40-50% of GPI neurons in MPTP-treated monkeys and PD patients. These oscillations are predominantly at tremor frequency and at 13-14 Hz in MPTP-treated monkeys. Linear regression analysis has failed to show any significant relationship between the frequencies of tremor and neuronal oscillation (Heimer et al., 2006).

There are few studies comparing GPI sensory-motor fields in normal and MPTP-treated monkeys. These reveal a dramatic loss of spatial focal selectivity in the latter condition. Another change after MPTP intoxication is that the response of GPI neurons to voluntary movement begins prior to the onset of muscular activity. This implies that dopaminergic depletion induces a complete reversal of temporal sequences.

L-dopa or dopamin agonist stimulation can reverse some of the above pathophysiological activity. Firing rate and bursting pattern are decreased in tandem with clinical improvement. On the other hand, an excessive decrease in GPi firing rate and modification of discharge pattern results in dyskinesia. Overall, this implies that the pattern of neuronal discharge may be more important than the firing rate in the generation of movement disorders.

In the rate coding model of Albin and DeLong it was proposed that a decreased activity of GPi output neurons would be found in idiopathic dystonias and other hyperkinetic movements. However, studies from different groups haven't shown consistent features in these movement disorders. Vitek (Vitek et al., 1999) reported a decrease of the firing rate of GPi in dystonia patients undergoing functional neurosurgery. Hutchinson (Hutchison et al., 2003) recorded GPi activity from a heterogeneous group of dystonic patients and revealed that the firing rate is not significantly distinct from PD patients who underwent the same surgical procedure. They argued that the discrepant results may be due to anesthesia. They also failed to find a correlation between firing rate in GPi and the severity of dystonic movement. This raises the possibility that the firing patterns of GPi neuron are more important in dystonia. Indeed, neurons in GPi tend to fire in bursts in the GPi of patients with dystonia. Phasic and tonic increases and decreases in firing rates of neurons during movements are observed both in GPi and thalamus, and can be found before, during and after dystonic movement. In addition, Lenz et al. (Lenz et al., 1998) reported expanded receptive fields in thalamus of dystonic patients. But studies in GPi

show neurons with multijoint receptive fields are rather sparse in patients with dystonia, and clear single joint movement-related activation is still preserved.

In line with this, in *dr^{sz}* hamsters (Gernert et al., 2002), a unique model for idiopathic paroxysmal dystonia, also demonstrate an alteration of neuronal discharge pattern in the entopeduncular neurons (internal globus pallidus in primate). The discharge pattern of entopeduncular neurons was highly irregular and was burst-like in *dr^{sz}* hamsters. This supports the notion that altered discharge pattern may be more important for the occurrence of dystonia than a reduced discharge rate.

1.2.4.2 Local field potentials in the basal ganglia during movement

Physiological studies in the sensory system suggest that brain is able to focus on and group together particular aspects of distributed neuronal responses to specific sensory stimulation, by making these responses synchronised (Gray et al., 1989; Singer, 1993b). Coherent and synchronized elements are assumed to be more effective when convergence occurs during later stages of processing, so that particular channels of activity can be biased over others. These findings contribute to the hypothesis that the motor system uses similar mechanisms to bind input to output in the executive motor cortex. Such mechanisms provide the automatic link between voluntary effort and the recruitment and operation of a sequence of motor programs. The motor areas of the cortex (sensorimotor, lateral premotor and dorsolateral prefrontal cortices, and SMA and cingulate motor areas) may select and group together particular aspects of the distributed

neuronal responses related to an intended movement, by making these responses coherent in the high frequency gamma band.

In order to appreciate the putative functional and pathological significance of synchronised oscillations in the BG, studies in health and disease need to be considered separately.

1.2.4.2.1 Synchronized oscillations in the healthy basal ganglia

Most electrophysiology studies suggest there are only low levels of oscillations in the BG of the healthy animal. However, a recent study (Courtemanche et al., 2003) provides evidence that robust oscillatory activity can be recorded from the striatum in alert and behaving monkeys, and this activity is modulated as the animals are engaged in saccadic eye movements. The predominant frequency of this activity is at 10-25 Hz. LFPs recorded in this beta frequency band are synchronized across recording electrodes. Some striatal neurons also show in-phase or anti-phase firing with the LFPs. These findings indicate that LFPs are locally generated and globally synchronized within striatum. They argue that beta oscillatory synchrony is not a de novo development in PD; instead it may be an exacerbation of a physiological mechanism.

It's noteworthy that in the above the synchronization between LFPs only shows a task-related modulation for sites that are neuronally engaged in the saccade eye movement task, termed saccade-related activity. Saccade-related neurons become disengaged from general LFP synchrony during the eye movement.

During oculomotor fixation, before saccades are made, high levels of beta synchronization are observed. This movement-related suppression in the beta frequency band was also manifest in the putamen of an epileptic human (Sochurkova and Rektor, 2003). It is therefore reasonable to assume the execution of movement relies, at least partially, on the ability to deftly engage and disengage task-related neurons from synchronization evident in the LFP at the basal ganglia level.

This and other studies have raised some important questions. What's the origin of this synchronous activity? Is it locally generated or a product of afferent input? Is this activity primarily pathological, or an exacerbation of a physiological mechanism? What's the functional role of these oscillations? The increase in this synchronous activity in dopaminergic depletion would provide some clue that when oscillatory activities in the BG go wrong, then abnormal behavioural states are likely to occur.

1.2.4.2.2 Synchronized oscillations in the basal ganglia in movement disorders

LFP activity in the BG may be subdivided into 3 bands, <10, 10-30, and >60 Hz, here are termed as alpha, beta and gamma activity, respectively.

Tremor-related oscillations (4-7 Hz), which are readily recorded by microelectrodes, are not consistent features in BG LFP recording. There are numbers of reports about the elevated coupling both between STN and GPi

(Foffani et al., 2005) and between the GPi and muscle activity (Silberstein et al., 2003) at frequency <10 Hz in patients with levodopa dyskinesia. Of relevance in this regard is the observation that LFP power at this frequency band may also increase in the pallidum and STN of PD patients following Levodopa or dopaminergic agonist stimulation.

There is also increasing evidence suggesting that low frequency oscillatory local field potential activity in the pallidum may be somehow related to the pathophysiology of dystonia. The first report of relevant activity in the pallidal LFP was in a patient with myoclonic dystonia, and involved the 4-8 Hz frequency band (Liu et al., 2002). Soon after this, prominent activity was reported over an overlapping frequency band of 4-10 Hz in a large series of patients with primary dystonia (Silberstein et al., 2003). The level of this activity was shown to exceed that in patients with PD. Silberstein et al, proposed that pallidal LFP activity in the 4-10 Hz band might relate to synchronized bursting across neurons. Such bursting may be particularly prominent during dyskinesia in primates and PD patients and during hemiballism (Silberstein et al., 2005a), which bear some phenomenological resemblance to dystonia. However, there is, to date, no evidence that directly links pallidal LFP activity < 10 Hz with neuronal activity. This is important as oscillations in the LFP might represent volume conduction from distant sources such as the cerebral cortex, or even movement-related artifact secondary to dystonic movement of the head and neck. To refute this would require evidence from intraoperative recording in dystonic patients to demonstrate that local neuronal discharges in GPi are locked to oscillatory LFP activity at low

frequency. In Chapter 4, we will investigate this question in detail. We simultaneously record LFPs and neuronal activity from microelectrodes inserted into the pallidum in awake patients with primary dystonia during functional neurosurgery to determine the extent to which low frequency band LFP activity is concentrated in GPi and is synchronous with local neuronal discharge.

LFP activity in the 10-30 Hz band is the best characterized in the human BG. It can be recorded from striatum, STN and GPi, and observed to be temporally coupled between GPi and STN and between these nuclei and cortical EEG in patients with PD.

In MPTP-treated monkeys, the pathological synchronization in the beta band is suppressed by the injection of apomorphine. Similar to this, the oscillatory LFP activity in PD patients is suppressed by treatment with dopaminergic drugs in tandem with clinical improvement. It is noteworthy that the predominant frequency in MPTP-treated monkeys and PD patients centres at about 10 Hz and 20 Hz, respectively. One possible explanation for this difference is the greater severity of the parkinsonism in the monkey model. If so then one might expect the peak frequency of synchronization would inversely correlate with the severity of parkinsonism in patients with PD. This needs to be investigated by further experiments.

The evidence above has suggested that prominent synchronized beta activity in the untreated parkinsonism state may be related to motor impairment. It raises the question as to what is the relationship between motor processing and beta

synchrony. Several correlative studies have demonstrated an inverse correlation between these two. Beta activity in STN and GPi is attenuated prior to and during self and externally paced voluntary movement (Doyle et al., 2005; Kuhn et al., 2004). There is also a positive correlation between the onset of desynchronization of beta activity and reaction time across patients (Kuhn et al., 2004). However, the major deficit in PD is bradykinesia, rather than prolongation of reaction time. In order to explain this bradykinesia, one needs to prove that beta synchronization is more resistant to suppression during and before movement in patients who are withdrawn from levodopa. In this regard, several studies have compared the reduction of suppression during movement in untreated patients with treated patients. However, the results are inconsistent. Accordingly, the anti-kinetic properties of beta activity were examined in a movement paradigm which necessitated patients to cancel a preprepared movement. Consistent with the results above, there was an augmentation of beta activity in STN when patients with PD had to suppress a movement (Kuhn et al., 2004).

1.2.4.3 What is the mechanism by which excessive synchrony might impair motor processing?

There is growing evidence to suggest that synchronization between neurons may facilitate information flow. However, a system must reach a point when correlation between neurons reduces information processing and this prevails over any potential advantage conferred upon the transmission by synchrony. It

should not be forgotten that prominent synchrony limits the space available for information coding.

The increase in beta activity and its less ready suppression in dopamine deficiency may tie to the BG model proposed by Bergman and colleagues. Here the putative role of the BG play is to maximize the representation of the cortical information by using dimensionality reduction controlled by dopamine reinforcement signals. The selection and compression of cortical information may be impaired in PD due to the prominence of beta synchrony and its resistance to suppression.

Nevertheless, it's an intriguing question as to how synchronization in the BG network is correlated with the progression of PD. A study designed to mimic the evolution of PD by step-wise lesioning of the substantia nigra in monkeys has demonstrated that abnormal synchronization appears later in the depletion process than the first parkinsonism symptoms (Heimer et al., 2006). The significance of this study is twofold. Firstly, it implies that the phenomenon of neuronal synchronization in the BG can be a result of phase transition instead of linear correlation with striatal dopamine level. Secondly, it argues against a causal relationship between bradykinesia and synchronized oscillation in the BG.

So does excessive synchronization cause bradykinesia? Another approach would be to demonstrate significant impairment of motor function during extrinsic synchronization of BG activity through direct stimulation at

frequencies within the beta band. It has been shown that stimulation in this frequency band in the BG of the cat causes akinesia. In humans, worsening of bradykinesia has been reported following 10 Hz and 20 Hz stimulation in the region of the STN in patients with PD. However, it is conspicuous that the effect is relatively small. In Chapter 6, we will investigate whether externally imposed synchronization through direct stimulation of the region of the STN at 20 Hz can slow motor performance in a simple unimanual tapping task and whether this effect is frequency selective.

In contrast to beta band activity, which is usually recorded from the BG of PD patients when they are withdrawn from levodopa, gamma frequency (60-100 Hz) band activity in local field potentials (LFPs) is preferentially observed after restoring dopaminergic medication in patients with PD. The appearance of gamma activity is less consistent than the recording of lower frequency activities, such as alpha or beta activity. There are several possibilities. First, LFP activity at 60-100 Hz may be dependent on a good clinical response to levodopa, not always realized in post-operative levodopa challenges. Second, spontaneously occurring field potential oscillations appear to follow the rule that the amplitude of the fluctuations decreases with increasing frequency of the oscillation, as rapidly oscillating cell assemblies comprise fewer neurons than slowly oscillating cell assemblies (Singer, 1993b). Therefore, the recording of gamma activity may rely on more accurate localization of the macroelectrode than the recording of activities with lower frequencies. Last but not least, the appearance of gamma activity may be related to some specific symptoms, such as dyskinesia.

Spike triggered averages (STAs) of LFP activity have suggested that the discharges of neurons in the STN are locked to gamma oscillations in the LFP in PD patients undergoing functional neurosurgery. In particular, gamma activity may represent synchronous activity in populations of neurons in the upper STN and bordering zona incerta of patients with PD (Trottenberg et al., 2006). To what extent does this high frequency activity relate to motor processing in the BG? The reciprocal relationship between beta and gamma activity has led to the suggestion that activity at 60-100 Hz is prokinetic. Several studies have revealed the similarity between the pattern of LFP gamma activity in the STN following treatment of levodopa in PD patients and that found in the cerebral motor cortex of patients without obvious movement disorders, suggesting that it may be a physiological characteristic of normal movement. Indeed, the same activity can be detected in the STN of patients who have intact dopaminergic innervation (Androulidakis et al., 2007).

Despite all the evidence that beta and gamma activities are focally generated, one should not underestimate the importance of the network character of these oscillations. These oscillatory activities recorded from different nuclei in the BG are coherent with each other and with activity in the cerebral cortex. In the rest state, there is a net drive to the STN from the cortex in the beta band, but a reversal of net information flow in the gamma band, where activity tends to temporally lead over that in the cortex. The pattern of functional connectivity during movement has not been tested yet and a dynamic model of connectivity

between subcortical and cortical levels needs to be established for differing stages of movement.

1.3 Parkinson's disease

1.3.1 Introduction of Parkinson's disease

Parkinson's disease (PD) is considered to be the second most common degenerative disorder of the aging human brain after Alzheimer's disease. The prevalence of this disorder is between 18 and 418 per 100,000 worldwide (Zhang and Roman, 1993). Reported annual incidence rates of PD range from 4.9 to 26 per 100,000 (Bower et al., 1999; MacDonald et al., 2000). PD is rare before 50 years age and increases with age to affect approximately 2% in those aged 65 and above (de Riji, 1997).

The main neuropathological characteristic of PD is the loss of the neuromelanin-containing dopaminergic neurons of the nigrostriatal pathway (Hirsch et al., 1988), which leads to the appearance of motor symptoms such as bradykinesia, hypo-/akinesia, muscular rigidity, resting tremor and postural instability (Fahn, 2006) . The definite diagnosis of PD often relies on autopsy. The essential neuropathological feature of this disorder is not only the finding of loss of nigrostriatal dopaminergic neurons, but also the identification of intraneuronal inclusions, Lewy's bodies, in affected brain regions (Shults, 2006;

Spillantini et al., 1997). Onset of this disorder is prior to the motor manifestation of PD. By the time patients become symptomatic, around 60% of nigral dopaminergic neurons have been lost and striatal content of dopamine has been reduced by around 80% (Moller et al., 1996).

PD arises as a sporadic condition in more than 90% of the cases. Nevertheless, the etiology of the onset of PD remains unknown. It may be the complex interplay between multiple genetic and environmental factors that contributes to the occurrence of PD.

1.3.2 Electrophysiology of PD

1.3.2.1 EMG, EEG and MEG in PD

The fact that slowness is a main feature of patients with PD has implied some abnormality of the function or control of function of muscles during movement. Nevertheless, there have been difficulties in identifying these abnormalities at a single motor unit level. Slight changes in motor unit activity have been detected by spectral analysis and reveal a tendency for motor unit firing to be modulated at around 10 Hz in PD patients (Brown, 1997). In normal subjects, a tonic contraction is associated with a spectral peak at about 20 Hz and again at about 40 Hz (Piper frequency)(Brown et al., 1998). In patients with PD, these peaks are absent and replaced by a lower frequency at around 10 Hz, which is inappropriate for fast and strong contraction. The normal pattern can be restored with dopaminergic treatment (Brown, 1997).

The source of the 20 Hz and 40 Hz peaks is unclear, but coherence analysis between magnetic encephalography (MEG) and surface electromyography (EMG) suggests a cortical origin. Salenius and colleagues have demonstrated that the amount of coherence between the EMG and MEG signals in the 20 Hz and 40 Hz ranges varies dependence on dopaminergic treatment. In patients with PD who are withdrawn from levodopa, the corticospinal coherence between 15-30 Hz and between 35-60 Hz is reduced. The restitution of dopaminergic medication returns a more normal pattern of coherence. Phase analysis indicates that MEG signals recorded from the contralateral motor cortex lead the EMG (Salenius et al., 2002). However, to which extent these abnormalities contribute to the appearance of bradykinesia remains unclear.

Another approach is to investigate the coupling between cortical areas rather than between cortex and muscle. Cassidy and Brown (Cassidy et al., 2002) investigated functional coupling between different cortical areas in PD using cortico-cortical EEG coherence. Scalp EEG activity from several cortical areas was recorded in PD patients when they were engaged in a visual tracking task or copied the task from memory. Differences in EEG-EEG coherence between the tracking and copying tasks were determined in the on and off levodopa conditions. Levodopa treatment greatly increased task-related cortico-cortical coherence. The authors suggested that the ascending dopaminergic projection from the mesencephalon may be important in determining the pattern and extent of functional couplings during executive tasks. One unusual aspect of this study

was that coherence was broad band (0-80 Hz); one would expect functional coherence to be restricted to narrower frequency ranges.

1.3.2.2 BG electrophysiology in PD

The basal ganglia are the primary locus of pathology in PD. It is, therefore, reasonable to assume that PD symptoms are due to abnormalities within these circuits.

The renaissance of functional neurosurgery has provided a unique opportunity to study the neurophysiological characteristics of the BG in patients with PD. Oscillatory synchronization within the BG and between subcortical and cortical structures is of particular significance in the pathophysiology of PD.

1.3.2.2.1 Abnormal synchronization in PD

An increase in synchronized oscillation has been observed in GPe, GPi and STN (Levy et al., 2000; Raz et al., 2000). The excitatory STN and inhibitory GPe form a feedback system that engages in synchronized bursting. Frequency domain analysis of LFP recordings from patients with PD has revealed oscillations in three main frequency bands: 4-10 Hz, 11-30 Hz and 60-100 Hz. The first band contains activity in the frequency range of parkinsonian rest and action tremor. In the pallidum of patients with PD tremor, 12.3% of the cells were found to fire at the tremor frequency (Hutchinson et al., 1997; Mandir et al., 1997). The rhythm of tremor cells within the pallidum is correlated with the frequency of the tremor in the periphery. In line with the data from humans,

pallidal activity in MPTP-treated monkeys showed an increase in oscillations in pallidal cells. The oscillation frequencies of the single cells were bimodally distributed around 7 and 13 Hz, in parallel with the tremor frequencies of these monkeys. However, this relationship may be fleeting (Hurtado et al., 1999), and synchronization between neurons may only occur within small local ensembles, consistent with the multiple peripheral oscillators manifest in parkinsonian rest tremor (Hurtado et al., 2000). It is also unclear whether tremor relates to striatal dopamine deficit. The clinical severity of parkinsonism tremor is neither correlated to the severity of dopaminergic deficit in the striatum nor clinical disease progression.

Taken together, the emergence of PD tremor may depend on the nigrostriatal deficit but once this is present, the tremor does not depend on the severity of dopaminergic depletion. Instead, other neurotransmitter systems, such as the cholinergic or serotonergic systems, or neural circuits other than the BG play an important role in tremor.

The second major band recorded from STN or GPi in patients with PD is 11-30 Hz, (Kuhn et al., 2004; Priori et al., 2002; Priori et al., 2004; Williams et al., 2005; Williams et al., 2003; Williams et al., 2002) termed the 'beta' band. It can be recorded from single, pairs and populations of neurons in STN (Amirnovin et al., 2004; Brown et al., 2001; Kuhn et al., 2005; Levy et al., 2002b) and pallidum (Brown, 2003; Priori et al., 2002; Silberstein et al., 2003).

Synchronized oscillation activity in the STN and GPi of patients with PD may also occur at frequencies in excess of 60 Hz, termed the “gamma” band (Brown et al., 2002; Cassidy et al., 2002; Williams et al., 2002).

1.3.2.2.2 Relation to movement execution

The gamma band activity recorded from GPi or STN in patients with PD who have been treated with dopaminergic medication is observed at rest and is increased with movement (Brown et al., 2002; Williams et al., 2002). Before and during voluntary movement, the STN-GPi coherence and the coherence between STN and cortex are increased (Cassidy et al., 2002), with STN and GPi oscillation leading the cortical activity (Williams et al., 2002). Thus the gamma band is considered as *prokinetic*. In line with this, stimulation of STN or GPi at frequencies >60 Hz alleviate akinesia. However, it is unlikely that this activity is directly linked to the execution of movement, as it occurs both in movement and at rest. Interestingly, this activity in STN disappears when the patient becomes drowsy (Brown et al., 2001). These observations have led to the suggestion that gamma activity is related to attentional processes in the motor domain rather than to the actual execution of movement, and possibly acts through the thalamus to favour cortico-cortico interactions.

As mentioned above, in the dopamine depleted state, beta oscillation is enhanced and gamma activity depressed. The increase in background levels of beta and decrease in the reactivity of beta oscillations prior to and during

movement might contribute to paucity and slowness of voluntary movements, respectively.

Interestingly, drug and task-dependent effects on the beta band are reciprocal to those on the gamma band. Because of this functional reciprocity it has been proposed that in the dopamine depleted state, *antikinetic* beta oscillatory input from the cortex suppresses *prokinetic* gamma oscillations in the BG (Brown et al., 2001; Levy et al., 2002b). This is further supported by a recent study in patients with chronically implanted DBS electrodes. It was found that the degree of synchronization in the beta band between cortical sites over central motor areas correlated with motor impairment, when patients were withdrawn from medication and therapeutic stimulation. In addition, both the reduction in beta synchronization effected by high frequency stimulation of the STN, and that achieved with levodopa, correlated with treatment induced improvements in motor performance (Silberstein et al., 2005b). If beta activity is essentially antikinetic in nature, could its excessive suppression following antiparkinsonian therapy or lesioning of the STN help explain the emergence of hyperkinesias? Recent recordings in the GP of PD patients during levodopa-induced dyskinesias demonstrate that dyskinetic muscle activity may inversely correlate with pallidal beta activity, in keeping with the latter's posited antikinetic nature (Silberstein et al., 2005a).

1.3.2.3 PET studies of Parkinson's disease

Position emission tomography (PET) with [^{18}F] fluorodopa allows the integrity of presynaptic dopaminergic neurons within the BG to be assessed. Typically fluorodopa PET scans of patients with PD show markedly reduced tracer uptake within the striatum, while [^{11}C]raclopride PET scanning (with measures binding of dopamine to D2 receptors) may initially show upregulation. PET studies using H_2^{15}O may be used to assess changes in regional cerebral blood flow during different tasks. Patients with PD show reduced activation of the dorsolateral and mesial frontal regions compared with control groups. These areas are considered to subserve motor preparation.

1.3.3 Treatment for Parkinson's disease

1.3.3.1 Medical treatment for Parkinson's disease

L-dopa

L-dopa, the precursor of dopamine, was introduced as a treatment for PD in the early 1960s (Birkmayer and Hornykiewicz, 1961; Birkmayer and Hornykiewicz, 2001; Gotzias 1967) and has since remained the gold standard among antiparkinsonian drugs. L-dopa continues to be the most powerful orally active antiparkinsonian drug, with a marked symptomatic effect on all components of the cardinal parkinsonian motor signs, such as bradykinesia and rigidity. However, its use is limited by several factors. After 5 years, 25-50% of patients (90% of young onset patients) develop motor fluctuations, whereby the individual fluctuates between periods of high and low mobility, often described as on and off states respectively. In addition, many patients develop

dyskinesia over a period of months or years of L-dopa treatment, which most commonly manifests as chorea during the 'on' state. L-dopa also has no or little effect on clinically important non-dopaminergic problems such as dementia, depression, on-period freezing, autonomic dysfunction, and sleep disturbances; and it does not modify the underlying neurodegenerative process.

Strategies to overcome motor complications in PD

Once motor complications have occurred, there are various ways in which L-dopa can be administered for better effect. L-dopa can be administered in a frequent smaller dose in order to minimize peak-dose complications. In patients without disabling peak-dose dyskinesias, a larger L-dopa dose may be helpful to extend the duration of on periods. Controlled-release L-dopa leads to a longer delay to peak plasma concentrations with prolonged half-life and a slower decline in plasma levels and clinical effect. Some patients with motor complications or wearing off benefit from this formulation. However, the advantage of controlled-release L-dopa is partially limited by its lower bioavailability and lack of reliability.

COMT inhibitors

L-dopa is metabolized via two main pathways: decarboxylation and O-methylation. Blocking peripheral decarboxylation by adding a decarboxylase (AADC) inhibitor has long been the standard in L-dopa treatment. When AADC is inhibited, methylation of L-dopa to 3-O-methyldopa becomes more prominent. This process is catalyzed by catechol-O-methyltransferase (COMT). By inhibiting COMT, slower degradation of L-dopa and thus prolonged

maintenance of plasma levels can be achieved. Two COMT-inhibitors are clinically available: entacapone and tolcapone. Whereas the former acts only on peripheral L-dopa, the latter also can penetrate the blood-brain barrier. When administered in combination with L-dopa, both drugs lead to prolonged availability of L-dopa and to increased plasma half-life.

Dopamine Agonists

Dopamine agonist drugs alleviate parkinsonism symptoms by means of stimulating dopamine (DA) receptors. The various dopamine agonists in use have distinct receptor stimulation profiles and different effects on non-DA receptors. Studies (Piercey et al., 1996; Piercey et al., 1997), have shown that most of the clinical benefits of dopamine agonists are from the stimulation of D2 receptors.

Starting treatment of early PD with dopamine agonists has been proved to reduce the risk of motor complications. In PD patients with motor complications, some dopamine agonists such as pergolide (Jankovic, 1985; Olanow et al., 1994; Sage and Duvoisin, 1986) pramipexole (Guttman, 1997; Mizuno et al., 2003; Pinter et al., 1999), or ropinirole (Rascol et al., 1996) effectively reduce off time.

Parenteral Apomorphine

Apomorphine is the oldest and the most potent dopamine agonist in clinical practice, acting on both D1 and D2 receptors. Intermittent subcutaneous injection of apomorphine can be a useful option for quick relief from off

periods. It leads to large reductions in daily off-time when given via continuous subcutaneous infusion during waking hours. It has been shown that continuous subcutaneous apomorphine therapy can significantly reduce dyskinesia by 40-80%, -believed to be due to the replacement of pulsatile with continuous dopamine receptor stimulation.

MAO-B inhibitors

MAO-B plays an important role in the biotransformation of dopamine in the human brain. It constitutes about 80% of the total MAO activity in the human brain and is the predominant form of the enzyme in the striatum. Inhibition of this enzyme blocks the oxidative deamination of dopamine and increases its half-life in the brain. There are currently two MAO-B inhibitors commercially available for the treatment of PD: selegiline (deprenyl) and rasagiline.

Amantadine

Amantadine hydrochloride (ATD) is a noncompetitive antagonist of the N-methyl-D-aspartate (NMDA) receptor. It is suggested that ATD can interact with catecholamines, especially dopamine pre-and post-synaptically. ATD has been used for the symptomatic treatment of parkinsonism. Its effectiveness is inferior to that of L-dopa. Several clinical trials have confirmed a potent antidyskinetic effect in patients taking L-dopa (Metman et al., 1999), but this effect may fail to persist long-term and may be inconsistent.

Anticholinergic medication

It has been stated that anticholinergic medications improve parkinsonism through a central anticholinergic effect exerted in the striatum, and these drugs are more effective in alleviating resting tremor and rigidity than akinesia. However, several recent studies have indicated the propensity of anticholinergic drugs to induce adverse effects. On top with this, the wider choice of alternative antiparkinsonian drugs with better clinical effectiveness and tolerability has led to the decline of importance of anticholinergic medication.

1.3.3.2 Surgical treatment for PD

See Section 5.2.1

1.4 Dystonia

The origin of the concept

The concept of dystonia was somehow vague a century ago. It was assumed to be a psychogenic rather than organic disorder. The term “dystonia” was coined by Oppenheim in 1911 to describe two patients, one with “dysbasia lordotica progressive” and the other with “dystonia musculorum deformans”. The first patient had an abnormal gait with twisted postures and the second patient abnormal muscle spasms and postures of the limbs. Afterwards, the term ‘dystonia’ was used to describe patients with abnormal, especially mobile, postures.

1.4.1 Definition and classification of dystonia

Dystonia is “a syndrome of sustained muscle contraction, frequently causing twisting and repetitive movements or abnormal postures” (Fahn and Eldridge, 1976).

The initial classification system of patients with dystonia was an anatomical one. Patients are classified as focal (one body part only affected), segmental (two contiguous body parts affected), multifocal (two or more non-contiguous body parts affected), hemidystonia (one side of the body affected), or generalized dystonia (two or more contiguous body parts affected plus trunk)(Fahn and Eldridge, 1976). This classification system is still clinically relevant.

Another classification system describes the anatomical distribution of dystonia, and is used as a diagnostic label in some cases. These terms include: blepharospasm (dystonia affecting orbicularis oculi), oromandibular dystonia, laryngeal dystonia, torticollis (a general term for dystonia affecting the neck, as well as specific description of head turning caused by dystonia, in order to differentiate it from laterocollis (head tilt to the side), anterocollis (forward) or back (retrocollis)), and writer’s cramp (task-specific dystonia affecting the action of writing, but not other tasks).

When this anatomical system of classification is applied to patients with dystonia, pattern of anatomical involvement that relate to age at onset are revealed. Dystonia with childhood or teenage onset is typically the generalized

form, whereas adult-onset dystonia is typically focal (Fahn and Eldridge, 1976). In addition, there emerges to be a somatotopic “gradient” of dystonia related to age at onset. Dystonia affecting the feet or legs is only usually seen in those with young-onset primary dystonia, and even though generalization of symptoms is typical, involvement of cranio-cervical structures is unusual (Bressman, 2000; Bressman et al., 1998). Task-specific dystonias, in particular writer’s cramp, tend to have an age of onset of about 30–40 years old (Jedynak et al., 2001). Cervical dystonia tends to have a later age at onset of about 40–50 years old of age (Jahanshahi et al., 1990), with blepharospasm having the latest average age at onset at about 50–60 years old (Jankovic and Orman, 1984).

Recent classification systems of dystonia depend on etiology. In this system, dystonia is divided into ‘primary’ and ‘secondary’ (Fahn and Eldridge, 1976). In primary dystonia, dystonia is the only clinical feature (with or without tremor), and neither structural nor neurodegenerative cause is present. Patients with secondary dystonia may have other clinical features apart from dystonia, such as cerebellar or extrapyramidal symptoms, and a structure or environmental cause is usually observed.

Most lesions responsible for symptomatic dystonia involve the BG or thalamus (Marsden et al., 1985; Pettigrew and Jankovic, 1985). Bhatia and Marsden (Bhatia and Marsden, 1994) reported their results of a meta-analysis of 240 patients with lesions affecting the BG and causing movement disorders. 36% exhibited dystonia. The lentiform nucleus (putamen and GP) was the most frequent site affected in those with dystonia. Dystonia was also observed in

30% of patients with movement disorders associated with lesions of thalamus and subthalamic region (Lee and Marsden, 1994). Thalamic lesions producing dystonia involved the posterior and midline thalamic nuclei.

In dopa-responsive dystonia (DRD) and myoclonic dystonia there is an underlying deficit in the gene encoding guanidine triphosphate cyclohydrolase 1 (GTPCH1), which is a rate limiting step in the metabolism of dopamine from tyrosine (Ichinose et al., 1994; Ichinose et al., 2001). These patients typically have young onset limb dystonia. Parkinsonism and extrapyramidal signs are not unusually observed. A diurnal fluctuation of symptoms is reported in some patients with worsening of symptoms throughout the day (Bandmann et al., 1998a; Bandmann et al., 1998b). In the vast majority of patients, a dramatic and sustained response to levodopa is seen.

In myoclonic dystonia, familial early childhood onset dystonia, typically affecting the neck and arms is associated with myoclonus. The myoclonus commonly responds to alcohol (Quinn, 1996). Recently, mutations in the epsilon sarcoglycan gene (SGCE) have been found in a proportion of patients with myoclonic dystonia (Zimprich et al., 2001).

1.4.2 The pathophysiology underlying dystonia -electrophysiology

1.4.2.1 EMG studies in dystonic movement

Co-contraction of agonist and antagonist muscles is a characteristic feature of dystonia. Voluntary movement exacerbates the co-contraction of antagonist muscle pairs. The first demonstration of abnormal EMG in dystonia was reported by Herz (Herz, 1944), who showed that dystonic postures are produced by long periods of continuous EMG activity lasting several seconds. Repeated shorter EMG bursts are occasionally recorded superimposed with the longer spasm. It may represent as postural or action tremor (Jedynak et al., 1991; Yanagisawa and Goto, 1971), slow myorhythmia (Herz, 1994) or myoclonus (Obeso et al., 1983), depending on the regularity and duration of bursts. In addition to the involuntary movement, many abnormalities which interfere with the voluntary movement are also found in dystonic patients. The most remarkable one is the lack of selectiveness in attempting to perform discrete independent movements, so that there is an overflow of activity to remote muscle groups that are not normally activated in the movement, including co-contraction.

The characteristic di or triphasic pattern of activation of agonist and antagonist muscles (Berardelli et al., 1998) when normal subjects perform simple rapid movements about a single joint appears to be lost in the EMG in dystonic patients. In contrast, EMG bursts are prolonged in these patients and the agonist and antagonist activities may overlap in time for a longer period than normal. This contributes to the appearance of co-contraction. In addition, simple finger or hand movements may be accompanied by unexpected activity in remote muscles of the upper and trunk muscles. As a consequence, these abnormalities

are probably responsible for the slowness and high degree of variability of voluntary movements in dystonic patients.

Deficits have been found in performing sequences of movement in dystonic patients. The time required to switch from one movement to the next is prolonged. Similar findings are seen in PD. In the latter, the movements also became progressively slower through the sequence ('fatigue'), a finding not seen in dystonia. This is an important distinction between PD and dystonia, as both of them are bradykinetic, and tremor can be observed in both disorders.

In summary, EMG and kinematic studies in dystonia show that simple voluntary movement are bradykinetic and characterized by excessive and overlapping activity in agonist and antagonist muscles together with overflow of activity to muscles not normally involved in the task. The time taken to switch between components of a complex movement is prolonged.

1.4.2.2 Spinal cord reflexes in dystonia

Although primary dystonia by definition does not present clinically with signs of corticospinal dysfunction, electrophysiological testing has revealed deficits in spinal reflex control.

The H reflex (Hoffmann, 1918) is effectively an electrical method of mimicking the tendon reflex. The H-reflex in those with dystonia has been found to have a shorter recovery cycle compared to normal subjects. In addition, reciprocal

inhibition is a technique that experimentally explores the interaction between agonist and antagonist muscles, an issue of core importance to the pathophysiology of dystonia. Studies in those with dystonia, regardless of site of involvement, have found a reduction of inhibition.

1.4.2.3.1 Brainstem motor function in dystonia

At a brainstem level, the most studied circuit is the blink reflex and in particular the blink reflex recovery cycle. A stimulus to the supraorbital nerve of sufficient intensity will trigger an ipsilateral contraction of orbicularis oculi (R1 component) followed by a bilateral contraction of orbicularis oculi (R2 component). The blink reflex recovery cycle is typically assessed by delivering paired stimuli to the supraorbital nerve at different interstimulus intervals, and comparing the size of the R2 response to that obtained when a single stimulus is given. In normal subjects interstimulus intervals of less than 750ms typically result in a significantly reduced R2 size. In certain types of dystonia (blepharospasm, cervical dystonia, generalized dystonia) this recovery cycle is enhanced such that the R2 component is large even at ISIs of 250-500ms (Berardelli et al., 1985; Eekhof et al., 1996; Nakashima et al., 1990; Tolosa et al., 1988). Although abnormalities of the blink reflex recovery cycle are clearly seen in some types of dystonia that clinically do not involve orbicularis oculi, some studies have failed to find blink reflex recovery cycle abnormalities in other types of dystonia such as segmental dystonia not involving the head or neck (Nakashima et al., 1990).

1.4.2.3.2 Other brainstem abnormalities in dystonia

Vestibular abnormalities have been reported in those with torticollis (Bronstein and Rudge, 1988; Stell et al., 1989), although it remains unclear to which extent these are primary to the dystonia or are secondary to a prolonged period of abnormal head position (Bronstein and Rudge, 1988; Stell et al., 1989). The masseteric inhibitory reflex is obtained by stimulating the masseteric nerve during voluntary muscle contraction. Similar to the blink reflex, studies in dystonia have found that reflex recovery cycle is more excitable than normal subjects. This is found both in patients with and without oromandibular dystonia (Pauletti et al., 1993).

1.4.2.4 Cortical function in dystonia

Transcranial magnetic stimulation (TMS)

TMS is a non-invasive method of stimulating cortical neurons. It tends to activate corticospinal neurons trans-synaptically (Di Lazzaro et al., 2001). As stimulation intensity is increased, a rising proportion of activation occurs directly. TMS is useful as a technique to explore the integrity and excitability of motor pathways, and can be applied before and after interventions to determine whether a change in synaptic excitability has occurred.

Several abnormalities in dystonia have been revealed based on TMS studies.

Firstly, TMS has demonstrated increased motor system excitability in dystonia.

It is reflected in the size of motor evoked responses (MEP) from the target muscle. Secondly, studies on the effect of short interval intracortical inhibition (SICI) using a paired pulse TMS technique have shown a reduction in SICI in dystonic individuals. This has been interpreted as a failure of inhibitory control of motor pathways, which would lead to problems in focusing desired movement and could lead to unwanted muscle activity (Beradelli 1998). Thirdly, the silent period following a TMS shock is shortened (Beradelli 1998). This would suggest a deficit in GABA_B mediated inhibition in dystonia.

More recently, a TMS study on a DYT1 cohort has shown that abnormalities in cortical motor inhibition can be present to the same severity in manifesting and non-manifesting carriers of the DYT1 mutation (Edwards et al., 2003). The author therefore developed a new hypothesis regarding the manifestation of symptoms in DYT1 mutation carriers based on abnormalities in synaptic plasticity in the motor system. They found an excessive synaptic plasticity in manifesting mutation carriers, but sub-normal plasticity in non-manifesting carriers. These data suggest abnormalities in the sensitivity of the “synaptic plasticity system” in DYT1 dystonia, and by inference, primary dystonia in general. (Edward et al. 2006).

CNV and MRCP

Two types of pre-movement potential have been recorded in the EEG in dystonia; the Bereitschaftspotential (BP) and the contingent negative variation (CNV). The BP is a slow rising (negative) EEG potential that begins 1.5-2

seconds prior to a self-paced voluntary movement. Initially the potential is diffuse and bilateral (NS1: bilateral primary and supplementary motor area activity), and then becomes lateralized (NS2: contralateral primary motor area activity). The CNV is recorded in a different fashion. Here EEG is recorded between a warning cue and a “go” signal to perform a particular movement. During the gap between the two stimuli, a slow negative potential is recorded which, like the BP, is at first bilateral and then lateralized to the representative hemisphere for the planned movement.

Studies of the BP and CNV in patients with primary dystonia have found a reduction in amplitude of the potentials compared to normal subjects. In most experiments this abnormality was only present when the planned movement involved a body part affected by dystonia (Deuschl et al., 1995; Ikeda et al., 1996; Van der Kamp et al., 1995).

1.4.2.5 Sensory dysfunction in dystonia

There are several lines of evidence suggesting that abnormal sensory function may play an important role in the development of dystonia and Byl (Byl et al., 1996a) proposed sensory signs in dystonia patients may be a consequence of defective sensorimotor integration. It's not uncommon that sensory symptoms precede the appearance of dystonia. Common examples were a gritty sensation in the eye preceding blepharospasm and irritation of the throat preceding spasmodic dysphonia. The presence of “geste antagoniste” or “sensory trick” in those with dystonia has long been viewed as a pointer to a possible role for

abnormal sensory function in dystonia. It describes a phenomenon in which dystonic spasms and postures can be improved by a voluntary manoeuvre such as touching the face. Conversely, vibration of a dystonic limb at rest can induce involuntary co-contractions of muscle that reproduces the dystonic posture of limb (Kaji et al., 1995). It should be noted that vibration can sometimes improve spasmodic torticollis (Leis et al., 1992).

However, to prove in principle that sensory input is, at least, partly responsible for the appearance of dystonia would rely on the demonstration that reducing sensory input from the affected limb can alleviate dystonia. Injection of local anesthesia directly to block muscle afferent function has successfully reduced the action dystonia in writer's cramp patients (Kaji et al., 1995). It's also worthy of note that intramuscular injection of botulinum toxin modifies reciprocal inhibition between flexor and extensor muscles (Priori et al., 1995).

1.4.3 Pathophysiology underling dystonia -imaging studies

1.4.3.1 Structural imaging

Simple structural imaging is normal in primary dystonia. Nevertheless, high field studies in spasmodic torticollis have identified prolonged T2 relaxation times in the lentiform nucleus compared to normal subjects (Schneider et al., 1994).

Recently, voxel-based morphometry has been used to look at brain anatomy in dystonia. In one study of 10 patients with torticollis (Draganski et al., 2003),

voxel-based morphometry revealed an increase in gray matter density bilaterally in the motor cortex and in the cerebellar flocculus and unilaterally in the right GPi. In addition, a decrease in gray matter density was observed in the right caudal SMA as well as in the right DLPFC and visual cortex.

A more recent study of 36 patients with focal hand dystonia, again using voxel-based morphometry, revealed significant bilateral increases in gray matter in the hand representation area of primary somatosensory and, to a lesser extent, primary motor cortex. The finding of bilateral abnormalities in those with unilateral dystonia led the authors to suggest that these abnormalities might to some extent be primary (Garraux et al., 2004).

1.4.3.2 Functional imaging

Regional blood flow changes have been examined during movement. A study compared dystonic patients to normal subjects has shown an underactivity in primary and SMA and excessive activation of prefrontal, cerebellar, insula and parietal cortex when patients are engaged in a paced freely selected movement (Ceballos-Baumann and Brooks, 1997).

Levy and Hallett (Levy and Hallett, 2002) have studied a cohort of patients with focal arm dystonia using magnetic resonance spectroscopy. They found a reduction of GABA in the sensorimotor cortex and lentiform nucleus contralateral to the affected hand, but no such change on the ipsilateral side.

1.4.4 Basal Ganglia dysfunction in dystonia

Given the fact that structural lesions in the BG are noted in the majority of patients with secondary dystonia, it's not unreasonable to suspect that altered BG motor output may contribute to dystonia. This "noisy" BG output could either engage the motor areas of cerebral cortex via the thalamus, or descend directly to the brainstem regions that control posture, balance and locomotion.

Early studies of the BG in dystonia relied on lesions in patients and imaging techniques with poor temporal resolution. Animal models of dystonia have been limited compared to PD. The recent renaissance in functional neurosurgery, however, has provided a unique opportunity to record directly from the BG in human. The usual target for the treatment of dystonia is GPi. Two recording possibilities exist; single unit recording and the LFP. Here we investigate how abnormal neuronal activity in the pallidum may contribute to dystonia.

Dystonia is classified as a hyperkinesia and has been attributed to reduced pallidal inhibition of a tonic thalamocortical excitatory input in the classical model of BG function. However, this explanation has been challenged by the observation that pallidotomy, and GPi DBS, reduce dystonia while abolishing pallidal outflow (for more detail see DBS effect section). Accordingly, recent attention has focused on whether it could be the patterning of pallidal activity, rather than the mean level of tonic activity, that underlies dystonia. Abnormal patterning could involve disturbed somatosensory relationships within the pallidum, altered patterning of pallidal activity over time, or combination of the two.

1.4.4.1 Disorganisation of sensory representation in pallidum

The pallidum is partly somatotopically organized so that abnormal spatial patterning may lead to abnormal representation of the body. Several observations suggest sensory inputs play an important role in dystonia (Byl et al., 1997; Byl et al., 1996b; Hallett, 1995; Tinazzi et al., 2003). Enlargement of receptive fields of neurons in the BG-cortical loop may be a key pathophysiological feature in this disorder. For example, reorganization occurs in the somato-sensory thalamus, a pallidal-receiving structure, in patients with dystonia (Lenz and Byl, 1999; Lenz et al., 1999). In particular, the number of cells with receptive fields in the thalamus is significantly higher in dystonia than in other movement disorders (Lenz et al., 1998). Furthermore, cells with sensory inputs in patients with dystonia have receptive fields that include the dystonic limb, in line with an enlarged sensory representation of the affected limb.

However, the exact relationship between changes in receptive fields and neuronal activity in the pallidum and the development of dystonia remains unclear. Vitek has proposed that focal changes in the receptive region of one pallidal area representing the arm or hand would lead to focal dystonia involving the arm or hand, and changes throughout the pallidum bilaterally may be expected to result in general dystonia (Vitek, 2002b).

1.4.4.2 Disorganization of temporal patterning of pallidal activity

Microelectrode recordings from the GPi in dystonic patients reveal marked abnormalities in the temporal patterning of neuronal discharge; neurons fire irregularly grouped discharges with intermittent pauses (Suarez et al., 1997; Vitek, 2002a; Vitek et al., 1999). In line with this, analysis of interspike intervals in the endopeduncular nucleus (homologue of GPi) in the dystonic *dr^{sz}* (mutant dystonic) hamster shows an increased proportion of neurons with burst-like firing pattern compared to normal animals (Gernert et al., 2002). Evidence also exists from animal models of dystonia of burst discharge in other nodes of the cortico-basal ganglia loop involved in motor control. Increased bursting has been noted in monkey motor thalamus after induction of dystonia by intrathalamic injection of the GABA antagonist bicuculline (Macia et al., 2002) and dystonic movements corresponding to putaminal bursting discharge have been seen after intraputaminal injection of bicuculline in the cat (Yamada et al., 1995).

1.4.4.3 Spatio-temporal disorganization of pallidal neuronal activity

Of course spatial and temporal disorganization of pallidal activity may not be mutually exclusive aspects of dystonia. One way that the two may be combined that has received considerable interest in PD (Brown and Williams, 2005) is through abnormal synchronization across neurons displaying burst-like firing patterns. Neurons might then lose some of their spatial and temporal independence in information encoding, and, in so far as the pallidum is topographically organized, this would lead to loss of the type of specificity

stressed by Lenz (Lenz et al., 1998). No microrecording has so far attempt to explore the degree of synchronization between pairs of neurons in dystonia. However, an alternative means of studying changes in the pattern of local neuronal synchrony is through a frequency-based analysis of LFPs.

The first report of activity in the pallidal LFP was in a patient with myoclonic dystonia, and involved the 4-8 Hz frequency band (Liu et al., 2002). Soon after this, prominent activity was reported over an overlapping frequency band of 4-10 Hz in a large series of patients with primary dysotnia (Silberstein et al., 2003). The level of this activity was shown to exceed that in PD patients. Silberstein and colleagues proposed that pallidal LFP in the 4-10 Hz band might relate to the synchronized, relatively non-oscillatory bursting across neurons. Such bursting may be particularly predominant during dyskinesia in primates and PD patients (Leone et al., 2001; Levy et al., 2001; Yoshida, 1991) and during hemiballismus (Suarez et al., 1997), which bear some phenomenological resemblance to dystonia. Nevertheless, in order to support the relevance of pallidal LFP activity in this frequency band and this disabling condition, the correlation between LFPs in GPi and the involuntary muscle spasm in dystonia needs to be established. Accordingly, in Chapter 3, we test the hypothesis that the pattern of synchronized neuronal activity in the pallidum correlates with the intensity of involuntary EMG activity in dystonia.

However, not all patients with primary dystonia have prominent LFP power over 4-10 Hz band. One important consideration when dealing with the LFP is can it be merely due to movement related artifact or volume conduction. There

is, to date, no evidence that directly links pallidal LFP activity at frequencies under 12 Hz with neuronal activity.

Another feature that might increase the patho-physiological significance of LFP <10 Hz would be a possible concentration of this activity in GPi as this represents the most effective therapeutic target for lesioning of DBS implantation in dystonia. However, the relative topography of this activity within the pallidum remains unclear. Indeed, Silberstein and colleagues reported that the prominent LFP power over the 4-10 Hz band was located in GPe (Silberstein et al., 2003). It is worthy of note that these LFP recordings were through DBS electrodes with relatively poor spatial resolution.

In Chapter 4, we simultaneously record LFPs and neuronal activity from microelectrodes inserted into the pallidum in awake patients with primary dystonia during functional neurosurgery to determine the extent to which 3-12 Hz LFP activity is concentrated in GPi and is synchronized with local neuronal discharge.

1.4.5 Treatment for dystonia

1.4.5.1 Medical treatment for dystonia

For young-onset primary dystonia, a trial of levodopa is appropriate in all patients to exclude the possibility of dopa-responsive dystonia. If the levodopa is ineffective, other medications like trihexyphenidyl, clonazepam,

tetrabenazine and baclofen can be considered. These medications only offer limited benefit to adult-onset primary limb dystonia patients. In severe dystonia, combinations of these drugs can be used.

1.4.5.2 Botulinum toxin treatment for dystonia

Botulinum toxin treatment is the first line therapy for blepharospasm, adductor spasmodic dysphonia, jaw-closing oromandibular dystonia and cervical dystonia, as recommended by National Institutes of Health consensus statement. Botulinum toxin is produced by the anaerobic organism *Clostridium botulinum*. It mostly works by blocking neuromuscular transmission. It weakens the muscle, thereby reducing the muscle spasm. Several randomized placebo-controlled studies have evaluated the short-term effect of Botulinum toxin A (BoNT-A) on cervical dystonia. All reported a benefit of a single injection cycle of BoNT –A and further injections maintained efficacy in most patients.

A small percentage of patients chronically treated with botulinum will develop circulating antibodies to the toxin, rendering it ineffective. In this condition, BoNT-B is an alternative. However, evidence is currently lacking with respect to the direct comparison of the clinical efficacy and safety of BoNT-A versus BoNT-B.

1.4.5.3 Stereotactic functional neurosurgery for dystonia

Two means of surgery are available for the treatment of dystonia, lesioning and GPi stimulation. Two targets are considered, thalamus and GPi. Pallidotomy and more rarely thalamotomy have been used as a treatment for dystonia. The first bilateral pallidotomy for treatment of primary dystonia was reported by Lozano on a DYT1 patient (Lozano et al., 1997). This procedure can be beneficial in treatment of severe generalised dystonia, but risks from the operation and long term ineffectiveness are notable. Thus lesion operations have largely been replaced by deep brain stimulation.

The most dramatic improvements with bilateral GPi stimulation are seen in patients with genetically proven DYT1 dystonia, although improvement can be achieved in idiopathic segmental axial dystonia (Muta et al., 2001), dystonia-plus syndrome (myoclonus-dystonia)(Trottenberg et al., 2001a), secondary dystonia (tardive dystonia)(Trottenberg et al., 2001b) and PKAN (Castelnau et al., 2005). Bilateral GPi stimulation has shown, in both controlled (Kupsch et al., 2006; Vidailhet et al., 2005) and open-label (Cif et al., 2003; Coubes et al., 2004; Coubes et al., 2000; Coubes et al., 2002; Krauss, 2003) studies, improvement in motor symptoms, motor disability, and quality of life. A sustained benefit of pallidal stimulation has been reported in patients with primary general dystonia (Bittar et al., 2005; Krauss et al., 2004), or cervical dystonia (Bittar et al., 2005; Eltahawy et al., 2004; Krauss et al., 2002), and also in a large open-label study (Cif et al., 2003; Coubes et al., 2004).

A recent prospective multicenter study reports the long-term efficacy and safety of bilateral GPi stimulation for primary generalized dystonia (Vidailhet et al.,

2007). The therapeutic effect was sustained at 3 years after surgery, and in some cases, a further mild improvement in limb disability and quality of life, was noted after 1 year. Still there is a need for careful studies on larger series that compare outcomes of surgery or neurostimulation in primary dystonia, dystonia-plus syndromes, secondary dystonia, in distinct genetic primary dystonia. Finally, the mechanism that underlies the improvement of dystonia through GPi stimulation should be further assessed.

1. 5 Deep brain stimulation

1.5.1 Concept and history of DBS

The idea that the electrostimulation of deep brain structures may constitute an effective therapy for certain chronic diseases is not a recent one. It was first applied in the hypothalamus for the treatment of chronic pain (Pool et al., 1956). Since then there have been two milestones in the introduction of DBS for movement disorders. First is the introduction of Vim stimulation for tremor. This procedure was based on clinical research and empirical surgery without a reliable animal model. In the sixties, surgeons noted that stimulation used to localize thalamic targets prior to lesioning improved the symptoms of movement disorders (Hassler et al., 1960; Narabayashi, 1982; Narabayashi, 1989). It was noted that the suppression of tremor was frequency-dependent,

and Benabid (Benabid et al., 1987) found the tremor was only suppressed when stimulation frequency was above 100 Hz and immediately reversible when stimulation was discontinued. This led to the concept of using chronic stimulation as an alternative therapy to thalamotomy for PD patients with tremor.

The second milestone was the extension of DBS to the STN (Limousin et al., 1995), mainly driven by models of basal ganglia pathophysiology (DeLong, 1990). The model proposed by DeLong proposed that overactivity of STN was central to the pathophysiology of Parkinsonism. Lesioning (Aziz et al., 1991; Bergman et al., 1990) and chronic stimulation (Benazzouz et al., 1993) of STN in animal models of parkinsonism alleviated parkinsonism. The spectacular reversal of rigidity and bradykinesia observed in these animal studies led to the development of STN stimulation for the treatment of PD.

An empiric application of DBS therapy for movement disorders not predicted by the current model of the BG, is the success of GPi stimulation for levodopa induced dyskinesia and dystonia (Siegfried and Lippitz, 1994).

1.5.2 Current indications for DBS

1.5.2.1 DBS for Parkinson's disease

The efficacy of stimulation at GPi or STN has been demonstrated in several reports. Krack et al reported a 5-year following up of the effectiveness of bilateral STN stimulation for PD. Motor scores and activities of daily living scores (UPDRS and ADL) were improved during the off-medication state. On the other hand, “on” medication akinesia, speech, postural stability and freezing of gait worsened between years 1 and 5 of following up (Krack et al., 2003). Several groups have noted substantial reductions in anti-parkinsonism medications.

Since the GPi, the main output structure of the BG network, is also hyperactive in PD, it was proposed then that the activity of this structure could be inhibited by stimulation of its posteroventral zone, the target which had been proved most effective in pallidotomy (Laitinen et al., 1992; Siegfried and Lippitz, 1994; Siegfried and Wellis, 1997). The initial reports of this therapy for PD gave conflicting results. Certain groups have found a significant reduction of levodopa induced dyskinesia, a moderate improvement in rigidity but not akinesia (Siegfried and Wellis, 1997). Others have reported a dramatic attenuation of all the main symptoms (Davis et al., 1997; Gross et al., 1997; Pahwa et al., 1997). The disparities could be due to the selection of slightly different target locations (Bejjani et al., 1997). Two distinct effects were observed from stimulating differing areas of GP. Stimulation of the posteroventral part of GP aggravated akinesia, but alleviated dyskinesia and rigidity. On the other hand, stimulation of a more dorsal and more medial target has a “prokinetic” effect which alleviates parkinsonian symptoms (akinesia, rigidity and gait) but can induce abnormal involuntary movement.

However, hitherto, no large randomized studies have aimed to compare the effects of stimulation at the STN and GPi. A small randomized study compared 1-year follow up data from equal numbers of PD patients who were given GPi-DBS or STN DBS. This showed significant reduction in the UPDRS motor scale at 12 months for both GPi and STN stimulation. There was a trend for more improvement with STN stimulation in terms of medication dose reduction, as well as the bradykinesia score of UPDRS, although this did not reach statistical significance (Anderson et al., 2005).

Another target currently being explored for future stimulation in the context of PD is the pedunculopontine nucleus (PPN) (Mazzone et al., 2005; Plaha and Gill, 2005; Stefani et al., 2007). The PPN is believed to be involved in the initiation and modulation of gait, given electrical stimulation and the application of neuroactive substances in the PPN can elicit locomotor activity in experimental animals. Furthermore patients with PD have significant loss of PPN neurons, and experimental lesions within the PPN of normal monkeys result in akinesia. Degeneration of PPN neurons or their dysfunction may be important in the pathophysiology of locomotor and postural disturbances of parkinsonism (Pahapill and Lozano, 2000). The effectiveness PPN stimulation on patients with PD reveals conflicting results, with one group reporting significant improvement in all cardinal parkinsonism symptoms, including gait and speech, and another group demonstrating limited relatively modest efficacy of this surgery (Mazzone et al., 2005; Plaha and Gill, 2005).

The fact that stimulation at different BG ganglia targets has rather distinct effects on the treatment of PD has led to the hypothesis that each symptom is related to specific pathophysiological mechanisms involving specific brain structures. Our current knowledge is insufficient to predict or explain which structure and mechanism is responsible to which symptoms.

Despite the success in the treatment of PD by using STN DBS, therapeutic efficacy is limited by difficulties in consistently and correctly targeting the STN, particularly the 'motor' domain of this nucleus, while side effects may, in part, relate to poor positioning of electrodes. Single cell microelectrode recordings of the activity of local neurons were introduced to facilitate targeting and generally remain an important element of the surgical procedure (Hutchison et al., 1998). However, their use may considerably prolong surgery, does not always lead to satisfactory targeting and has been associated with an increased risk of intra-operative hemorrhage deep-brain stimulation for Parkinson's disease study group for PPN (Alkhani and Lozano, 2001; Binder et al., 2003; Binder et al., 2005; Hariz and Fodstad, 1999; The deep-brain stimulation for PD study group, 2001). In addition, microelectrodes must be withdrawn prior to introduction of the DBS electrode, which may introduce targeting errors, especially in the vertical plane. Thus, an electrophysiological signature of STN activity that could be directly and intra-operatively recorded from the DBS electrode would be of considerable potential value.

Although DBS electrodes cannot be used to record single neurons, they are suitable for recording aggregate activity of neuronal populations in the form of

the local field potential (Brown et al., 2001). The LFPs recorded from the STN in patients with PD are increasingly recognized as being characterized by prevalent activity in the so-called beta frequency (around 20 Hz) band (Brown and Williams, 2005). The focal nature of this beta activity has been demonstrated in patients through microelectrode recordings (Brown et al., 2001; Levy et al., 2000), polarity reversal in bipolar macroelectrode recordings (Brown et al., 2001; Doyle et al., 2005; Kuhn et al., 2004). Moreover, the recording of this activity from electrodes in STN has been confirmed histologically in rats with 6-OHDA lesions of midbrain dopamine neurons, an established rodent model of parkinsonism (Sharott et al., 2005). Thus, increased beta LFP activity may be a marker of the parkinsonian STN, particularly the dorsolateral (sensorimotor) portion of the nucleus (Kuhn et al., 2005), which, based on inactivation studies in MPTP treated primates is considered the optimal target (Wichmann et al., 1994a; Wichmann et al., 1994b).

In Chapter 7 we test the hypothesis that spontaneous beta LFP activity can be recorded intra-operatively from DBS electrode contacts in the STN of PD patients and that the contacts exhibiting the spontaneous beta activity of the highest amplitude would lie in dorsal 'sensorimotor' STN. This LFP 'signature' of STN activity could prove useful in the intra-operative confirmation of electrode placement in STN.

1.5.2.2 DBS for Tremor

Ventral intermedius nucleus (Vim)-the cerebellar relay of the thalamus, is the usual target for DBS therapy in essential tremor. In Parkinsonism tremor, it was widely been replaced by STN stimulation, given the latter is effective for all cardinal parkinsonism symptoms. Vim stimulation has demonstrated a long-lasting effectiveness for essential tremor (Koller et al., 2001; Sydow et al., 2003).

The successful treatment of STN stimulation in PD has led to the trial of this therapy for the treatment of essential tremor and non-primary dystonia. Significant reduction of tremor and dystonia have been reported (Chou et al., 2005; Krack et al., 1999; Murata et al., 2003; Stover et al., 2005).

The effect of DBS for treatment of severe kinetic tremor is usually limited and variable (Benabid et al., 1996; Geny et al., 1995). Tremor related to the cerebellar outflow pathway, mainly as a result of midbrain lesion and usually due to MS is particularly resistant to single target stimulation. Vim stimulation can be effective only if the rhythmic component prevails in cerebellar ataxia (Liu et al., 2000). Therefore, other targets have been proposed, such as zona incerta (ZI) and the prelemniscal radiation (PRL) (Nandi et al., 2002).

Stimulation at a variety of targets, such as Vim, Voa, zona incerta (ZI) and GPi has been recommended for tremor accompany with other neurological symptoms, like multiple sclerosis tremor, Holmes tremor or primary writing tremor (Goldman and Kelly, 1992; Krauss et al., 1992; Krauss et al., 1997;

Speelman et al., 1998; van Manen, 1974). However, no long-termed following up results have been reported.

1.5.2.3 DBS for Dystonia

Severe, medically refractory forms of primary dystonia seem to respond to GPi stimulation, consistent with the involvement of this structure in the pathophysiology of dystonia (Hallett, 1995; Lenz and Byl, 1999). This has been verified by a recent blinded controlled clinical trial in primary dystonia patients. The improvement is significant with an average reduction of the Burke-Fahn-Marsden Dystonia score of 51% at 12 months follow up. The effect is persistent and even improves over time. However, the effects of GPi stimulation for dystonia of other etiologies are limited.

1.5.2.4 DBS for other disorders

The application to DBS in these movement disorders has opened the way for this technique to be used in other neurological and psychiatric diseases, such as epilepsy, Tourette's syndrome, cluster headache, obsessive-compulsive disorder, depression, and obesity. (Benabid et al., 2002; Leone et al., 2001; Nuttin et al., 1999; Vandewalle et al., 1999). These therapies are still experimental and long-termed effect need to be determined.

1. 5.3 Mechanisms of action of DBS for movement disorders

Despite the fact that DBS has been effective in the treatment of movement disorders and is being explored for the treatment of other neurological disorders, the scientific understanding of its mechanism of actions has lagged. Albe-Fessard, who introduced microrecording and first described a tremorogenic rhythm in the thalamus (Albe-Fessard, 1962) (Albe-Fessard D, Arfel G, Guiot G, et al. *Derivaitons d'activites spontanees et evoquees dans les structures cerebrales profondes de l'homme Rev Neurol* 1962; 106:89-105) first raised the question about the mechanism underlying tremor suppression using stimulation: "The fact that the stimulation of this rhythmogenic zone inhibits the tremor may seem a paradox. Whether we are dealing with a true inhibition or a desynchronization of the rhythmic centers by a stimulation at high frequency, we are today unable to decide".

Recently, some possible mechanisms have been proposed:

1. Depolarization block: stimulation-induced alterations in the activation of voltage-gated currents that block neural output near the stimulating electrode (Beurrier et al., 2001);
2. Synaptic inhibition: indirect inhibition of neuronal output by means of activation of axon terminals that make synaptic connection with neurons near the stimulating electrode (Dostrovsky et al., 2000);
3. Synaptic depression: synaptic transmission failure of the efferent output of stimulated neurons as a result of transmitter depletion (Urbano et al., 2002);
4. Stimulation-induced disruption of pathologic network activity (Montgomery and Baker, 2000).

1.5.3.1 Suppression by DBS

The depolarization blockade and synaptic inhibition hypotheses explain the similar effect achieved by lesioning and DBS for the treatment of movement disorders. Several lines of evidence from single unit recording in vivo and in vitro have supported this notion. In vitro studies of the effect of HFS show a frequency-dependent suppression of activity that coincides with the frequency-dependent therapeutic response of DBS (Beurrier et al., 2001; Garcia et al., 2003; Kiss et al., 2002). In high frequency stimulation, stimulation has a dual effect: it completely suppresses spontaneous STN activity and generates a robust pattern of recurrent burst of spikes, with each spike being time-locked to a stimulus pulse (Garcia et al., 2003). This pattern may replace the pathological activity of the BG network in the parkinsonism state with a less intrusive high-frequency activity.

In vivo studies of neuronal activity made in the stimulated nucleus show decreased activity during and after high frequency stimulation trains (Benazzouz and Hallett, 2000; Benazzouz et al., 1995; Boraud et al., 1996; Dostrovsky et al., 2000; Tai et al., 2003). In rats, Benazzouz and colleagues (Benazzouz and Hallett, 2000; Benazzouz et al., 1995) found that HFS stimulation trains in the STN caused a depression of firing for 30-90 s. Boraud (Boraud et al., 1996) reported that HFS in GPi at therapeutic intensities in the MPTP-treated monkey results in a decreased firing rate through suppression of spontaneous activity. Similarly, long-duration high-frequency stimulation of either the GPi or STN of PD patients results in long-lasting periods of neuronal

silence (Dostrovsky et al., 2000). Most importantly, stimulation also reduces abnormal oscillatory activity at an individual STN neuron level as well as correlated and abnormal oscillatory activity between pairs of STN neurons (Meissner et al., 2005). Hence, it reduces the abnormal oscillatory activity in the cortex-basal ganglia-cortex network. A mounting of evidence suggests that the excessive synchronization of neuronal activity in BG may contribute to the symptoms of parkinsonism in non-human primates and PD patients (Bergman et al., 1994; Brown, 2003; Brown et al., 2001; Kuhn et al., 2004; Levy et al., 2000; Nini et al., 1995; Raz et al., 2000; Silberstein et al., 2003; Williams et al., 2002), the suppression of this abnormal synchronization may underlie the mechanism of action of STN HFS in PD.

1.5.3.2 Activation by DBS

The ‘silencing’ effect of DBS on neurons may also be accompanied by the activation of efferent axons of local cells or axons of passage. Evidence from theoretical and experimental studies suggests that the activation of myelinated axons is likely (McIntyre and Grill, 1999; McIntyre et al., 2004a; McIntyre et al., 2004b; Nowak and Bullier, 1998; Rattay, 1999). However, if DBS does excite the axon in the vicinity of the stimulation electrode, it seems difficult to explain the similar therapeutic effects of lesioning and DBS. One explanation is that neurons activated by the stimulus train are unable to sustain high frequency synaptic action on efferent targets due to depletion of neurotransmitter (Urbano et al., 2002; Wang and Kaczmarek, 1998; Zucker and Regehr, 2002). However,

this is at odds with several in vivo experiments, which have revealed increases in transmitter release and changes in firing pattern at efferent nuclei consistent with activation of neurons around the electrode and subsequent synaptic action on targets during HFS (Anderson and Mullins, 2003; Hashimoto et al., 2003; Windels et al., 2003).

In rats, STN HFS on downstream neurons has conflicting results. Benazzouz and colleagues reported that stimulation of the STN led to long-duration excitation of neurons in the GPe (Benazzouz et al., 2000; Benazzouz et al., 1995). In contrast, other groups report that stimulation does not excite GPe (Boraud et al., 1996). Windles's (Windels et al., 2003) group have shown that high-frequency stimulation in the STN leads to increased glutamate concentrations in the SNr and GPe, which suggests that the HFS is driving STN neurons or exciting glutamatergic efferent axons in the STN.

The work of Hashimoto (Hashimoto et al., 2003) addressed the effects of STN HFS on neuronal activity in the GPi and GPe of MPTP-treated primates. The results revealed that stimulation of STN increases the firing rate and alters the pattern of neuronal activity in both GPi and GPe. The excitation is likely to arise through the glutamatergic STN output that produces short-latency excitatory responses at downstream targets. In line with this, stimulation in the GPi and recordings in the thalamus of monkeys, also suggests activation of the GABA GPi output (Anderson and Mullins, 2003). The thalamic discharge frequency during GPi HFS was reduced by 77%. In addition, single stimuli

delivered to the STN of PD patients evoke potentials which can be recorded at the scalp (Ashby et al., 2001).

Human data are consistent with the above. Brown (Brown et al., 2004) stimulated STN and recorded from GPi in two PD patients. Stimulation at around 20 Hz exacerbated synchronization at similar frequencies in the GPi. In contrast, stimulating the STN at >70 Hz suppressed pallidal activity at about 20 Hz. Clinically, stimulation of STN at similar high frequencies reverses parkinsonism and forms the basis of therapeutic DBS in PD. The authors argued that the synchronization imposed by therapeutic stimulation of the STN replaces an abnormal and potentially deleterious synchronization of BG output at around 20 Hz.

Recently, there has been a model-based analysis aimed to assess whether the combination of distinct effects on neuron and axon could explain the paradoxical results of experiments (McIntyre et al., 2004c). The authors observed that subthreshold stimulation for direct activation of thalamocortical relay neurons suppressed intrinsic firing activity through activation of pre-synaptic terminals. In contrast, suprathreshold stimulation suppressed the intrinsic firing in the neuron, but generated efferent axonal output faithfully locked to the stimulus frequency (McIntyre et al., 2004c).

Considered together, the action of STN DBS may be to disrupt the pathological activity of the neuronal soma and replace it with tonic high-frequency axonal output.

1.5.3.3 Functional imaging studies

PET and fMRI can be used to assess the impact of functional neurosurgery in movement disorders by measuring regional cerebral flow and glucose and oxygen consumption as indicators of metabolic activity of specific brain regions. These studies, therefore, provide a system-level insight into the effects of stimulation.

Parkinson's disease

Stimulation of the GPi significantly increases regional glucose metabolism and cerebral flow in the areas that are underactive in PD, including premotor cortex ipsilateral to stimulation, and bilateral SMA (Fukuda et al., 2001a; Fukuda et al., 2001b). Interestingly, there is a significant correlation between the improvement in motor performance and the regional cerebral blood-flow changes mediated by stimulation. Clinically effective stimulation of the GPi also reduces the expression of an abnormal PD-related metabolic network involving elements of the cortico-striato-pallido-thalamocortical and the cerebello-cortical motor loops (Fukuda et al., 2001a; Fukuda et al., 2001b). These findings suggest suppression of the pathological output of the BG nuclei reverses parkinsonism by activation of brain areas involved in the initiation of movement.

Stimulation of the STN similarly increases activation of the rostral SMA and premotor cortex ipsilateral to stimulation during contralateral movement.

Furthermore, a H_2^{15}O PET study examining the regional Cerebral Blood Flow (rCBF) changes induced by GPi or STN stimulation in PD patients revealed that the difference between the effect of the two on movement-related activity was mainly localized to dorsolateral prefrontal cortex (DLPFC). The rCBF was significantly higher during STN stimulation. These results have suggested the dominant role of non-primary motor areas in the control of movement in parkinsonism patients and demonstrate the importance of STN input in the control of this area (Limousin et al., 1997).

Overall, chronic high frequency electrical stimulation of the GPi and STN through implanted electrodes has been shown to be clinically effective in improving variety of symptoms in movement disorders. Little deficit other than cognition functions involving executive processes is noted. This has led to the influential concept that the BG are not necessary for simple movement. This notion has been promoted by Mardsen and Obeso “the overall distributed system could continue to function without its basal ganglia component, except in those special contexts. Thus routine predictable and automatic movement might continue without BG support.” However, if deep brain stimulation suppresses spontaneous, including pathological, activity in the basal ganglia it must also remove any residual physiological functioning in these key motor structures. In Chapter 5, we test a simple movement when activity in a structure in the BG is suppressed through DBS or not. Our hypothesis was straightforward. Patients that, at the time of study, have performance in a simple motor task that is compromised by PD will improve with DBS, in tandem with the suppression of pathological activity by stimulation. In contrast, in those

patients with relatively intact task-related processing, DBS would be expected to suppress physiological processing and thereby impair performance.

CHAPTER 2: Methods

This chapter contains a description of the patients' characters and surgical procedures, experimental and analytical methods that are common to the investigations described in chapter 3-7. There are some distinct methods used in different centers where patients are operated and tested. The details of the different techniques will be discussed in these individual chapters. This chapter, therefore, exclusively concentrates on clinical evaluations and recordings in patients, concepts of signal processing and statistic analysis common to the following chapters.

2.1 Patients and operative procedure

All patients participated with informed consent and with the agreement of the local ethics committees in studies outlined in this thesis. All patients underwent DBS implantation for the treatment of their movement disorders. Patients with PD (Chapter 5, 6 and 7) all suffered from severe off periods and motor fluctuation with or without dyskinesia. Patients with dystonia (Chapter 3 and 4) were resistant to medical treatment.

Depth recordings (Chapter 3, 4 and 7), surface EMG (Chapter 3) and results of behavioral tests (Chapter 5 and 6) were obtained from patients in the following centers:

1. The National Hospital for Neurology and Neurosurgery, London, United

Kingdom (Chapter 5,6 and 7)

2. Department of Neurology, Chang Gung Memorial Hospital, Taipei, Taiwan
(Chapter 5 and 6)
3. Department of Neurosurgery, Charite Campus Virchow, Humboldt
University Berlin, Germany (Chapter 3 and 4).
4. University Hospital, Klinikum Mannheim, Germany (Chapter 3).

Implantation of DBS electrodes was performed in all subjects using stereotactic methods for the treatment of PD or dystonia. In patients with PD, the implanted target is STN and electrode used is model 3389 (Medtronic Neurological Division, Minneapolis, USA) with four platinum-iridium cylindrical surfaces (1.27-mm diameter and 1.5-mm length) and a centre-to-centre separation of 2mm. Contact 0 is the most caudal and contact 3 the most rostral. The intended coordinates at the tip of contact 0 are 10-12 mm from the midline, 0-2 mm behind the midcommissural point and 3-5mm below the anterior commissural-posterior commissural line. Adjustments to the intended coordinates are made in accordance with the direct visualization of STN in the individual stereotactic MRI (Hariz et al.2003) and, in the patients operated in Taiwan, the results of microrecordings. (Axon Guideline 3000 System, FHC, USA, or Leadpoint system, Medtronic Neurological Division, Minneapolis, USA).

All patients with dystonia were operated in Germany. The implanted target is the posteriolateral part of GPi determined by MRI or ventriculography. The intended coordinates for the target point are 2-3 mm in front of the

mid-commissural point, 20-22 mm lateral to the midline of the third ventricle, and 4-6 mm below the AC-PC line. Intraoperative recordings in Berlin are made with the TREC scanner electrophysiological neuronavigation system using a tetrode (Thomas RECORDING, Gissen, Germany). The macroelectrode implanted is model 3387 (Medtronic Neurological Division, Minneapolis, USA) with four platinum-iridium cylindrical surfaces (1.27mm diameter and 1.5mm length) and a centre-to-centre separation of 3mm.

All patients underwent post-operative imaging (MRI or CT) to confirm electrode placement prior to connection of the deep brain electrodes to a subcutaneous stimulator (Itrel II or Kinetra Medtronic Neurological Division Minneapolis, USA). Correct placement of the DBS electrodes in the region of the STN or GPi was further supported by 1. Effective intra-operative macrostimulation (for STN only) and 2. Significant improvement in validated clinical rating scales (see section 2.2.1, 2.2.2, 2.2.3) during chronic DBS off medication compared to off medication pre operation, or with stimulator switched off post-operation.

2.2 Clinical rating scales

2.2.1 The Unified Parkinson's Disease Rating Scale (UPDRS)

The UPDRS is a scale that was developed as an effort to incorporate elements from existing scales to provide a comprehensive but efficient and flexible means to monitor PD-related disability and impairment. The scale has a

multidimensional approach with 4 different sections, including Part I ,
Mentation, Behavior and Mood; Part II, Activities of Daily Living; Part III,
Motor; Part IV, Complications. The UPDRS is increasingly used as a gold
standard reference scale. The motor section (UPDRS III) has repeatedly been
employed in attempts to develop surrogate markers for disease severity and
progression. It's also used as an assessment for trials of surgical interventions
for PD. All subjects with PD in this thesis were rated using UPDRS III based on
clinical examination. There are 14 items, each item is constructed with 5-point
options, ranging from 0-without abnormality to 4-severe abnormality. Some of
the items are rated for different parts of body-such as tremor at rest (item 20)
rigidity(item 22) for the head and neck, right and left, upper and lower limbs.
Taken together, the maximum score is 108. Maximal points for the different
parkinsonism signs are: Speech (4), facial expression (4), tremor (28), rigidity
(20), akinesia (32), axial symptoms and gait (20). Details of the score for each
item are described in Appendix (UPDRS).

2.2.2 The Toronto Western Spasmodic Torticollis scale (TWSTR).

TWSTR is used to assess the severity and character of cervical dystonia in
Chapter 3 and Chapter 4. It contains 6 sections of assessment: (A) Maximal
excursion (B) Duration factor (C) Effect of sensory tricks (D) Shoulder
elevation and displacement (E) Range of motion and (F) Time that the patient is
able to maintain the neutral position. Section A consist 3 scores with respect to
the neck rotation, say laterocollis, anterocollis or retrocollis. The part B score
is doubled prior to calculating the final score. (See Appendix TWSTR)

2.2.3.BFMDRS (Burke-Fahn-Marsden Dystonia Rating Scale)

BFMDRS is utilized for the assessment of severity of general dystonia. This score is used in Chapter 3 and 4. The examination of dystonia at distinct body parts is scored according to the severity and provoking factor. The maximal score for BFMDRS is 120 (see Appendix BFMDRS)

2.3 Data collection

In Chapter 3, simultaneous recording of LFP and EMG were made during the post-operative period prior to implantation of the stimulator while leads from the DBS electrode (DBE) were still external. In Chapter 7 and chapter 4, recording were made by using a TETRODE and DBE, respectively. In chapter 5 and 6, the behaviour tests were evaluated under various stimulation parameters a minimum of 6 months post stimulator implantation.

2.3.1 LFP recording

In Chapters 3 and 7, STN and GPi LFP were recorded from the adjacent 4 contacts of each macroelectrode. LFPs were recorded bipolarly from contacts 01, 12 and 23. In Chapter 3, the LFPs were filtered at 0.5 to 300 Hz, and 1 to 80 Hz in Chapter 7. Amplification, filtering and recording were performed using a custom made 9V battery operated portable amplifier and recorded through an A-D card (PCN-DAS16S, ComputerBoards, Middleboro, MA 02346, U.S.A.)

using Spike 2 version 4.0 software (Cambridge Electronic Design, Cambridge, UK) on a portable computer using a custom written program in the study of Chapter 3.

In the study of Chapter 7, signals were amplified, filtered and recorded by a portable amplifier (Biopotential Analyzer Diana, St Petersburg, Russia), using a purpose written software.

In chapter 4, LFPs were recorded simultaneously with neuronal spikes by using a tetrode. The tetrode combined four platinum-tungsten fibers in a glass insulation electrode of outer diameter 100 μm with four circular contacts. The outer three contacts were 14 μm in diameter and the central contact, positioned at the tip of the electrode, 26 μm in diameter. The outer contacts were separated by a distance of 29 μm , and the central and outer contacts separated by 5 μm . Contacts were referenced to the uninsulated stainless steel guide tube of the tetrode using a single ended input configuration in the pre-amplifier system. The tip of the guide tube was usually $\leq 15,000$ μm dorsal to the tetrode tip. LFPs recording were derived from one of the four contacts of tetrode. Neuronal spike and LFPs were amplified 4000-20,000 times, band pass filtered at 0.5-10 kHz and 1-141Hz, respectively, and sampled at 25 kHz.

2.3.2 Surface EMG recordings

Surface EMG (sEMG) was performed simultaneously with pallidal LFP recording in Chapter 3. Here, sEMG recordings were made over the

sternocleidomastoid (SCM), using pairs of Ag/AgCl electrodes and high pass filtered at >10Hz.

2.3.3 Technical Basis of biological signal recording

This section explores the technical basis of LFPs and EMG recording used in this thesis. All recordings are in bipolar mode. The recorded signals are measured at electrode level as the potential difference between two contacts. Two potentials are then individually transmitted to the acquisition apparatus on separate but identical lines. The signals are then differentially amplified, filtered and analogue to digital converted to yield a time domain based signal that may be viewed on line or stored for off-line analysis. Figure 2.1 introduces the setup of a recording channel.

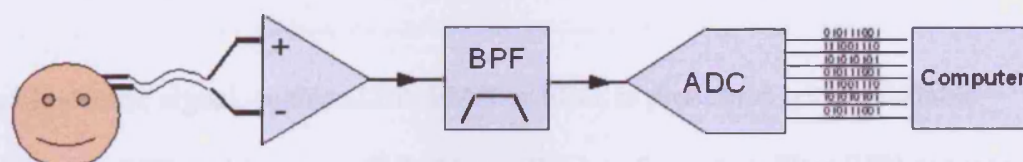


Figure 2.1 Schematic presentation of an EEG or LFP recording channel.

Abbreviations: BPF, Band pass filter; ADC, Analog-Digital Converter.

2.3.3.1 Amplifiers

The first operation in recording of bioelectric signal is the differential amplification. Differential refers to the ability of cancelling the interferences

which have been captured equally by both recording inputs (common mode rejection). The discriminative performance of the differential measurement is determined by the sensitivity of the input amplifier to common components in relation to the sensitivity to different components (discrimination factor) (Niedermeyer and Da Silva, 2000). Amplification increases the size of LFPs or EEG (usually in a range of microvolt) to a level (in the range of one volt) that can accurately drive analogue to digital conversion devices by reaching a sufficient level for best resolution.

Two types of EEG amplifiers exist nowadays. The first type of amplifier provides the analog amplified EEG signal at the output, and the second type of amplifier provides the amplified EEG signal already digitally converted at the output.

2.3.3.2. Filters of recorded bioelectric signals

A bioelectric signal, such as LFP, EMG or EEG, is processed with adjustable high-pass (HP) and low-pass (LP) filters. The low frequency filter (HP) reduces the amplitude of slow waves. The high frequency filter (LP) reduces the frequency of fast waves. The amplitude of electrical line interference (50Hz) can be alleviated by 'notch' filter.

A band-pass filter is a device that passes frequencies within a certain range and attenuates frequencies beyond this range. An ideal filter would have a completely flat *passband* (with no gain/attenuation throughout) and would

completely reject all frequencies outside the passband. In addition, the transition out of the passband would be instantaneous in frequency. However, no bandpass filter is ideal in practice. The filter does not attenuate all frequencies outside the desired frequency range completely; particularly, there is a region just outside the intended passband where frequencies are attenuated, but not rejected. This is known as the filter roll-off (filter steepness), and it is usually expressed in dB of attenuation per octave. In general, the ideal design would make the roll-off area as narrow as possible, thus allowing the filter to perform as close as possible to its intended design. Nevertheless, as the roll-off area is made narrower, the passband is no longer flat and begins to 'ripple'.

2.3.3.3 Analog-digital conversion (ADC)

The amplified filtered signals are digitized by means of the Analogue to Digital Converter (ADC), which converts the continuous electrical signal to a digitized waveform. The first operation performed by the ADC is the sampling, which consists in reading and storing the amplitude of the signal at regular intervals. The second operation is the digitizing of the amplitude. This operation compares the analogue amplitude with the input range of the converter and gives it an integer number. This comparison can only be expressed on a limited number of levels known as the resolution ADC. In the studies of this thesis, we use a 16 bits ADC, which means the number of digitizing levels is $2^{16} = 65536$ discrete levels.

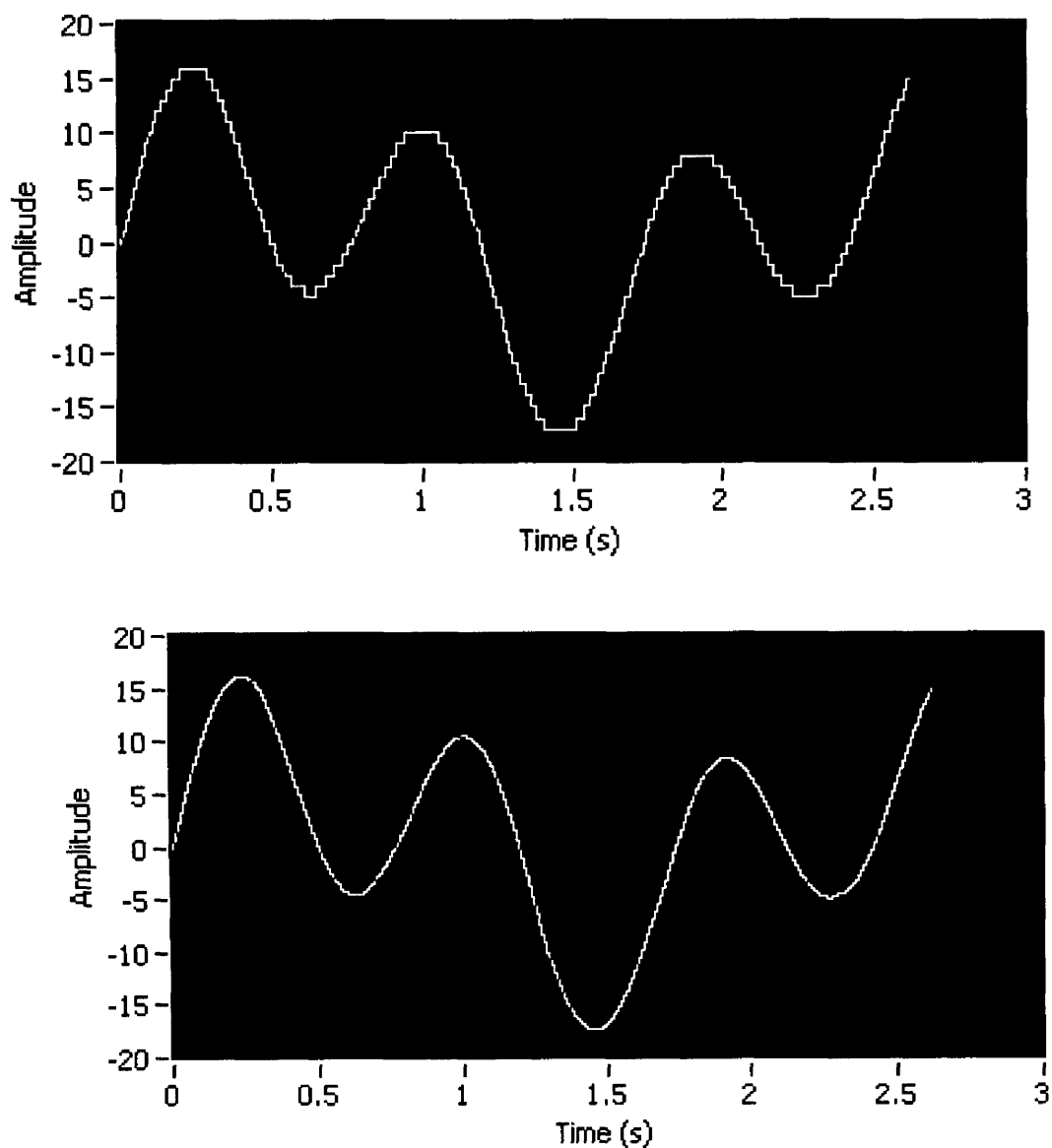


Figure 2.2 Signal obtained by using different numbers of digitizing levels. Upper panel represents signal recorded by using 5 bits ADC while lower panel represents 32 bits ADC recording.

2.3.4 Tapping task

In Chapter 5 and 6, patients were studied when the DBS stimulator was switched off, and during bilateral STN stimulation at different frequencies. The

task was a repetitive depression of a keyboard key as fast as possible by rapid alternating flexion and extension of the index finger at the level of the metacarpophalangeal joint. Tapping was performed in two runs of 30s, separated by ~30s rest and each hand tested separately (giving four runs per condition). The number of taps made with the index fingers in 30 s was recorded and two runs from each pair with the best performance selected for analysis, as this was less likely to be affected by fatigue, or the effects of impaired arousal/concentration.

2.4 Data analysis

The study of biological signals often results in simultaneous observations of several processes. They are divided into two categories of data series; one is a continuously varying waveform, so called time series; the other is the times of occurrence of discrete events, a stochastic point process. Examples of the former include recordings of LFP and EMG. An example of the later is the times of occurrence of extracellularly recorded action potentials, such as spike or single unit recordings (Halliday et al., 1995).

Most analyses carried out in this thesis involve the study of the dependence between two data series, such as the recordings of LFP and EMG, or spikes of neuron activities. These two data series may be two time series, two point processes, or one of each category. The parameters we have been using for characterizing the individual signal or interaction between signals are usually classified into two groups, that we are going to introduce in the next paragraphs:

the time domain parameters computed from the raw data and the frequency domain parameters computed from the Fourier transformed data.

2.4.1 Time domain analysis

A signal in the time domain is a function of the signal's amplitude versus time $x(t)$. Since the signals are accessed through a sampling and digitizing interface, they are practically described as the signal amplitude versus the sample index $x(n)$.

The parameters such as correlation can be defined on the continuous time signal $x(t)$. But they can only be calculated on the acquired signal $x(n)$, by means of estimates which have been optimised in order to minimise their bias and variance around the actual value of the parameter.

2.4.1.1 Correlation

The concept of correlation between two groups of data implies that they change with respect to each other in an organized way. If y always increases and decreases as x increases and decreases then x and y are positively correlated. If they always move in opposite directions then they are negatively correlated. The correlation coefficient, denoted as r is used to indicate the strength and sense of the correlation (Challis and Kitney, 1990).

Correlations between two signals activity $x(n)$ and $y(n)$ can be computed by the following estimate :

$$r_{xy} = \frac{\sum_{n=1}^N (x(n) - \bar{x})(y(n) - \bar{y})}{\sqrt{\sum_{n=1}^N (x(n) - \bar{x})^2 \sum_{n=1}^N (y(n) - \bar{y})^2}}$$

Where N denoted the numbers of pairs of data (x,y)

The denominator of the latter expression is a scaling factor, which thresholds the absolute value of r to 1. So, a coefficient r close to 1 or -1 indicates a maximum correlation of both signals, whereas a coefficient close to zero indicates a probable independence between them.

Note, the correlation coefficient is only useful while the relationship between the two variable x and y is linear or approximately linear. The correlation coefficient may be insensitive to the relationship between two variables that correlates in non-linear structure.

2.4.1.2. Cross-correlation function

Two signals may be obviously correlated but with a correlation coefficient close to zero, because of a phase shift between the two signals disrupts the synchronisation between the variations of the one with the variations of the other. Hence another parameter is used to refine the analysis, the cross-correlation, which is obtained by performing a correlation between the first signal and the second shifted by k samples. (Challis and Kitney, 1990).

The calculation of the discrete cross-correlation function between two sampled signals $x(n)$ and $y(n)$ is performed with the following estimate :

$$r_{xy(k)} = \frac{\frac{1}{N-1} \sum_{n=1}^N (x(n) - \bar{x})(y(n+k) - \bar{y})}{\sqrt{\frac{1}{N-1} \sum_{n=1}^N (x(n) - \bar{x})^2 \frac{1}{N-1} \sum_{n=1}^N (y(n) - \bar{y})^2}}$$

N denoted the numbers of samples of each signal.

\bar{x} and \bar{y} are the average values of x and y

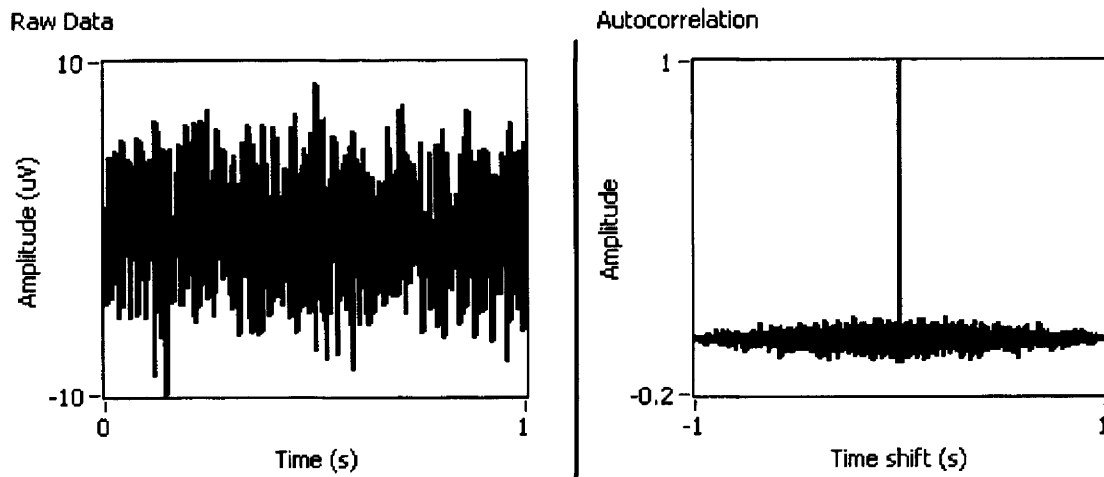
This cross-correlation is widely used to investigate the relationship between two single neurons, known as cross correlation histogram (CCH) (Vitek and Giroux, 2000).

Another parameter known as autocorrelation is the cross-correlation of a signal by itself. Its purpose is to selectively amplify the deterministic components of a signal embedded in noise, given that its random components are cancelled by the autocorrelation products.

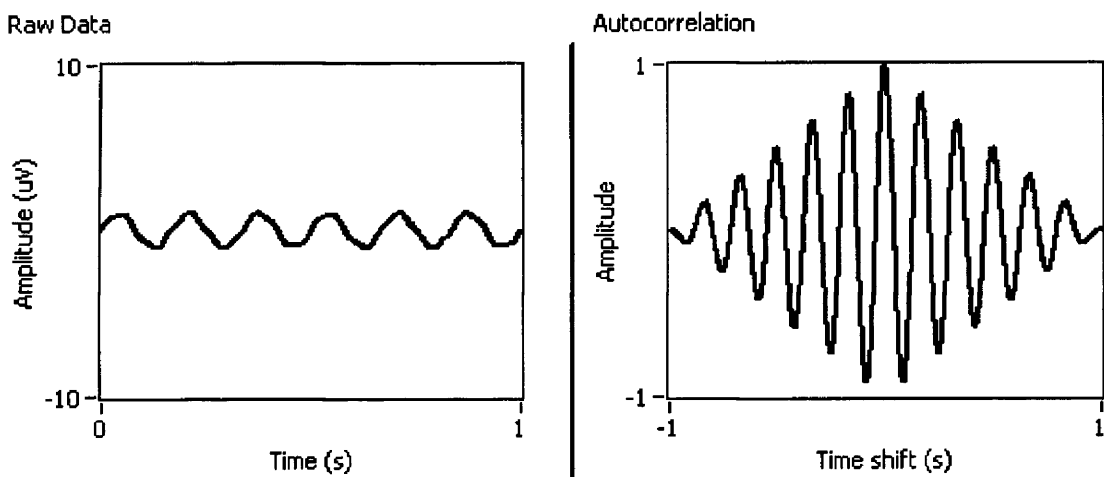
Here is the expression of its estimate:

$$r_{xx}(k) = \frac{\frac{1}{N-1} \sum_{n=1}^N (x(n) - \bar{x})(x(n+k) - \bar{x})}{\frac{1}{N-1} \sum_{n=1}^N (x(n) - \bar{x})^2}$$

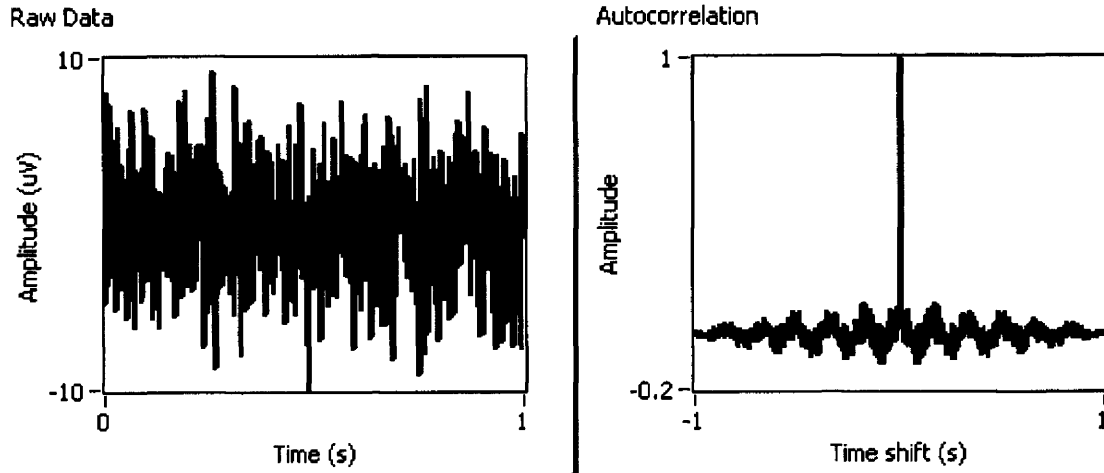
Figure 2.3 Introduces examples of autocorrelation.



2.3.a : pure noise



2.3.b : harmonic signal



2.3.c : harmonic signal embedded in noise

In Chapter 3, we investigate the relation between two times series, EMG and LFP. In another chapter (Chapter 4), we investigate the correlation between time series and a point process, spikes and LFP, which gives the result as spike triggered average (STA).

2.4.1.3 Spike triggered average (STA)

The spike-triggered average $c(\tau)$ is the average value of the stimuli a time interval τ before (and after) a spike is fired. The spike average is computed as the following: (Dayan and Abbott, 2001)

$$c(\tau) = \left\langle \frac{1}{n} \sum_{i=1}^n s(t_i - \tau) \right\rangle \approx \frac{1}{\langle n \rangle} \left\langle \sum_{i=1}^n s(t_i - \tau) \right\rangle$$

T_1 is the time when a spike occurs, n is the number of spikes in a trial, while $s(t_i - \tau)$ determines each signal in a time interval τ preceding the spike is recorded. The stimuli are only recorded over a finite time period. The recorded stimuli for all spikes are then summed and the procedure is repeated over multiple trials. The spike-triggered average stimulus is extensively used to characterize neural responses. Because $c(\tau)$ represents the average value of the stimulus at a time τ before a spike, larger values of τ represent times further in the past relative to the time of the triggering spike. To facilitate the visualization of significance, STAs of multiunit data were normalized by the standard deviation of the STA following time-shifting. So that y axes are plotted as z scores.

2.4.2 Frequency domain analysis

Frequency domain analysis refines the time domain analysis by emphasizing the frequency components of the signals themselves and of the relationships between different signals. The basic frequency domain tool is the spectral plot or power spectrum, which extracts the signal energy in proportions which represent the proportion of energy distributed in different bands of frequency (Challis and Kitney, 1991a).

2.4.2.1 Fourier series

The Fourier series (FS) represents a periodic continuous function of time series by the summation of an *infinite* series of sine waves and cosine waves of *rising* frequencies. The algebraic representation of the FS is (Challis and Kitney, 1991a)

$$f(t) = a_0 + \sum_{k=1}^K \{a_k \cos k\omega_0 t + b_k \sin k\omega_0 t\}$$

Where $\omega_0 = 2\pi / T$ and T is the basic repetition period.

The coefficients a_k and b_k are calculated as:

$$a_k = \frac{2}{T} \int_{-T/2}^{T/2} f(t) \cos k\omega_0 t dt$$

$$b_k = \frac{2}{T} \int_{-T/2}^{T/2} f(t) \sin k\omega_0 t dt$$

At a given frequency these terms can be re-expressed as a single amplitude and phase as:

$$a_k \cos k\omega_0 t + b_k \sin k\omega_0 t = c_k \cos(k\omega_0 t + \phi)$$

Where

$$c_k^2 = a_k^2 + b_k^2, \phi = \arctan \frac{b_k}{a_k}$$

A complex exponential function may be expressed as the sum of a sine and cosine components

$$e^{jx} = \cos x + j \sin x$$

It is then defined by the following summation:

$$f(t) = \sum_{k=-K}^{+K} F_k e^{jk\omega_0 t}$$

Where

$$F_k = \frac{1}{T} \int_{t_0}^{t_0+T} f(t) e^{-jk\omega_0 t} dt$$

The coefficients f_k , a_k and b_k are related as

$$a_k = F_k + F_{-k}$$

$$b_k = j(F_k - F_{-k})$$

$$F_k = \frac{1}{2}(a_k - jb_k)$$

The real and imaginary parts of the coefficients F_k correspond to the cosine and sine terms, respectively. (Challis and Kitney, 1991a)

The convergence of the FS is granted for the continuous and periodic functions of time. However this is not the case of the recorded signals, which are necessarily discrete because of the sampling process, and non-periodic because limited in time to the duration of acquisition. We therefore need to see how transforms can describe such functions and what is the impact of the sampling constraints.

2.4.2.2 Fourier Transform

The Fourier transform consists in changing the representation of a signal from the referential of the time domain to the referential of the frequency domain introduced above.

Mathematically, the result of the Fourier transform is a complex function totally equivalent to its time domain counterpart.

Its definition is: (Challis and Kitney, 1991a)

$$f(t) = \frac{1}{2} \int_{-\infty}^{\infty} F(\omega) e^{j\omega t} d\omega$$

$$F(\omega) = \int_{-\infty}^{\infty} f(t) e^{-j\omega t} dt$$

The Fourier transform is essentially a correlation between $f(t)$ and the complex exponential $e^{-j\omega t}$. Moreover its conditions for existence are weaker, than those of the Fourier series, since now $f(t)$ may be discontinuous and non periodic. The studied signals are all recorded over a finite period of time and digitized. The finite recording time generates a side-effect known as spectral leakage which is a spreading of the power over a larger frequency band than in the original signal. The use of specific windows over the recording, such as the Hanning windows, limits this leakage to a large extent. The second effect is known as aliasing, by which frequency components above $F_s/2$ may interfere with those below. In order to avoid aliasing, all signals are first low-pass filtered at a frequency lower than $F_s/2$ before sampling. Besides, this requires the sampling frequency F_s to be chosen higher than twice the highest frequency of interest, since all information contained in the signal above $F_s/2$ will be discarded. Conversely, the Nyquist theorem ensures that all information below $F_s/2$ will be represented in the sampled signal.

The computation method of the Fourier transform from the sampled data in the conditions exposed above is generally known as the discrete Fourier Transform (DFT). Indeed, the frequency domain representation of the sampled signal is

also a discrete function, which is featured by its frequency resolution, the unit bandwidth of frequency on which the energy of the signal is integrated:

$$\text{Frequency resolution} = F_s / N$$

where F_s is the sampling frequency.

The evaluation of the discrete Fourier transform is usually performed under its optimized form, the FFT for Fast Fourier Transform. Although today the power of processors enables the calculation of the Fourier Transform in a fraction of seconds, the FFT is still used as a habit. It requires the number of samples to be a power of two, usually 1024 in our data analyses.

In order to compensate the intrinsic loss of accuracy, the method of disjoint sections requires the acquisition of a large record R , which is divided into a large number L of subrecords T , where $R=LT$. Both time series and point process are segmented this way, and a Fourier transform is performed independently on both signals for each subrecord T_l . Once each process has been transformed, spectral estimates are constructed by algebraic combinations of these transforms. The finite Fourier transform of the l th segment ($l=1,2,\dots,L$) from process x at frequency λ is defined as

$$dxT(\lambda, l) = \int_{(l-1)T}^{lT} x(t) e^{-i\lambda t} dt \approx \sum_{t=(l-1)T}^{lT-1} e^{-i\lambda t} x_l$$

Where $i = \sqrt{-1}$ and $e^{it} = \cos(t) + i \sin(t)$

Using the DFT algorithm non-overlapping, discrete windows of spectral estimates of a signal can be made.

Frequency resolution = sampling rate/window of length (FFT points)

When EMG signals are computed, they are usually rectified prior to being Fourier transformed. The idea behind this is that it is the timing of the individual action potentials within EMG which is of interest, thus the full wave rectification can maximize information about action potential timing.

2.4.2.3 The power spectrum

In its complex expression presented in the definition, the Fourier transform does not have much physical meaning. Therefore, the signal spectra are usually plotted by means of the power spectrum, which is defined as the square modulus of the Fourier transform of the signal (Challis and Kitney, 1991b).

$$P(\omega) = F(\omega)F^*(\omega) = |F(\omega)|^2$$

Where $P(\omega)$ is the power spectrum and $F(\omega)$ the Fourier transform. The amplitude of $P(\omega)$ is always positive for a real signal and it represents the power of the signal in the unit frequency band. The total signal power which exists in the frequency ω_1 to ω_2 can be obtained as:

$$P(\omega_1, \omega_2) = \int_{\omega_1}^{\omega_2} P(\omega) d\omega$$

$P(\omega)$ can be seen as the distribution in frequency space of variance in the time-domain signal.

2.5 Statistical analysis

Statistical analyses used throughout the studies in this thesis were performed using SPSS 11.0 for windows (SPSS, Inc, Chicago, Illinois, USA) and Excel (Microsoft Office 2000 SR-1 Professional), unless described elsewhere.

2.5.1 Parametric tests

Parametric tests used in this thesis include correlation, student's t-test and repeated measures general linear models (GLM) of analysis of variance (ANOVA). The utilization of these analyses is based on the assumption that the data are normally distributed. The normal distribution refers to the observations that have a Gaussian distribution profile. A characteristic of this distribution is that 68% and 95% of all values under the curve lie within one and two standard

deviations of the mean, respectively. The Kolmogorov Smirnov test is used to determine whether a set of data are normally distributed. It compares the observed data with the theoretical normal distribution. If $p > 0.05$ then the distribution is not significantly different to the theoretical normal distribution. In contrast, the data are considered non-parametric if $p < 0.05$. In Chapter 3, where we seek to look at the relationship between recorded LFP and EMG, the principle statistical tool used is correlation. In Chapters 3 and 6, ANOVA is used for the purpose of comparing multiple variables within groups. Student's t-test is used across different studies within this thesis.

2.5.1.1 Correlation analysis

The concept of correlation has been discussed previously. Pearson's correlation is used when the data is parametric and normal distributed

For Pearson's correlation, the t-test is determined as:

$$t = r \sqrt{\frac{n-2}{1-r^2}}$$

p-value is determined by entering the t value at n-2 degrees of freedom.

Spearman's rank correlation is used when the data are non-parametric.

One should bear in mind that it doesn't prove causality.

2.5.1.2 ANOVA

Repeated measures general linear models (GLMs) of analysis of variance (ANOVA) were used to compare multiple variables within groups. ANOVAs allow the investigation of the effects of each variable, or factor, individually and the interaction between factors. The validity of ANOVA relies on the ‘sphericity’ of the dependent variables. This means that the variables have equal variances across time (Norman and Streiner). The Greenhouse Geisser correction for non-sphericity was incorporated in this thesis where this assumption was violated as assessed by the Mauchley’s test. If the ANOVA shows significant differences between groups, it is necessary to perform *post-hoc* t-tests to further investigate significant factors and interactions identified by ANOVAs.

When performing multiple post hoc tests, it’s necessary to apply a correction factor to the significance level. In the Chapter 3 Bonferroni correction is used to correct the significant level. If there are n independent significant tests at the p level, then the corrected significant level will be p/n .

2.5.1.3 Z-score

The Z-score is used as a way of representing the raw score by expressing it by means of measuring its location away from the mean of the distribution, in standard deviation units.

The Z-score is calculated by subtracting the mean of distribution from the raw score and further dividing by the standard deviation. Therefore, distributions are transformed to the same scale and are suitable when comparing scores from different measures or examinations.

2.5.1.4 The student's t-test

The student's t-test compares the means of two groups. The probability value (p-value) is usually determined as <0.05 . Paired t-tests were performed where the same samples are compared under different conditions. In contrast, unpaired t-tests are used when samples sizes in two groups are different or independent. T-tests may be one or two tailed. Only the two-tailed t-test is performed in this thesis.

2.5.2.1 Non-parametric tests

Wilcoxon and Mann Whitney signed rank tests are used for non-parametric data sets. The Wilcoxon signed rank test is performed for paired data and the Mann Whitney signed rank test is used for unpaired data.

2.5.2.2 Fisher's exact test

The Fisher's exact test is a way of determining if there are associations between two categories of variables. The test is based on a 2*2 table, with the frequency of an event in each cell. The test determines whether the ratios of the variables are significantly different.

Further details of statistical analysis are given in Chapters 3-7.

CHAPTER 3: Oscillatory pallidal local field potential activity correlates with involuntary EMG in dystonia

3.1 Introduction

Pallidotomy (Lozano et al., 1997; Vitek and Bakay, 1997) and high frequency stimulation of the pallidum (Coubes et al., 2004; Coubes et al., 2000; Krack and Vercueil, 2001; Krauss, 2003; Kumar et al., 1999; Kupsch et al., 2006; Vidailhet et al., 2005; Vidailhet et al., 2007) have been shown to be of therapeutic benefit in the treatment of dystonia, thereby implicating this structure in the pathophysiology of this movement disorder. However, little is known about the particular aspects of the pallidal activity that might relate to the involuntary muscle spasm in dystonia. Hitherto, intra-operative microrecording have afforded conflicting data regarding the firing rate of individual pallidal neurons in dystonia, partially explained by the form of anesthesia used (Hutchison et al., 2003; Starr et al., 2004; Vitek et al., 1999). No microelectrode study has so far attempted to explore the degree of synchronization between neurons in this condition, and yet the abnormal pattern of activity *across* populations of neurons is emerging as an important characteristic of basal ganglia dysfunction, at least in parkinsonism (Bergman et al., 1998; Bevan et al., 2002; Brown, 2003).

In this chapter we test the hypothesis that patterns of synchronized neuronal activity in the pallidum correlate with the intensity of involuntary EMG activity in dystonia. Local field potentials (LFPs) were recorded from the different

contacts of DBS electrodes inserted into the pallidum of 13 patients for the treatment of dystonia. Patients were studied while alert, during the interval between implantation and subsequent connection of the DBS electrodes to an implantable pulse generator stimulating device. By recording LFPs from DBS electrode contacts rather than single unit activity from microelectrodes we were able to concentrate on changes in the synchronous activity across many neurons, as non-synchronised activity is canceled out and lost in the LFP. We focused our attention on the 4-10 Hz, 11-30 Hz and 65-85 Hz bands, as past work suggests that these basal ganglia activities may have differing functional significance (Brown et al., 2001; Priori et al., 2002; Priori et al., 2004; Silberstein et al., 2003; Williams et al., 2002). The aim of this chapter is to determine whether synchronization of local activity indexed by the different spectral components of the pallidal LFP correlated with the intensity of involuntary EMG activity in dystonia, in keeping with the pathophysiological role for synchronization of pallidal activity in this disabling condition.

3.2 Methods

3.2.1 Patients and surgery

Thirteen cervical dystonia patients participated with informed consent and with the agreement of the local ethics committees. Their clinical details are summarized in the Table. Here, the clinical description of the dystonia was drawn from the blinded inspection of pre-operative video recording by the author. The indication for surgery was medication refractory severe dystonia.

Patients were recorded 2-6 days post-operatively. The operative procedure and beneficial clinical effects of stimulation have been described previously (Coubes et al., 2004; Coubes et al., 2000; Coubes et al., 2002; Krauss, 2003; Vidailhet et al., 2005; Vitek et al., 1998; Volkmann and Benecke, 2002). DBS electrodes were inserted bilaterally. The model of macroelectrode used (3387 Medtronic) has been described in detail in Section 2.1. Macroelectrodes were connected to a battery-operated programmable pulse-generator (Itrel II or Kinetra 7428, Medtronic) after an interval of 3-7 days. All patients except case 2 improved following continuous bilateral high frequency stimulation (Table).

Table 3.1. Summary of patient details

All patients had bilateral implantation of the globus pallidus. Case 13 was operated in Mannheim. The rest of the cases were operated in Berlin.

BFM=Burke-Fahn-Marsden dystonia rating scale, ME=Macroelectrode

Case	Age (yr) & Sex	Disease duration (yr)	Diagnosis & predominant symptoms pre-operatively	Pre-op BFM motor/ disability scales/ Tsui scales*	Post-op BFM motor/ disability scales/ Tsui scales*	Medication
1	17M	11	DYT1	75/13	44.5/9	Trihexyphenidyl

			generalised dystonia with non-mobile cervical dystonia			22.5mg
2	54M	29	Idiopathic generalised dystonia with non-mobile cervical dystonia	50/13	65/23	Trihexyphenidyl 6mg, Tetrabenazine 37.5 mg
3	42M	15	DYT1 generalised dystonia with phasic neck movement	37/5	9/2	Tilidate 45 mg
4	40M	1	Idiopathic fixed cervical dystonia	10*	5*	Metoprolol 100 mg, Primidone 125mg
5	41M	21	Idiopathic familial segmental dystonia with phasic neck movement	12/4	8/1	Trihexyphenidyl 15mg, Diazepam 12mg, Baclofen 30mg

6	36M	29	Idiopathic familial generalised dystonia with non-mobile cervical dystonia	82/18	50/18	Trihexyphenidyl 20mg
7	64M	7	Idiopathic segmental dystonia, involvement of neck with phasic movement	23/11	7/0	Diazepam 5mg
8	74M	13	Idiopathic segmental dystonia with phasic neck movement	16*	10*	Tilidate 15mg
9	38F	12	Idiopathic generalised dystonia with non-mobile cervical dystonia	9/3	9/2	Trihexyphenidyl 30mg, Tetrabenazine 150mg

10	56F	11	Tardive segmental dystonia	28/8	2/0	Lorazepam 1mg, Lithium 900 mg
11	65M	8	Idiopathic cervical dystonia with 5 Hz neck tremor (no-no)	14*	13*	Nebivolol 5mg
12	62F	13	Idiopathic dystonia with head-neck tremor	34*	29*	Metoprolol 190mg, Lactulose 30mg
13	36F	1	Idiopathic segmental non-mobile dystonia	20/6	8/0	None

Pallidal electrode trajectories were aimed at the postero-ventral portion of the globus pallidus internus (GPi) and the posterior ansa lenticularis. The target was identified on high resolution T2-weighted axial, coronal and sagittal MRI planes. This image was superimposed on coronal and lateral contrast ventriculography and drawn on the GP Tailairach Scheme, corresponding in

location to the GP area in the Schaltenbrand and Wahren atlas (Schaltenbrand and Wahren, 1977). The depth of the lowest contact was aimed to be at least 1 mm above the upper border of the optic tract (but see results). The location of the latter was established by the intra-operative induction of visual phosphenes by high frequency stimulation. Intra-operative microelectrode recordings and macrostimulation were performed in all patients. Details of the target coordinates were provided in Section 2.1.

3.2.2. Post-operative radiological reconstruction of contact placement

Post-operative contact localization was performed by adapting a three-dimensional anatomical atlas, consisting of MR images, two series of histological slices and 3D contours of basal ganglia structures (Bardinet, 2002), to the brain anatomy of each patient (Yelnik et al., 2003). The atlas was deformed automatically through coregistration of atlas and patient MR images (Fig. 1A). Localization of electrode contacts was obtained by reslicing each patient's MR image and atlas structures along the axis of each electrode (Fig. 1B).

3.2.3. Recordings and analysis

Patients were studied in the interval between macroelectrode implantation and subsequent connection to a subcutaneously placed stimulating device. Subjects were seated and recorded at rest, simultaneously with dystonic posturing or movement of the neck. LFPs were recorded bipolarly from the adjacent 4

contacts of each pallidal macroelectrode (contacts 01, 12, 23). They were filtered at 0.5-300 Hz. Simultaneous surface EMG (sEMG) recordings were made over the sternocleidomastoid (SCM) bilaterally in 5 patients and unilaterally in 8 patients, using pairs of Ag/AgCl electrodes taped 3-4 cm apart over the muscle bellies. Single runs of recordings were made in all subjects except 3 (one patient each with unilateral and bilateral SCM recordings had data from two sessions and a further patient with bilateral recordings had data from 4 sessions). EMG was filtered at 16-300 Hz in four patients and 10 Hz-3 kHz in nine. Signals were amplified and filtered using a custom-made. 9-V battery-operated portable high-impedance amplifier (which has as its front end input stage the INA 128 instrumentation amplifier, Texas Instruments, Dallas, TX, USA) and sampled at 625 Hz-1250 Hz through a 1401 analog to digital converter (Cambridge Electronic Design, Cambridge, UK) onto a portable computer using Spike2 software (Cambridge Electronic Design). Section 2.3 provides details of the recording set.

LFPs and sEMG were viewed off-line. Sections of visible movement artefact in both EMG and LFP channels were removed. The mean duration of data analysed per correlation was 622 seconds (range 199 to 1717 seconds). Signals were down-sampled to a common sampling rate of 512 Hz through spline interpolation in Matlab v6.0 (The Mathworks Inc, Natick, MA, USA). sEMG was rectified and LFP and sEMG data segmented into non-overlapping blocks of 512 data points before spectral analysis (Spike2). Log LFP power was determined over four frequency bands: three a priori candidate bands of 4-10 Hz, 11-30 Hz and 65-85 Hz and one control frequency band from 120-145 Hz,

where no correlations above chance levels were anticipated. In addition, log rectified sEMG power was determined in the same blocks over 4-200 Hz. The latter was used as a measure of the level of dystonic sEMG activity.

3.2.4. *Statistical analysis*

The concepts and application of parametric and non-parametric tests used in this study have been introduced in Section 2.5.

Pearson's test was estimated between sEMG and LFP activity in each of the three frequency bands for each of the three contact pairs of the pallidal electrodes. Correlations were only considered significant if $p \leq 0.05$ after Bonferroni correction for the three contact pairs. There are 168 possible correlations between macroelectrode contact pairs and ipsilateral/contralateral SCM, when all data were considered. The number of positive or negative correlation in the three frequency bands expected by chance was estimated as $[(0.05/3) * 168] / 2 = 1.6$, where $(0.05/3)$ was the significance level after correction for the three contact pairs. The division by two was because chance correlations would be expected to be equally distributed between positive and negative correlations. The final result was conservatively rounded up to 2 before incorporation in Fisher Exact tests. Normal data distributions were checked by the one-sample Kolmogorov Smirnov test. LFP power was analysed by a general linear model with Greenhouse-Geisser correction for non-sphericity, where necessary. Paired t-tests and non-parametric tests (Fisher Exact test, Wilcoxon signed ranks tests and Friedman tests) were corrected for multiple

comparisons using the Bonferroni correction. Paired t-tests, Fisher Exact and Wilcoxon signed ranks tests were two-tailed.

3.3 Results

3.3.1. Macroelectrode positioning

Thirteen patients were recorded following bilateral implantation (Table). In one patient (case 13), the limited sagittal acquisition and the large voxel size (3.6 mm) obviated MRI reconstruction. This section therefore applies to the 24 macroelectrodes in which reconstruction of contact sites was possible. Of these, none of the most caudal contact pairs (01) exclusively involved contacts outside of the target zone of GPi and ansa lenticularis, although in 8 macroelectrodes contact 0 was considered to lie within the optic tract. All but one of the middle contact pairs (12) involved one (n=9) or both (n=14) contacts in GPi. In the exception, contact 1 was considered to lie in the intramedullary lamina and contact 2 in the GPe. In seven macroelectrodes contact 2 was considered to lie in GPe. Of the most dorsal contact pairs (23) one (n=8, all contact 3) or both (n=7) contacts were thought to lie in GPe, but in seven both contacts lay in GPi. In two macroelectrodes contact 3 was considered to lie in the internal medullary lamina. The precise distribution of the different contact pairs is summarized in Figure 1C, while Figure 1A and B illustrates data from case 9.

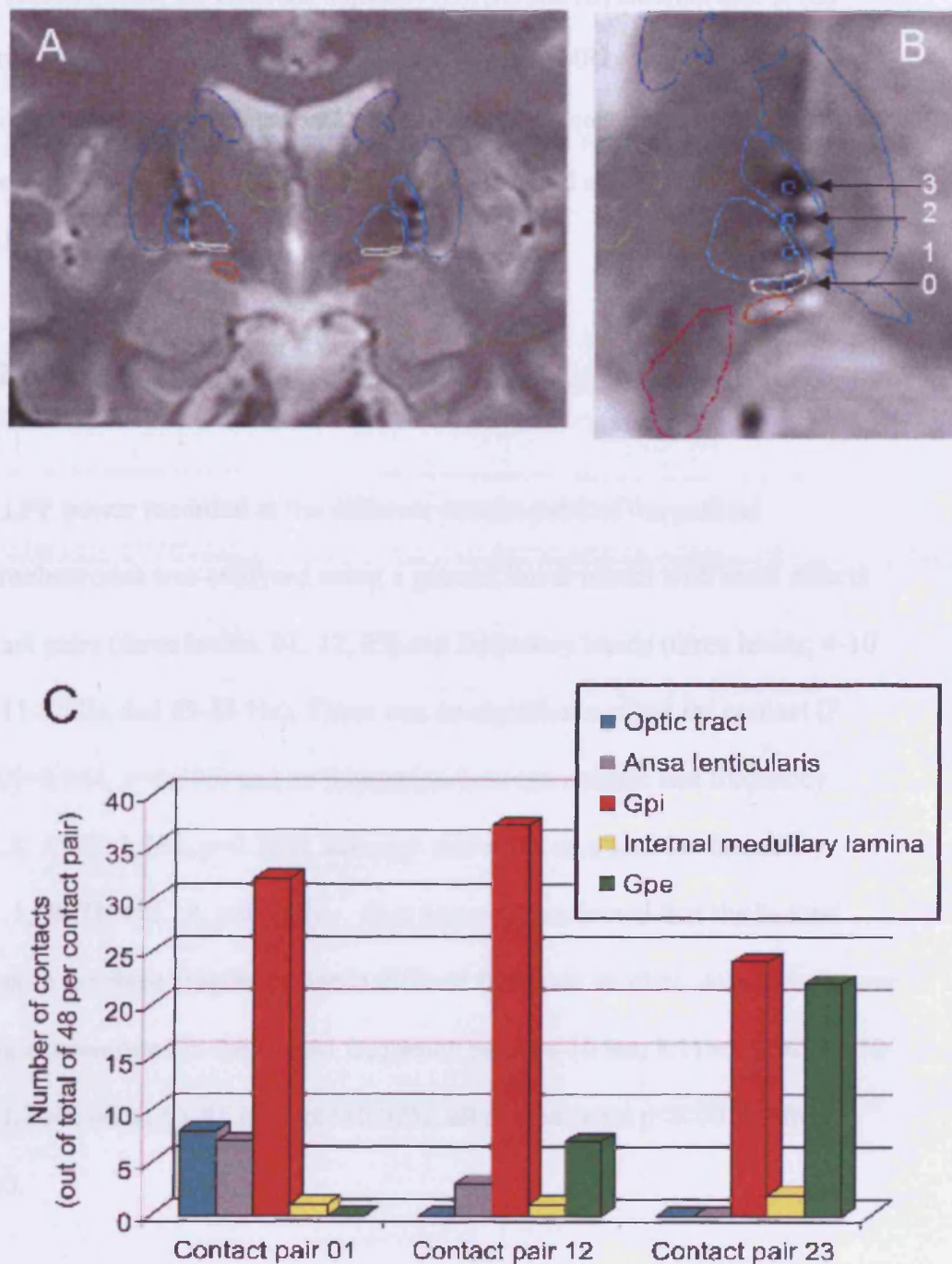


Figure 3.1. Positioning of macroelectrode contacts comprising the bipolar electrodes.

(A) The result of atlas/MRI coregistration is shown on a frontal MRI section: thalamus (green), caudate nucleus, putamen, external and internal pallidum (blue), optic tract (maroon), cerebral peduncle (pink) ansa lenticularis (white). The localization of the

four contacts (blue spheres) is determined with reference to the deformed atlas contours after reslicing along the electrode trajectory (B). (A) and (B) are from case 9. (C) Distribution of contacts across the 12 patients in whom MRI reconstruction was possible. Note that on one macroelectrode contact 0 was considered to lie just inferior to the ansa lenticularis, but this contact has been included as 'ansa lenticularis' for simplicity.

3.3.2. Spectral distribution of LFP power

The LFP power recorded at the different contact pairs of the pallidal macroelectrodes was analysed using a general linear model with main effects contact pairs (three levels; 01, 12, 23) and frequency bands (three levels; 4-10 Hz, 11-30 Hz and 65-85 Hz), There was no significant effect for contact ($F[2,50]=0.944$, $p=0.396$) and no interaction between contact and frequency ($F[1.8, 45.8]=1.280$, $p=0.286$), although there was an effect for frequency ($F[1.1, 26.7]=452.19$, $p<0.001$). *Post hoc* tests confirmed that the % total power in the three frequency bands differed from one another, with most power being concentrated in the lowest frequency band (4-10 Hz, $8.11\pm0.33\%$; 11-30 Hz, $1.36\pm0.08\%$; 65-85 Hz, $0.13\pm0.02\%$, all comparisons $p<0.001$, paired t-test).

3.3.3 Correlation between LFP and dystonic EMG

The spectral activities in the different frequency bands recorded from 26 pallidal macroelectrodes were correlated with contralateral and ipsilateral SCM sEMG in the 13 patients. Each correlation was repeated for each of the three

bipolar contacts of a given macroelectrode. An example of simultaneous recordings of pallidal LFPs and rectified sEMG in case 12 is shown in Figure 2. Figure 3 gives examples of the relationship between log pallidal LFP activity in three frequency bands of interests (4-10 Hz, 11-30 Hz and 65-85 Hz) and log rectified sEMG activity in case 1,5, and 8.

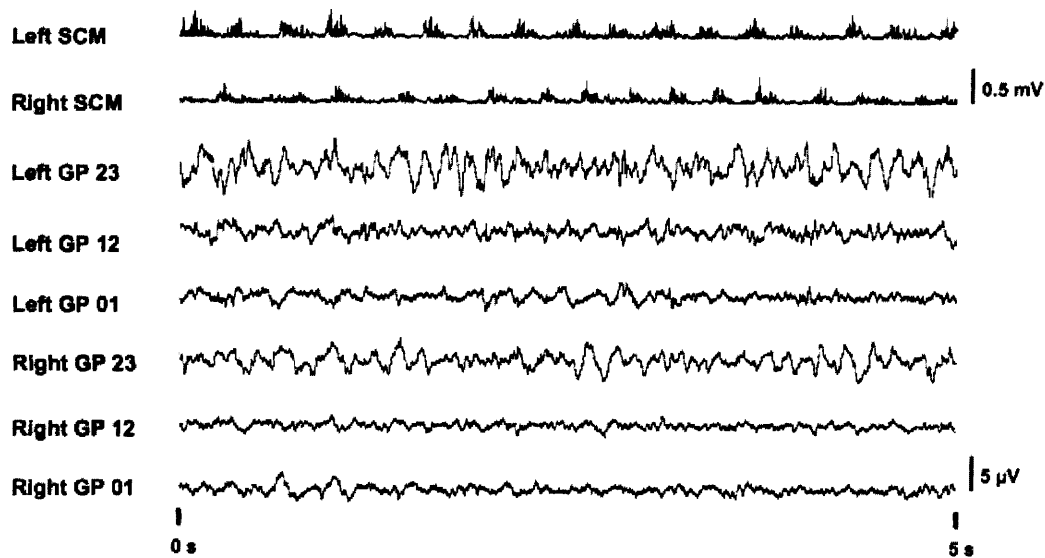


Figure 3.2. Example of simultaneous recordings of pallidal LFPs and rectified sEMG in case 12.

Figure 3

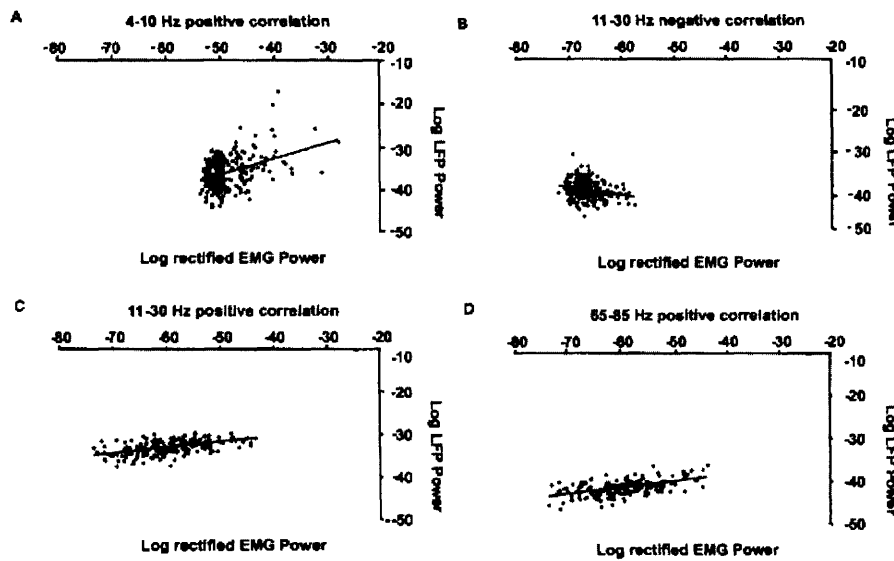


Figure 3.3. Relationship between log pallidal LFP activity in the three frequency bands of interest and log rectified sEMG activity in case 1, 5 and 8. B, D were from case 1, A and C were from case 8 and 6, respectively. All illustrated correlations had $p < 0.001$ and $r^2 > 0.05$.

The distribution of the significant correlations across frequency bands is shown in Figure 4. The proportion of positive correlation in the 4-10 Hz, 11-30 Hz and 65-85 Hz exceeded that expected by chance (each $p < 0.0001$, Fisher Exact test) as did the proportion of the negative correlations in the 11-30 Hz band ($p < 0.004$, Fisher Exact test). Significant correlations were not lateralized, whether considered separately for the positively correlating 4-10 Hz, 11-30 Hz and 65-85 Hz or negatively correlating 11-30 Hz activities, or collapsed across all frequency bands (Fisher Exact test, all not significant). Note too within the 11-30 Hz band all 18 macroelectrodes with two or more significant correlations

either showed exclusively positive (12 macroelectrodes) or negative (6 macroelectrodes) correlations at all contact pairs with significant correlations (regardless of the number of recording sessions performed and of whether correlations were with contralateral or ipsilateral SCM). Furthermore, macroelectrode pairs within the same subject tended to share the same form of correlation in the 11-30 Hz band (5 out of 6 macroelectrodes pairs with bilaterally significant correlations in the 11-30 Hz band involved correlations that were exclusively of the same sign: $p=0.08$, Fisher Exact test).

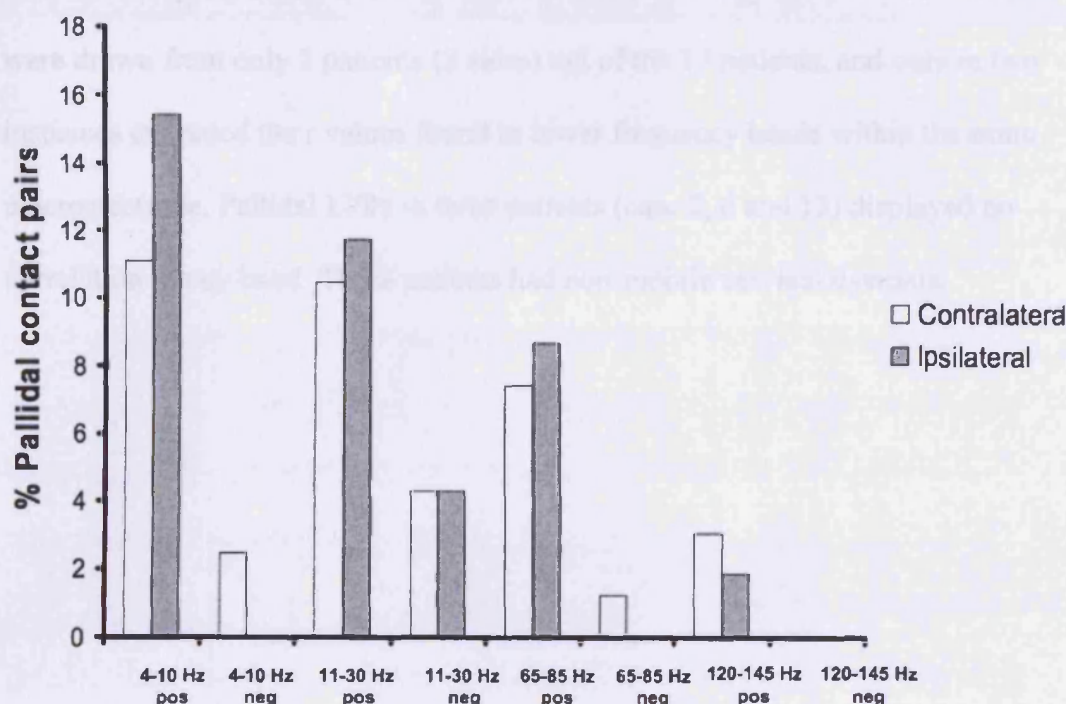


Figure 3.4. Incidence of GP LFP-EMG correlations per pallidal contact pair in the 4-10 Hz, 13-30 Hz, 65-85 Hz and 125-145 Hz band. % pallidal macroelectrode contact pairs (out of total of 168) with significant correlations between log spectral activity in a given band and log EMG power. All significant correlation coefficients in each band

were considered. No significant difference was found between sides in any group (Wilcoxon signed ranks tests).

In order to test whether or not the correlations in the three candidate frequency bands were non-specific, correlations between SCM sEMG and a control frequency band (120-145 Hz) were analyzed. Eight significant correlations were found; no more than expected by chance (Fisher Exact test). Figure 5 gives the mean correlation coefficient per contact pair in the different frequency bands, with the exception of the 120-145 Hz band where the 8 significant correlations were drawn from only 2 patients (3 sides) out of the 13 patients, and only in two instances exceeded the r values found in lower frequency bands within the same macroelectrode. Pallidal LFPs in three patients (case 2, 6 and 13) displayed no correlation in any band. These patients had non-mobile cervical dystonia.

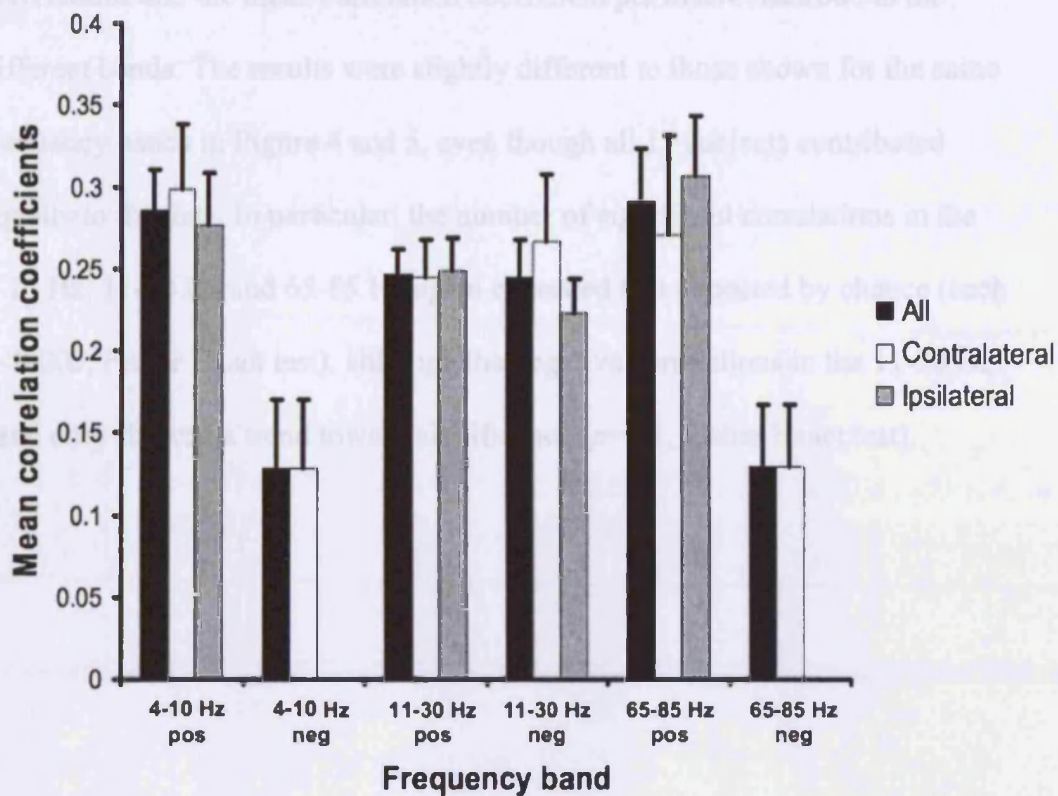


Figure 3.5. Size of GP LFP-EMG correlations per pallidal contact pair in the 4-10 Hz, 13-30 Hz and 65-85 Hz bands. Mean peak correlation coefficient (+SEM) per contact in each band. Data Fisher transformed before averaging, then back-transformed. All significant correlation coefficients in each band were considered. No significant difference was found between sides in any group (Wilcoxon signed ranks tests).

To make sure that the significant correlations in the frequency bands of interest (4-10 Hz, 11-30 Hz and 65-85 Hz) were not dominated by data from only one or two patients we found the peak correlations in each frequency band in each macroelectrode in each patient, regardless of the contact pair or recording used, or whether correlations were derived with respect to ipsilateral (total of 26 significant correlations) or contralateral sEMG (22 correlations). Figure 6 A and B summarise the percentage of macroelectrodes affording significant

correlations and the mean correlation coefficient per macroelectrode in the different bands. The results were slightly different to those shown for the same frequency bands in Figure 4 and 5, even though all 13 subjects contributed equally to the data. In particular, the number of significant correlations in the 4-10 Hz, 11-30 Hz and 65-85 Hz again exceeded that expected by chance (each $p < 0.005$, Fisher Exact test), although the negative correlations in the 11-30 Hz band only showed a trend toward significance ($p = 0.1$, Fisher Exact test).

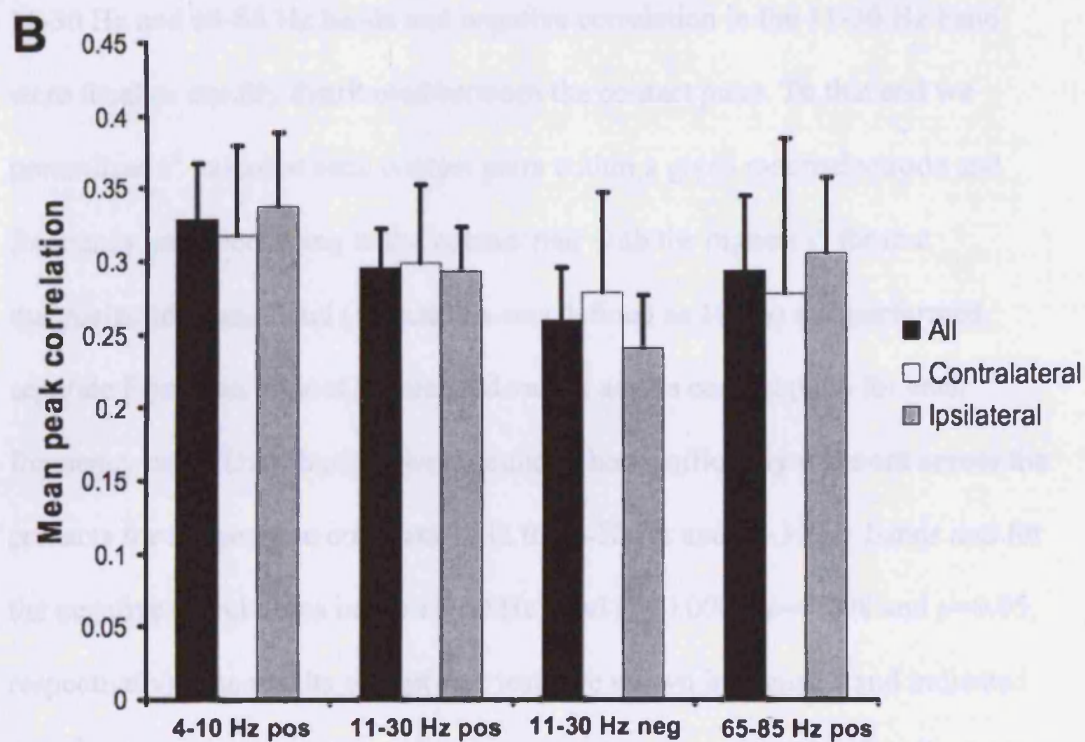
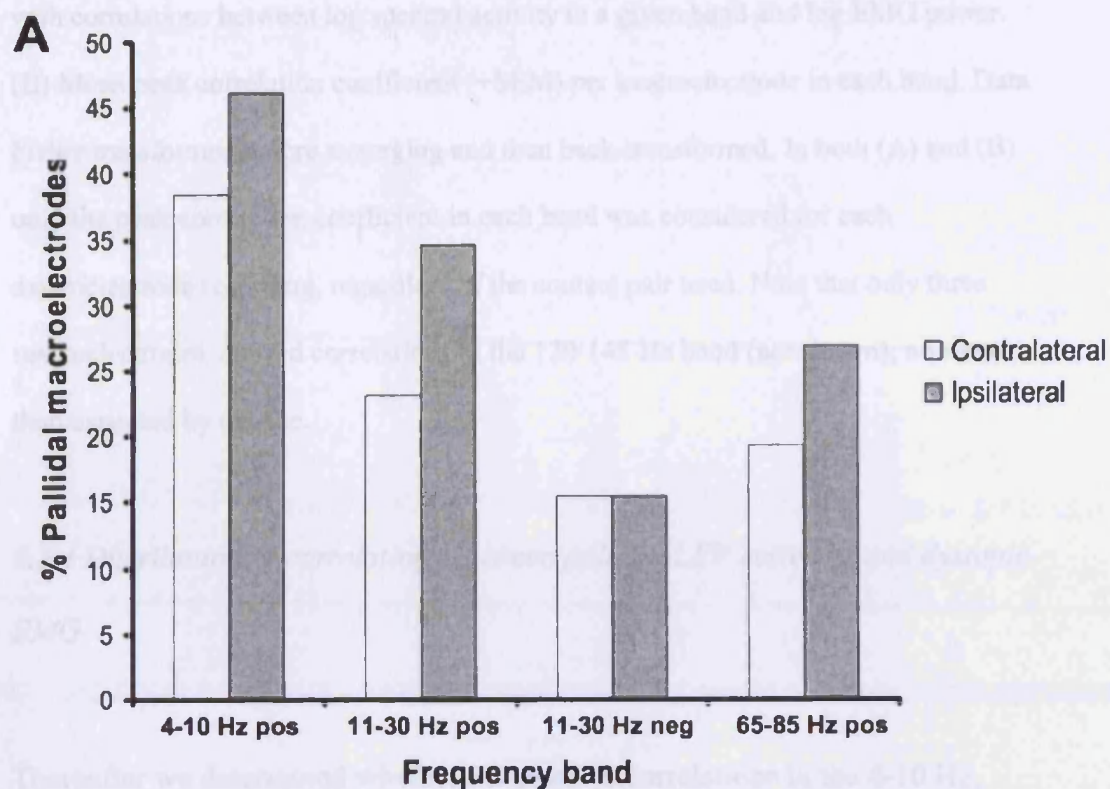


Figure 3 6. Incidence and size of GP LFP-EMG correlations per pallidal macroelectrode in the three frequency bands of interest. (A) % Pallidal macroelectrodes

with correlations between log spectral activity in a given band and log EMG power.

(B) Mean peak correlation coefficient (+SEM) per macroelectrode in each band. Data Fisher transformed before averaging and then back-transformed. In both (A) and (B) only the peak correlation coefficient in each band was considered for each macroelectrode recording, regardless of the contact pair used. Note that only three macroelectrodes showed correlations in the 120-145 Hz band (not shown); no more than expected by chance.

3.3.4 Distribution of correlations between pallidal LFP activities and dystonic EMG

Thereafter we determined whether the positive correlations in the 4-10 Hz, 11-30 Hz and 65-85 Hz bands and negative correlation in the 11-30 Hz band were focal or equally distributed between the contact pairs. To this end we normalized r^2 values at each contact pairs within a given macroelectrode and frequency band according to the contact pair with the highest r^2 for that macroelectrode and band (so that this was defined as 100%) and performed separate Friedman tests of normalized values across contact pairs for each frequency band. Distributions were found to be significantly different across the contacts for the positive correlations in the 4-10 Hz and 11-30 Hz bands and for the negative correlations in the 11-30 Hz band ($p < 0.0001$, $p = 0.008$ and $p = 0.05$, respectively). The results of post-hoc tests are shown in Figure 7 and indicated that r^2 values were maximal at the most caudal contact pairs (01) for all positive correlations and the middle contact pair (12) for the negative correlation in the 11-30 Hz band ($p < 0.05$, post-hoc Wilcoxon signed ranks test).

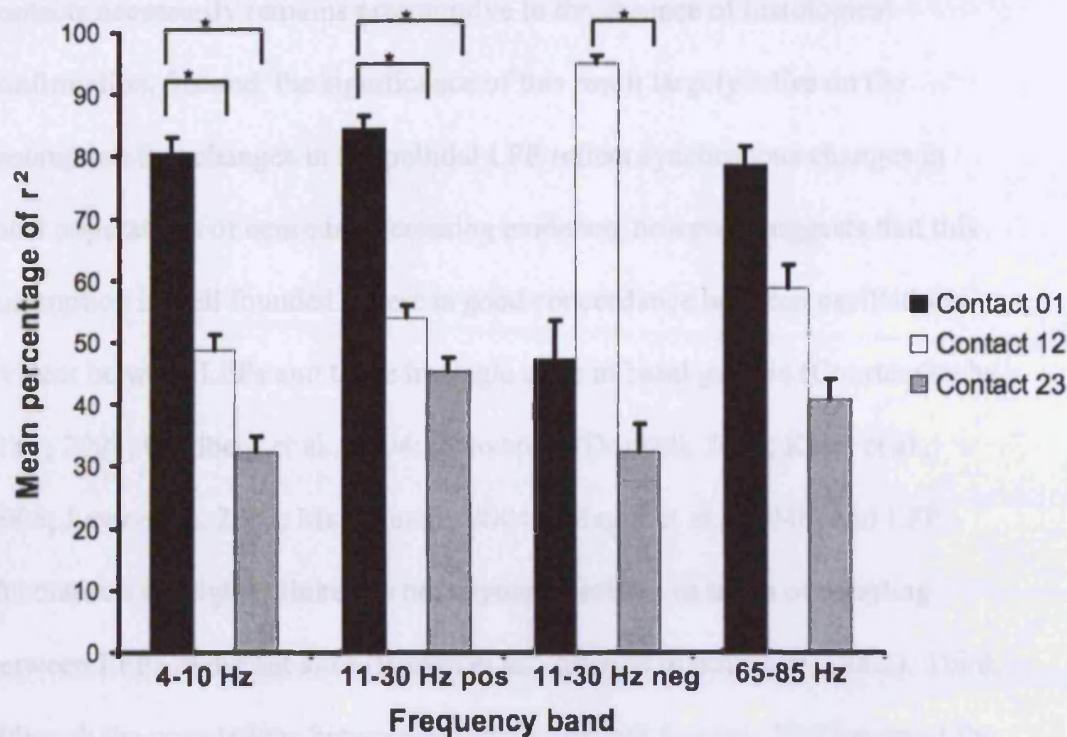


Figure 3. 7. Distribution of significant GP LFP-SCM EMG correlations among the three contact pairs in the three frequency bands of interest. Positive correlations in all three frequency bands were strongest at the lowermost contact pair, 01, the strongest negative correlations in the 11-30 Hz band were at contact 12. Only those activities correlating above chance levels are shown. * $p < 0.005$ (post-hoc Wilcoxon signed ranks Tests).

3.4 Discussion

3.4.1 Experimental limitations

Before considering this finding in greater detail we should bear in mind some limitations of this study. First, the precise location of the macroelectrode

contacts necessarily remains presumptive in the absence of histological confirmation. Second, the significance of this result largely relies on the assumption that changes in the pallidal LFP reflect synchronous changes in local populations of neurons. Increasing evidence, however, suggests that this assumption is well founded. There is good concordance between oscillations evident between LFPs and those in single units in basal ganglia (Courtemanche et al., 2003; Goldberg et al., 2004; Goto and O'Donnell, 2001; Kuhn et al., 2005; Levy et al., 2002; Magill et al., 2004a; Magill et al., 2004b) and LFP fluctuations are tightly linked to post-synaptic effects in terms of coupling between LFPs in distant sites (Brown et al., 2001; Williams et al., 2002). Third, although the correlations between pallidal LFPs and dystonic EMG support the notion that pallidal dysfunction is central to the pathogenesis of dystonia (Bhatia and Marsden, 1994; Vitek, 2002), it should be stressed that correlation cannot prove causality. Nevertheless, the fact that our positive correlations were maximal at those contact pairs considered to include the GPi and/or posterior ansa lenticularis, where lesioning or high frequency stimulation is most effective (Bittar et al., 2005; Krack and Vercueil, 2001) would support a mechanistic link between synchronized oscillatory activity and dystonic EMG activity.

3.4.2 Correlations involving LFP activity in the 4-10 Hz band

The positive correlation between 4-10 Hz LFP activity and dystonic EMG levels is consistent with the predominance of LFP power in this band in the pallidum of dystonic patients as reported here and by others (Liu et al., 2002;

Silberstein et al., 2003). Silberstein et al (2003) proposed that pallidal activity in the 4-10 Hz band might relate to the relatively non-oscillatory bursting across neurons. This form of discharge may be important in dystonia. Section 1.4.4.2 stressed the disorganization of temporal patterning of pallidal activity in dystonic animal models and patients. Microelectrode recordings from the globus pallidus in dystonic patients reveal marked abnormalities in the temporal patterning of neuronal discharge; neurons firing in irregularly grouped discharges with intermittent pauses (Lenz et al., 1999; Vitek, 2002; Vitek and Giroux, 2000). Similarly, analysis of interspike intervals in the endopeduncular nucleus (homologue of GPi) of dystonic dt^{sz} hamsters shows an increased proportion of neurons with a burst-like firing pattern compared to normal animals (Gernert et al., 2002).

Together, the above observations coupled with the positive correlation low frequency LFP activity and dystonic sEMG suggest pallidal LFP oscillations in the 4-10 Hz band may be an important pathophysiologic substrate for the development of dystonia, although it is unclear whether this relates to an abnormal processing of afferent information at the pallidal level or to a more direct influence on the motor drive to the dystonic muscles. Note that increases in LFP activity at the similar frequencies occur during and, more importantly, between paroxysms of dystonia in the dystonic dt^{sz} mutant hamster, suggesting that the spectral changes are not merely a consequence of the attacks and do not simply accompany afferent activity (Gernert et al., 1998). In addition, the positive correlations between the pallidal LFP activity at 4-10 Hz and dystonic EMG activity found here would also be consistent with the abnormal

descending drive at similar frequencies noted to neck muscles in dystonia (Tijssen et al., 2000; Tijssen et al., 2002).

Nevertheless, physiological data suggested that there may indeed be a bidirectional flow between the pallidum and muscles in dystonic patients, both efferent and afferent (Sharott et al., 2007). In this context, Directed Transfer Function (DTF) analysis, which estimates the directed coherence due to flow round coupled loops in each direction, would help interpret such a complex bidirectional system. The results confirm a bidirectional flow of information between muscle and pallidum, but with significantly more coherent activity being driven from pallidum to muscle.

3.4.3 Correlations involving LFP activity in the 11-30 Hz band

It has been previously suggested that synchronization of neuronal activity in the 11-30 Hz band may have an essentially antikinetic effect in the basal ganglia, acting instead to promote existing postural sets (Brown, 2003). If correct, then it might be reasonably predicted that there would be a negative correlation between LFPs power in the 11-30 Hz band and pallidal EMG levels in patients with predominantly mobile torticollis. Consistent with this two parkinsonism patients with pallidal DBS have been reported who showed negative correlations between pallidal LFP in the 11-30 Hz band and dyskinetic EMG activity following treatment with levodopa (Silberstein et al., 2005). Similar findings were made in LFPs recorded in a patient with Parkinson's disease and levodopa induced dyskinesias with double, bilateral deep brain stimulation

electrode implants in the subthalamic nucleus (STN) and the globus pallidus internus (GPi). Synchronisation studied through coherence analysis showed that in the nuclei contralateral to the dyskinetic side of the body there was decreased STN-GPi coherence in the high beta range (20-30 Hz) (Foffani et al., 2005). In our study, however, negative correlations were found across contacts above chance levels in the 11-30 Hz band, but, surprisingly, were out numbered by positive correlation in the same band. The locations of pallidal activities maximally correlating positively and negatively with dystonic EMG were spatially separate. The latter raises the speculative hypothesis that the 11-30 Hz activities in cases showing positive correlation with dystonic EMG is related either to compensatory processes trying to counter abnormal movement or to primarily pathophysiological activity promoting tonic elements of neck dystonia. Relevant to this, patients showed either positive or negative correlations in the 11-30 Hz band, rather than a mix of effects within a given macroelectrode or across a pair of macroelectrode, consistent with a relationship between 11-30 Hz correlations of different sign and a specific aetiologic or phenotypic characteristic among the patients. Nevertheless, no clear phenotypic characteristic emerged among those 5 patients (case 3, 5, 7, 9, 10) who had negative correlations in the 11-30 Hz band, perhaps because of the small number of patients involved. Note that the topographic difference between positive and negative correlations in the beta band parallels evidence for functional topographic differences within GP in PD (Bejjani et al., 1997; Krack et al., 1998; Yelnik et al., 2000).

3.4.4 *Correlations involving LFP activity in the 65-85 Hz band*

It has been previously suggested that synchronization of neuronal activities in the 65-85 Hz band within the basal ganglia may be prokinetic and contribute to the development of dyskinesia (Alonso-Frech et al., 2006; Brown, 2003; Brown and Marsden, 1998). This hypothesis was supported in the present investigation as positive correlations between pallidal 65-85 Hz band LFP and dystonic EMG levels were found more often than predicted by chance. However, unlike those at lower frequency, these positive correlations did not have clear topographic distribution across macroelectrode contacts. Positive correlations between pallidal 65-85 Hz band LFP power and dyskinetic EMG levels have also been reported in a patient with Parkinson's disease and levodopa induced dyskinesias (Silberstein et al., 2005). In contrast, a study reporting power spectra of LFPs from the subthalamic nucleus during complete treatment cycles in patient with PD suggested that low frequency activities determine dyskinesia, while gamma activities determine the 'On' state (Alonso-Frech et al., 2006).

3.4.5 Patients with insignificant correlations

Three out of the 13 patients exhibited no correlations between sEMG and pallidal LFPs in any frequency band. The most obvious conclusion is that any pathophysiological mechanisms associated with the correlations were not relevant in these cases. However, there are several alternative explanations. First, the three patients without correlations had relatively fixed cervical dystonia, so that there may have been too little dynamic variation in the sEMG to afford correlations with LFP features. In support of this, a study examining

the coherence between pallidal LFPs and EMG activity in patients with dystonia showed that significant coherence was only observed between the pallidal LFPs and rhythmic EMG bursts, but not sustained tonic EMG activities (Liu et al., 2006). The author suggested that different mechanisms may underlie the generation of different components of the dystonic symptoms. Second, only one muscle (sternocleidomastoid) and not all pallidal locations were sampled so that negative findings may have arisen through sampling error. Note the sensorimotor territory of GPe may lie outside the area recorded by the macroelectrode (DeLong, personal communication). Third, it is possible that drug effects may have obscured correlation and finally it should be remembered that recordings were performed several days post-implantation, when regional edema may have still been significant. This, too, may have obscured the correlations.

3.5 Summary

1. The central finding of this study is the demonstration of correlations between wide band spectral components of the pallidal LFP and levels of dystonic EMG.
2. LFP activity in the 4-10 Hz, 11-30 Hz and 65-85 Hz bands positively correlated with the level of dystonic EMG. Negative correlation, however, was limited to the 11-30 Hz band.

3. The correlations were topographically distributed. Positive correlations were maximal at the lowermost contact pair (01), which included at least one contact in the globus pallidus interna and /or posterior ansa lenticularis. In contrast, negative correlations in the 11-30 Hz band were maximal more dorsally, at the middle contact pair (12).
4. Albeit significant and topographically focal, correlations were generally weak, in keeping with any pallidal effect on muscle spasm being necessarily indirect, perhaps through pallido-thalamo-cortico-spinal pathways.
5. These correlations provide support for a pathophysiological role for synchronized basal ganglia population activity in dystonia.

CHAPTER 4: Neuronal activity in globus pallidus interna can be synchronized to local field potential activity over 3-12 Hz in patients with dystonia

4.1 Introduction

In chapter 3 we demonstrated the correlations between pallidal activity in the low frequency band and the intensity of dystonic EMG. This evidence suggests that low frequency (<12 Hz) oscillatory local field potentials (LFPs) in the pallidum may be somehow related to the pathophysiology of dystonia (Liu et al., 2002; Silberstein et al., 2003). In line with this, LFP power is prominent in this band in patients with dystonia, and is also coherent with dystonic EMG (Liu et al., 2006). Silberstein et al. (2003) proposed that pallidal LFP activity in the 4-10 Hz band might relate to the synchronized bursting across neurons, given that single neurons in the globus pallidus tend to fire in irregularly grouped discharges with intermittent pauses in dystonic patients (Lenz et al., 1999; Vitek, 2002; Vitek et al., 1999; Zhuang et al., 2004). However, there is, to date, no evidence that directly links pallidal LFP activity at frequency under 12 Hz with neuronal activity. This is important as oscillations in the LFP might represent volume conduction from distant sources such as cerebral cortex, or even movement-related artefacts secondary to dystonic movement of the head and neck.

Another feature that might increase the patho-physiological significance of LFP activity <12 Hz would be a possible concentration of this activity in globus

pallidus internus (GPi) as this represent the most effective therapeutic target for lesioning or deep brain stimulation (DBS) in dystonia (Bittar et al., 2005; Krack and Vercueil, 2001; Lozano et al., 1997; Vidailhet et al., 2005; Vidailhet et al., 2007; Yianni et al., 2003). However, the relative topography of this activity within the pallidum remains unclear, with contrast reports (Chapter 3; Silberstein et al., 2003), perhaps because the latter study was based on LFP recordings through DBS electrodes with relatively poor spatial resolution.

In the experiment described in this chapter, we simultaneously recorded LFPs and neuronal activity from microelectrodes inserted to the pallidum in awake patients with primary dystonia during functional neurosurgery to determine the extent to which the 3-12 Hz LFP activity is concentrated within GPi and synchronous with local neuronal discharge.

4.2 Methods

4.2.1 Patients and surgery

We studied nine sides in six patients with primary dystonia (4 men, mean age 46 years, range 36-64 years) who underwent bilateral implantation of deep brain electrodes in GPi. Their clinical details were summaries in Table 1.

Microelectrode recordings were used to assist the localization of GPi intra-operatively. Three patients (cases 2, 4 and 6) were recorded bilaterally, and in the remaining patients coordinates from one side were mirrored on the other.

The stereotactic frame (Riechert-Mundinger) was placed at the plan of the external auditory canal under general anesthesia with propofol. The way of localizing the target was described in details in Chapter 2.

Table 4.1 Clinical details of patients.

Case	Age in yr & Sex	Disease duration (yr)	Diagnosis and predominant pre-op symptoms	Mobile dystonia (& site)	Pre-op BFM motor/ disability scales	Post-op BFM motor/ disability scales	Medication
1.	36M	29	Idiopathic familial general dystonia	No	82/18	50/18	Trihexyphenidyl 20mg Haloperidol 3 mg Pirenzepine 50 mg Tiaprid 400mg
2	40M	1	Idiopathic cervical dystonia	Yes/Neck	8/0	2/0	Metoprogamma 100mg

3.	46F	41	Idiopathic generalized dystonia	No	50/10	21/6	Trihexyphenidyl 4mg Tetrabenazine 50 mg
4.	43M	3	Segmental dystonia	No	11/3	1/0	Pimozide 1mg Clonazepam 2mg
5.	64M	7	Idiopathic segmental dystonia	Yes/Neck	23/11	7/0	Diazepam 5mg
6.	47F	30	Segmental Dystonia	No	7/0	5/0	Amitriptylin 100 mg Tetrazepam 150 mg

Mobile=jerky component to dystonia. BFM=Burke, Fahn and Marsden Dystonia Rating Scale.

4.2.2 Intra-operative recordings

Intra-operative recordings were made with the TREC scanner electrophysiological neuronavigation system using a tetrode. The tetrode contained four circular contacts. The details of this electrode were introduced in Chapter 2. Local field potentials (LFPs) were derived from one of the four contacts of the tetrode, and this contact was not used for further analysis of unit activity. In all patients, propofol was stopped 30-60 min prior to the start of microrecordings. All patients were alert at the start of recording. Patients were instructed to rest during the recordings, although some patients did experience spontaneous dystonic movements. Electrodes impedance was $\sim 500 \text{ k}\Omega$ and showed little difference between the beginning and end of the recordings.

The microelectrode track used was aimed at the ventro-posterior-lateral part of GPi. The track was then simulated on the computerized Schaltenbrand and Wahren atlas in the sagittal view, and recordings were correlated with the track in the atlas. In a typical surgical procedure, the parasagittal microelectrode penetrations were made through Putamen, GPe and GPi. The internal medullary lamina was identified by a change in discharge pattern across a silence of at least 1 mm (\pm the presence of the border cells). Only those sides/trajectories in which an internal medullary lamina could be identified were included in this chapter. The optic track was detected by light-evoked action potential discharges at the pallidal base. Neurons were recorded on average every 984 μm along each trajectory. Neuronal activities encountered between the internal medullary lamina and optic track were considered to arise in

GPI, whereas that between striatum and the internal medullary lamina was considered to arise in GPe.

4.2.3 Off-line analyses

Off line analyses were performed with Spike 2 software. Neuronal spike data were only included in this chapter if discharges exceeded 200 events (range 242-44,942). Only those recordings that were made between 10 mm above and 8 mm below the GPi-GPe border (and excluded the optic track) were analysed. LFPs were adjusted to the same amplification and analysed using the discrete Fourier transform with non-overlapping segments 1024 data points (~1 Hz frequency resolution). Mean power across 3-12 Hz band was then determined for each LFP recording. The distribution of this power across subjects was determined by first expressing power at each site in a given microelectrode trajectory as the percentage of the highest LFP power over the 3-12 Hz band recorded in that trajectory between 10 mm above and 6 mm below the GPi-GPe border. Recording sites were then divided according to their distance in 2 mm increments from where the recording electrode crossed the microelectrode defined GPe-GPi border in each trajectory. The % power from those sites falling within each 2 mm step was averaged within each trajectory and across all patients. In total there were 94 (87 in GPe) and 32 sites above and below the GPi-GPe border, respectively, from the nine sides.

Spike triggered averages (STAs) of LFPs were also calculated, after discriminating multiunit spike discharges (Kuhn et al., 2005). To this end, the spike channel with

clearest spike activity was selected and multiunit activity was discriminated into a point process by recording all instances in which the microelectrode signal crossed a threshold level of 100 μ V at minimum interval of 0.001 s. Simultaneously recorded LFP signals were band pass filtered from 1 to 20 Hz, prior to average to give STAs (with 4 s duration and 2 s offset). The 1 Hz high pass filter was used so as to limit the effects of LFP activity of very low frequency, which was sometimes of high gain and attributable to pulse and respiratory movements of the brain. Although STAs are usually performed using single unit data, the identification of single unit data often relies on subjective criteria. With multiple unit data, the only experimenter controlled variables is the threshold level and this was fixed across all recordings in this chapter. However, the STAs derived from multiunit data have the disadvantage that they may underestimate unit-LFP synchrony (see discussion).

The STAs were considered as significant if they (1) exhibited a central peak at 0 ± 30 ms that exceeded 97.7% confidence levels (CL) established in time-shifted data (Kuhn et al., 2005) (2) corresponding peaks in power spectra exceeded 99.7% CL. To facilitate the visualization of significance, STAs of the multiunit data were normalized by the standard deviation of the STA following the time-shifting of the LFP by 7 s, so that the y axis was plotted as z-scores. The frequency content of STAs was quantified by spectral analysis in Spike2, using a block of 1024 data points (~ 1 Hz frequency resolution) centred on zero time (center of STA). Peaks in the spectra of STAs were defined as more than two contiguous bins with mean power greater than the 99.7% confidence level (CL) determined from activity over 2-35 Hz. The power in peaks with frequencies above 2 Hz was expressed as a

percentage of total power in the STA spectrum from 2 to 20 Hz. Here the 0-2 Hz frequency range was omitted so as to avoid the inclusion of pulse artefact.

4.3 Results

4.3.1 Topographical distributions of LFP power over 3-12 Hz band

Representative pallidal LFP and multiunit activity are illustrated in case 5 (Fig. 1). LFP power over 3-12 Hz was higher more distally along the microelectrode track. This is illustrated for both a single case (left track in case 4) in Fig. 2 and for the group (Fig.3). Note that Fig. 3A includes data from 7 sites between 10 mm above and 8 mm below the GPe-GPi border considered to be non-pallidal, based on microelectrode recordings characteristics. The mean percentage maximum LFP power over this frequency band at sites within GPi (n=32) was significantly greater than that at pallidal sites above the GPi-GPe border (n=87; $p=0.001$, two-tailed unpaired t test; non-pallidal sites excluded). The difference between LFP power in GPe and GPi remained if criteria were made even more stringent, and only those sites considered to lie in GPi that had appropriate microelectrode recording characteristics and were also no more than 6 mm above the GPi-GPe border (n=77 and n=2, respectively; $p=0.005$, two-tailed unpaired t test).

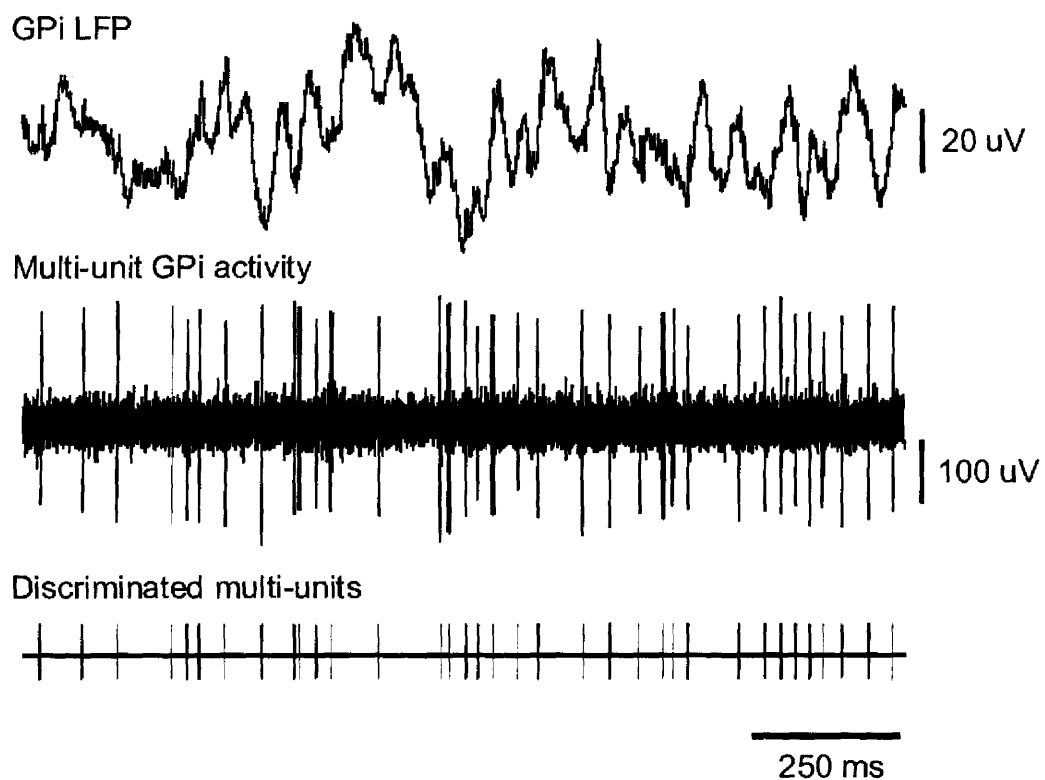


Figure 4.1. Example of raw data. Pallidal LFP (band pass 1-141 Hz), multiunit activity (band pass 0.5-10 kHz) and corresponding discriminated multiunit activity from the right side in case 6 at the level of lower GPi.

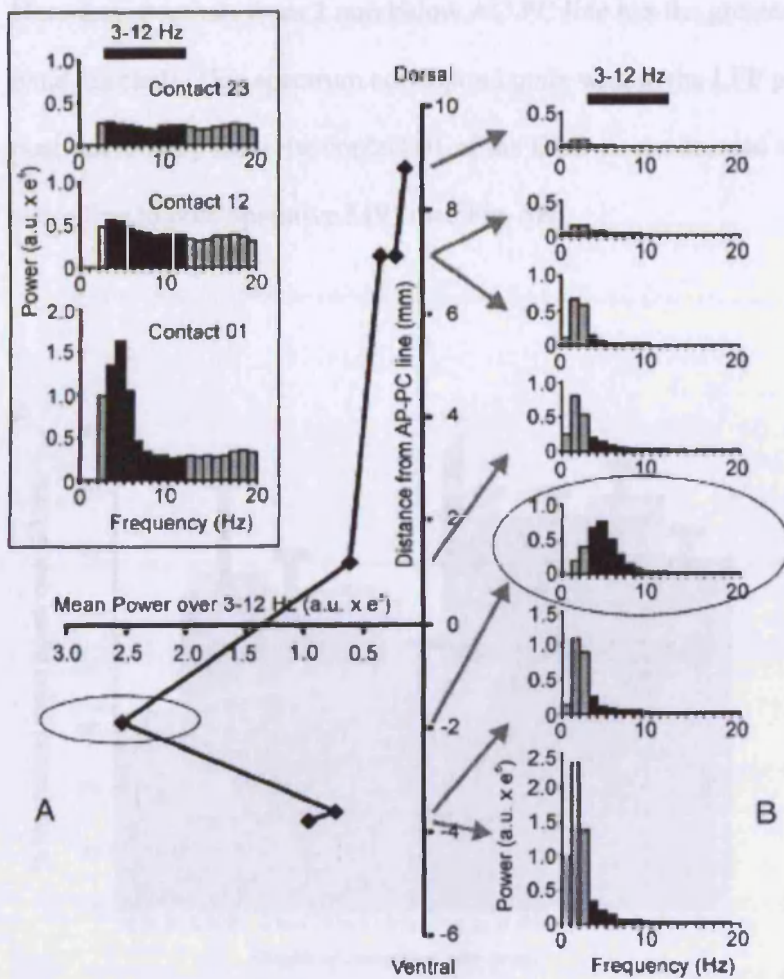


Figure 4.2. Distribution of LFP power in the 3-12 Hz band along microelectrode track in case 4 (left side). (A) Mean 3-12 Hz power along the microelectrode trajectory. Power is greatest 2 mm below the AC-PC line (circled) in ventral GPi as defined by microelectrode recording characteristics. In particular, flash evoked signals were picked up 2 mm move ventrally. The box inset shows the power recorded post-operatively from the bipolar contacts of DBS electrode on the same side. Power ≤ 2 Hz was very high and has been omitted for visualization purposes. (B) Power spectra along the microelectrode trajectory.

Note that spectrum from 2 mm below AC-PC line has the greatest power in the 3-12 Hz band (circled). This spectrum correspond quite well to the LFP power spectrum recorded post-operatively from the contact 01 of the DBS electrode, also considered to lie in GPi according to post-operative MRI (see Fig. 5B).

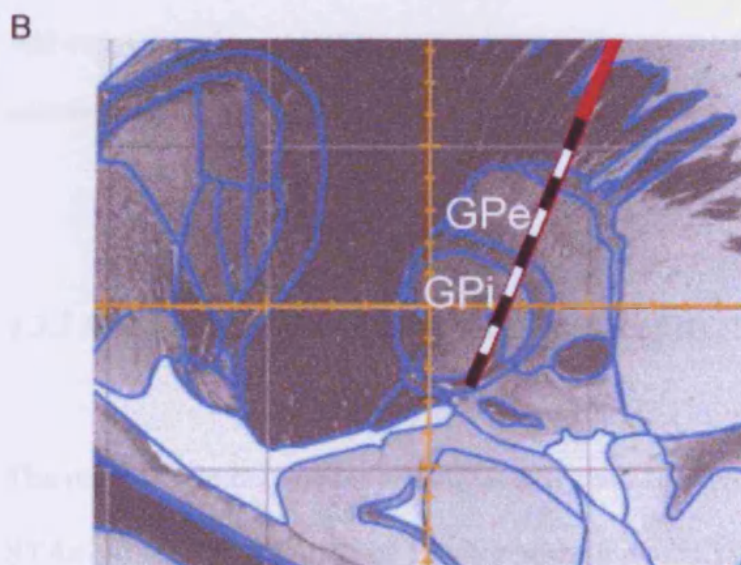
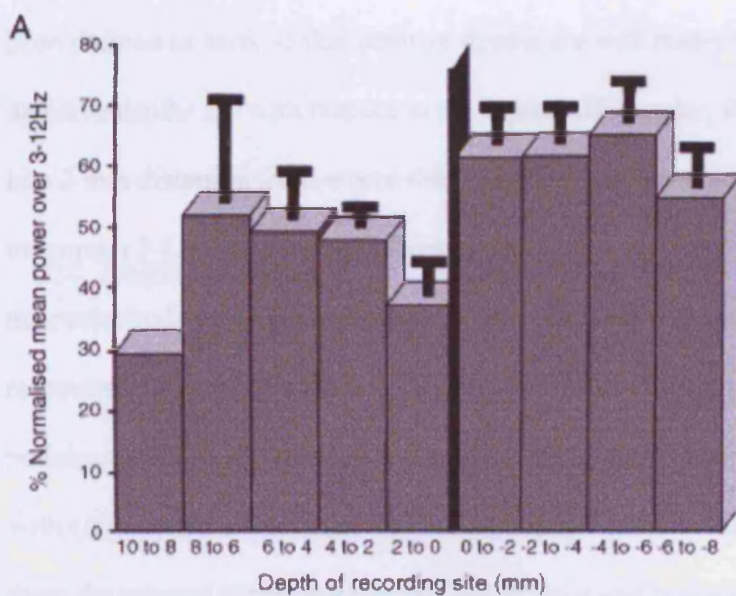


Figure 4.3.. Distribution of LFP power in the 3-12 Hz band along microelectrode trajectory across cases. (A) Mean % of maximum 3-12 LFP power along the microelectrode trajectory in 6 patients (126 recording sites, 119 of which were considered to be in the globus pallidus according to recording characteristics; sites in the optic track have been excluded). Distribution is defined with respect to the internal medullary lamina (positive=dorsal, negative=ventral), which is schematically shown as a black bar and has been defined as zero, so that positive depths are with respect to the GPe-lamina border and negative depths are with respect to the lamina-GPi border. Recording sites were divided into 2 mm distances from where the microelectrode traversed the lamina, and the % maximum 3-12 Hz LFP power from sites falling within each 2 mm bin along the microelectrode trajectory averaged. Where there were ≥ 3 sites in each bin, the SEM for the respective estimate is provided. (B) Mean microelectrode trajectory superimposed on the pallidum from the 20 mm lateral sagittal plate of the atlas by Nowinski. For comparison with (A), the mean microelectrode trajectory has been divided into steps of 2 mm distance from the internal medullary lamina. The vertical and horizontal lines are the mid-commissural point (MCP) and the level of line joining the anterior and posterior commissures. The interval between ticks on the axis is 2 mm.

4.3.2 Relationship between multiunit spike and LFP

The relationship between multiunit activity and LFP was objectively assessed by STAs of the LFP. STAs from 11 sites in the 6 patients (9 sides) had a significant central peak, which was negative in polarity in all but three averages (Fig. 4). Eight of the 11 (73%) STAs had more than one significant peak centered around zero and

were therefore suggestive of oscillatory synchronization. All 11 STAs had discrete peaks in their spectra, ranging in frequency from 2.9 to 10.7 Hz (Fig. 4). The low frequency of this activity makes spike contamination of the LFP an unlikely explanation for the oscillatory and non-oscillatory STAs.

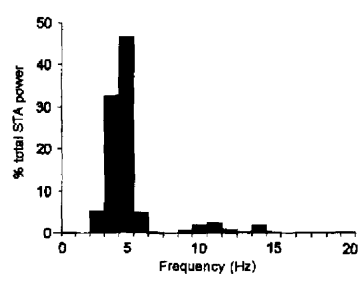
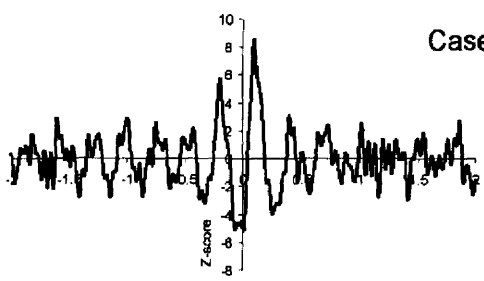
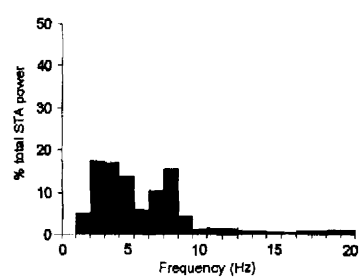
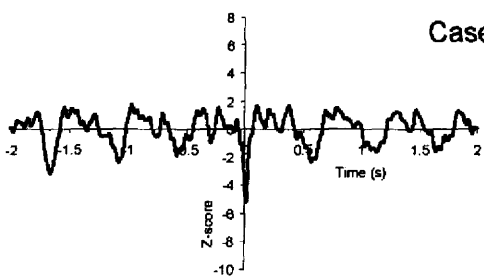
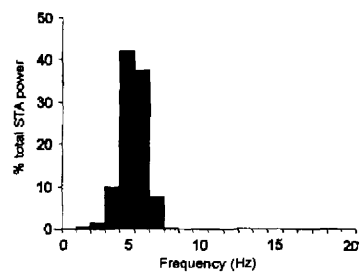
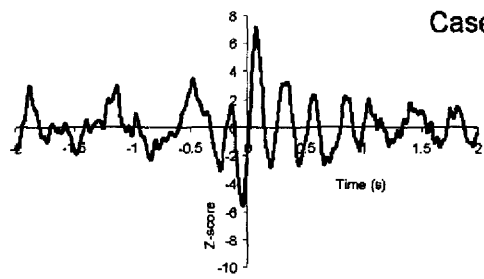
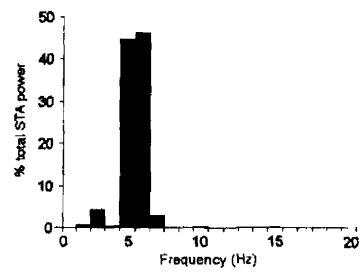
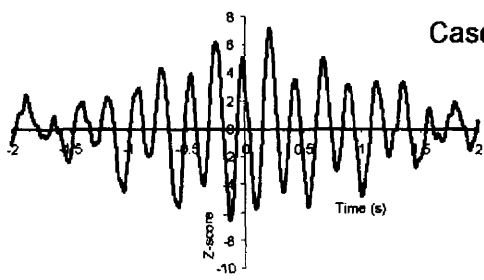
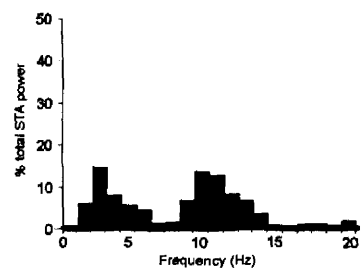
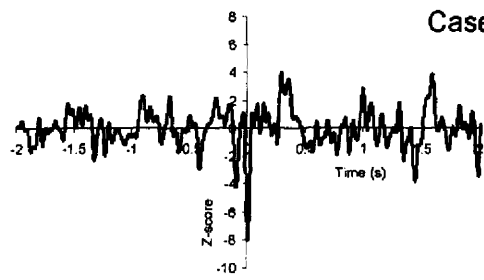
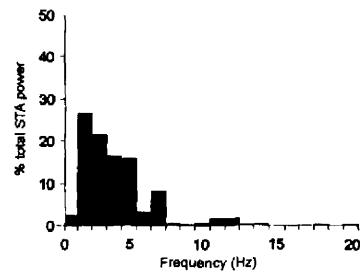
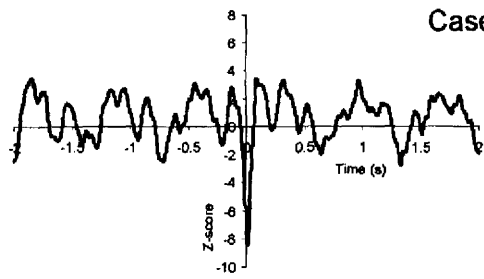


Figure 4.4. STAs and the corresponding STA spectra in the six patients. The STA with the most positive and negative central peak in each subject is shown, together with the power spectrum of the central 1024 ms of each STA. STAs were derived from multiunit data and were normalized by the standard deviation of the STA of the same LFP but after time-shifting the late, so the *y* axes are plotted as *z* scores. Spectra are plotted as % of the total power in the 2-20 Hz band. Most STAs had more than one significant peak centered around time zero, and all spectra had peaks at 3-12 Hz band. Note that the spectrum of the STA in case 4 has a peak centered around 5 Hz that was also seen in the spectrum of the LFP from this level (circled spectrum in Fig. 2B) and in the contact pairs of the DBS electrode finally implanted close to this region (spectrum of LFP from contact 01 in the boxed area of Fig. 2A).

All but two (left side in case 2 and right side in case 3) of the sites giving STAs with components in the 3-12 Hz band were in GPi according to microelectrode recordings. In addition, all but two sites (left side in case 2 and left side in case 6) were in GPi and bordering medullary lamina according to comparison of their coordinates with the Schaltenbrand and Wahren atlas. Thus, 28% of the 32 sites sampled in GPi had evidence of synchronization between multiunit activity and LFP within the 3-12 Hz band, regardless of whether GPi was defined according to microelectrode recording characteristics or coordinates. In contrast, only 2 % of the 87 sites sampled in GPe had evidence of synchronization between multiunit activity and LFP within the 3-12 Hz band. This difference is highly significant (Fisher's Exact test on numbers rather than %, $p < 0.001$). DBS electrodes placed according to

the microelectrode defined anatomy were confirmed to include the target GPi by post-operative MRI, as shown, for example, in Figs. 5A and B.

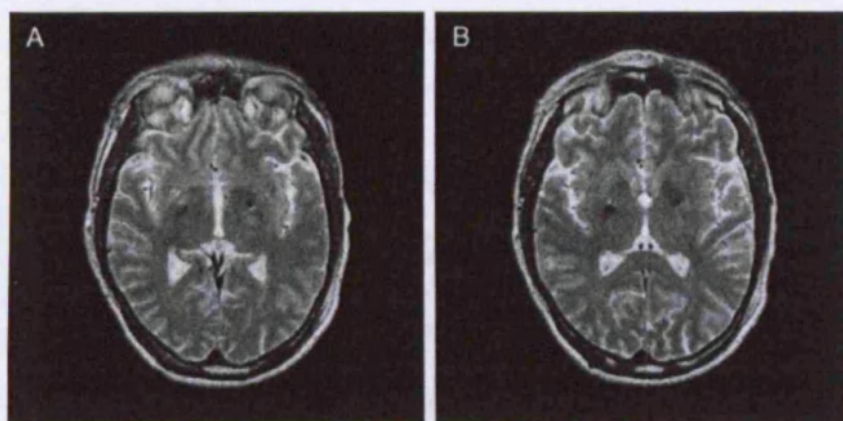


Figure 4.5. Eventual placement of deep brain stimulation (DBS) electrode. Representative post-operative MRI showing placement of DBS electrode in GPc (A) and GPi (B) in case 4.

4.4 Discussion

The principle findings in this chapter are twofold: the relative predilection for LFP activity in the 3-12 Hz band to occur within GPi and the potential locking between neuronal spike activity and the LFP in this frequency band in patients with primary dystonia. It seems unlikely that the LFP oscillations were due to the previous anesthesia with propofol (Hutchison et al., 2003; Starr et al., 2006). This was terminated 30-60 minutes before the start of recording and would not have explained the topographic distributions of the LFP power. More importantly,

Nevertheless, LFPs recorded with microelectrodes will not be identical to those identified in previous recordings with DBS electrodes. This is because of obvious differences in electrode recording areas and impedances, but also in the timing of recordings. Microelectrode recordings are made intra-operatively, in the setting of recent general anaesthesia, whereas recordings are made through DBS electrodes several days after implantation, when local edema may be prominent and dystonia accordingly temporarily improved. However, the LFP recorded in both cases includes prominent power in the 3-12 Hz band (see for example the direct comparison of microelectrode and DBS electrode recordings in Fig. 2) and our microelectrode data suggest that at least some of this involves neuronal synchronization.

Perhaps related to the differences between recording techniques, the greater 3-12 Hz power in GPi in this chapter is at odds with a previous investigation (Silberstein et al., 2003). The latter failed to demonstrate any difference in LFP activity in a similar pass band (4-10 Hz) between the rostral and caudal contact pairs of pallidal stimulating macroelectrodes in patients with dystonia. However, spatial resolution was limited in this study, which was performed with DBS electrodes, and spectral gradient over bipolar derivations of DBS contacts can be misleading. Power, for

example, is paradoxically low when bipolar electrodes bridge an electrical source.

In Chapter 3, we considered correlations between pallidal LFP activity and dystonic EMG rather than LFP spectra *per se*, the results showed correlations to be maximal in GPi, in line with the findings in this chapter. Another study only reported LFP findings from GPi (Liu et al., 2006).

4.4.2 Synchronization between LFPs and neuronal activity over 3-12 Hz

Our data confirmed that activity at 3-12 Hz in the LFP can be synchronized to neuronal discharge in the GPi in patients with primary dystonia and these cases is not the product of volume conduction of synchronous cerebral activity or due to movement artefact secondary to dystonic head or neck movements. The latter would also not explain the prominent of the 3-12 Hz activity in GPi. Thus, this chapter adds to the growing evidence that LFP recordings in the basal ganglia reflect, at least in part, synchronized current flow in a population of local neurons (Brown and Williams, 2005; Kuhn et al., 2005). On the other hand, it should be stressed that, while the LFP oscillations recorded in Gpi may be generated by synchronized local population activity, this is not necessarily imply that synchronization arises through intrinsic local network properties rather being driven by afferent to GPi.

Nevertheless, it is important to stress that we only recorded STAs with significant activity in the 3-12 Hz band in a small proportion (28%) of recording sites in GPi and that we have also recorded from patients with primary dystonia who have had

no significant STAs. This may be partly explained by methodological considerations. We used relatively conservative criteria to define STAs and based on these multiunit data that may have underestimated the incidence of LFP locking in STAs. This is because a central feature only appears in the STA if the different units comprising the multiunit activity have fairly similar phase relationship with the LFP.

4.4.3 Topographical distributions of LFP power

LFP power in the 3-12 Hz band tends to be greater in the GPi than GPe and STAs with component in this band almost exclusively limited to GPi. As this is the site where lesioning or high-frequency stimulation is most effective (Bittar et al., 2005; Krack and Vercueil, 2001; Lozano et al., 1997; Vidailhet et al., 2005; Vidailhet et al., 2007; Yianni et al., 2003), these topographical findings support a functional link between population synchrony in this band and dystonia. They also reinforce evidence from patients with Parkinson's disease pointing to a functional distinction between GPi and GPe (Krack et al., 1998; Starr et al., 2006; Vitek et al., 1999). Nevertheless, it remains unclear whether the link between pallidal activity over 3-12 Hz and dystonia relates to afferent information at the pallidal level or to a more direct influence on the motor drive to dystonic muscles. Note that LFP activity at similar frequencies occur during and, importantly, between paroxysms of dystonia in the *dr^{sz}* mutant hamster, suggesting that spectral change at low frequency are not merely a consequence of the attacks of dystonia and do not simply accompany afferent activity (Bennay et al., 2001; Gernert et al., 1998). It

may be relevant, therefore, that patients with primary dystonia have evidence of an abnormal descending drive to muscles at similar frequencies (Grosse et al., 2004; Tijssen et al., 2000; Tijssen et al., 2002).

4.5 Summary

1. We have demonstrated that pallidal oscillations at 3-12 Hz bands are maximal in GPi, the surgical target.
2. Spike triggered averages (STAs) indicated that discharge of neuronal activities were locked to 3-12 Hz oscillations in the LFP. All but two of these STAs were in GPi.
3. This lends support to a pathophysiological relationship between LFP activity at 3-12 Hz and dystonia.
4. The findings also have clinical implications. The low frequency oscillatory activity may provide intra-operative confirmation of GPi targeting in patients undergoing GPi DBS implantation for the treatment of dystonia, given that the correct placement of the DBS electrodes in the GPi region is difficult to confirm by intra-operative stimulation.

CHAPTER 5: Deep brain stimulation of the subthalamic nucleus: a two-edged sword

5.1 Introduction

Chronic high frequency stimulation of the subthalamic nucleus (STN) of the basal ganglia is a highly effective treatment for Parkinson's disease (PD) (for review see section 1.5). Such deep brain stimulation is thought to suppress spontaneous, including pathological, activity in the basal ganglia (Brown et al., 2001; Garcia et al., 2003; Garcia et al., 2005; Meissner et al., 2005; Wingeier et al., 2006). Equally, however, it must also remove any residual physiological function in these key motor structures. And yet there is paradoxically little evidence to suggest that the motor action of the limb is in any way further impaired by stimulation or even focal ablation of the STN in PD patients (Brown et al., 1999; Marsden and Obeso, 1994; Vaillancourt et al., 2004). This has led to the influential hypothesis that the human basal ganglia are not necessary for simple limb movement, but are particularly involved in more subtle and complex functions, such as the promotion of motor flexibility, that are not readily revealed by standard tests of motor behavior (Marsden and Obeso, 1994).

In this chapter we aimed to test the hypothesis that the basal ganglia are involved in processing simple limb movements in the human, by separating the effects of deep

brain stimulation on pathological and physiological activities based on baseline task performance.

Our hypothesis is straightforward:

6. Patients that, at the time of study, have performance in a simple motor task that is compromised by PD will improve with deep brain stimulation (Brown et al., 2001; Garcia et al., 2003; Garcia et al., 2005; Meissner et al., 2005; Wingeier et al., 2006).
7. In contrast, in those patients with relatively intact processing, as evidenced by a baseline performance within normal limits, deep brain stimulation would be expected to suppress the physiological processing and thereby impair the motor performance.

5.2 Methods

5.2.1 Patients and surgery

Thirteen patients participated in this study. Their clinical details are summarized in the table. The details of surgical techniques could be found in Section 2.2. The adjustment of the intended coordinates were made in accordance with the direct visualization of STN in individual stereotactic MRI in the patients who were operated in National Hospital for Neurology and Neurosurgery (cases 1-9), whereas in the patients in Taiwan (cases 10-13), the adjustment was made according to the

results of microelectrode recordings. Correct placement of the DBS electrodes in the region of the subthalamic nucleus was further supported by: [1] effective intra-operative macrostimulation; [2] post-operative T2 weighted MRI compatible with the placement of at least one electrode contact in the STN region; [3] significant improvement in UPDRS motor score during chronic DBS off medication ($23.6 \pm [\text{SEM}] 4.0$) compared to UPDRS off medication with stimulator switched off (51.6 ± 3.5 , $t=11.593$ $p<0.001$, paired t-test).

Age/ Sex	Disease Duration (years)	Predominant symptoms	UPDRS 3 Off Drug On/Off stim ≥6months post op	Pre-op medication	Post-op medication	Stimulations parameters
60/M	13	Off periods, gait freezing	4/41	L-dopa 1250 mg/d Ropinirole 20 mg/d Amantadine 100 mg/d	L-dopa 400 mg/d Ropinirole 8mg/d Amantadine 100 mg/d	Lstn: 1-, 2.1V, 60ms, 130 Hz Rstn; 5-, 2.1V, 60ms, 130 Hz
59/M	11	Off periods, gait freezing	20/46	L-dopa 600mg/d Cabergoline 3mg/d	L-dopa 600mg/d Cabergoline 3mg/d	Lstn: 0-, 2.8V, 60ms, 130 Hz Rstn; 5-, 3.3V, 60ms, 130 Hz
64/M	19	Off periods, gait freezing	13/39	L-dopa 1150 mg/d Pergolide 4m/d Apomorphine 3mg/d Entacapone 1000 mg/d	L-dopa 250 mg/d Pergolide 1 mg/d	Lstn: 2-, 3.0V, 60ms, 130 Hz Rstn; 5-, 3.3V, 60ms, 130 Hz

52/M	24	Off periods, gait freezing, tremor, dykinesia NB: L pallidotomy 1995	32/45	L-dopa 800 mg/d Pergolide 1.25 mg/d Trihexphenydy 6 mg/d Entacapone 800 mg/d	L-dopa 400 mg/d Cabergoline 4 mg/d Entacapone 800 mg/d	Lstn: 1-, 2.0V, 60ms, 180 Hz Rstn; 5-, 5.0V, 90ms, 180 Hz
51/F	19	Off periods gait freezing	12/52	L-dopa 700 mg/d Cabergoline 1 mg/d Apomorphine 20 mg/d	L-dopa 300 mg/d Cabergoline 3mg/d	Lstn: 2-, 3.3V, 60ms, 130 Hz Rstn; 5-, 3.0V, 60ms, 130 Hz
53/M	14	Off periods, gait freezing, rigidity, tremor	23/52	N.A.	L-dopa 100 mg/d Cabergoline 5 mg/d	Lstn: 2-, 3.2V, 60ms, 130 Hz Rstn; 5-, 2.4V, 60ms, 130 Hz
54/F	15	Off periods, dyskinesia	16/46	L-dopa 300 mg/d Cabergoline 5m/d	Ropinirole 34 mg/d	Lstn: 1-, 2.75V, 60ms, 145 Hz Rstn; 5-, 3.6V, 90ms, 145 Hz

62/F	9	Off periods gait freezing	20/37	L-dopa 800 mg/d Ropinirole 24 mg/d Entacapone 1200 mg/d	L-dopa 750 mg/d Ropinirole 13 mg/d	Lstn: 1-, 3.5V, 60ms, 130 Hz Rstn; 4-, 2.5 V, 60ms, 130 Hz
61/M	20	Off periods gait freezing, rigidity, tremor. NB Unable to perform task with left hand due to severe tremor	12/56	L-dopa 800 mg/d Ropinirole 36 mg/d	L-dopa 700 mg/d	Lstn: 1-, 3.0 V, 60ms, 185 Hz Rstn; 5-, 3.5V, 60ms, 185 Hz
61/M	19	Off periods, akinetic-rigid, drug-induced hallucination	58/82	L-dopa 1200 mg/day	L-dopa 600 mg/day Pergolide 1mg/day	Lstn: 0+ 1-, 3.3 V, 60ms, 130 Hz Rstn; 6-, 3.2V, 60ms, 130 Hz
67/M	16	Off periods, akinetic-rigid, tremor	38/69	L-dopa 1875 mg/day	L-dopa 300 mg/day Ropinirole 8 mg/day	Lstn: 2-, 3.3 V, 60ms, 145 Hz Rstn; 2-, 3.0V, 60ms, 130 Hz (ltrel 2)

67/M	20	Off period, akinetic-rigid, tremor, dyskinesia	35/60	L-dopa 1400 mg/day Pergolide 1 mg/day Amantadine 100 mg/day	L-dopa 400 mg/day Amantadine 100 mg/day	Lstn: 3-, 3.3 V, 60ms, 130 Hz Rstn; 7-, 3.5V, 60ms, 130 Hz
60/M	13	Off period, dyskinesia	24/46	L-dopa 1000 mg/day Pergolide 3 mg/day Amantadine 300 mg/day	L-dopa 200 mg/day Pergolide 0.5 mg/day Amantadine 300 mg/day	Lstn: 2-, 3.3 V, 60ms, 145 Hz Rstn; 6-, 3.0V, 60ms, 135 Hz

Table 5.1. Clinical details of patients.

5.2.2 Protocol

All patients were assessed after overnight withdrawal of anti-parkinsonism medication. Patients were studied when the stimulator was switched off and during bilateral STN stimulation at 130 Hz. The stimulation types were assessed in pseudo-randomised order across patients, as was the presentation order of trials within a stimulation type. Stimulation contacts, amplitude and pulse width were the same as utilized for therapeutic high frequency stimulation in each subject (see Table). Patients were not informed of the stimulation type. We did not stimulate one side at a time to avoid possible functional compensation by the non-stimulated side. We waited ~20 minutes after changing between conditions (no DBS or bilateral DBS) before testing. This is sufficient to elicit about 75% of DBS effects. Tapping was performed in two runs of 30 s, separated by ~30 seconds rest and each hand tested separately (giving four runs per condition). Data from two sides were rejected; one contralateral to previous unilateral pallidotomy (case 4 in Table) and the other because severe rest tremor prevented tapping (case 9 in Table). The number of the taps made with the index finger in 30 s was recorded in two runs per hand for each condition and the run from each pairs with the best performance selected for analysis. Changes in tapping rate during DBS relative to no DBS was then calculated as $[(\text{taps per 30s on bilateral DBS} - \text{taps per 30s off DBS}) / (\text{taps per 30s off DBS})] * 100$. Thus the positive % change represented an improvement in performance with DBS.

Six healthy age matched control subjects (4 males, mean age 58 years, range 52-67 years) were also tested. The lower limit of the normal range in this control group was 138 taps per 30 s.

5.2.3 Statistical analysis

Absolute and percentage change in tapping rates were normally distributed (One-sampled Kolmogorov Smirnov tests $p>0.05$). Correlation was performed by Person's correlation test. Significant data remained significant at $p<0.05$ after correction for multiple testing using the false discovery rate procedure.

5.3 Results

5.3.1 Dependency of deep brain stimulation effects on baseline performance

There was a striking correlation between baseline performance in the task and percentage change with deep brain stimulation. A negative correlation ($r=-0.742$, $p<0.001$) between % change in tapping rate of each hand with deep brain stimulation and tapping rate prior to onset of deep brain stimulation was found. Those sides showing the best performance with deep brain stimulation actually slowed during stimulation, whereas those with poorer performance got quicker in the task (Figure 1A).

Next, we divided sides into two groups according to whether or not tapping performance off deep brain stimulation was within the normal limits established in 12 sides in six healthy age-matched subjects (see methods). Tapping rates were confirmed to improve on those sides where performance was compromised by parkinsonism at the time of study, but deteriorated on those sides in which tapping rates were within normal limits, whether absolute (Figure 1B) or percentage change (Figure 1C) tapping rates were considered.

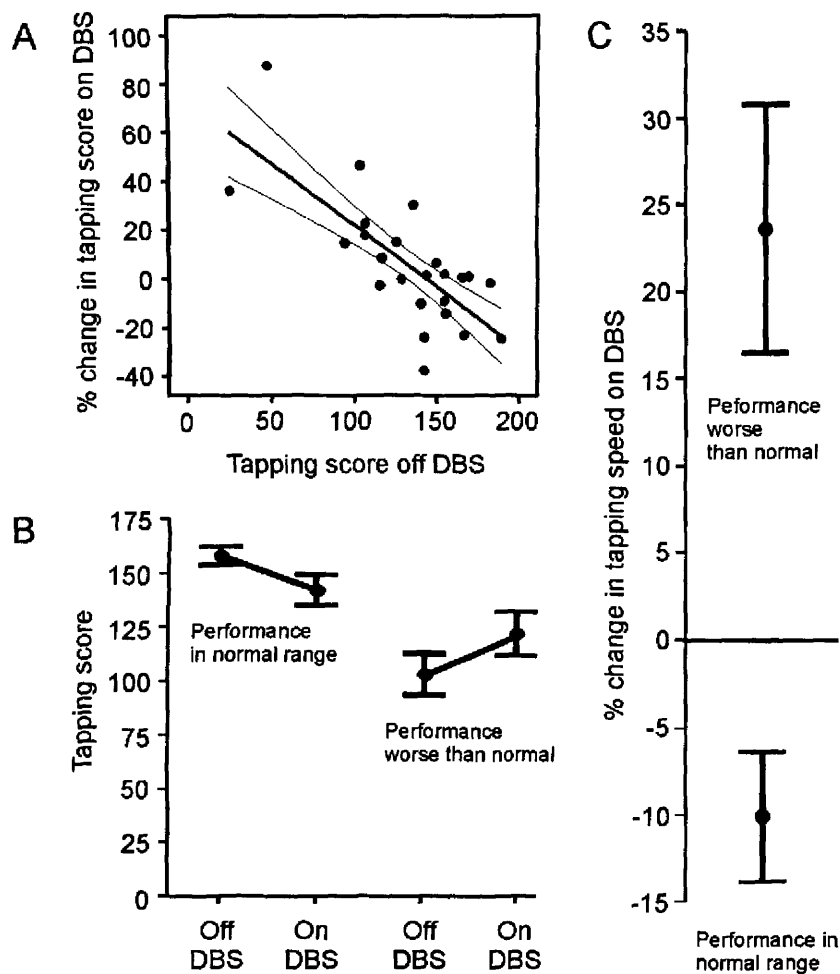


Figure 5. 1. Dependency of deep brain stimulation effects on baseline performance.

(A) Negative correlation (thick line, $r=-0.742$, $p<0.001$) between % change in tapping rate of each hand with deep brain stimulation and tapping rate prior to onset of deep brain stimulation. Positive % change =improvement with deep brain stimulation. Thin lines=95% confidence limit. N=24 tapping sides in 13 patients (right hand rejected from case 4 as contralateral to previous pallidotomy and tapping made impossible by tremor in the left hand in case 9). (B) Mean (\pm s.e.m.) tapping rate off and on deep brain stimulation in hands with baseline tapping performance within ($n=13$) or less than ($n=11$) normal range (difference on and off deep brain stimulation $p=0.018$ and $p=0.003$, respectively, two-tailed paired t-tests). (C) Mean (\pm s.e.m.) % change in tapping rate with deep brain stimulation in hands with baseline tapping performance within or less than normal range ($p<0.001$ for difference between groups, unpaired two-tailed t-test and $p=0.019$ and $p=0.008$ for each group differing from zero, two-tailed one-sample t-test).

5.3.2 Reproducibility of the results

Finally, we confirmed the reproducibility of our finding by repeating the experiments on seven patients (13 sides) with PD. Again there was a negative correlation ($r=-0.558$, $p=0.048$) between the percentage change in tapping rate of each hand with deep brain stimulation and tapping rate prior to the onset of deep brain stimulation. More importantly, tapping rate deteriorated on those six sides in which performance was within normal limits without deep brain stimulation,

whether absolute (tapping rate 154.7 ± 3.3 off deep brain stimulation, 144.5 ± 5.5 , $p=0.02$, unpaired two-tailed t test) or percentage change (mean % deterioration 6.7 ± 2.1 , $p=0.025$, two tailed t-test) tapping rate were considered.

5.4 Discussion

5.4.1 Differing effects of high frequency stimulation in basal ganglia

The principle finding in this chapter is the striking negative correlation between the percentage change in tapping rate of each hand with deep brain stimulation and tapping rate prior to the onset of stimulation. Thus, sides with performance compromised at the time of study improve with deep brain stimulation. It is the subthalamic nuclei contralateral to these sides that are likely to have the most pronounced pathological synchronization at the time of testing and, in line with this, there is a linear relationship between pathological synchronization as evidenced by oscillatory activity in the STN local field potential and motor impairment (Kuhn et al., 2006). Subjects with existing difficulties therefore have more to gain from the suppression of local activity. On the other hand, sides with relatively normal performance in a given task are likely to have less contralateral pathological synchronization at the time of study, so that the effect of suppression of physiological activity dominates motor performance during deep brain stimulation. Simple tapping was slowed in these subjects. Although the degree of slowing was relatively small and likely to be overlooked in retrospective

assessments of the effects of basal ganglia lesions (Bhatia and Marsden, 1994), it was reproducible in our paired comparisons using reversible functional blockade . Indeed, the slowing in tapping rate observed here may represent the lower limit of basal ganglia function in the task, as this is the impairment despite any compensation by other motor systems.

We infer that the basal ganglia are involved in processing of simple limb movements in humans, something that could not be assumed by the ‘release’ phenomena of improvement in motor performance in parkinsonian patients following local lesioning/deep brain stimulation or development of hemiballismus in previously healthy subjects after subthalamic infarction (Bhatia and Marsden, 1994). The finding is in keeping with the increasing evidence from focal recordings that activity in the STN of patients with PD changes prior to and during simple movements of the upper limb (Brown and Williams, 2005), although these studies by themselves only suggest and do not approve the involvement of basal ganglia in these tasks. Only a behavioral approach, showing a decrement in motor performance, as here, can prove that the basal ganglia are necessary for the normal execution of simple limb movement.

Hitherto, evidence of impairment of performance during STN deep brain stimulation has been limited to selected cognitive tasks (Hershey et al., 2004; Jahanshahi et al., 2000) and to occasional reports of diminished intelligibility of speech (Rousseaux et al., 2004). Interestingly, a recent study investigated whether

the human STN was involved in offline feedback control of voluntary movement (Brown et al., 2006). In this study, patients were engaged in a 'PC' game (Papakostopoulos, 1978), in which they had to produce a movement under circumstances that required temporal accuracy. The results showed that the disruption of the STN activity by stimulation at high frequency compromised the feedback-based modulation of motor performance compared to performance prior to deep brain stimulation.

5.4.2 Clinical implications of the current findings

The negative correlation between the percentage change in task performance with deep brain stimulation and performance prior to onset of deep brain stimulation also has important therapeutic implications. First, it suggests that the efficacy of deep brain stimulation in patients with mild PD may be limited and counsels against the use of this intervention very early in the course of the disease, whether or not to slow future deterioration (Benabid et al., 2005). Second, it suggests that the effectiveness of deep brain stimulation in PD may be improved by using an on-demand mode, possibly with stimulation being triggered by the level of pathological local field potential activity in the STN . Continuous stimulation, as utilized recently, may even impair performance in tasks relatively spared by parkinsonism or temporarily improved by concurrent medication.

5.5 Summary

1. Human basal ganglia are involved in processing of simple limb movement.
2. High frequency stimulation in STN has a dual effect in patients with PD, subject to the baseline performance of patients without stimulation; first, high frequency stimulation ameliorates behavioral impairments because of dopaminergic denervation and consequent abnormal functioning of STN. Second, high frequency stimulation can disturb remaining physiological STN function, such as those contributing to simple limb movements.
- 3 There is a negative correlation between change in task performance with deep brain stimulation and performance prior to onset of deep brain stimulation.

CHAPTER 6: Excessive synchronization of basal ganglia neurons at 20 Hz slows movement in Parkinson's disease

6.1 Introduction

What is the nature of pathological activity in Parkinson's disease (PD)? In Section 1.2 and 1.3 we have stressed the recent shift of attention from changes in discharge rate to elevations in population synchrony in the basal ganglia of patients with PD (Uhlhaas and Singer, 2006). In particular, recordings in the subthalamic nucleus (STN) in PD patients have consistently revealed prominent oscillations in the local field potential (LFP) in a broad 'beta' frequency band centered around 20 Hz (Alegre et al., 2005; Alonso-Frech et al., 2006; Amirnovin et al., 2004; Brown et al., 2001a; Cassidy et al., 2002; Fogelson et al., 2006; Kuhn et al., 2006; Kuhn et al., 2004; Levy et al., 2002a; Priori et al., 2002; Silberstein et al., 2003; Weinberger et al., 2006; Williams et al., 2005; Williams et al., 2002). These oscillation likely reflect summed activity in synchronized and local neuronal elements, and in accordance with this, local neuronal discharges are locked to the oscillatory LFP activity (Kuhn et al., 2005; Levy et al., 2002b; Wingeier et al., 2006) and to one another (Amirnovin et al., 2004; Levy et al., 2000; Wingeier et al., 2006) in the beta frequency band. There is increasing correlative evidence to suggest this form of synchronization in the basal ganglia is associated with impairment of movement (Alonso-Frech et al., 2006; Dostrovsky and Bergman, 2004; Kuhn et al., 2006; Kuhn et al., 2004; Williams et al., 2005) and that it is this activity that may be

suppressed by dopaminergic therapy (Brown et al., 2001b; Priori et al., 2002; Silberstein et al., 2003) and deep brain stimulation (Brown et al., 2004; Wingeier et al., 2006), thereby improving function. However, the correlative evidence linking excessive synchrony in the beta band with parkinsonism cannot distinguish between a causal or epiphenomenal association. Proof of principle that excessive beta synchrony contributes to parkinsonism would require the demonstration of a significant deterioration in motor performance during direct stimulation of the STN in the beta band.

That STN stimulation can simultaneously suppress local neuronal activity and enforce some degree of synchronization through direct activation of local axons with one-to-one following of stimulation rates is suggested by model-based analyses (Brown et al., 2004; McIntyre et al., 2004; Miocinovic et al., 2006; Wingeier et al., 2006), in vitro recordings (Garcia et al., 2003; Garcia et al., 2005), simultaneous recordings from globus pallidus interna (Brown et al., 2004; Hashimoto et al., 2003) and from effects evoked in cerebral cortex and muscle (Ashby et al., 1999; Ashby et al., 2001; MacKinnon et al., 2005). However, a previous attempt at stimulating the STN in the beta band was only able to show a relative rather than absolute deterioration in task performance with stimulation, superimposed upon a more striking linear improvement in performance with increasing stimulation frequency (Fogelson et al., 2005). This study therefore suggested the hypothesis that DBS in the beta band might have two effects,-a frequency selective impairment in task performance due to the synchrony imposed

by electrical stimulation and a confounding ameliorative effect. The latter meant that performance did not fall significantly below baseline levels during stimulation at 20 Hz and the study fell short of the desired 'proof of principle'.

Thus, attempts to demonstrate any deleterious effects of direct stimulation at 20 Hz should take into account any simultaneous ameliorative effects of stimulation at this frequency (all be they less marked than with higher frequency stimulation as demonstrated in Chapter 5). Moreover, the frequency selectivity of any potential effect of stimulation at 20 Hz should be established, so as to distinguish it from the impairment of motor performance in selected patients during high frequency stimulation as shown in Chapter 5, where it was suggested that deterioration was due to the suppression of physiological task-related activity in the STN during stimulation.

One possible way to separate any disruptive effects of STN stimulation from any possible therapeutic action is to consider the level of baseline performance at the time of study, as this may index the level of spontaneous pathological activity and determine which effect of stimulation dominates as described in Chapter 5. Thus, the effects of suppression of pathological activity may dominate and patients improve with stimulation where baseline performance is poor and spontaneous pathological synchronization likely prevails. On the other hand, pathological activity is likely minimal when baseline performance is relatively intact. Under this circumstance, the deleterious effects of suppression of physiological activity may

prevail with stimulation at high frequency or those of direct synchronization at 20 Hz dominate with stimulation in the beta band. In this chapter we investigated whether stimulation at 20 Hz can have significant deleterious effects on motor function in PD patients with relatively preserved performance, and whether this effect can be distinguished from that seen with stimulation at higher frequencies in similar patients as examined in Chapter 5.

6.2 Methods

6.2.1 Patients and surgery

Twenty-two patients participated in this study. The surgical procedure and the method utilized to adjust the placement of electrodes were described in Chapter 2. There was a significant improvement in UPDRS motor score during chronic DBS off medication ($26.4 \pm [\text{SEM}] 3.5$) compared to UPDRS off medication with stimulation switched off (53.1 ± 3.0 , $t=13.030$, $p<0.001$, paired t-test).

Case	Age/ Sex	Disease Duration (years)	Main symptoms	UPDRS 3 Off Drug On/Off stim ≥6 months post op	Pre-op medication	Post-op medication	Stimulations parameters
1	60/M	13	Off periods, gait freezing	4/41	L-dopa 1250 mg/d Ropinirole 20 mg/d Amantadine 100 mg/d	L-dopa 400 mg/d Ropinirole 8mg/d Amantadine 100 mg/d	Lstn: 1-, 2.1V, 60µs, 130 Hz Rstn: 5-, 2.1V, 60µs, 130 Hz
2	58/M	20	Off periods, gait freezing, rigidity, drug induced dyskinesia	5/26	L-dopa 700 mg/d Ropinirole 10 mg/d Apomorphine 84 mg/d Amantadine 200 mg/d	L-dopa 800 mg/d Ropinirole 15 mg/d Amantadine 200 mg/d	Lstn: 1-, 3.0 V, 60µs, 130 Hz Rstn: 6-, 2.5V, 60µs, 130 Hz
3	57/M	14	Off periods, gait freezing	20/51	L-dopa 700 mg/d Cabergoline 2 mg/d Amantadine 300 mg/d Entacapone 600 mg/d	L-dopa 600 mg/d Cabergoline 2 mg/d Amantadine 200 mg/d	Lstn: 1-, 3.3 V, 60µs, 130 Hz Rstn: 5-, 3.3 V, 60µs, 130 Hz
4	52/M	24	Off periods, gait freezing, tremor, dyskinesia NB: L pallidotomy 1995	32/45	L-dopa 800 mg/d Pergolide 1.25 mg/d Trihexphenidyl 6 mg/d Entacapone 800 mg/d	L-dopa 400 mg/d Cabergoline 4 mg/d Entacapone 800 mg/d	Lstn: 1-, 2.0V, 60µs, 180 Hz Rstn: 5-, 5.0V, 90µs, 180 Hz
5	68/M	22	Off periods, gait freezing, rigidity	6/48	L-dopa 800 mg/d Pergolide 6 mg/d Entacapone 1200 mg/d Selegeline 10mg/d	L-dopa 500 mg/d Pergolide 3 mg/d	Lstn: 1-, 3.0 V, 60µs, 130 Hz Rstn: 5-, 3.5V, 60µs, 130 Hz
6	53/M	14	Off periods, gait freezing, rigidity, tremor	23/52	L-dopa 300 mg/d Cabergoline 2 mg/d	L-dopa 350 mg/d Cabergoline 2 mg/d	Lstn: 2-, 3.2V, 60µs, 130 Hz Rstn: 5-, 2.4V, 60µs, 130 Hz
7	54/F	15	Off periods, dyskinesia	16/46	L-dopa 300 mg/d Cabergoline 5mg/d	Ropinirole 24 mg/d	Lstn: 1-, 2.75V, 60µs, 145 Hz Rstn: 5-, 3.6V, 90µs, 145 Hz
8	61/M	20	Off periods gait freezing, rigidity,	12/56	L-dopa 800 mg/d Ropinirole 18 mg/d	L-dopa 700 mg/d	Lstn: 1-, 3.6 V, 60µs, 185 Hz Rstn: 5-, 3.5V, 60µs, 185 Hz

Table 6.1. Clinical details of patients.

6.2.2 Protocol

All patients were assessed after overnight withdrawal of antiparkinsonian medication, although the long-action of many of the drug used to treat PD meant that patients may still have been partially treated when assessed. They were studied when the stimulator was switched off and during bilateral STN stimulation at 20 Hz, 50 Hz and 130 Hz. The stimulation types were assessed in pseudo-randomised order across patients, as was the presentation order of trials within a stimulation type. Stimulation contact, pulse width and amplitude were the same as utilized for therapeutic high frequency stimulation in each patient (see Table 1). There was no evidence of capsular spread during stimulation, as determined by clinical examination. Patients were not informed of the stimulation type. Why we did not stimulate one side and wait ~ 20 minutes after changing between conditions was discussed in Chapter 5.

6.2.3 Task

The details of the task are given in Chapter 2. Tapping data from one side were rejected as these were collected contralateral to a previous unilateral pallidotomy (case 4 in Table 1) and were also rejected from another side where tapping was obviated by severe tremor (case 8 in Table 1). The number of taps made with the index finger in 30 s was recorded and the run from each pair with the best

performance selected for analysis, as this was less likely to be affected by fatigue, or the effect of impaired arousal/concentration.

6.2.4 Statistical analysis

Ten healthy age matched control subjects (20 sides, 4 males, mean age 57 years, range 52-64 years) were also tested. The lower limit of the normal range (*e.g.* mean-[2*standard deviation]) in this control group was 127 taps per 30 s. Tapping sides were divided into those with baseline performance within normal limits (the mean tapping performance across this group, 152 taps/30s, was still lower than the mean tapping performance in healthy subjects of 162 taps/30s) and those with baseline tapping rates lower than normal limits ($n=15$, 10 sides were in patients operated in Taiwan). Nine subjects had sides distributed across the two groups. Tapping rates were normally distributed (One-sample Kolmogorov Smirnov tests $p>0.05$). Repeated measures of ANOVAs with within subjects simple contrasts (comparing different frequencies of stimulation to no stimulation) were performed in SPSS. Within-subjects contrasts were planned, so correction for multiple comparisons was unnecessary. However, a single *post-hoc* paired two-way t-test was also performed to compare tapping during stimulation at 20 Hz with that during 50 Hz stimulation in those subjects with good baseline performance. Non-sphericity was corrected where unnecessary using the Greenhouse Geisser correction. For correlations with baseline tapping performance change in tapping rate during DBS relative to no DBS was calculated as [taps per 30s on bilateral

DBS-taps per 30s off DBS]. Thus a positive change represented an improvement in performance with DBS. Linear regression was performed in SPSS.

6.3 Results

6.3.1 Dependency of stimulation effects on baseline performance

We divided the tapping sides into two groups according to whether or not tapping performance off DBS was within normal limits established in 20 sides in 10 healthy age-matched subjects (Fig.1). An ANOVA of tapping scores with factors FREQUENCY (four levels: 0, 20, 50 and 130 Hz) and BASELINE TAPPING PERFORMANCE (two levels: within normal limits and less than normal limits) demonstrated an interaction between FREQUENCY and BASELINE TAPPING PERFORMANCE ($F_{[3,120]} = 7.336, p < 0.001$, as well as an additional effect of FREQUENCY; $F_{[3,120]} = 6.264, p = 0.001$). Accordingly, the data were further analysed with separate GLMs for each baseline tapping performance group. In those patients with baseline tapping performance within normal limits an ANOVA with factor FREQUENCY (four levels: 0, 20 50 and 130 Hz) confirmed that the latter was a significant main effect ($F_{[3, 78]} = 3.116, p = 0.031$). Within subjects contrasts indicated that tapping during 20 Hz stimulation was worse than during no stimulation ($F_{[1, 26]} = 6.921, p = 0.014$). The average deterioration in tapping rate during 20 Hz stimulation in this group was $8.2 \pm 3.2\%$. However, tapping during 50 Hz and 130 Hz stimulation was no different to that during no stimulation ($F_{[1, 26]}$

=0.519, $p=0.478$ and $F [1, 26] = 2.411$, $p=0.113$, respectively). A single *post-hoc* paired two-way t-test confirmed that tapping during stimulation at 20 Hz was worse than 50 Hz stimulation ($t_{[df\ 26]} = 2.094$, $p=0.046$), so that the deleterious effects of stimulation upon task performance were frequency selective within this group.

In those patients with baseline tapping performance below normal limits an ANOVA with factor FREQUENCY (four levels: 0, 20, 50 and 130 Hz) also confirmed that the latter was a significant main effect ($F [1.74, 24.278] = 7.477$, $p=0.004$; Fig 1). Within subject contrast indicated that tapping during 20 Hz stimulation was no different to that during no stimulation ($F [1, 13] = 2.346$, $p=0.148$). There was a trend for tapping during 50 Hz to be better than during no stimulation ($F [1, 14] = 3.226$, $p=0.094$) and 130 Hz was clearly improved (by $67\pm 25\%$) relative to no stimulation ($F [1, 14] = 23.831$, $p<0.001$).

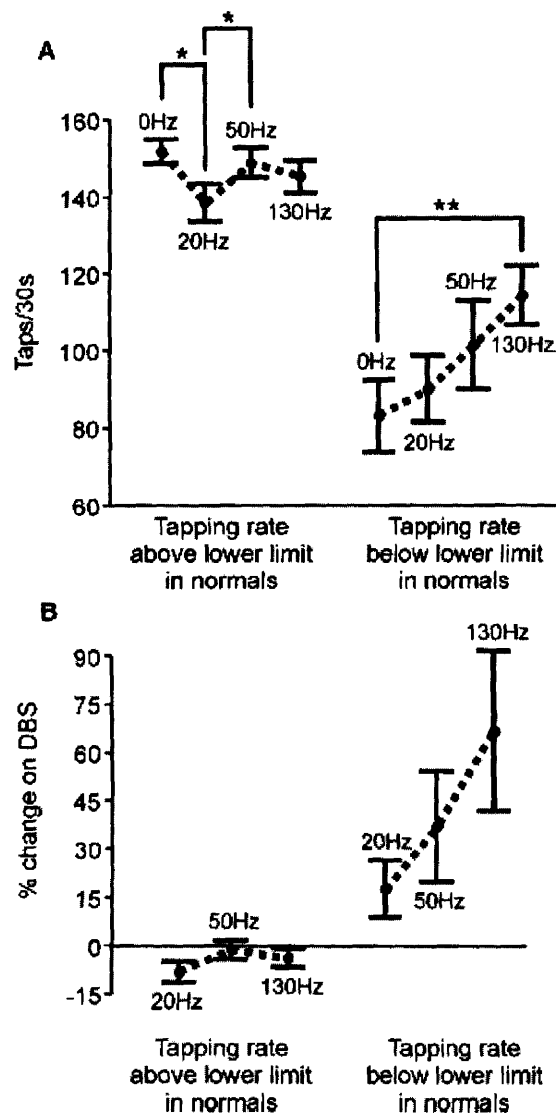


Figure 6.1. Dependence of stimulation effects on baseline performance. [A] Mean (\pm s.e.m.) tapping rate off ('0 Hz') and on stimulation at 20, 50 and 130 Hz in hands with baseline tapping performance within normal range (left) and below normal range (right). In those sides with baseline performance within normal limits tapping during 20 Hz

stimulation was worse than without stimulation or stimulation at 50 Hz. In those sides with baseline performance below normal limits tapping during stimulation at 130 Hz was better than without stimulation. $* < 0.05$, $** < 0.001$. [B] Mean (\pm s.e.m) % change in tapping rate on stimulation at 20, 50 and 130 Hz relative to baseline performance in hands with baseline performance within normal range (left) and below normal range (right). Negative % change means a drop in tapping rate in stimulation.

6.3.2 Correlation between change in tapping during DBS and baseline tapping performance

In the above analysis we divided tapping performance in patients into two groups with respect to the lower limit of performance in healthy controls. Next we determined the extent to which the different responses to stimulation in these two groups depended on the chosen cut-off point between the two groups. Figure 2 shows the correlation between the change in tapping performance during stimulation at different frequencies and baseline tapping performance. The relationship could be described using a linear model in each case ($p < 0.001$), but more important is the distribution of sides in which tapping performance deteriorated during stimulation (show in red in scatter plots). These sides tended to be those with the best baseline performance. Whether or where this distribution was significant for each frequency of stimulation was tested using serial two-tailed paired t-tests of cumulative tapping rates with and without stimulation (shown by red line graphs which run from right to left in the log probability plots). This

demonstrated that there was a significant impairment of tapping rates during stimulation at 20 Hz and 130 Hz for sides with baseline tapping rates ≥ 51 taps/30s and ≥ 135 taps/30s (*i.e.* above the lower limit of performance in our healthy controls, and therefore missed with our chosen cutoff in the above ANOVAs), respectively. In contrast, stimulation at 50 Hz did not consistently impair tapping, regardless of baseline performance. Thus the deleterious effect of stimulation at 20 Hz was robust over a wide range of baseline performance. In contrast, the deleterious effect of stimulation at 130 Hz, although significant, was limited to only those sides with the very best performance at baseline.

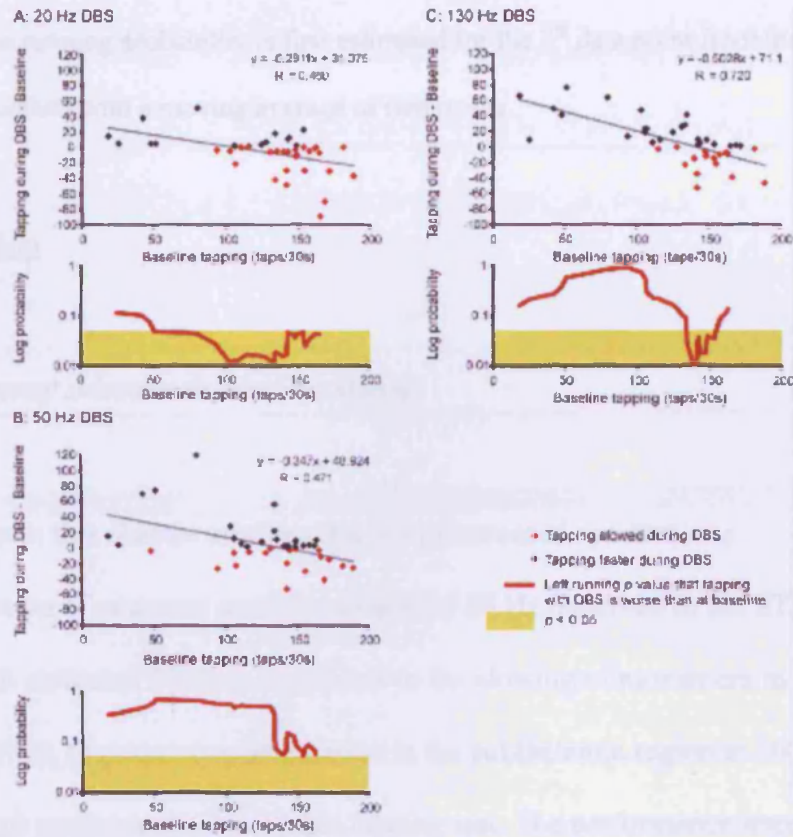


Figure 6.2. Correlation between change in tapping rate during DBS and baseline tapping performance. [A]. Bilateral stimulation of STN at 20 Hz. [B]. Stimulation of STN at 50 Hz. [C]. Stimulation at 130 Hz. Upper panels are correlations. All correlations are significant ($p < 0.001$). Correlation coefficient, r , and regression equation are shown. Lower panels are

left running probabilities (red lines) representing the probability that tapping during DBS is slower than baseline (serial two-way paired t-tests) for the data point shown and those to the right. This running probability is first estimated for the 7th data point from the right and has been smoothed with a moving average of two points.

6.4 Discussion

6.4.1 Frequency selective deleterious effects

The findings in this chapter confirm that the pronounced spontaneous synchronization of neuronal activities at around 20 Hz observed in the STN of patients with untreated PD may contribute to the slowing of movement in this condition. Thus, imposed synchronization in the subthalamic region at 20 Hz was able to impair performance in a simple tapping test. The performance impairment was relatively frequency dependant as it was absent with stimulation at 50 Hz. The latter would also appear to rule out a deleterious effect due to capsular spread of stimulation, the effect of which would be expected to be greater at 50 Hz than 20 Hz.

6.4.2 Dual effects of 20 Hz stimulation

The overall impairment of tapping performance during imposed synchronization at 20 Hz was limited to those sides with relatively preserved baseline tapping performance (see also Chapter 5 and Brown et al., 2006 for similar observation).

This seems reasonable, as pathological activity is likely minimal when baseline task performance is relatively intact. Under these circumstances, the deleterious effect of direct stimulation at 20 Hz dominated. In contrast, synchronization at 20 Hz did not impair function on those sides with poor baseline performance.

Significant spontaneous activity is likely in these cases, so perhaps the effects of any additional synchronization was limited by ceiling effects. In addition, it is possible that direct stimulation at 20 Hz has a dual effect; a direct driving of efferent axons and a simultaneous suppression of spontaneous, local background activity,-similar but weaker to the dual effects of stimulation reported in vitro (Garcia et al., 2003; Garcia et al., 2005) and in vitro (Brown et al., 2004; Filali, 2004; Fogelson et al., 2005). These effects may tend to cancel each out when spontaneous pathological activity is significant.

6.4.3. Limitations of the experiment

Even among those sides with relatively preserved baseline tapping function, the degree of slowing due to 20 Hz stimulation was relatively small,-about 8%.

Perhaps it is not surprising as DBS is likely to provide a poor stimulation of spontaneous beta synchrony, which occurs simultaneously at many nodes in the basal ganglia-loop in PD (Brown et al., 2001b; Fogelson et al., 2006; Williams et al., 2002), and may involve multiple discharge with each cycle of the endogenous rhythm (see Fig 1 in Levy et al., 2002 and Fig 1 in Kuhn et al., 2005). In contrast, direct stimulation is relatively focal and only involves a single pulse in each

stimulation cycle. In addition, it is possible that the effects of imposed synchrony were partially obscured by any simultaneous suppression of spontaneous pathological synchrony (see above). Finally, higher stimulation voltage and/or longer pulse durations may have lead to greater impairment of tapping during 20 Hz stimulation, but we elected to keep these parameters the same as those used clinically, to avoid capsular effects.

6.4.4 Differing mechanism underlies the deleterious effects induced by high and low frequency stimulation

The slowing of motor performance during subthalamic nucleus stimulation at 20 Hz must be distinguished from impairments of performance due to the suppression of physiological activity in patients with good baseline performance at the time of study (see Chapter 5 and Brown et al., 2006)). The suppression of physiological activity will lead to impairment in task performance that increases with increasing frequencies of stimulation, and so does not explain the lack of deleterious effect of stimulation at 50 Hz, despite worsening at 20 Hz. However, the suppression of physiological activity may explain the worsening seen in patients with the very best baseline performance during stimulation at 130 Hz in this chapter.

6.5 Summary

1. Task performance was slowed during 20 Hz stimulation in the subthalamic

nucleus in PD patients with relatively preserved baseline function in the task.

2. The worsening of the task performance with stimulation at 20 Hz may be the consequence of the imposed synchronization of efferent axons in the vicinity of stimulation.
3. The data in this chapter provide proof of principle that excessive beta synchrony within the basal ganglia-cortical loop may contribute to the slowing of movement in Parkinson's disease.

CHAPTER 7: Intraoperative recording of local field potential can help localize the subthalamic nucleus in Parkinson's disease surgery

7.1 Introduction

High frequency 'deep brain stimulation' (DBS) of the subthalamic nucleus (STN) can be an effective treatment in Parkinson's disease (for review see Section 1.5; The Deep-Brain stimulation for Parkinson's Disease Study Group 2001). However, therapeutic efficacy is limited by consistently and correctly targeting the STN, particularly the 'motor' domain of this nucleus, while side effects may, in part, relate to poor positioning of electrodes. Single cell microelectrode recordings of the activity of local neurons were introduced to facilitate the targeting and generally remain an important element of the surgical procedure (Hutchison et al., 1998). However, their use may considerably prolong surgery, does not always lead to satisfactory targeting and has been associated with an increased risk of intra-operative hemorrhage (Alkhani and Lozano, 2001; Binder et al., 2005; Hariz and Fodstad, 1999). In addition, microelectrodes must be withdrawn prior to introduction of the DBS electrode, which may introduce targeting errors, especially in the vertical plane. Thus, an electrophysiological signature of STN activity that could be directly and intra-operatively recorded from the DBS electrode would be of considerable potential value.

Although DBS electrodes can not be used to record single neurons, they are suitable for recording aggregate activity of neuronal populations in the form of local field potentials (LFPs). The LFPs recorded from STN in patients with Parkinson's disease (PD) are increasingly recognized as being characterized by prevalent activity in the so-called beta frequency (~20 Hz) band. The focal nature of this beta activity has been demonstrated in patients through microelectrode recordings, polarity reversal in bipolar macroelectrode recordings and correlation with post-operative MRI. Moreover, the recording of this activity in STN has been confirmed histologically in rats with 6-hydroxydopamine (6-OHDA) lesions of midbrain dopamine neurons, an established rodent model of parkinsonism. Thus, an increase in beta activity may be a marker of the parkinsonian STN, particularly the dorsolateral (sensorimotor) portion of the nucleus, which, based on inactivation studies in 1-methyl-4-phenyl-1, 2, 3, 6-tetrahydropyridine treated primates is considered the optimal target. In this chapter, we hypothesized that spontaneous beta LFP activity can be recorded intra-operatively from DBS electrode contacts in the STN of PD patients and that the contact exhibiting the spontaneous activity of the highest amplitude would lie in the 'sensorimotor' STN. This LFP 'signature' of STN would prove useful in the intra-operative confirmation of electrode placement in STN.

7.2 Methods

7.2.1 Patients and surgery

Nine patients participated in this study (5 males; mean age 56.9 ± 4.3 years, range 51-63). All had advanced idiopathic PD with motor fluctuation and/or dyskinesias. The mean disease duration was 13 years (range 8-23 years). One patient had a right pallidotomy nine years ago. The mean Unified Parkinson's Disease Rating Scale (UPDRS) motor score was 40 ± 24 off drugs and 9 ± 8 after levodopa treatment ($p < 0.01$, two tailed t-test). Implantation of bilateral STN DBS electrodes was performed in the same operative session under local anesthesia in all patients for treatment of PD. Patients were operated on after overnight withdrawal of their anti-parkinsonian medication. The DBS electrode used was model 3389 (Medtronic Division, MN); details of this electrode can be found in Chapter 2. Fast acquisition T2 weighted axial and coronal stereotactic MRI scan using Leksell's Frame (Elekta, Sweden) were performed with contiguous slices of 2 mm thickness. This visualized the STN and especially its medial border. The anatomical target point within the centre of STN was selected at a level 1 mm in front of the anterior border of the red nuclei on the axial image showing the largest diameter of the red nucleus. Contact 0 was intended to reach this point. The double oblique trajectory to the target was planned on the coronal images to avoid entry into the ventricles. Calculations of Cartesian coordinates of the target point were performed both manually on enlarged MRI film copies and on the Framelink software (Medtronic, Minneapolis). The DBS electrode was advanced with steps of 2 mm from 4-6 mm above to 4 mm below the intended target point. Rigidity at the wrist \pm bradykinesia of the hand was assessed at each step contralateral to the DBS electrode by an

experienced neurologist. An intra-operative stun effect was determined by a definite, sudden sustained reduction in rigidity and /or onset of dyskinesias occurring shortly after an electrode step. Intra-operative high frequency test stimulation and further clinical evaluation of the patient were performed monopolarly at 1-3 selected levels (usually intended target and/or level of stun effect) to detect further clinical benefits as well as any side effects once the DBS electrode had completed its trajectory to 4 mm below target. No microelectrode recordings were made. Once the optimum target point for stimulation was identified, the electrode was fixed in position with the Medtronic burrhole cap or the Navigus system (Image Guided Neurologics, FL, USA). The same procedure was then repeated for the other side. Both electrodes were then attached to Medtronic cables with the distal ends externalized. All patients received immediate post-operative stereotactic MRI to confirm the location of the DBS electrode. Electrodes were then connected to a battery-operated programmable pulse generator (Kinetra 7428, Medtronic).

7.2.2 Recordings

Recordings were made continuously from 4-6 mm above to 4 mm below the intended target in descending 2 mm steps. Each level was maintained for 60-65 s. STN LFPs were recorded bipolarly from the four adjacent contacts of each DBS electrode (contact pairs 01, 12, 23). The spatial resolution of such a chain of different recordings is about 2 mm. Signals were amplified, pass band filtered

between 1 and 80 Hz and sampled at 184 Hz (Biopotential Analyzer Diana, St Petersburg, Russia). Purpose written software saved the original time series on a portable PC and displayed on-line the evolving patterns of beta band power from contact pairs 01, 12 and 23 as the DBS electrode was advanced. The on-line assessment was only performed to show that such evaluation of LFP activity is possible in real time. Neurosurgeons and neurologists remained blinded to this intra-operative LFP assessment. The recording and on-line assessment of beta power took, in total, 6-7 minutes per side.

Thereafter LFPs were examined off-line, and sections of visible artefact (movement artefact recorded during the descent between steps) were removed before frequency analysis was performed. In two patients (2 sides) the DBS electrode slipped ventrally an indeterminate few mm between steps of the recording track so that the DBS electrode had to be pulled back and the graded descent procedure restarted. Recording from the latter two sides, were rejected so that the analysed data set were known to be from penetration through an otherwise undisturbed, hereafter termed 'virgin' trajectory. Sixteen recordings were analysed from such virgin trajectories. Spectra of LFP power was estimated in Spikes2 using the discrete Fourier transform (see Chapter 2 for details). LFP power was determined over successive (non-overlapping) 0.7 s blocks for the three contact pairs. 84.9 ± 0.4 blocks were available for each step.

7.2.3 Post-operative radiological reconstruction of contact placement

Post-operative stereotactic imaging was performed using fast spin-echo T2 weighted axial and coronal MRI scans with contiguous slices of 2 mm thickness. Contact localization was performed on commercial dedicated software (FrameLink TM, Medtronic Inc.) The centre of the electrode artefact on post-operative images was used to calculate the coordinates of the DBS electrode contacts. The software allowed reconstruction of the imaging data in multiple planes, including trajectory views along the centre of the electrode contacts. In such views, the four contacts of the quadripolar electrode (Medtronic 3389) created a recognizable artefact in brain parenchyma (Fig 1A). A template of the electrode was superimposed on the trajectory views allowing calculation of the likely position of the centre of each electrode contact. As electrode artefact partially obscures the MR signal of adjacent brain parenchyma, the coordinates of each contact were transposed onto the pre-operative MR images (Fig 1B). A neurosurgeon and a neuroradiologist, neither of whom were present during surgery, independently assessed the anatomical position of each contact with relation to the visualized STN in the axial, coronal and sagittal dimensions. Both assessors were also blinded to the physiological and clinical data. Contacts were rated as outside (score 0), touching (score 1) or inside (score 2) the STN in each dimension. Due to the poor resolution of the STN in sagittal planes, we used the scores for only axial and coronal planes for each evaluator to give a two dimensional (2-D) additive score. Cohen's κ coefficient with linear weighting between 2- scores was 0.4974 (\pm SE 0.181, $p=0.02$). The level

with the highest intra-operative 13-35 Hz activity was defined as being 'in STN' if the average 2-D score of the two observers was ≥ 2 out of a maximal of 4.

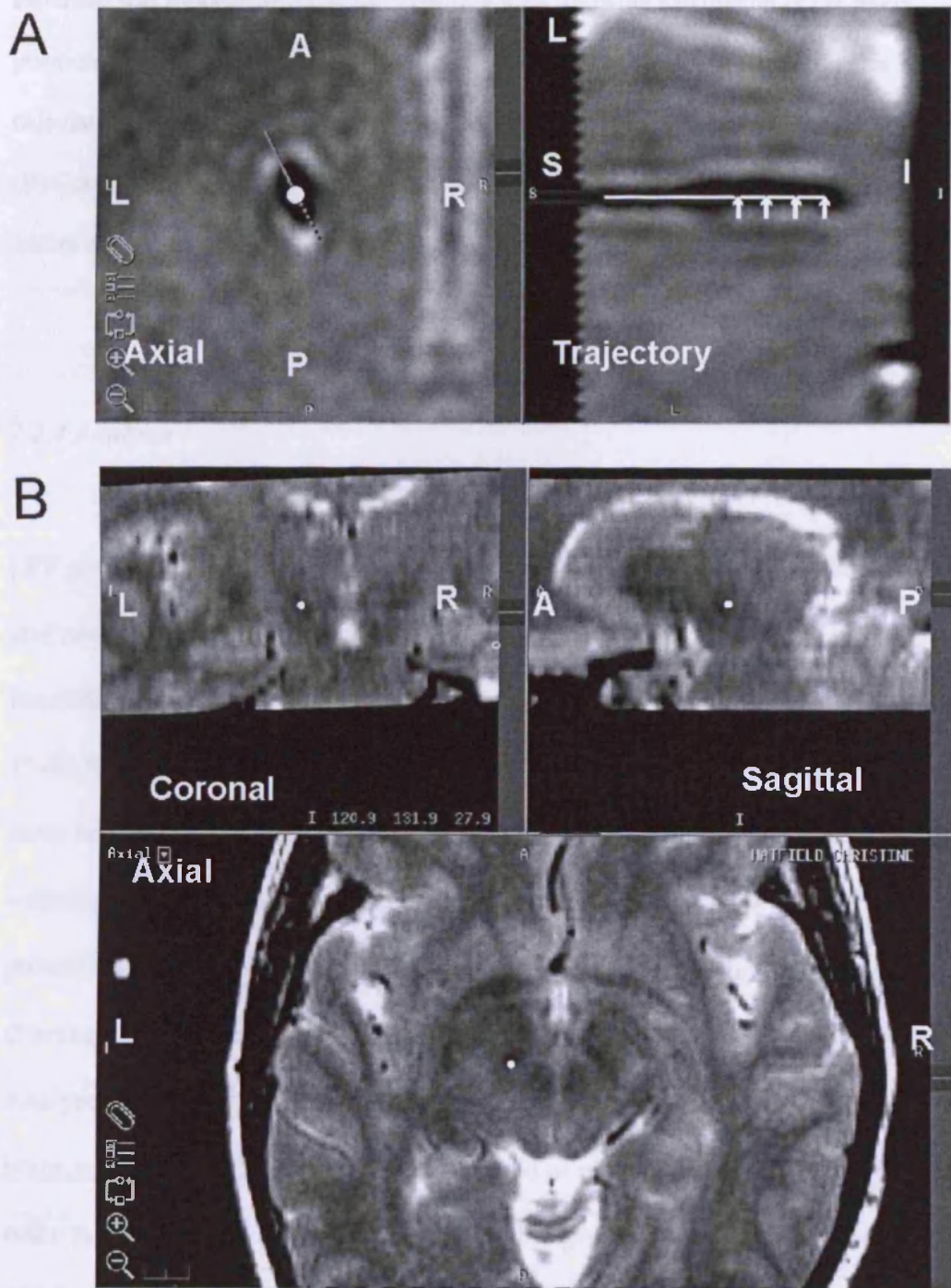


Figure 7.1. Localization of DBS electrode contacts on MRI. (A) Postoperative stereotactic MRI. Software used allowed reconstruction of the imaging data in multiple planes, including trajectory views along the center of the implanted electrode. A template of the electrode was superimposed on the trajectory view allowing calculation of the likely position of the center of each electrode contact (arrowed), from which coordinates were calculated. L, R, A, P, S and I denote left, right, anterior, posterior, superior and inferior. (B) Coordinates of contact 2 transposed onto corresponding preoperative MR. White circles denote coordinates of contact. Left STN in case 1.

7.2.4 Analysis

LFP power was determined in three candidate frequency bands, -the 13-35 Hz band and two further bands selected with the aim of establishing whether the potential localizing significance of intra-operatively recorded LFP activity was limited to the 13-35 Hz band. The additional bands were 4-10 Hz and 65-85 Hz. LFP activities in these range have also been reported in recording from the STN made in patients with Parkinson's disease. Changes in LFP power in serial 0.7 sec blocks (128 data points) and periods of sustained power were evaluated in the three bands by control charting and change point analysis, using commercial software (Changing-Point Analyser 2.0 shareware program; Taylor Enterprises, Illinois, IA, USA, <http://www.variation.com>). Control charts consisted of plots of serial deviations from the mean power. Control limits were determined to give the maximum range over which values were expected to vary with 99% probability, assuming no change had

occurred. Ten thousand bootstraps were performed in each test. Band powers were averaged across groups of five to six blocks prior to analysis, so as to avoid violation of the assumption of independent errors, and were ranked to avoid problems with outlying values. The application of this technique to power changes in the basal ganglia has been reported previously. The timing of change of LFP power ($p < 0.01$) was then related to the level of the DBS electrode at that time.

To determine the degree of agreement between the level at which maximal stun effect was reported intra-operatively by the neurologist and the level affording the highest LFP power in a particular band at the lower-most contact pair (01) determined as significant by changing point analysis, we used Cohen's κ with linear weighting, expressed as the observed kappa as a proportion of the maximum possible (<http://faculty.vassar.edu/lowry/kappa.html>). The linear weighting was used to reflect the equal spacing between 2 mm steps. Cohen's κ coefficients of < 0.40 , $0.40-0.75$ and > 0.75 are considered to indicate poor, fair to good, and excellent agreement between the sets of observations.

7.3 Results

7.3.1 On-line recording of LFP activity in the 13-35 Hz band

The time evolving and color-coded pattern of beta band power from contact pairs 01, 12 and 23 was displayed on-line as the DBS electrode was advanced during

surgery. Fig.2 gives some representative examples of the screen displays obtained intra-operatively in three patients. The x-axes are the distance of contact 0 along the electrode trajectory with respect to the intended target and therefore reflect the depth of activity picked up by contact pair 01. Rostral contact pairs 12 and 23 were further 2 mm and 4 mm above the intended target at any given level. Accordingly, the depth at which the stun effect was obtained, if present, was shifted across contact pairs and is shown by the vertical black arrows. Specific features of note in Fig. 2 are highlighted in the section below. Nevertheless, the figure serves to stress that on-line determination of LFP spectral power in the 13-35 Hz band is possible intra-operatively, and that the depth of contact pair 01 with the maximal power in this band corresponded to the depth of any intra-operative stun effect (Figs. 2A, B) or was adjacent to the depth of any stun effect (Fig. 2D). The recording and the assessment of on-line beta band power took, in total, 6-7 min per side.

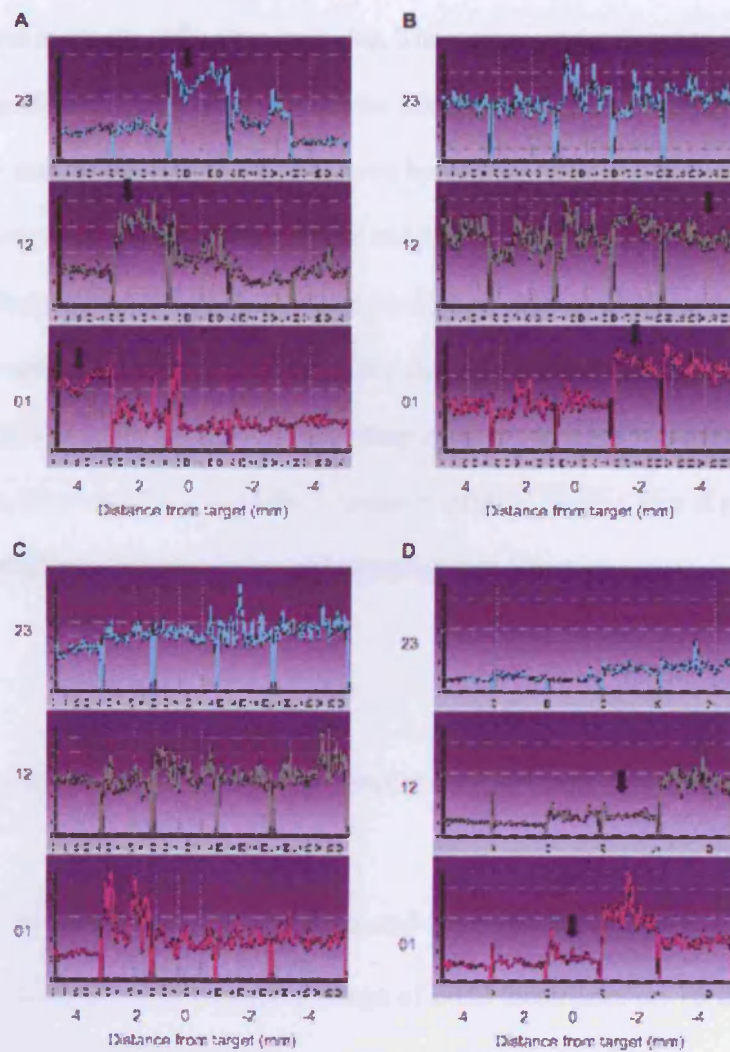


Figure 7.2. On-line displays of spectral change in LFP as DBS electrode descends through target, obtained intra-operatively. Recordings from case 9 right (A), 9 left (B), 5 right (C) and (8) left (D). The intended target at 0 mm was the center of STN. DBS

electrodes were introduced in 2 mm steps from (+) 4 mm above target to (-) 4 mm below. Recordings were made for ~60 s after each step. The x-axes are the distance of contact 0 along the electrode trajectory with respect to the intended target. The depth at which the intra-operative stun effect was obtained is shown by vertical black arrows. The highest level of beta activity is seen in contact 01 first and then recorded in more rostral contact pairs after further descent (A and D). Power is in arbitrary units and its range is independently optimized for each channel by the software. The depth of contact pair 01 with maximal power in the 13-35 Hz band corresponded to (A, B) or was adjacent to (D) the depth of the intra-operative stun effect, except in panel C where a step in power was recorded at contact pair 01 without an accompanying stun effect.

7.3.2 Off-line analysis of the predictive value of LFP recordings

The LFP activity in the 4-10 Hz, 13-35 Hz and 65-85 Hz frequency bands was analysed in recordings from 'virgin' passage of DBS electrodes on 16 sides (9 patients) and changes in power corresponding to different levels of the DBS electrode were objectively confirmed by control charting. Examples of the LFP in the 13-35 Hz band over successive levels with corresponding control charts are illustrated for each of the three contact pairs on both sides in case 1 in Fig. 3. The core results are summarized in Table 1.

Table 1: Comparison of results in different frequency bands.

Band	≥ 1 significant increase in contact pair 01	Concordance between level of peak activity & level of intra-operative stun effect (k coefficient)*	Peak activity at a level considered within STN on imaging
4-10 Hz	13/16 (81%)	Poor (<0.4, N.S.)	11/15 (73%)
13-34 Hz	15/16 (94%)	Excellent (0.792, $p < 0.01$)	15/15 (100%)
65-85 Hz	15/16 (94%)	Poor (<0.4: N.S.)	10/15 (67%)

*Cohen's κ coefficient with linear weighting, given the equal spacing between 2 mm steps. Cohen's κ coefficients of <0.40, 0.40 - 0.75 and >0.75 are considered to indicate poor, fair to good, and excellent agreement between sets of observations (Landis and Koch, 1977).

Table 7.1 Core results: Off-line analysis of the predictive value of LFP recordings

All sides showed at least one significant increase in the power in the 13-35 Hz band recorded at the lowermost contact pair (01) during the descent of the DBS electrode, with the exception of the left side in case 3. Thereafter, signals from

contact 12 showed a steep increase in the 13-35 Hz activity, but only after a median of a further 2 mm of descent. As contacts were 2 mm apart, this indicates that both contact pair 01 and 12 encountered the beta activity at the same depth in the brain. The picture was less consistent in the case of contact pair 23. In five sides there was an orderly progression, so that steep increase in 13-35 Hz activity was recorded in contact pair 23 after a further 2 mm of descent, as shown in Figure 2. However, the results in the remaining sides were more variable (see below). In two of these sides contact pair 23 picked up maximum beta activity 4 mm and 6 mm above the level at which contact 01 displayed its peak beta activity, *i.e.* at a point in the brain that was likely to lie in the ventral thalamus, another source of focal beta activity (Marsden et al., 2000).

All sides also showed at least one significant increase in the power in the 65-85 Hz band recorded at lowermost contact pair (01) during the descent of DBS electrode, again with the exception of the left side in case 3. However, in the 3-10 Hz band only 13 out of the 16 sides showed at least one significant increase in power at contact 01 (exceptions were case 3, 4 right and 6 left).

An intra-operative stun effect was observed in 13 out of the 16 sides (all cases except case 3 left, 6 right and 7 left). For these sides we evaluated the concordance between the level with the highest LFP power at the contact 01 in each of the three frequency bands and the level of maximal stun effect. In the 13-35 Hz band there was an excellent agreement between the two assessments (Cohen's κ coefficient

with linear weighting $=0.792 \pm \text{SE } 0.150$, $p < 0.01$). However, the agreement between the level of highest LFP power in the 4-10 Hz and 65-85 Hz bands with the level of stun effect was poor ($n = 9$ and 10 , respectively; $\kappa < 0.4$, both N.S.). The concordance between the intended target level determined from pre-operative MRI and the level of the highest LFP in three bands was poor, as was, however, the concordance between intended target point level and the level of the maximal intra-operative stun effect ($\kappa < 0.4$, both N.S.).

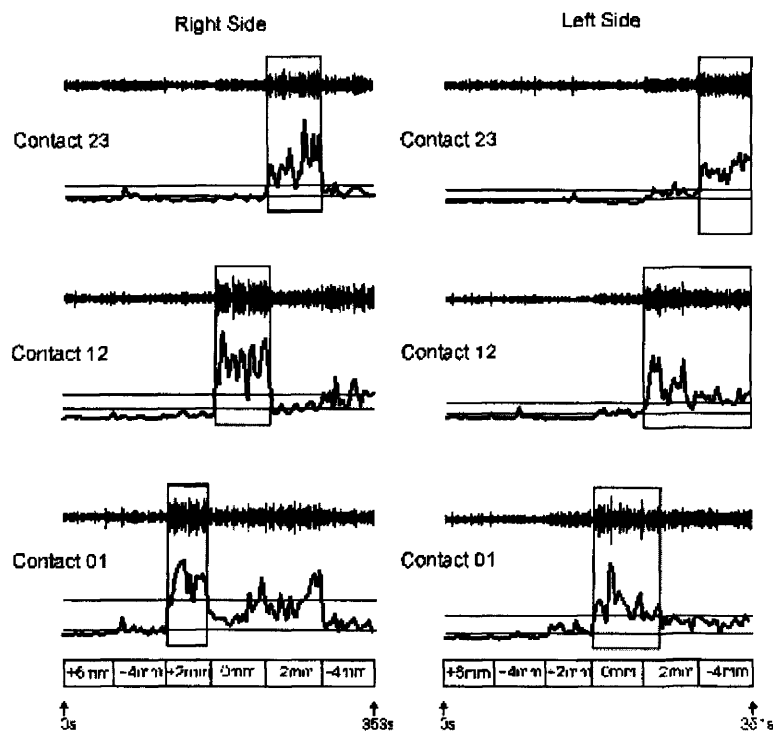


Figure 7.3. Off-line analysis of spectral change of LFP as DBS electrode descends through target. Recording from case 1. The intended target at 0 mm was the center of STN. DBS electrode was introduced in 2 mm steps from 6 mm above target to 4 mm below.

Recording were made for 53-61 s after each step (this excludes movement artefact during descent, which was not recorded or otherwise removed during earlier processing). For each contact pair, the upper trace is the LFP after pass band filtering in the beta band, and the lower trace is the control chart of the spectral power in serial 0.7 s blocks. The horizontal lines are the 99% confidence limits of the control chart and the boxed areas are the limits over which the highest level of beta activity was maintained as defined by change point analysis. Note that the highest level of beta activity is seen in contact 01 first and then recorded in contacts 12 and 23 after further descents of 2 mm and 4 mm, respectively. The highest level of beta activity was ~limited to one level, except for contact 12 on the left side. Gains are separately tied for filtered LFPs and control charts (arbitrary units). The intra-operative stun effect was maximal at 2 mm and 0 mm on the right and left.

The above suggested that the level at which the highest LFP power was recorded in the 13-35 Hz band at contact 01 corresponded to the level of the 'functional' target, in so far as this is defined by the stun effect, consistent with microelectrode recordings demonstrating beta band LFP activity focal to the STN (Kuhn et al., 2005; Levy et al., 2002). The presence of a focal source of 13-35 Hz activity along the trajectory of the DBS electrode was further supported by the fact that the recorded 13-35 Hz activity was 47.2% ($\pm 13\%$) less when the upper most contact pair (23) traversed the level that had previously afforded the highest 13-35 Hz activity when first penetrated by the lowermost contact pair (two tailed Wilcoxon signed ranks test, $p=0.04$). This effect would also make the contact pair 23 a less reliable index of the level of the beta source (see above). In addition, we also

determined the spatial extent of the peak 13-35 Hz activity detected by contact pair 01. The source of this activity spanned ≤ 4 mm (*e.g.* was limited to either 1 or 2 steps) along the trajectory. This compared with the 6-8 mm extent of the STN along the chosen trajectory suggests that the 13-35 Hz activity is limited to a portion of STN.

7.3.3. Relationship between 'physiologically' and 'radiologically' defined STN

The level at which recordings exhibited peak 13-35 Hz activity was confirmed to lie within the radiologically defined STN on all 15 sides. The DBS electrode on the one side without a 13-35 Hz peak (case 3 left) was confirmed to lie outside of (and just anterolateral) to STN, probably in the lateral part of Zona Incerta, adjacent to the internal capsule. Thus the depth of peak beta activity showed 100% specificity and 100% sensitivity for placement within STN in comparison to postoperative stereotactic MRI. The picture was less consistent when levels with peak activity in the 4-10 Hz and 65-85 Hz bands were assessed. These were confirmed to be within STN only 11 and 10 sides, respectively (Table 1).

7.4 Discussion

The results in this chapter suggest that the LFP activity recorded directly from the lower most contact pair of the DBS electrode can be used intra-operatively to confirm the placement within the STN in patients operated on under local

anesthesia, after overnight withdrawal of antiparkinsonian medication. In this study STN was defined both functionally, in terms of intra-operative stun effect, and radiologically, on narrow slice stereotactic MRI. The relevant 'signature' of STN was a local increase in beta activity in the LFP, in line with similar findings made using semi-microelectrodes in 6-OHDA midbrain lesioned parkinsonian rodents (Sharott et al., 2005) and microelectrodes in parkinsonian patients (Kuhn et al., 2005). The localizing benefit of the peak in beta activity was frequency specific, with neither the 4-10 Hz and nor the 65-85 Hz activities helping to localize STN intra-operatively. The latter probably because the 4-10 Hz LFP activity has a more diffuse origin in the subthalamic region, whereas a well defined spectral peak in the 65-85 Hz band is a more consistent feature of recordings made from patients after they have been turned 'on' following levodopa intake (Brown et al., 2001; Cassidy et al., 2002; Fogelson et al., 2005a; Fogelson et al., 2005b; Obeso et al., 2004).

It should be pointed out that the evidence of placement in STN derived from the LFP was not merely duplicative: an intra-operative stun effect could not be determined in about 20% of sides. Although anatomical targeting based on pre-operative stereotactic MRI appeared excellent in selecting an appropriate target and electrode trajectory, it was relatively poor in identifying the rostral-caudal level of either the maximal stun effect or peak beta activity. A robust peak in beta activity was recorded along the electrode trajectory on all but one side, and showed excellent concordance with the level of the maximal stun effect when this could be determined and 100% specificity and sensitivity for placement of the DBS

electrode within STN, as judged by stereotactic MRI. Worthy of note too was that the peak beta activity was limited in its spatial extent along the DBS trajectory, consistent with the observation made in a recent microelectrode study that beta activity is predominantly generated in the dorsal region of the STN (Kuhn et al., 2005).

This experiment described in this chapter provides two important implications. First, the reduction in the beta activity recorded by rostral contact pairs as they enter the levels previously traversed by lower contacts with consequent stun effects is strongly supportive that elevated levels of beta activity may promote parkinsonian motor impairment. Thus the acute disruption of the synchronized activity in this frequency band associated with the trauma of penetration is accompanied by an acute amelioration of rigidity and, where tested, improvement in bradykinesia. This interventional evidence supplements the correlative data linking excessive beta activity with parkinsonian deficits (Williams et al., 2005). Second, the current observations offer a means by which the level of STN can be confirmed intra-operatively with respect to the actual DBS electrode. We found the on-line evaluation of LFP in power in the beta band to be quick and feasible. At the very least, this could be useful in limiting errors that arise between the trajectory and depth of microelectrode recordings and those of the final DBS electrode, as the former have to be withdrawn prior to implantation of the DBS electrode. In time, however, this technique may potentially provide an alternative to microelectrode recordings, with attendant advantages in terms of the duration of the operation and

reduction in the risks of intra-operative hemorrhage. It remains to be established whether the same LFP 'signature' activity can be recorded under general anesthesia, raising the possibility that the whole surgical procedure could be attempted under this state, when clinically demanded.

7.5 Summary

1. The core results of this chapter suggest that functional physiological localization of STN by the on-line spectral analysis of LFPs is quick to perform and may provide information directly relevant to the position of the electrode contact actually used for DBS.
2. The results also provide evidence in support of the focal generation of beta activity in STN region in patients with PD as opposed to volume conduction.

CHAPTER 8: Conclusions

This aim of this thesis is to investigate oscillatory activity in the basal ganglia, and the extent to which its exaggeration contributes to differing symptoms of movement disorders. Furthermore, it explores the relevance of basal ganglia oscillations to DBS interventions for patients with movement disorders.

The principle findings of this thesis can be summarised as follows:

Chapter 3: Findings on the correlation between oscillatory pallidal local field potential activity and EMG in dystonia

1. The central finding of this study is the demonstration of correlations between wide band spectral components of the pallidal LFP and levels of dystonic EMG.
2. LFP activity in the 4-10 Hz, 11-30 Hz and 65-85 Hz bands positively correlated with the level of dystonic EMG. Negative correlation, however, was limited to the 11-30 Hz band.
3. The correlations were topographically distributed. Positive correlations were maximal at the lowermost contact pair (01), which included at least one contact in the globus pallidus interna and /or posterior ansa lenticularis. In contrast, negative correlations in the 11-30 Hz band were maximal more dorsally, at the middle contact pair (12).

4. Albeit significant and topographically focal, correlations were generally weak, in keeping with any pallidal effect on muscle spasm being necessarily indirect, perhaps through pallido-thalamo-cortico-spinal pathways.
5. These correlations provide support for a pathophysiological role for synchronized basal ganglia population activity in dystonia.

Chapter 4: Findings on the synchronization between neuronal activity in Globus pallidus interna and local field potential activity over 3-12 Hz in dystonia.

1. We have demonstrated that pallidal oscillations over the 3-12 Hz band are maximal in GPi, the surgical target.
2. Spike triggered averages (STAs) indicated that the discharge of neuronal activities were locked to 3-12 Hz oscillations in the LFP. All but two of these STAs were in GPi.
3. This lends support to a pathophysiological relationship between LFP activity at 3-12 Hz and dystonia.
4. The findings also have clinical implications. The low frequency oscillatory activity may provide intra-operative confirmation of GPi targeting in patients undergoing GPi DBS implantation for the treatment of dystonia, given that the correct placement of DBS electrodes in the GPi region is difficult to confirm by intra-operative macrostimulation.

Chapter 5: Findings on the effect of deep brain stimulation of the subthalamic nucleus: a two-edged sword.

1. Human basal ganglia are involved in processing of simple limb movement.
2. High frequency stimulation in STN has a dual effect in patients with PD, subject to the baseline performance of patients without stimulation; first, high frequency stimulation ameliorates behavioral impairments because of dopaminergic denervation and consequent abnormal functioning of STN. Second, high frequency stimulation can disturb remaining physiological STN functions, such as those contributing to simple limb movements.
3. There is a negative correlation between change in task performance with deep brain stimulation and performance prior to onset of deep brain stimulation.
4. The effectiveness of DBS therapy for patients with Parkinson's disease is related, at least partly, to the baseline performance of patients.

Chapter 6: Findings on how excessive synchronization of basal ganglia neurons at 20 Hz slows movement in Parkinson's disease.

1. Task performance was slowed during 20 Hz stimulation in the subthalamic nucleus in PD patients with relatively preserved baseline function in the task.
2. The worsening of the task performance with stimulation at 20 Hz may be

the consequence of the imposed synchronization of efferent axons in the vicinity of stimulation.

3. The data in this chapter provide proof of principle that excessive beta synchrony within the basal ganglia-cortical loop may contribute to the slowing of movement in Parkinson's disease.

Chapter 7: Intra-operative recordings of local field potentials can help localize the subthalamic nucleus in Parkinson's disease surgery.

1. The core results of this chapter suggest that functional physiological localization of STN by the on-line spectral analysis of LFPs is quick to perform and may provide information directly relevant to the position of the electrode contact actually used for DBS.
2. The results also provide evidence in support of the focal generation of beta activity in the STN region in patients with PD as opposed to volume conduction.

8.1 What is the pathophysiological role for synchronization of pallidal activity in hyperkinetic movement disorders?

Dystonia is generally classified as a hyperkinetic movement disorder and has been attributed to reduced pallidal inhibition of tonic thalamocortical excitatory input in the classical model of basal ganglia function (Vitek, 2002).

Nevertheless, this explanation has been challenged by the observation that pallidotomy, and high frequency pallidal stimulation, reduce dystonia while abolishing pallidal outflow (Marsden and Obeso, 1994). Accordingly, recent interest has shifted to whether it could be the '*pattern*' rather than the '*rate*' of pallidal activity that underlies dystonia. Abnormal patterning could involve disturbed somatosensory relationships within the pallidum, altered patterning of pallidal activity over time, or a combination of the two.

Several observations have suggested sensory inputs play an important role in dystonia (Byl et al., 1997; Byl et al., 1996; Hallett, 1995; Tinazzi et al., 2003). Enlargement of the receptive fields of neurons in the basal ganglia-cortical loop may be a key pathophysiological feature in this disorder. This has been supported by reorganization in the thalamus (Lenz and Byl, 1999; Lenz et al., 1999) and pallidum (Lenz et al., 1998) in dystonia.

Microelectrode recordings from the globus pallidus in dystonic patients reveal marked abnormalities in the temporal patterning of neuronal discharge, with neurons firing in irregular grouped discharges with intermittent pauses (Suarez et al., 1997; Vitek, 2002; Vitek et al., 1999). Similar findings were observed in the endopeduncular nucleus of dystonic *dt^{sz}* hamsters.

To which extent does spatio-temporal disorganization of pallidal activity contribute to dystonia? One aspect worthy of consideration is the abnormal

synchronization across neurons displaying burst-like firing patterns. So far, no microelectrode study has attempted to explore the degree of synchronization between pairs of neurons in dystonia. However, local field potential (LFP) recordings have demonstrated predominant LFP activity in the pallidum in dystonia.

The first report of activity in the pallidal LFP was in a patient with myoclonic dystonia, and involved the 4-8 Hz frequency band (Liu et al., 2002). Soon after this, a report on a large cohort of patients with primary dystonia revealed prominent activity over 4-10 Hz band (Silberstein et al., 2003). The level of this activity exceeded that in untreated patients with PD. Silberstein et al. proposed that pallidal LFP activity in the 4-10 Hz band might relate to synchronized, relatively non-oscillatory bursting across neurons. Such bursting has also been observed in other hyperkinetic movement disorders, such as dyskinesias in primates and PD patients (Levy et al., 2001; Yoshida, 1991) and hemiballismus (Suarez et al., 1997). There are also data to suggest that excessive synchrony in this frequency band may contribute to levodopa-induced dyskinesias (LID). A report on STN-GPi coherence has revealed that activity <10 Hz increased during contralateral dyskinesias in a patient with PD (Foffani, 2005).

Furthermore, a study reporting power spectra of LFPs from the subthalamic nucleus during complete treatment cycles in patients with PD suggested that low frequency activities determine dyskinesia (Alonso-Frech et al., 2006). The relevance of pallidal LFP activity in this frequency band is further supported by

the results of Chapter 3 which indicated that such activity correlates with levels of dystonic EMG. In line with this, another study reported coherence between pallidal LFP and dystonic EMG (Liu et al., 2006). Together, the above evidence suggests that synchronised activity over 4-10Hz at the pallidal level may be an important pathophysiological substrate for the development of hyperkinetic movement disorders.

8.2 Is the 4-10 Hz LFP in Globus Pallidus focally generated in dystonia?

The evidence therefore suggests that activity in the 4-10 Hz frequency band plays an important pathophysiological role in dystonia. However, when dealing with LFP oscillations, it is important to consider whether they can be epiphenomena (through movement related artifact or through movement related re-afference). Nevertheless, there are several lines of evidence against this possibility. In Chapter 3, we have shown a selective spatial distribution of the LFP-EMG correlations. Positive correlations between LFP activity and dystonic EMG over the 4-10 Hz mode were strongest at the pair of contacts within globus pallidus interna (GPi), where lies the most effective therapeutic target for lesioning or deep brain stimulation in dystonia. (Krack 2001, Lozano 1997, Vidailhei 2005, Yanni 2003). In line with this, Chapter 4 demonstrates that LFP activity recorded with microelectrodes is concentrated in GPi and spike triggered averages with components in this band are almost exclusively limited to GPi in patients with primary dysotonia. Furthermore, LFP power in this

frequency band tends to be greater in GPi than GPe (Chapter 4). These topographical findings support a functional link between population synchrony in this band and dystonia. They also reinforce evidence from patients with Parkinson's disease pointing to a functional distinction between GPi and GPe (Krack et al., 1998; Starr et al., 2006; Vitek et al., 1999). However, it remains unclear whether the link between pallidal LFP activity over this frequency band and dystonia is related to an abnormal processing of afferent information at the pallidal level or to a more direct influence on the motor drive to dystonic muscles. The correlative evidence linking excessive synchrony at 4-10 Hz band with dystonia and drug-induced dyskinesia cannot distinguish between a causal or epiphenomenal association. Proof of the principle that excessive synchrony at this mode contributes to dystonia/dyskinesia would require the demonstration of the occurrence of dystonia/dyskinesia during direct stimulation of BG nuclei in 4-10 Hz frequency range (Alonso-Frech et al., 2006).

8.3 The effect of high frequency deep brain stimulation : more or less?

As mentioned above, deranged synchrony in the BG may underlie the pathophysiology of movement disorders (Chapter 3, 4, (Alonso-Frech et al., 2006; Amirnovin et al., 2004; Brown et al., 2001; Cassidy et al., 2002; Fogelson et al., 2006; Kuhn et al., 2006; Kuhn et al., 2004; Levy et al., 2002; Priori et al., 2002; Silberstein et al., 2003; Williams et al., 2002). It is suggested that high frequency stimulation or lesioning of basal ganglia nuclei (STN or

GPI) may improve distinct movement disorders by disrupting spontaneous, pathological synchronization at the BG level, and therefore release motor cortex from similar aberrant synchronization (Brown, 2003; Silberstein et al., 2005). In support of this, an in vivo study has shown that high frequency stimulation of the STN suppresses all spontaneous STN spikes and replaces them by spikes entirely driven by stimulation (Garcia et al., 2005a; Garcia et al., 2005b), while high frequency stimulation of the STN of MPTP primates decreases oscillatory activity in the STN (Meissner et al., 2005).

It is reasonable to assume that high frequency stimulation must also remove any residual physiological activity in the BG. Hitherto, evidence of impairment of performance during STN deep brain stimulation has been restricted to selected cognitive tasks (Hershey et al., 2003; Jahanshahi et al., 2000), a complex bimanual task (Brown et al., 2006) and occasional reports of diminished intelligibility of speech (Rousseaux et al., 2004). Importantly, DBS related impairment in a simple limb movement task is shown in Chapter 5. This sheds some light on the physiological function of STN and its therapeutic implications for high frequency stimulation. STN is involved in processing of differing motor and cognitive actions. It would be worthwhile investigating whether DBS of this nucleus could compromise other task-related processing, such as on-line learning and attentional tasks, by separating the effects of deep brain stimulation on pathological and physiological activities based on baseline task performance. In addition, it is not unreasonable to assume that deep brain

stimulation may have different effects in the 'On' state, when the filtering properties of the BG may have changed, moving closer to a more physiological state.

The above has important therapeutic implications, as there may be a tipping point at which stimulation will worsen rather than improve net function (Chapter 5). Therefore, the effectiveness of DBS in PD may be improved by using an on-demand mode, possibly with stimulation being triggered by the level of pathological local field potential activity in the STN. Continuous stimulation, as utilized presently, may even impair performance in tasks relatively spared by parkinsonism or temporarily improved by concurrent medication.

8.4 The effect of beta band stimulation: amelioration and/or disruption?

Evidence presented thus far indicates that at high frequency, stimulation may have two effects: a suppression of pathological activity which then ameliorates parkinsonism and a direct stimulation of local neuronal elements which may or may not have effects in its own right (Brown et al., 2004; Garcia et al., 2003; Garcia et al., 2005a; McIntyre et al., 2004b; Meissner et al., 2005; Miocinovic et al., 2006; Wingeier et al., 2006). What is the nature of the pathological activity in PD which may be suppressed by DBS? There is increasing

correlative evidence to suggest that this synchronised activity in the beta band is associated with impairment of movement (Alonso-Frech et al., 2006; Dostrovsky and Bergman, 2004; Kuhn et al., 2006; Kuhn et al., 2004), and that it is this activity that may be suppressed by DBS, thereby improving function (Brown et al., 2004; Wingeier et al., 2006).

STN stimulation can enforce some degree of synchronization through direct activation of local axons with one-to-one following of stimulation rates, as suggested by model-based analysis (McIntyre et al., 2004a; Miocinovic et al., 2006), simultaneous recordings from GPi (Brown et al., 2004; Hashimoto et al., 2003) and from the effects evoked in cerebral cortex and muscle (Ashby et al., 1999; Ashby et al., 2001). Studies attempting to estimate the deleterious effects of stimulation at low frequency have suggested a rather small effect size (Fogelson et al., 2006; Timmermann et al., 2004). But these did not separate the disruptive effects of stimulation from the confounding ameliorative effects of stimulation at the same frequency, and made no allowance for baseline task performance. In Chapter 6, we show that externally imposed synchrony can impair task performance on those sides with good performance. This effect, however, was unlikely to be due to suppression of physiological activity (Chapter 5) because stimulation at 20 Hz has weaker suppressive effects than stimulation at higher frequency, and yet DBS at 50 Hz did not impair performance. The effect at 20 Hz is more likely to be due to a mimicking of the effects of pathological synchronization in the beta band. Chapter 6 strongly suggests that the excessive synchronization of basal ganglia activity in the beta

band may compromise motor function. Hitherto, this was only suspected on the basis of correlative evidence, but it is shown here that externally imposed synchrony has similar effects.

8.5 Can local field potential recordings help localize the subthalamic nucleus in Parkinson's disease surgery?

DBS of the STN can be a highly effective treatment for Parkinson's disease. However, therapeutic efficacy is limited by difficulties in consistently and correctly targeting this nucleus. Single unit microelectrode recordings remain an important element of the surgical procedure (Hutchison et al., 1998).

However, their use may considerably prolong surgery, does not always lead to satisfactory targeting and has been associated with an increased risk of intra-operative hemorrhage (Alkhani and Lozano, 2001; Binder et al., 2005; Hariz and Fodstad, 1999). Thus, alternative electrophysiological signatures of STN activity that could be directly and intra-operatively recorded from DBS electrodes would be of considerable potential value.

Increasing correlative (Alonso-Frech et al., 2006; Kuhn et al., 2006; Kuhn et al., 2004; Williams et al., 2005) and direct (Chapter 6) evidence has suggested that there is abnormal synchronization of activity in the beta frequency band in the STN in PD patients and it is this oscillatory activity that contributes to slowness in PD. Studies made using semi-microelectrodes in 6-OHDA

midbrain lesioned parkinsonian rodents (Sharott et al., 2005) and microelectrodes in parkinsonian patients (Kuhn et al., 2005) have demonstrated a local increase in beta activity in the LFP in the sensorimotor domain of STN. Chapter 7 provided a quick way of localizing functional physiological STN by means of on-line spectral analysis of LFPs. This technique may potentially provide an alternative to microelectrode recordings for the provision of this information. It also remains to be explored whether the LFP 'signature' can be recorded in other hyperkinetic movement disorders, such as dystonia or dyskinesia during GPi DBS surgery (Chapter 3, 4), in which clinical benefit is not always realized by intra-operative stimulation.

8.6 Conclusion and future directions

We conclude that deranged synchronisation of neuronal activities in basal ganglia nuclei may underlie the pathophysiology of movement disorders, such as dystonia (hyperkinesias) and Parkinson's disease (hypokinesias). In dystonia, there appears to be a pathophysiological relationship with LFP activity over 3-12Hz. Whether this excessive synchrony relates to abnormal descending drive to muscles at comparable frequencies or is epiphenomenal, remains obscure. There is a need for studies that establish whether or not this excessive synchrony is causative in dystonia. One approach would be the demonstration of the same characteristic pattern between paroxysms of dystonia in patients.

with paroxysmal dystonia, a condition which shares some phenomenological similarities with the dystonic dt^{sz} mutant hamster.

In Parkinson's disease, correlative and direct evidence suggests that this spontaneous activity contributes to slowness of movement in this condition. Recently, studies have demonstrated that externally imposed synchronization through direct stimulation of the STN at 5, 10 and 20 Hz can impair motor performance. However, so far it has been impossible to determine which precise frequencies in this band are the most important in impairing movement. This is an important question, as studies in MPTP treated primates suggest that it is synchronization at 8-12 Hz that is important, whereas studies in PD patients suggest that it is synchronization at 13-30 Hz that is more important. The severity of parkinsonism may not be the only factor determining the level of impairment of behavioural performance seen with stimulation of the basal ganglia at different frequencies ≤ 20 Hz. BG-cortical loops subserving different features of motor function may have their own distinct network characteristics and resonances. The latter may lead to different susceptibilities to pathologically synchronised activity according to frequency. Further investigation is warranted as to whether some frequencies of imposed synchronization have more effects on movement than others in PD. Another issue that requires further clarification is whether there is an interaction between the effects of imposed synchronization at different frequencies and type of movement in PD. Furthermore, there remains the need for establishing whether there is an interaction between the frequency of stimulation and the

cortical topography of evoked steady state potentials in PD. Finally, the studies above may contribute to a smart regime, such as on-demand mode of DBS therapy for patients with movement disorders.

BIBLIOGRAPHY

- Abeles M, Gerstein GL. Detecting spatiotemporal firing patterns among simultaneously recorded single neurons (1998) *J Neurophysiol* 60: 909-24.
- Agid Y, Ahlskog E, Albanese A, Calne D, Chase T, De Yebenes J, et al. Levodopa in the treatment of Parkinson's disease: a consensus meeting (1999) *Mov Disord* 14: 911-3.
- Agid Y, Arnulf I, Bejjani P, Bloch F, Bonnet AM, Damier P, et al. Parkinson's disease is a neuropsychiatric disorder (2003) *Adv Neurol* 91: 365-70.
- Agid Y, Graybiel AM, Ruberg M, Hirsch E, Blin J, Dubois B, et al. The efficacy of levodopa treatment declines in the course of Parkinson's disease: do nondopaminergic lesions play a role? (1990) *Adv Neurol* 53: 83-100.
- Albe Fessard D, Arfel G, Guiot G, Derome P, Dela H, Korn H, et al. [Characteristic Electric Activities of Some Cerebral Structures in Man.] (1963) *Ann Chir* 17: 1185-214.

Albe-Fessard AG, Guiot G, et al. Derivations d'activités spontanées et évoquées dans les structures cérébrales profondes de l'homme (1962) *Rev Neurol* 106: 89-105.

Albe-Fessard D, Arfel G, Guiot G, Derome P, Guilbaud G. Thalamic unit activity in man. *Electroencephalogr* (1967) *Clin Neurophysiol Suppl* 25:132+.

Albe-Fessard D, Arfel G, Guiot G, Derome P, Hertzog E, Vourc'h G, et al. Electrophysiological studies of some deep cerebral structures in man (1966) *J Neurol Sci* 3: 37-51.

Albin RL, Kearney JA. Alessandro Agnoli Lecture. Models of basal ganglia dysfunction: predictions and pitfalls (2000) *Funct Neurol* 15: 135-46.

Albin RL, Young AB, Penney JB (1989) The functional anatomy of basal ganglia disorders. *Trends Neurosci* 12: 366-75.

Alegre M, Alonso-Frech F, Rodriguez-Oroz MC, Guridi J, Zamarbide I, Valencia M, et al. Movement-related changes in oscillatory activity in the human subthalamic nucleus: ipsilateral vs. contralateral movements (2005) *Eur J Neurosci* 22: 2315-24.

Alexander GE, Crutcher MD. Functional architecture of basal ganglia circuits: neural substrates of parallel processing (1990) *Trends Neurosci* 13: 266-71.

Alexander GE, DeLong MR. Microstimulation of the primate neostriatum. I.

Physiological properties of striatal microexcitable zones (1985a). J

Neurophysiol 53: 1401-16.

Alexander GE, DeLong MR. Microstimulation of the primate neostriatum. II.

Somatotopic organization of striatal microexcitable zones and their relation

to neuronal response properties (1985b) J Neurophysiol 53: 1417-30.

Alexander GE, DeLong MR, Strick PL. Parallel organization of functionally

segregated circuits linking basal ganglia and cortex (1986) Annu Rev

Neurosci 9: 357-81.

Alkhani A, Lozano AM. Pallidotomy for parkinson disease: a review of

contemporary literature (2001) J Neurosurg 94: 43-9.

Allers KA, Ruskin DN, Bergstrom DA, Freeman LE, Ghazi LJ, Tierney PL, et al.

Multisecond periodicities in basal ganglia firing rates correlate with theta

bursts in transcortical and hippocampal EEG (2002) J Neurophysiol 87:

1118-22.

Alonso-Frech F, Zamarbide I, Alegre M, Rodriguez-Oroz MC, Guridi J, Manrique M, et al. Slow oscillatory activity and levodopa-induced dyskinesias in Parkinson's disease (2006) *Brain* 129: 1748-57.

Alusi SH, Aziz TZ, Glickman S, Jahanshahi M, Stein JF, Bain PG. Stereotactic lesional surgery for the treatment of tremor in multiple sclerosis: a prospective case-controlled study (2001) *Brain* 124: 1576-89.

Alvarez L, Macias R, Guridi J, Lopez G, Alvarez E, Maragoto C, et al. Dorsal subthalamotomy for Parkinson's disease (2001) *Mov Disord* 16: 72-8.

Amirnovin R, Williams ZM, Cosgrove GR, Eskandar EN. Visually guided movements suppress subthalamic oscillations in Parkinson's disease patients (2004) *J Neurosci* 24: 11302-6.

Amirnovin R, Williams ZM, Cosgrove GR, Eskandar EN. Experience with microelectrode guided subthalamic nucleus deep brain stimulation (2006) *Neurosurgery* 58: ONS96-102; discussion ONS96-102.

Amjad AM, Breeze P, Conway BA, Halliday DM, Rosenberg JR. A framework for the analysis of neuronal networks (1989) *Prog Brain Res* 80: 243-55; discussion 239-42.

Anderson KE, Mullins J. Behavioral changes associated with deep brain stimulation surgery for Parkinson's disease (2003) *Curr Neurol Neurosci Rep* 3: 306-13.

Anderson VC, Burchiel KJ, Hogarth P, Favre J, Hammerstad JP. Pallidal vs subthalamic nucleus deep brain stimulation in Parkinson disease (2005) *Arch Neurol* 62: 554-60.

Anderson WS, Lenz FA. Surgery insight: Deep brain stimulation for movement disorders (2006) *Nat Clin Pract Neurol* 2: 310-20.

Androulidakis AG, Kuhn AA, Chen CC, Blomstedt P, Kempf F, Kupsch A, et al. Dopaminergic therapy promotes lateralized motor activity in the subthalamic area in Parkinson's disease (2007) *Brain* 130: 457-68.

Apicella P. Tonically active neurons in the primate striatum and their role in the processing of information about motivationally relevant events (2002) *Eur J Neurosci* 16: 2017-26.

Ashby P, Kim YJ, Kumar R, Lang AE, Lozano AM. Neurophysiological effects of stimulation through electrodes in the human subthalamic nucleus (1999) *Brain* 122 (Pt 10): 1919-31.

Ashby P, Paradiso G, Saint-Cyr JA, Chen R, Lang AE, Lozano AM. Potentials recorded at the scalp by stimulation near the human subthalamic nucleus (2001) Clin Neurophysiol 112: 431-7.

Aziz TZ, Peggs D, Sambrook MA, Crossman AR. Lesion of the subthalamic nucleus for the alleviation of 1-methyl-4-phenyl-1,2,3,6-tetrahydropyridine (MPTP)-induced parkinsonism in the primate (1991) Mov Disord 6: 288-92.

Balagura S, Katz RG. Undecussated innervation to the sternocleidomastoid muscle: a reinstatement (1980) Ann Neurol 7: 84-5.

Bandmann O, Marsden CD, Wood NW. Atypical presentations of dopa-responsive dystonia (1998) Adv Neurol 78: 283-90.

Bandmann O, Valente EM, Holmans P, Surtees RA, Walters JH, Wevers RA, et al. Dopa-responsive dystonia: a clinical and molecular genetic study (1998b) Ann Neurol 44: 649-56.

Bar-Gad I, Bergman H. Stepping out of the box: information processing in the neural networks of the basal ganglia (2001) Curr Opin Neurobiol 11: 689-95.

Bar-Gad I, Elias S, Vaadia E, Bergman H. Complex locking rather than complete cessation of neuronal activity in the globus pallidus of a 1-methyl-4-phenyl-1,2,3,6-tetrahydropyridine-treated primate in response to pallidal microstimulation (2004) *J Neurosci* 24: 7410-9.

Bar-Gad I, Havazelet-Heimer G, Goldberg JA, Ruppin E, Bergman H. Reinforcement-driven dimensionality reduction--a model for information processing in the basal ganglia (2000) *J Basic Clin Physiol Pharmacol* 11: 305-20.

Bar-Gad I, Heimer G, Ritov Y, Bergman H. Functional correlations between neighboring neurons in the primate globus pallidus are weak or nonexistent (2003a) *J Neurosci* 23: 4012-6.

Bar-Gad I, Morris G, Bergman H. Information processing, dimensionality reduction and reinforcement learning in the basal ganglia (2003b) *Prog Neurobiol* 71: 439-73.

Bardinet EO, S. Malandain, G. Tande, D. Parain, K. Ayache, N. Yelnik, J. Three dimensional functional cartography of the human basal ganglia by registration of optical and histological serial sections (2002) In *IEEE Internatinal Symposium on Biomedical Imaging*, Washington, USA, 329-332.

Bejjani B, Damier P, Arnulf I, Bonnet AM, Vidailhet M, Dormont D, et al. Pallidal stimulation for Parkinson's disease. Two targets? (1997) *Neurology* 49: 1564-9.

Bejjani BP, Arnulf I, Vidailhet M, Pidoux B, Damier P, Papadopoulos S, et al. Irregular jerky tremor, myoclonus, and thalamus: a study using low-frequency stimulation (2000a) *Mov Disord* 15: 919-24.

Bejjani BP, Dormont D, Pidoux B, Yelnik J, Damier P, Arnulf I, et al. Bilateral subthalamic stimulation for Parkinson's disease by using three-dimensional stereotactic magnetic resonance imaging and electrophysiological guidance (2000b) *J Neurosurg* 92: 615-25.

Benabid AL. Deep brain stimulation for Parkinson's disease (2003) *Curr Opin Neurobiol* 13: 696-706.

Benabid AL, Benazzouz A, Hoffmann D, Limousin P, Krack P, Pollak P. Long-term electrical inhibition of deep brain targets in movement disorders (1998) *Mov Disord* 13 Suppl 3: 119-25.

Benabid AL, Chabardes S, Seigneuret E. Deep-brain stimulation in Parkinson's disease: long-term efficacy and safety - What happened this year? (2005) *Curr Opin Neurol* 18: 623-30.

Benabid AL, Koudsie A, Pollak P, Kahane P, Chabardes S, Hirsch E, et al. Future prospects of brain stimulation (2000) *Neurol Res* 22: 237-46.

Benabid AL, Minotti L, Koudsie A, de Saint Martin A, Hirsch E. Antiepileptic effect of high-frequency stimulation of the subthalamic nucleus (corpus luyisi) in a case of medically intractable epilepsy caused by focal dysplasia: a 30-month follow-up: technical case report (2002) *Neurosurgery* 50: 1385-91; discussion 1391-2.

Benabid AL, Pollak P, Gao D, Hoffmann D, Limousin P, Gay E, et al. Chronic electrical stimulation of the ventralis intermedius nucleus of the thalamus as a treatment of movement disorders (1996) *J Neurosurg* 84: 203-14.

Benabid AL, Pollak P, Gross C, Hoffmann D, Benazzouz A, Gao DM, et al. Acute and long-term effects of subthalamic nucleus stimulation in Parkinson's disease (1994) *Stereotact Funct Neurosurg* 62: 76-84.

Benabid AL, Pollak P, Louveau A, Henry S, de Rougemont J. Combined (thalamotomy and stimulation) stereotactic surgery of the VIM thalamic

nucleus for bilateral Parkinson disease (1987) *Appl Neurophysiol* 1987; 50: 344-6.

Benabid AL, Vercueil L, Benazzouz A, Koudsie A, Chabardes S, Minotti L, et al.
Deep brain stimulation: what does it offer? (2003) *Adv Neurol* 91: 293-302.

Benazzouz A, Gao D, Ni Z, Benabid AL. High frequency stimulation of the STN influences the activity of dopamine neurons in the rat (2000a) *Neuroreport* 11: 1593-6.

Benazzouz A, Gao DM, Ni ZG, Piallat B, Bouali-Benazzouz R, Benabid AL.
Effect of high-frequency stimulation of the subthalamic nucleus on the neuronal activities of the substantia nigra pars reticulata and ventrolateral nucleus of the thalamus in the rat (2000b) *Neuroscience* 99: 289-95.

Benazzouz A, Gross C, Feger J, Boraud T, Bioulac B. Reversal of rigidity and improvement in motor performance by subthalamic high-frequency stimulation in MPTP-treated monkeys (1993) *Eur J Neurosci* 5: 382-9.

Benazzouz A, Hallett M. Mechanism of action of deep brain stimulation (2000) *Neurology* 55: S13-6.

Benazzouz A, Piallat B, Pollak P, Benabid AL. Responses of substantia nigra pars reticulata and globus pallidus complex to high frequency stimulation of the subthalamic nucleus in rats: electrophysiological data (1995) *Neurosci Lett* 189: 77-80.

Bennay M, Gernert M, Richter A. Spontaneous remission of paroxysmal dystonia coincides with normalization of entopeduncular activity in dt(SZ) mutants (2001) *J Neurosci* 21: RC153.

Bennett JP, Jr., Piercey MF. Pramipexole--a new dopamine agonist for the treatment of Parkinson's disease (1999) *J Neurol Sci* 163: 25-31.

Berardelli A, Hallett M, Rothwell JC, Agostino R, Manfredi M, Thompson PD, et al. Single-joint rapid arm movements in normal subjects and in patients with motor disorders (1996) *Brain* 119 (Pt 2): 661-74.

Berardelli A, Rothwell JC, Day BL, Marsden CD. Pathophysiology of blepharospasm and oromandibular dystonia. (1985) *Brain* 108 (Pt 3): 593-608.

Berardelli A, Rothwell JC, Day BL, Marsden CD. The pathophysiology of cranial dystonia (1988) *Adv Neurol* 50: 525-35.

Berardelli A, Rothwell JC, Hallett M, Thompson PD, Manfredi M, Marsden CD.

The pathophysiology of primary dystonia (1988) *Brain* 121 (Pt 7):
1195-212.

Bergman H, Deuschl G. Pathophysiology of Parkinson's disease: from clinical

neurology to basic neuroscience and back (2002). *Mov Disord* 17 Suppl 3:
S28-40.

Bergman H, Feingold A, Nini A, Raz A, Slovin H, Abeles M, et al. Physiological

aspects of information processing in the basal ganglia of normal and
parkinsonian primates (1998a) *Trends Neurosci* 21: 32-8.

Bergman H, Raz A, Feingold A, Nini A, Nelken I, Hansel D, et al. Physiology of

MPTP tremor (1998b) *Mov Disord* 13 Suppl 3: 29-34.

Bergman H, Wichmann T, DeLong MR. Reversal of experimental parkinsonism by

lesions of the subthalamic nucleus (1990) *Science* 249: 1436-8.

Bergman H, Wichmann T, Karmon B, DeLong MR. The primate subthalamic

nucleus. II. Neuronal activity in the MPTP model of parkinsonism (1994) *J*
Neurophysiol 72: 507-20.

Berke JD, Okatan M, Skurski J, Eichenbaum HB. Oscillatory entrainment of striatal neurons in freely moving rats (2004) *Neuron* 43: 883-96.

Beurrier C, Bioulac B, Audin J, Hammond C. High-frequency stimulation produces a transient blockade of voltage-gated currents in subthalamic neurons (2001) *J Neurophysiol* 85: 1351-6.

Bevan MD, Magill PJ, Terman D, Bolam JP, Wilson CJ. Move to the rhythm: oscillations in the subthalamic nucleus-external globus pallidus network (2002) *Trends Neurosci* 25: 525-31.

Bezard E, Boraud T, Bioulac B, Gross CE. Involvement of the subthalamic nucleus in glutamatergic compensatory mechanisms (1999) *Eur J Neurosci* 11: 2167-70.

Bhatia KP, Marsden CD. The behavioural and motor consequences of focal lesions of the basal ganglia in man (1994) *Brain* 117 (Pt 4): 859-76.

Binder DK, Rau G, Starr PA. Hemorrhagic complications of microelectrode-guided deep brain stimulation (2003) *Stereotact Funct Neurosurg* 80: 28-31.

- Binder DK, Rau GM, Starr PA. Risk factors for hemorrhage during microelectrode-guided deep brain stimulator implantation for movement disorders (2005) *Neurosurgery* 56: 722-32; discussion 722-32.
- Birkmayer W, Hornykiewicz O. [The L-3,4-dioxyphenylalanine (DOPA)-effect in Parkinson-akinesia.] (1961) *Wien Klin Wochenschr* 73: 787-8.
- Birkmayer W, Hornykiewicz O. The effect of l-3,4-dihydroxyphenylalanine (= DOPA) on akinesia in parkinsonism. 1961 (2001) *Wien Klin Wochenschr* 113: 851-4.
- Bittar RG, Yianni J, Wang S, Liu X, Nandi D, Joint C, et al. Deep brain stimulation for generalised dystonia and spasmodic torticollis (2005) *J Clin Neurosci* 12: 12-6.
- Boraud T, Bezard E, Bioulac B, Gross C. High frequency stimulation of the internal Globus Pallidus (GPi) simultaneously improves parkinsonian symptoms and reduces the firing frequency of GPi neurons in the MPTP-treated monkey (1996) *Neurosci Lett* 215: 17-20.
- Boraud T, Bezard E, Bioulac B, Gross CE. Dopamine agonist-induced dyskinesias are correlated to both firing pattern and frequency alterations of pallidal neurones in the MPTP-treated monkey (2001) *Brain* 124: 546-57.

Boraud T, Bezard E, Bioulac B, Gross CE. From single extracellular unit recording in experimental and human Parkinsonism to the development of a functional concept of the role played by the basal ganglia in motor control (2002) *Prog Neurobiol* 66: 265-83.

Boraud T, Bezard E, Guehl D, Bioulac B, Gross C. Effects of L-DOPA on neuronal activity of the globus pallidus externalis (GPe) and globus pallidus internalis (GPi) in the MPTP-treated monkey (1998) *Brain Res* 787: 157-60.

Bower JH, Maraganore DM, McDonnell SK, Rocca WA. Incidence and distribution of parkinsonism in Olmsted County, Minnesota, 1976-1990 (1999) *Neurology* 52: 1214-20.

Brainard MS, Doupe AJ. Interruption of a basal ganglia-forebrain circuit prevents plasticity of learned vocalizations (2000) *Nature* 404: 762-6.

Bressman SB. Dystonia (1998) *Curr Opin Neurol* 11: 363-72.

Bressman SB. Dystonia update (2000) *Clin Neuropharmacol* 23: 239-51.

Bressman SB, de Leon D, Raymond D, Greene PE, Brin MF, Fahn S, et al. The role of the DYT1 gene in secondary dystonia (1998) *Adv Neurol* 78: 107-15.

Bressman SB, Greene PE. Dystonia (2000) *Curr Treat Options Neurol* 2: 275-285.

Bronstein AM, Rudge P. Vestibular involvement in spasmodic torticollis (1986) *J Neurol Neurosurg Psychiatry* 49: 290-5.

Bronstein AM, Rudge P. The vestibular system in abnormal head postures and in spasmodic torticollis (1988) *Adv Neurol* 50: 493-500.

Brown P. Muscle sounds in Parkinson's disease (1997) *Lancet* 349: 533-5.

Brown P. Cortical drives to human muscle: the Piper and related rhythms (2000) *Prog Neurobiol* 60: 97-108.

Brown P. Oscillatory nature of human basal ganglia activity: relationship to the pathophysiology of Parkinson's disease (2003) *Mov Disord* 18: 357-63.

Brown P. Bad oscillations in Parkinson's disease (2006) *J Neural Transm Suppl* 27-30.

- Brown P, Chen CC, Wang S, Kuhn AA, Doyle L, Yarrow K, et al. Involvement of human basal ganglia in offline feedback control of voluntary movement (2006) *Curr Biol* 16: 2129-34.
- Brown P, Marsden CD. What do the basal ganglia do? (1998) *Lancet* 351: 1801-4.
- Brown P, Marsden CD. Bradykinesia and impairment of EEG desynchronization in Parkinson's disease (1999) *Mov Disord* 14: 423-9.
- Brown P, Marsden J, Defebvre L, Cassim F, Mazzone P, Oliviero A, et al. Intermuscular coherence in Parkinson's disease: relationship to bradykinesia (2001a) *Neuroreport* 12: 2577-81.
- Brown P, Mazzone P, Oliviero A, Altibrandi MG, Pilato F, Tonali PA, et al. Effects of stimulation of the subthalamic area on oscillatory pallidal activity in Parkinson's disease (2004) *Exp Neurol* 188: 480-90.
- Brown P, Oliviero A, Mazzone P, Insola A, Tonali P, Di Lazzaro V. Dopamine dependency of oscillations between subthalamic nucleus and pallidum in Parkinson's disease (2001b) *J Neurosci* 21: 1033-8.

Brown P, Salenius S, Rothwell JC, Hari R. Cortical correlate of the Piper rhythm in humans (1998) *J Neurophysiol* 80: 2911-7.

Brown P, Williams D. Basal ganglia local field potential activity: character and functional significance in the human (2005) *Clin Neurophysiol* 116: 2510-9.

Brown P, Williams D, Aziz T, Mazzone P, Oliviero A, Insola A, et al. Pallidal activity recorded in patients with implanted electrodes predictively correlates with eventual performance in a timing task (2002) *Neurosci Lett* 330: 188-92.

Brown RG, Dowsey PL, Brown P, Jahanshahi M, Pollak P, Benabid AL, et al. Impact of deep brain stimulation on upper limb akinesia in Parkinson's disease (1999) *Ann Neurol* 45: 473-88.

Burke RE, Fahn S, Marsden CD, Bressman SB, Moskowitz C, Friedman J. Validity and reliability of a rating scale for the primary torsion dystonias (1985) *Neurology* 35: 73-7.

Byl N, Wilson F, Merzenich M, Melnick M, Scott P, Oakes A, et al. Sensory dysfunction associated with repetitive strain injuries of tendinitis and focal hand dystonia: a comparative study (1996a) *J Orthop Sports Phys Ther* 23: 234-44.

Byl NN, Merzenich MM, Cheung S, Bedenbaugh P, Nagarajan SS, Jenkins WM. A primate model for studying focal dystonia and repetitive strain injury: effects on the primary somatosensory cortex (1997) *Phys Ther* 77: 269-84.

Byl NN, Merzenich MM, Jenkins WM. A primate genesis model of focal dystonia and repetitive strain injury: I. Learning-induced dedifferentiation of the representation of the hand in the primary somatosensory cortex in adult monkeys (1996b) *Neurology* 47: 508-20.

Capelle HH, Weigel R, Krauss JK. Bilateral pallidal stimulation for blepharospasm-ormandibular dystonia (Meige syndrome) (2003) *Neurology* 60: 2017-8.

Cassidy M, Brown P. Task-related EEG-EEG coherence depends on dopaminergic activity in Parkinson's disease (2001) *Neuroreport* 12: 703-7.

Cassidy M, Mazzone P, Oliviero A, Insola A, Tonali P, Di Lazzaro V, et al. Movement-related changes in synchronization in the human basal ganglia (2002) *Brain* 125: 1235-46.

Castelnau P, Cif L, Valente EM, Vayssiere N, Hemm S, Gannau A, et al. Pallidal stimulation improves pantothenate kinase-associated neurodegeneration (2005) *Ann Neurol* 57: 738-41.

Ceballos-Baumann AO, Brooks DJ. Basal ganglia function and dysfunction revealed by PET activation studies (1997) *Adv Neurol* 74: 127-39.

Challis RE, Kitney RI. Biomedical signal processing (in four parts). Part 1. Time-domain methods (1990) *Med Biol Eng Comput* 28: 509-24.

Challis RE, Kitney RI. Biomedical signal processing (in four parts). Part 2. The frequency transforms and their inter-relationships (1991a) *Med Biol Eng Comput* 29: 1-17.

Challis RE, Kitney RI. Biomedical signal processing (in four parts). Part 3. The power spectrum and coherence function (1991b) *Med Biol Eng Comput* 29: 225-41.

Chen CC, Brucke C, Kempf F, Kupsch A, Lu CS, Lee ST, et al. Deep brain stimulation of the subthalamic nucleus: a two-edged sword (2006a) *Curr Biol* 16: R952-3.

Chen CC, Kuhn AA, Hoffmann KT, Kupsch A, Schneider GH, Trottenberg T, et al.

Oscillatory pallidal local field potential activity correlates with involuntary EMG in dystonia (2006b) *Neurology* 66: 418-20.

Chen CC, Kuhn AA, Trottenberg T, Kupsch A, Schneider GH, Brown P. Neuronal activity in globus pallidus interna can be synchronized to local field potential activity over 3-12 Hz in patients with dystonia (2006c) *Exp Neurol* 202: 480-6.

Chen CC, Litvak V, Gilbertson T, Kuhn A, Lu CS, Lee ST, et al. Excessive synchronization of basal ganglia neurons at 20 Hz slows movement in Parkinson's disease (2007) *Exp Neurol* 205: 214-21

Chen CC, Pogosyan A, Zrinzo LU, Tisch S, Limousin P, Ashkan K, et al.

Intra-operative recordings of local field potentials can help localize the subthalamic nucleus in Parkinson's disease surgery (2006d) *Exp Neurol* 198: 214-21.

Chen H, Hua SE, Smith MA, Lenz FA, Shadmehr R. Effects of human cerebellar thalamus disruption on adaptive control of reaching (2006) *Cereb Cortex* 16: 1462-73.

Chen H, Smith M, Shadmehr R. Effects of deep brain stimulation on adaptive control of reaching 2005 Conf Proc IEEE Eng Med Biol Soc 5: 5445-8.

Chou KL, Hurtig HI, Jaggi JL, Baltuch GH. Bilateral subthalamic nucleus deep brain stimulation in a patient with cervical dystonia and essential tremor (2005) Mov Disord 20: 377-80.

Cif L, El Fertit H, Vayssiere N, Hemm S, Hardouin E, Gannau A, et al. Treatment of dystonic syndromes by chronic electrical stimulation of the internal globus pallidus (2003) J Neurosurg Sci 47: 52-5.

Coubes P, Cif L, El Fertit H, Hemm S, Vayssiere N, Serrat S, et al. Electrical stimulation of the globus pallidus internus in patients with primary generalized dystonia: long-term results (2004) J Neurosurg 101: 189-94.

Coubes P, Roubertie A, Vayssiere N, Hemm S, Echenne B. Treatment of DYT1-generalised dystonia by stimulation of the internal globus pallidus (2000) Lancet 355: 2220-1.

Coubes P, Vayssiere N, El Fertit H, Hemm S, Cif L, Kienlen J, et al. Deep brain stimulation for dystonia (2002) Surgical technique. Stereotact Funct Neurosurg 78: 183-91.

Courtemanche R, Fujii N, Graybiel AM. Synchronous, focally modulated beta-band oscillations characterize local field potential activity in the striatum of awake behaving monkeys (2003) *J Neurosci* 23: 11741-52.

Damier P, Hirsch EC, Agid Y, Graybiel AM. The substantia nigra of the human brain. I. Nigrosomes and the nigral matrix, a compartmental organization based on calbindin D(28K) immunohistochemistry (1999a) *Brain* 122 (Pt 8): 1421-36.

Damier P, Hirsch EC, Agid Y, Graybiel AM. The substantia nigra of the human brain. II. Patterns of loss of dopamine-containing neurons in Parkinson's disease (1999b) *Brain* 122 (Pt 8): 1437-48.

Davis KD, Hutchison WD, Lozano AM, Tasker RR, Dostrovsky JO. Human anterior cingulate cortex neurons modulated by attention-demanding tasks (2000a) *J Neurophysiol* 83: 3575-7.

Davis KD, Taub E, Duffner F, Lozano AM, Tasker RR, Houle S, et al. Activation of the anterior cingulate cortex by thalamic stimulation in patients with chronic pain: a positron emission tomography study (2000b) *J Neurosurg* 92: 64-9.

Davis KD, Taub E, Houle S, Lang AE, Dostrovsky JO, Tasker RR, et al. Globus pallidus stimulation activates the cortical motor system during alleviation of parkinsonian symptoms (1997) *Nat Med* 3: 671-4.

De Toledo JD, R. Sternomastoid function during hemispheric suppression by amytal: Insights into the inputs to the spinal accessory nerve nucleus (2004) *Mov Disord* 13: 809-812.

Dejean C, Gross CE, Bioulac B, Boraud T. Synchronous high-voltage spindles in the cortex-basal ganglia network of awake and unrestrained rats (2007) *Eur J Neurosci* 25: 772-84.

DeLong MR. Activity of pallidal neurons during movement (1971) *J. Neurophysiol* 34: 414-427.

DeLong MR. Primate models of movement disorders of basal ganglia origin (1990) *Trends Neurosci* 13: 281-5.

DeLong MR, Crutcher MD, Georgopoulos AP. Primate globus pallidus and subthalamic nucleus: functional organization (1985) *J Neurophysiol* 53: 530-43.

Deuschl G, Toro C, Matsumoto J, Hallett M. Movement-related cortical potentials in writer's cramp (1995) *Ann Neurol* 38: 862-8.

Di Lazzaro V, Oliviero A, Saturno E, Pilato F, Insola A, Mazzone P, et al. The effect on corticospinal volleys of reversing the direction of current induced in the motor cortex by transcranial magnetic stimulation (2001) *Exp Brain Res* 138: 268-73.

Diedrichsen J, Hashambhoy Y, Rane T, Shadmehr R. Neural correlates of reach errors (2005) *J Neurosci* 25: 9919-31.

Dostrovsky J, Bergman H. Oscillatory activity in the basal ganglia--relationship to normal physiology and pathophysiology (2004) *Brain* 127: 721-2.

Dostrovsky JO. Role of thalamus in pain (2000) *Prog Brain Res* 129: 245-57.

Dostrovsky JO, Levy R, Wu JP, Hutchison WD, Tasker RR, Lozano AM. Microstimulation-induced inhibition of neuronal firing in human globus pallidus (2000) *J Neurophysiol* 84: 570-4.

Dostrovsky JO, Lozano AM. Mechanisms of deep brain stimulation (2002) *Mov Disord* 17 Suppl 3: S63-8.

- Doupe AJ, Perkel DJ, Reiner A, Stern EA. Birdbrains could teach basal ganglia research a new song (2005) *Trends Neurosci* 28: 353-63.
- Doyle LM, Kuhn AA, Hariz M, Kupsch A, Schneider GH, Brown P.
Levodopa-induced modulation of subthalamic beta oscillations during self-paced movements in patients with Parkinson's disease (2005) *Eur J Neurosci* 21: 1403-12.
- Draganski B, Thun-Hohenstein C, Bogdahn U, Winkler J, May A. "Motor circuit" gray matter changes in idiopathic cervical dystonia (2003) *Neurology* 61: 1228-31.
- Edwards MJ, Huang YZ, Wood NW, Rothwell JC, Bhatia KP. Different patterns of electrophysiological deficits in manifesting and non-manifesting carriers of the DYT1 gene mutation (2003) *Brain* 126: 2074-80.
- Eekhof JL, Aramideh M, Bour LJ, Hilgevoord AA, Speelman HD, Ongerboer de Visser BW. Blink reflex recovery curves in blepharospasm, torticollis spasmodica, and hemifacial spasm (1996) *Muscle Nerve* 19: 10-5.
- Eekhof JL, Aramideh M, Speelman JD, Ongerboer de Visser BW. Orbicularis oculi and orbicularis oris reflexes in blepharospasm and torticollis spasmodica during spasm-free intervals (2001) *Eur Neurol* 46: 75-8.

- Elder CM, Hashimoto T, Zhang J, Vitek JL. Chronic implantation of deep brain stimulation leads in animal models of neurological disorders (2005) *J Neurosci Methods* 142: 11-6.
- Elliott R, Newman JL, Longe OA, Deakin JF. Differential response patterns in the striatum and orbitofrontal cortex to financial reward in humans: a parametric functional magnetic resonance imaging study (2003) *J Neurosci* 23: 303-7.
- Eltahawy HA, Saint-Cyr J, Poon YY, Moro E, Lang AE, Lozano AM. Pallidal deep brain stimulation in cervical dystonia: clinical outcome in four cases (2004) *Can J Neurol Sci* 31: 328-32.
- Engel AK, Fries P, Singer W. Dynamic predictions: oscillations and synchrony in top-down processing (2001) *Nat Rev Neurosci* 2: 704-16.
- Engel AK, Kreiter AK, König P, Singer W. Synchronization of oscillatory neuronal responses between striate and extrastriate visual cortical areas of the cat (1991) *Proc Natl Acad Sci U S A* 88: 6048-52.
- Engel AK, Singer W. Temporal binding and the neural correlates of sensory awareness (2001) *Trends Cogn Sci* 5: 16-25.

Ernst Niedermeyer and Fernando Lopes Da Silva. Electroencephalography, Basic principles, clinical applications, and related fields. 5th Edition, Lippincott Williams&Wilkins.

Everitt BJ, Wolf ME. Psychomotor stimulant addiction: a neural systems perspective (2002) J Neurosci 22: 3312-20.

Fahn S, Eldridge R. Definition of dystonia and classification of the dystonic states (1976) Adv Neurol 14: 1-5.

Fahn S, Elton RL. UPDRS program members, UPDRS. In/ Fahn S, Marsden CD, Goldstein M, Calne DB, editors. Recent development in Parkinson's disease, Vol 2, Florham Park, NJ: Macmillan Healthcare Information; 1987, p 153-163.

Farmer SF, Halliday DM, Conway BA, Stephens JA, Rosenberg JR. A review of recent applications of cross-correlation methodologies to human motor unit recording (1997) J Neurosci Methods 74: 175-87.

Farmer SF, Sheean GL, Mayston MJ, Rothwell JC, Marsden CD, Conway BA, et al. Abnormal motor unit synchronization of antagonist muscles underlies

pathological co-contraction in upper limb dystonia (1998) Brain 121 (Pt 5): 801-14.

Filali MH, WD. Peter, VN. Lozano, AM. Dostrovsky, JO. . Stimulation-induced inhibition of neuronal firing in human subthalamic nucleus (2004) Exp. Brain Res. 156: 274-281.

Filion M. Physiologic basis of dyskinesia (2000) Ann Neurol 47: S35-40; discussion S40-1.

Filion M, Tremblay L. Abnormal spontaneous activity of globus pallidus neurons in monkeys with MPTP-induced parkinsonism (1991) Brain Res 547: 142-51.

Filion M, Tremblay L, Bedard PJ. Abnormal influences of passive limb movement on the activity of globus pallidus neurons in parkinsonian monkeys (1988) Brain Res 444: 165-76.

Filion M, Tremblay L, Bedard PJ. Effects of dopamine agonists on the spontaneous activity of globus pallidus neurons in monkeys with MPTP-induced parkinsonism (1991) Brain Res 547: 152-61.

Flaherty AW, Williams ZM, Amirnovin R, Kasper E, Rauch SL, Cosgrove GR, et al. Deep brain stimulation of the anterior internal capsule for the treatment of Tourette syndrome: technical case report (2005) *Neurosurgery* 57: E403; discussion E403.

Foffani G, Ardolino G, Egidì M, Caputo E, Bossi B, Priori A. Subthalamic oscillatory activities at beta or higher frequency do not change after high-frequency DBS in Parkinson's disease (2006) *Brain Res Bull* 69: 123-30.

Foffani G, Ardolino G, Meda B, Egidì M, Rampini P, Caputo E, et al. Altered subthalamo-pallidal synchronisation in parkinsonian dyskinesias (2005a) *J Neurol Neurosurg Psychiatry* 76: 426-8.

Foffani G, Ardolino G, Rampini P, Tamma F, Caputo E, Egidì M, et al. Physiological recordings from electrodes implanted in the basal ganglia for deep brain stimulation in Parkinson's disease. the relevance of fast subthalamic rhythm (2005b). *Acta Neurochir Suppl* 93: 97-9.

Foffani G, Ardolino, G., Rampini, P., Tamma, F., Caputo, E., Egidì, M., . Physiological recordings from electrodes implanted in the basal ganglia for deep brain stimulation in Parkinson's disease. The relevance of fast subthalamic rhythms (2005c) *Acta Neurochir Suppl*. 93: 97-99.

Foffani G, Bianchi AM, Priori A, Baselli G. Adaptive autoregressive identification with spectral power decomposition for studying movement-related activity in scalp EEG signals and basal ganglia local field potentials (2004) *J Neural Eng* 1: 165-73.

Foffani G, Priori A. Involvement of the human subthalamic nucleus in movement preparation (2004) *Neurology* 63: 195-6; author reply 196.

Foffani G, Priori A, Egidi M, Rampini P, Tamma F, Caputo E, et al. 300-Hz subthalamic oscillations in Parkinson's disease (2003) *Brain* 126: 2153-63.

Fogelson N, Kuhn AA, Silberstein P, Limousin PD, Hariz M, Trottenberg T, et al. Frequency dependent effects of subthalamic nucleus stimulation in Parkinson's disease (2005a) *Neurosci Lett* 382: 5-9.

Fogelson N, Pogosyan A, Kuhn AA, Kupsch A, van Bruggen G, Speelman H, et al. Reciprocal interactions between oscillatory activities of different frequencies in the subthalamic region of patients with Parkinson's disease (2005b) *Eur J Neurosci* 22: 257-66.

Fogelson N, Williams D, Tijssen M, van Bruggen G, Speelman H, Brown P.

Different functional loops between cerebral cortex and the subthalamic area
in Parkinson's disease (2006) *Cereb Cortex* 16: 64-75.

Frank MJ, Seeberger LC, O'Reilly R C. By carrot or by stick: cognitive

reinforcement learning in parkinsonism (2004) *Science* 306: 1940-3.

Freeman A, Ciliax B, Bakay R, Daley J, Miller RD, Keating G, et al. Nigrostriatal

collaterals to thalamus degenerate in parkinsonian animal models (2001)

Ann Neurol 50: 321-9.

Freeman W, Morton AJ. Differential messenger RNA expression of complexins in

mouse brain (2004) *Brain Res Bull* 63: 33-44.

Fukuda M, Mentis M, Ghilardi MF, Dhawan V, Antonini A, Hammerstad J, et al.

Functional correlates of pallidal stimulation for Parkinson's disease (2001a)

Ann Neurol 49: 155-64.

Fukuda M, Mentis MJ, Ma Y, Dhawan V, Antonini A, Lang AE, et al. Networks

mediating the clinical effects of pallidal brain stimulation for Parkinson's
disease: a PET study of resting-state glucose metabolism (2001b) *Brain*

124: 1601-9.

Garcia L, Audin J, D'Alessandro G, Bioulac B, Hammond C. Dual effect of high-frequency stimulation on subthalamic neuron activity (2003) *J Neurosci* 23: 8743-51.

Garcia L, D'Alessandro G, Bioulac B, Hammond C. High-frequency stimulation in Parkinson's disease: more or less? (2005a) *Trends Neurosci* 28: 209-16.

Garcia L, D'Alessandro G, Fernagut PO, Bioulac B, Hammond C. Impact of high-frequency stimulation parameters on the pattern of discharge of subthalamic neurons (2005b) *J Neurophysiol* 94: 3662-9.

Garraux G, Bauer A, Hanakawa T, Wu T, Kansaku K, Hallett M. Changes in brain anatomy in focal hand dystonia (2004) *Ann Neurol* 55: 736-9.

Geny C, N'Guyen JP, Cesaro P, Goujon C, Brugieres P, Degos JD. Thalamic stimulation for severe action tremor after lesion of the superior cerebellar peduncle (1995) *J Neurol Neurosurg Psychiatry* 59: 641-2.

Geny C, Nguyen JP, Pollin B, Fève A, Ricolfi F, Cesaro P, et al. Improvement of severe postural cerebellar tremor in multiple sclerosis by chronic thalamic stimulation (1996) *Mov Disord* 11: 489-94.

- Gernert M, Bennay M, Fedrowitz M, Rehders JH, Richter A. Altered discharge pattern of basal ganglia output neurons in an animal model of idiopathic dystonia (2002) *J Neurosci* 22: 7244-53.
- Gernert M, Hamann M, Bennay M, Loscher W, Richter A. Deficit of striatal parvalbumin-reactive GABAergic interneurons and decreased basal ganglia output in a genetic rodent model of idiopathic paroxysmal dystonia (2000) *J Neurosci* 20: 7052-8.
- Gernert M, Richter A, Rundfeldt C, Loscher W. Quantitative EEG analysis of depth electrode recordings from several brain regions of mutant hamsters with paroxysmal dystonia discloses frequency changes in the basal ganglia (1998) *Mov Disord* 13: 509-21.
- Gill SS, Heywood P. Bilateral dorsolateral subthalamotomy for advanced Parkinson's disease (1997) *Lancet* 350: 1224.
- Gill SS, Patel NK, Hotton GR, O'Sullivan K, McCarter R, Bunnage M, et al. Direct brain infusion of glial cell line-derived neurotrophic factor in Parkinson disease (2003) *Nat Med* 9: 589-95.
- Goldberg JA, Boraud T, Maraton S, Haber SN, Vaadia E, Bergman H. Enhanced synchrony among primary motor cortex neurons in the

1-methyl-4-phenyl-1,2,3,6-tetrahydropyridine primate model of Parkinson's disease (2002) *J Neurosci* 22: 4639-53.

Goldberg JA, Rokni U, Boraud T, Vaadia E, Bergman H. Spike synchronization in the cortex/basal-ganglia networks of Parkinsonian primates reflects global dynamics of the local field potentials (2004a) *J Neurosci* 24: 6003-10.

Goldberg JA, Rokni U, Sompolinsky H. Patterns of ongoing activity and the functional architecture of the primary visual cortex (2004b) *Neuron* 42: 489-500.

Goldman MS, Kelly PJ. Stereotactic thalamotomy for medically intractable essential tremor (1992) *Stereotact Funct Neurosurg* 58: 22-5.

Goto Y, O'Donnell P. Network synchrony in the nucleus accumbens in vivo (2001a) *J Neurosci* 21: 4498-504.

Goto Y, O'Donnell P. Synchronous activity in the hippocampus and nucleus accumbens in vivo (2001b) *J Neurosci* 21: RC131.

Gray CM. Synchronous oscillations in neuronal systems: mechanisms and functions (1994) *J Comput Neurosci* 1: 11-38.

Gray CM, Konig P, Engel AK, Singer W. Oscillatory responses in cat visual cortex exhibit inter-columnar synchronization which reflects global stimulus properties (1989) *Nature* 338: 334-7.

Gray CM, McCormick DA. Chattering cells: superficial pyramidal neurons contributing to the generation of synchronous oscillations in the visual cortex (1996) *Science* 274: 109-13.

Gray CM, Viana Di Prisco G. Stimulus-dependent neuronal oscillations and local synchronization in striate cortex of the alert cat. *J Neurosci* (1997) 17: 3239-53.

Graybiel AM, Hirsch EC, Agid Y. The nigrostriatal system in Parkinson's disease (1990) *Adv Neurol* 53: 17-29.

Gross C, Rougier A, Guehl D, Boraud T, Julien J, Bioulac B. High-frequency stimulation of the globus pallidus internalis in Parkinson's disease: a study of seven cases (1997) *J Neurosurg* 87: 491-8.

Grosse P, Cassidy MJ, Brown P. EEG-EMG, MEG-EMG and EMG-EMG frequency analysis: physiological principles and clinical applications (2002) *Clin Neurophysiol* 113: 1523-31.

Grosse P, Edwards M, Tijssen MA, Schrag A, Lees AJ, Bhatia KP, et al. Patterns of EMG-EMG coherence in limb dystonia (2004) *Mov Disord* 19: 758-69.

Grosse P, Kuhn A, Cordivari C, Brown P. Coherence analysis in the myoclonus of corticobasal degeneration (2003) *Mov Disord* 8: 1345-50.

The deep-brain stimulation for Parkinson's disease study group . Deep-brain stimulation of the subthalamic nucleus or the pars interna of the globus pallidus in Parkinson's disease (2001) *N Engl J Med* 345: 956-963.

Guttman M. Double-blind comparison of pramipexole and bromocriptine treatment with placebo in advanced Parkinson's disease. International Pramipexole-Bromocriptine Study Group (1997) *Neurology* 49: 1060-5.

Haber SN. The primate basal ganglia: parallel and integrative networks (2003) *J Chem Neuroanat* 26: 317-30.

Hallett M. Is dystonia a sensory disorder? (1995) *Ann Neurol* 38: 139-40.

Halliday DM, Conway BA, Farmer SF, Rosenberg JR. Using electroencephalography to study functional coupling between cortical activity and electromyograms during voluntary contractions in humans (1998) *Neurosci Lett* 241: 5-8.

Halliday DM, Rosenberg JR, Amjad AM, Breeze P, Conway BA, Farmer SF. A framework for the analysis of mixed time series/point process data--theory and application to the study of physiological tremor, single motor unit discharges and electromyograms (1995) *Prog Biophys Mol Biol* 64: 237-78.

Hamada I, DeLong MR. Excitotoxic acid lesions of the primate subthalamic nucleus result in reduced pallidal neuronal activity during active holding (1992) *J Neurophysiol* 68: 1859-66.

Hamani C, Ewerton FI, Bonilha SM, Ballester G, Mello LE, Lozano AM. Bilateral anterior thalamic nucleus lesions and high-frequency stimulation are protective against pilocarpine-induced seizures and status epilepticus (2004a) *Neurosurgery* 54: 191-5; discussion 195-7.

Hamani C, Lozano AM. Special lecture: Brain stimulation: perspectives for the future (2004b) *Clin Neurosurg* 51: 271-4.

Hamani C, Saint-Cyr JA, Fraser J, Kaplitt M, Lozano AM. The subthalamic nucleus in the context of movement disorders (2004c) *Brain* 127: 4-20.

Hariz MI, Fodstad H. Do microelectrode techniques increase accuracy or decrease risks in pallidotomy and deep brain stimulation? A critical review of the literature (1999) *Stereotact Funct Neurosurg* 72: 157-69.

Hariz MI, Krack P, Melvill R, Jorgensen JV, Hamel W, Hirabayashi H, et al. A quick and universal method for stereotactic visualization of the subthalamic nucleus before and after implantation of deep brain stimulation electrodes (2003) *Stereotact Funct Neurosurg* 80: 96-101.

Hashimoto T, Elder CM, Okun MS, Patrick SK, Vitek JL. Stimulation of the subthalamic nucleus changes the firing pattern of pallidal neurons (2003) *J Neurosci* 23: 1916-23.

Hassler R, Riechert T, Mundinger F, Umbach W, Ganglberger JA. Physiological observations in stereotaxic operations in extrapyramidal motor disturbances (1960) *Brain* 83: 337-50.

Heimer G, Bar-Gad I, Goldberg JA, Bergman H. Dopamine replacement therapy reverses abnormal synchronization of pallidal neurons in the 1-methyl-4-phenyl-1,2,3,6-tetrahydropyridine primate model of parkinsonism (2002) *J Neurosci* 22: 7850-5.

Heimer G, Rivlin M, Israel Z, Bergman H. Synchronizing activity of basal ganglia and pathophysiology of Parkinson's disease (2006a) J Neural Transm Suppl 17-20.

Heimer G, Rivlin-Etzion M, Bar-Gad I, Goldberg JA, Haber SN, Bergman H. Dopamine replacement therapy does not restore the full spectrum of normal pallidal activity in the 1-methyl-4-phenyl-1,2,3,6-tetra-hydropyridine primate model of Parkinsonism (2006b) J Neurosci 26: 8101-14.

Hershey T, Revilla FJ, Wernle A, Gibson PS, Dowling JL, Perlmutter JS. Stimulation of STN impairs aspects of cognitive control in PD (2004) Neurology 62: 1110-4.

Hershey T, Revilla FJ, Wernle AR, McGee-Minnich L, Antenor JV, Videen TO, et al. Cortical and subcortical blood flow effects of subthalamic nucleus stimulation in PD (2003) Neurology 61: 816-21.

Hirsch E, Graybiel AM, Agid YA. Melanized dopaminergic neurons are differentially susceptible to degeneration in Parkinson's disease (1988) Nature 334: 345-8.

Hirsch EC, Graybiel AM, Duyckaerts C, Javoy-Agid F. Neuronal loss in the pedunculopontine tegmental nucleus in Parkinson disease and in

progressive supranuclear palsy (1987) Proc Natl Acad Sci U S A 84:
5976-80.

Hirsch EC, Mouatt A, Faucheux B, Bonnet AM, Javoy-Agid F, Graybiel AM, et al.
Dopamine, tremor, and Parkinson's disease (1992) Lancet 340: 125-6.

Hollerman JR, Schultz W. Dopamine neurons report an error in the temporal
prediction of reward during learning (1998) Nat Neurosci 1: 304-9.

Hurtado JM, Gray CM, Tamas LB, Sigvardt KA. Dynamics of tremor-related
oscillations in the human globus pallidus: a single case study (1999) Proc
Natl Acad Sci U S A 96: 1674-9.

Hurtado JM, Lachaux JP, Beckley DJ, Gray CM, Sigvardt KA. Inter- and intralimb
oscillator coupling in parkinsonian tremor (2000) Mov Disord 15: 683-91.

Hutchinson WD, Levy R, Dostrovsky JO, Lozano AM, Lang AE. Effects of
apomorphine on globus pallidus neurons in parkinsonian patients (1997)
Ann Neurol 42: 767-75.

Hutchison WD, Allan RJ, Opitz H, Levy R, Dostrovsky JO, Lang AE, et al.
Neurophysiological identification of the subthalamic nucleus in surgery for
Parkinson's disease (1998) Ann Neurol 44: 622-8.

Hutchison WD, Dostrovsky JO, Walters JR, Courtemanche R, Boraud T, Goldberg J, et al. Neuronal oscillations in the basal ganglia and movement disorders: evidence from whole animal and human recordings (2004) *J Neurosci* 24: 9240-3.

Hutchison WD, Lang AE, Dostrovsky JO, Lozano AM. Pallidal neuronal activity: implications for models of dystonia (2003) *Ann Neurol* 53: 480-8.

Hwang EJ, Smith MA, Shadmehr R. Adaptation and generalization in acceleration-dependent force fields (2006) *Exp Brain Res* 169: 496-506.

Ichinose H, Ohye T, Takahashi E, Seki N, Hori T, Segawa M, et al. Hereditary progressive dystonia with marked diurnal fluctuation caused by mutations in the GTP cyclohydrolase I gene (1994) *Nat Genet* 8: 236-42.

Ichinose H, Suzuki T, Inagaki H, Ohye T, Nagatsu T. DOPA-responsive dystonia. From causative gene to molecular mechanism (2001) *Adv Neurol* 86: 173-6.

Ikeda A, Shibasaki H, Kaji R, Terada K, Nagamine T, Honda M, et al. Abnormal sensorimotor integration in writer's cramp: study of contingent negative variation (1996) *Mov Disord* 11: 683-90.

Jahanshahi M, Ardouin CM, Brown RG, Rothwell JC, Obeso J, Albanese A, et al.
The impact of deep brain stimulation on executive function in Parkinson's
disease (2000) *Brain* 123 (Pt 6): 1142-54.

Jahanshahi M, Marion MH, Marsden CD. Natural history of adult-onset idiopathic
torticollis (1990) *Arch Neurol* 47: 548-52.

Jankovic J. Long-term study of pergolide in Parkinson's disease (1985) *Neurology*
35: 296-9.

Jankovic J, Orman J. Blepharospasm: demographic and clinical survey of 250
patients (1984) *Ann Ophthalmol* 16: 371-6.

Jasper H, Lende R, Rasmussen T. Evoked potentials from the exposed
somato-sensory cortex in man (1960) *J Nerv Ment Dis* 130: 526-37.

Jedynak CP, Bonnet AM, Agid Y. Tremor and idiopathic dystonia (1991) *Mov*
Disord 6: 230-6.

Jedynak PC, Tranchant C, de Beyer DZ. Prospective clinical study of writer's cramp
(2001) *Mov Disord* 16: 494-9.

Jenkinson N, Nandi D, Aziz TZ, Stein JF. Pedunculopontine nucleus: a new target for deep brain stimulation for akinesia (2005) *Neuroreport* 16: 1875-6.

Jenkinson N, Nandi D, Miall RC, Stein JF, Aziz TZ. Pedunculopontine nucleus stimulation improves akinesia in a Parkinsonian monkey (2004) *Neuroreport* 15: 2621-4.

Jenkinson N, Nandi D, Oram R, Stein JF, Aziz TZ. Pedunculopontine nucleus electric stimulation alleviates akinesia independently of dopaminergic mechanisms (2006) *Neuroreport* 17: 639-41.

Jueptner M, Frith CD, Brooks DJ, Frackowiak RS, Passingham RE. Anatomy of motor learning. II. Subcortical structures and learning by trial and error (1997a) *J Neurophysiol* 77: 1325-37.

Jueptner M, Ottinger S, Fellows SJ, Adamschewski J, Flerich L, Muller SP, et al. The relevance of sensory input for the cerebellar control of movements. *Neuroimage* (1997b) 5: 41-8.

Jueptner M, Stephan KM, Frith CD, Brooks DJ, Frackowiak RS, Passingham RE. Anatomy of motor learning. I. Frontal cortex and attention to action (1997c) *J Neurophysiol* 77: 1313-24.

Kaji R, Ikeda A, Ikeda T, Kubori T, Mezaki T, Kohara N, et al. Physiological study of cervical dystonia. Task-specific abnormality in contingent negative variation (1995a) Brain 118 (Pt 2): 511-22.

Kaji R, Rothwell JC, Katayama M, Ikeda T, Kubori T, Kohara N, et al. Tonic vibration reflex and muscle afferent block in writer's cramp (1995b) Ann Neurol 38: 155-62.

Kaji R, Shibasaki H, Kimura J. Writer's cramp: a disorder of motor subroutine? (1995c) Ann Neurol 38: 837-8.

Kaneoke Y, Vitek JL. The role of the basal ganglia in movement control (1995) Rinsho Shinkeigaku 35: 1518-21.

Kao MH, Doupe AJ, Brainard MS. Contributions of an avian basal ganglia-forebrain circuit to real-time modulation of song (2005) Nature 433: 638-43.

Kelly AM, Hester R, Murphy K, Javitt DC, Foxe JJ, Garavan H. Prefrontal-subcortical dissociations underlying inhibitory control revealed by event-related fMRI (2004) Eur J Neurosci 19: 3105-12.

Kimura M, Kato M, Shimazaki H, Watanabe K, Matsumoto N. Neural information transferred from the putamen to the globus pallidus during learned movement in the monkey (1996) *J Neurophysiol* 76: 3771-86.

Kiss ZH, Mooney DM, Renaud L, Hu B. Neuronal response to local electrical stimulation in rat thalamus: physiological implications for mechanisms of deep brain stimulation (2002) *Neuroscience* 113: 137-43.

Klostermann F, Nikulin VV, Kuhn AA, Marzinzik F, Wahl M, Pogosyan A, et al. Task-related differential dynamics of EEG alpha- and beta-band synchronization in cortico-basal motor structures (2007) *Eur J Neurosci* 25: 1604-15.

Knowlton BJ, Mangels JA, Squire LR. A neostriatal habit learning system in humans (1996) *Science* 273: 1399-402.

Koch GG, Landis JR, Freeman JL, Freeman DH, Jr., Lehnen RC. A general methodology for the analysis of experiments with repeated measurement of categorical data (1997) *Biometrics* 33: 133-58.

Koller WC, Lyons KE, Wilkinson SB, Troster AI, Pahwa R. Long-term safety and efficacy of unilateral deep brain stimulation of the thalamus in essential tremor (2001) *Mov Disord* 16: 464-8.

Kopell BH, Rezai AR, Chang JW, Vitek JL. Anatomy and physiology of the basal ganglia: implications for deep brain stimulation for Parkinson's disease (2006) *Mov Disord* 21 Suppl 14: S238-46.

Krack P, Batir A, Van Blercom N, Chabardes S, Fraix V, Ardouin C, et al. Five-year follow-up of bilateral stimulation of the subthalamic nucleus in advanced Parkinson's disease (2003) *N Engl J Med* 349: 1925-34.

Krack P, Benazzouz A, Pollak P, Limousin P, Piallat B, Hoffmann D, et al. Treatment of tremor in Parkinson's disease by subthalamic nucleus stimulation (1998a) *Mov Disord* 13: 907-14.

Krack P, Limousin P, Benabid AL, Pollak P. Chronic stimulation of subthalamic nucleus improves levodopa-induced dyskinesias in Parkinson's disease (1997a) *Lancet* 350: 1676.

Krack P, Pollak P, Limousin P, Benazzouz A, Benabid AL. Stimulation of subthalamic nucleus alleviates tremor in Parkinson's disease (1997b) *Lancet* 350: 1675.

- Krack P, Pollak P, Limousin P, Benazzouz A, Deuschl G, Benabid AL. From off-period dystonia to peak-dose chorea. The clinical spectrum of varying subthalamic nucleus activity (1999) *Brain* 122 (Pt 6): 1133-46.
- Krack P, Pollak P, Limousin P, Hoffmann D, Benazzouz A, Benabid AL. Inhibition of levodopa effects by internal pallidal stimulation (1998b) *Mov Disord* 13: 648-52.
- Krack P, Pollak P, Limousin P, Hoffmann D, Benazzouz A, Le Bas JF, et al. Opposite motor effects of pallidal stimulation in Parkinson's disease (1998c) *Ann Neurol* 43: 180-92.
- Krack P, Pollak P, Limousin P, Hoffmann D, Xie J, Benazzouz A, et al. Subthalamic nucleus or internal pallidal stimulation in young onset Parkinson's disease (1998d) *Brain* 121 (Pt 3): 451-7.
- Krack P, Vercueil L. Review of the functional surgical treatment of dystonia (2001) *Eur J Neurol* 8: 389-99.
- Krauss JK. Deep brain stimulation for cervical dystonia (2003) *J Neurol Neurosurg Psychiatry* 74: 1598.

Krauss JK, Loher TJ, Pohle T, Weber S, Taub E, Barlocher CB, et al. Pallidal deep brain stimulation in patients with cervical dystonia and severe cervical dyskinesias with cervical myelopathy (2002) J Neurol Neurosurg Psychiatry 72: 249-56.

Krauss JK, Loher TJ, Weigel R, Capelle HH, Weber S, Burgunder JM. Chronic stimulation of the globus pallidus internus for treatment of non-dYT1 generalized dystonia and choreoathetosis: 2-year follow up (2003) J Neurosurg 98: 785-92.

Krauss JK, Mundinger F. Thalamic stimulation for severe action tremor after lesion of the superior cerebellar peduncle (1996) J Neurol Neurosurg Psychiatry 61: 234.

Krauss JK, Nobbe F, Wakhloo AK, Mohadjer M, Vach W, Mundinger F. Movement disorders in astrocytomas of the basal ganglia and the thalamus (1992) J Neurol Neurosurg Psychiatry 55: 1162-7.

Krauss JK, Pohle T, Weber S, Ozdoba C, Burgunder JM. Bilateral stimulation of globus pallidus internus for treatment of cervical dystonia (1999) Lancet 354: 837-8.

Krauss JK, Trankle R, Kopp KH. Posttraumatic movement disorders after moderate or mild head injury (1997) *Mov Disord* 12: 428-31.

Krauss JK, Yianni J, Loher TJ, Aziz TZ. Deep brain stimulation for dystonia (2004) *J Clin Neurophysiol* 21: 18-30.

Kuhn AA, Doyle L, Pogosyan A, Yarrow K, Kupsch A, Schneider GH, et al. Modulation of beta oscillations in the subthalamic area during motor imagery in Parkinson's disease (2006a) *Brain* 129: 695-706.

Kuhn AA, Kupsch A, Schneider GH, Brown P. Reduction in subthalamic 8-35 Hz oscillatory activity correlates with clinical improvement in Parkinson's disease (2006b) *Eur J Neurosci* 23: 1956-60.

Kuhn AA, Trottenberg T, Kivi A, Kupsch A, Schneider GH, Brown P. The relationship between local field potential and neuronal discharge in the subthalamic nucleus of patients with Parkinson's disease (2005) *Exp Neurol* 194: 212-20.

Kuhn AA, Williams D, Kupsch A, Limousin P, Hariz M, Schneider GH, et al. Event-related beta desynchronization in human subthalamic nucleus correlates with motor performance (2004) *Brain* 127: 735-46.

Kumar R, Dagher A, Hutchison WD, Lang AE, Lozano AM. Globus pallidus deep brain stimulation for generalized dystonia: clinical and PET investigation (1999) *Neurology* 53: 871-4.

Kupsch A, Benecke R, Muller J, Trottenberg T, Schneider GH, Poewe W, et al. Pallidal deep-brain stimulation in primary generalized or segmental dystonia (2006) *N Engl J Med* 355: 1978-90.

Laitinen LV, Bergenheim AT, Hariz MI. Leksell's posteroventral pallidotomy in the treatment of Parkinson's disease (1992a) *J Neurosurg* 76: 53-61.

Laitinen LV, Bergenheim AT, Hariz MI. Ventroposterolateral pallidotomy can abolish all parkinsonian symptoms (1992b) *Stereotact Funct Neurosurg* 58: 14-21.

Landis JR, Koch GG. An application of hierarchical kappa-type statistics in the assessment of majority agreement among multiple observers (1977a) *Biometrics* 33: 363-74.

Landis JR, Koch GG. The measurement of observer agreement for categorical data (1977b) *Biometrics* 33: 159-74.

Landis JR, Koch, G.G., . The measurement of observer agreement for categorical data (1977) *Biometrics* 33: 159-174.

Leblois A, Boraud T, Meissner W, Bergman H, Hansel D. Competition between feedback loops underlies normal and pathological dynamics in the basal ganglia (2006a) *J Neurosci* 26: 3567-83.

Leblois A, Meissner W, Bezard E, Bioulac B, Gross CE, Boraud T. Temporal and spatial alterations in GPi neuronal encoding might contribute to slow down movement in Parkinsonian monkeys (2006b) *Eur J Neurosci* 24: 1201-8.

Lee MS, Marsden CD. Movement disorders following lesions of the thalamus or subthalamic region (1994) *Mov Disord* 9: 493-507.

Leis AA, Dimitrijevic MR, Delapasse JS, Sharkey PC. Modification of cervical dystonia by selective sensory stimulation (1992) *J Neurol Sci* 110: 79-89.

Lenz FA, Byl NN. Reorganization in the cutaneous core of the human thalamic principal somatic sensory nucleus (Ventral caudal) in patients with dystonia (1999) *J Neurophysiol* 82: 3204-12.

Lenz FA, Jaeger CJ, Seike MS, Lin YC, Reich SG, DeLong MR, et al. Thalamic single neuron activity in patients with dystonia: dystonia-related activity and somatic sensory reorganization (1999) *J Neurophysiol* 82: 2372-92.

Lenz FA, Suarez JI, Metman LV, Reich SG, Karp BI, Hallett M, et al. Pallidal activity during dystonia: somatosensory reorganisation and changes with severity (1998) *J Neurol Neurosurg Psychiatry* 65: 767-70.

Lenz FA, Vitek JL, DeLong MR. Role of the thalamus in parkinsonian tremor: evidence from studies in patients and primate models (1993) *Stereotact Funct Neurosurg* 60: 94-103.

Leone M, Franzini A, Broggi G, Bussone G. Hypothalamic deep brain stimulation for intractable chronic cluster headache: a 3-year follow-up (2003) *Neurol Sci* 24 Suppl 2: S143-5.

Leone M, Franzini A, Bussone G. Stereotactic stimulation of posterior hypothalamic gray matter in a patient with intractable cluster headache (2001) *N Engl J Med* 345: 1428-9.

Levy LM, Hallett M. Impaired brain GABA in focal dystonia (2002) *Ann Neurol* 51: 93-101.

Levy R, Ashby P, Hutchison WD, Lang AE, Lozano AM, Dostrovsky JO.

Dependence of subthalamic nucleus oscillations on movement and dopamine in Parkinson's disease. *Brain* (2002a) 125: 1196-209.

Levy R, Czernecki V. Apathy and the Basal Ganglia (2006) *J Neurol* 253 Suppl 7: vii54-vii61.

Levy R, Dostrovsky JO, Lang AE, Sime E, Hutchison WD, Lozano AM. Effects of apomorphine on subthalamic nucleus and globus pallidus internus neurons in patients with Parkinson's disease (2001a) *J Neurophysiol* 86: 249-60.

Levy R, Hazrati LN, Herrero MT, Vila M, Hassani OK, Mouroux M, et al.

Re-evaluation of the functional anatomy of the basal ganglia in normal and Parkinsonian states (1997) *Neuroscience* 76: 335-43.

Levy R, Hutchison WD, Lozano AM, Dostrovsky JO. High-frequency synchronization of neuronal activity in the subthalamic nucleus of parkinsonian patients with limb tremor (2000) *J Neurosci* 20: 7766-75.

Levy R, Hutchison WD, Lozano AM, Dostrovsky JO. Synchronized neuronal discharge in the basal ganglia of parkinsonian patients is limited to oscillatory activity. *J Neurosci* (2002) 22: 2855-61.

Levy R, Lang AE, Dostrovsky JO, Pahapill P, Romas J, Saint-Cyr J, et al.

Lidocaine and muscimol microinjections in subthalamic nucleus reverse
Parkinsonian symptoms (2001b) *Brain* 124: 2105-18.

Limousin P, Brown RG, Jahanshahi M, Asselman P, Quinn NP, Thomas D, et al.

The effects of posteroventral pallidotomy on the preparation and execution
of voluntary hand and arm movements in Parkinson's disease (1999) *Brain*
122 (Pt 2): 315-27.

Limousin P, Greene J, Pollak P, Rothwell J, Benabid AL, Frackowiak R. Changes
in cerebral activity pattern due to subthalamic nucleus or internal pallidum
stimulation in Parkinson's disease (1997) *Ann Neurol* 42: 283-91.

Limousin P, Pollak P, Benazzouz A, Hoffmann D, Broussolle E, Perret JE, et al.

Bilateral subthalamic nucleus stimulation for severe Parkinson's disease
(1995a) *Mov Disord* 10: 672-4.

Limousin P, Pollak P, Benazzouz A, Hoffmann D, Le Bas JF, Broussolle E, et al.

Effect of parkinsonian signs and symptoms of bilateral subthalamic nucleus
stimulation (1995b) *Lancet* 345: 91-5.

Limousin P, Pollak P, Hoffmann D, Benazzouz A, Perret JE, Benabid AL.

Abnormal involuntary movements induced by subthalamic nucleus stimulation in parkinsonian patients (1996) *Mov Disord* 11: 231-5.

Loher TJ, Gutbrod K, Fravi NL, Pohle T, Burgunder JM, Krauss JK. Thalamic stimulation for tremor. Subtle changes in episodic memory are related to stimulation per se and not to a microthalamotomy effect (2003) *J Neurol* 250: 707-13.

Louis ED, Levy G, Cote LJ, Mejia H, Fahn S, Marder K. Clinical correlates of action tremor in Parkinson disease (2001) *Arch Neurol* 58: 1630-4.

Love S, Plaha P, Patel NK, Hotton GR, Brooks DJ, Gill SS. Glial cell line-derived neurotrophic factor induces neuronal sprouting in human brain (2005) *Nat Med* 11: 703-4.

Lozano AM, Eltahawy H. How does DBS work? (2004) *Suppl Clin Neurophysiol* 57: 733-6.

Lozano AM, Hamani C. The future of deep brain stimulation (2004) *J Clin Neurophysiol* 21: 68-9.

Lozano AM, Hutchison WD. Microelectrode recordings in the pallidum (2002)

Mov Disord 17 Suppl 3: S150-4.

Lozano AM, Kumar R, Gross RE, Giladi N, Hutchison WD, Dostrovsky JO, et al.

Globus pallidus internus pallidotomy for generalized dystonia (1997) Mov Disord 12: 865-70.

Lozano AM, Lang AE, Levy R, Hutchison W, Dostrovsky J. Neuronal recordings

in Parkinson's disease patients with dyskinesias induced by apomorphine (2000) Ann Neurol 47: S141-6.

MacDonald BK, Cockerell OC, Sander JW, Shorvon SD. The incidence and

lifetime prevalence of neurological disorders in a prospective community-based study in the UK (2000) Brain 123 (Pt 4): 665-76.

Macia F, Escola L, Guehl D, Michelet T, Bioulac B, Burbaud P. Neuronal activity

in the monkey motor thalamus during bicuculline-induced dystonia (2002) Eur J Neurosci 15: 1353-62.

MacKinnon CD, Webb RM, Silberstein P, Tisch S, Asselman P, Limousin P, et al.

Stimulation through electrodes implanted near the subthalamic nucleus activates projections to motor areas of cerebral cortex in patients with Parkinson's disease (2005) Eur J Neurosci 21: 1394-402.

Magill PJ, Bolam JP, Bevan MD. Relationship of activity in the subthalamic nucleus-globus pallidus network to cortical electroencephalogram (2000) J Neurosci 20: 820-33.

Magill PJ, Bolam JP, Bevan MD. Dopamine regulates the impact of the cerebral cortex on the subthalamic nucleus-globus pallidus network (2001) Neuroscience 106: 313-30.

Magill PJ, Pogosyan A, Sharott A, Csicsvari J, Bolam JP, Brown P. Changes in functional connectivity within the rat striatopallidal axis during global brain activation in vivo (2006a) J Neurosci 26: 6318-29.

Magill PJ, Sharott A, Bevan MD, Brown P, Bolam JP. Synchronous unit activity and local field potentials evoked in the subthalamic nucleus by cortical stimulation. J Neurophysiol (2004a) 92: 700-14.

Magill PJ, Sharott A, Bolam JP, Brown P. Brain state-dependency of coherent oscillatory activity in the cerebral cortex and basal ganglia of the rat (2004b) J Neurophysiol 92: 2122-36.

Magill PJ, Sharott A, Bolam JP, Brown P. Delayed synchronization of activity in cortex and subthalamic nucleus following cortical stimulation in the rat (2006b) *J Physiol* 574: 929-46.

Magill PJ, Sharott A, Harnack D, Kupsch A, Meissner W, Brown P. Coherent spike-wave oscillations in the cortex and subthalamic nucleus of the freely moving rat (2005) *Neuroscience* 132: 659-64.

Mandir AS, Rowland LH, Dougherty PM, Lenz FA. Microelectrode recording and stimulation techniques during stereotactic procedures in the thalamus and pallidum (1997) *Adv Neurol* 74: 159-65.

Marsden CD. Problems with long-term levodopa therapy for Parkinson's disease (1994) *Clin Neuropharmacol* 17 Suppl 2: S32-44.

Marsden CD, Obeso JA. The functions of the basal ganglia and the paradox of stereotaxic surgery in Parkinson's disease (1994) *Brain* 117 (Pt 4): 877-97.

Marsden CD, Obeso JA, Zarranz JJ, Lang AE. The anatomical basis of symptomatic hemidystonia (1985) *Brain* 108 (Pt 2): 463-83.

Marsden JF, Ashby P, Limousin-Dowsey P, Rothwell JC, Brown P. Coherence between cerebellar thalamus, cortex and muscle in man: cerebellar thalamus interactions (2000a) *Brain* 123 (Pt 7): 1459-70.

Marsden JF, Ashby P, Rothwell JC, Brown P. Phase relationships between cortical and muscle oscillations in cortical myoclonus: electrocorticographic assessment in a single case (2000b) *Clin Neurophysiol* 111: 2170-4.

Marsden JF, Limousin-Dowsey P, Ashby P, Pollak P, Brown P. Subthalamic nucleus, sensorimotor cortex and muscle interrelationships in Parkinson's disease (2001) *Brain* 124: 378-88.

Marsden JF, Werhahn KJ, Ashby P, Rothwell J, Noachtar S, Brown P. Organization of cortical activities related to movement in humans (2000c) *J Neurosci* 20: 2307-14.

Matsumura M, Kojima J, Gardiner TW, Hikosaka O. Visual and oculomotor functions of monkey subthalamic nucleus (1992) *J Neurophysiol* 67: 1615-32.

Matsumura M, Tremblay L, Richard H, Filion M. Activity of pallidal neurons in the monkey during dyskinesia induced by injection of bicuculline in the external pallidum (1995) *Neuroscience* 65: 59-70.

Mayberg HS, Lozano AM, Voon V, McNeely HE, Seminowicz D, Hamani C, et al.
Deep brain stimulation for treatment-resistant depression (2005) *Neuron* 45:
651-60.

Mazzone P, Lozano A, Stanzione P, Galati S, Scarnati E, Peppe A, et al.
Implantation of human pedunculopontine nucleus: a safe and clinically
relevant target in Parkinson's disease (2005) *Neuroreport* 16: 1877-81.

McIntyre CC, Grill WM. Excitation of central nervous system neurons by
nonuniform electric fields (1999) *Biophys J* 76: 878-88.

McIntyre CC, Grill WM. Finite element analysis of the current-density and electric
field generated by metal microelectrodes (2001) *Ann Biomed Eng* 29:
227-35.

McIntyre CC, Grill WM, Sherman DL, Thakor NV. Cellular effects of deep brain
stimulation: model-based analysis of activation and inhibition (2004a) *J*
Neurophysiol 91: 1457-69.

McIntyre CC, Savasta M, Kerkerian-Le Goff L, Vitek JL. Uncovering the
mechanism(s) of action of deep brain stimulation: activation, inhibition, or
both (2004b) *Clin Neurophysiol* 115: 1239-48.

McIntyre CC, Savasta M, Walter BL, Vitek JL. How does deep brain stimulation work? Present understanding and future questions (2004c) *J Clin Neurophysiol* 21: 40-50.

Meissner W, Leblois A, Hansel D, Bioulac B, Gross CE, Benazzouz A, et al. Subthalamic high frequency stimulation resets subthalamic firing and reduces abnormal oscillations (2005) *Brain* 128: 2372-82.

Meissner W, Ravenscroft P, Reese R, Harnack D, Morgenstern R, Kupsch A, et al. Increased slow oscillatory activity in substantia nigra pars reticulata triggers abnormal involuntary movements in the 6-OHDA-lesioned rat in the presence of excessive extracellular striatal dopamine (2006) *Neurobiol Dis* 22: 586-98.

Mena-Segovia J, Bolam JP, Magill PJ. Pedunculo pontine nucleus and basal ganglia: distant relatives or part of the same family? (2004a) *Trends Neurosci* 27: 585-8.

Mena-Segovia J, Favila R, Giordano M. Long-term effects of striatal lesions on c-Fos immunoreactivity in the pedunculo pontine nucleus (2004b) *Eur J Neurosci* 20: 2367-76.

Mena-Segovia J, Giordano M. Striatal dopaminergic stimulation produces c-Fos expression in the PPT and an increase in wakefulness (2003) *Brain Res* 986: 30-8.

Metman LV, Del Dotto P, LePoole K, Konitsiotis S, Fang J, Chase TN. Amantadine for levodopa-induced dyskinesias: a 1-year follow-up study (1999) *Arch Neurol* 56: 1383-6.

Miller WC, DeLong MR. Parkinsonian symptomatology. An anatomical and physiological analysis (1988) *Ann N Y Acad Sci* 515: 287-302.

Mink JW. The basal ganglia: focused selection and inhibition of competing motor programs (1996) *Prog Neurobiol* 50: 381-425.

Mink JW. The Basal Ganglia and involuntary movements: impaired inhibition of competing motor patterns (2003) *Arch Neurol* 60: 1365-8.

Mink JW, Thach WT. Basal ganglia motor control. I. Nonexclusive relation of pallidal discharge to five movement modes (1991a) *J Neurophysiol* 65: 273-300.

Mink JW, Thach WT. Basal ganglia motor control. II. Late pallidal timing relative to movement onset and inconsistent pallidal coding of movement parameters (1991b) *J Neurophysiol* 65: 301-29.

Mink JW, Thach WT. Basal ganglia motor control. III. Pallidal ablation: normal reaction time, muscle cocontraction, and slow movement (1991c) *J Neurophysiol* 65: 330-51.

Miocinovic S, Parent M, Butson CR, Hahn PJ, Russo GS, Vitek JL, et al. Computational analysis of subthalamic nucleus and lenticular fasciculus activation during therapeutic deep brain stimulation (2006) *J Neurophysiol* 96: 1569-80.

Mitzdorf U, Singer W. Excitatory synaptic ensemble properties in the visual cortex of the macaque monkey: a current source density analysis of electrically evoked potentials (1979) *J Comp Neurol* 187: 71-83.

Mizuno Y, Yanagisawa N, Kuno S, Yamamoto M, Hasegawa K, Origasa H, et al. Randomized, double-blind study of pramipexole with placebo and bromocriptine in advanced Parkinson's disease (2003) *Mov Disord* 18: 1149-56.

- Moffitt MA, McIntyre CC, Grill WM. Prediction of myelinated nerve fiber stimulation thresholds: limitations of linear models (2004) *IEEE Trans Biomed Eng* 51: 229-36.
- Moller JC, Sautter J, Kupsch A. Potential of neurotrophic factors in therapy of Parkinson's disease. *J Neural Transm Suppl* (1996) 48: 103-12.
- Montgomery EB, Jr., Baker KB. Mechanisms of deep brain stimulation and future technical developments (2000) *Neurol Res* 22: 259-66.
- Moran A, Bar-Gad I, Bergman H, Israel Z. Real-time refinement of subthalamic nucleus targeting using Bayesian decision-making on the root mean square measure (2006) *Mov Disord* 21: 1425-31.
- Moro E, Esselink RA, Van Blercom N, Caputo E, Pollak P, Limousin P, et al. Bilateral subthalamic nucleus stimulation in a parkinsonian patient with previous unilateral pallidotomy and thalamotomy (2000) *Mov Disord* 15: 753-5.
- Morris G, Nevet A, Arkadir D, Vaadia E, Bergman H. Midbrain dopamine neurons encode decisions for future action (2006) *Nat Neurosci* 9: 1057-63.

Murata J, Kitagawa M, Uesugi H, Saito H, Iwasaki Y, Kikuchi S, et al. Electrical stimulation of the posterior subthalamic area for the treatment of intractable proximal tremor (2003) *J Neurosurg* 99: 708-15.

Murer MG, Tseng KY, Kasanetz F, Belluscio M, Riquelme LA. Brain oscillations, medium spiny neurons, and dopamine (2002) *Cell Mol Neurobiol* 22: 611-32.

Muta D, Goto S, Nishikawa S, Hamasaki T, Ushio Y, Inoue N, et al. Bilateral pallidal stimulation for idiopathic segmental axial dystonia advanced from Meige syndrome refractory to bilateral thalamotomy (2001) *Mov Disord* 16: 774-7.

Nakashima K, Rothwell JC, Thompson PD, Day BL, Berardelli A, Agostino R, et al. The blink reflex in patients with idiopathic torsion dystonia (1990) *Arch Neurol* 47: 413-6.

Nambu A. A new dynamic model of the cortico-basal ganglia loop (2004) *Prog Brain Res* 143: 461-6.

Nambu A, Tokuno H, Hamada I, Kita H, Imanishi M, Akazawa T, et al. Excitatory cortical inputs to pallidal neurons via the subthalamic nucleus in the monkey (2000) *J Neurophysiol* 84: 289-300.

- Nambu A, Tokuno H, Takada M. Functional significance of the cortico-subthalamo-pallidal 'hyperdirect' pathway (2002) *Neurosci Res* 43: 111-7.
- Nandi D, Aziz TZ, Liu X, Stein JF. Brainstem motor loops in the control of movement (2002a) *Mov Disord* 17 Suppl 3: S22-7.
- Nandi D, Chir M, Liu X, Bain P, Parkin S, Joint C, et al. Electrophysiological confirmation of the zona incerta as a target for surgical treatment of disabling involuntary arm movements in multiple sclerosis: use of local field potentials (2002b) *J Clin Neurosci* 9: 64-8.
- Nandi D, Jenkinson N, Stein JF, Aziz TZ. Laboratory and clinical investigations of the region of the rostral brainstem in motor control (2006) *Suppl Clin Neurophysiol* 58: 71-84.
- Narabayashi H. Stereotaxic Vim thalamotomy for treatment of tremor (1989) *Eur Neurol* 29 Suppl 1: 29-32.
- Nini A, Feingold A, Slovin H, Bergman H. Neurons in the globus pallidus do not show correlated activity in the normal monkey, but phase-locked

oscillations appear in the MPTP model of parkinsonism (1995) J Neurophysiol 74: 1800-5.

Nowak LG, Bullier J. Axons, but not cell bodies, are activated by electrical stimulation in cortical gray matter. I. Evidence from chronaxie measurements (1998) Exp Brain Res 118: 477-88.

Nowinski WT, A. Kennedy, DN. . Brain atlas for functional imaging: Clinical and research applications (2001) Thieme, Heidelberg, Germany

Nuttin B, Cosyns P, Demeulemeester H, Gybels J, Meyerson B. Electrical stimulation in anterior limbs of internal capsules in patients with obsessive-compulsive disorder (1999) Lancet 354: 1526.

Obeso JA, Rodriguez-Oroz MC, Rodriguez M, DeLong MR, Olanow CW. Pathophysiology of levodopa-induced dyskinesias in Parkinson's disease: problems with the current model (2000a) Ann Neurol 47: S22-32; discussion S32-4.

Obeso JA, Rodriguez-Oroz MC, Rodriguez M, Lanciego JL, Artieda J, Gonzalo N, et al. Pathophysiology of the basal ganglia in Parkinson's disease (2000b) Trends Neurosci 23: S8-19.

Obeso JA, Rodriguez-Oroz, M., Marin, C., Alonso, F., Zamarbide, I., Lanciego, J.L., . The origin of motor fluctuations in Parkinson's disease: importance of dopaminergic innervation and basal ganglia circuits (2004) . Neurology 62: S17-S30.

Obeso JA, Rothwell JC, Lang AE, Marsden CD. Myoclonic dystonia (1983) Neurology 33: 825-30.

Olanow CW, Fahn S, Muentner M, Klawans H, Hurtig H, Stern M, et al. A multicenter double-blind placebo-controlled trial of pergolide as an adjunct to Sinemet in Parkinson's disease (1994) Mov Disord 9: 40-7.

Pahapill PA, Lozano AM. The pedunculopontine nucleus and Parkinson's disease (2000) Brain 123 (Pt 9): 1767-83.

Pahwa R, Wilkinson S, Smith D, Lyons K, Miyawaki E, Koller WC. High-frequency stimulation of the globus pallidus for the treatment of Parkinson's disease (1997) Neurology 49: 249-53.

Paluzzi A, Bain PG, Liu X, Yianni J, Kumarendran K, Aziz TZ. Pregnancy in dystonic women with in situ deep brain stimulators (2006) Mov Disord 21: 695-8.

Papakostopoulos D. Multidisciplinary perspectives in event related brain potentials research (1978) D.A. Otto,ed.(Washington, D.C.: US Environmental Protection Agency) 134-137.

Parent A, Cote PY, Lavoie B. Chemical anatomy of primate basal ganglia (1995) Prog Neurobiol 46: 131-97.

Parent A, Hazrati LN. Functional anatomy of the basal ganglia. I. The cortico-basal ganglia-thalamo-cortical loop (1995a) Brain Res Brain Res Rev 20: 91-127.

Parent A, Hazrati LN. Functional anatomy of the basal ganglia. II. The place of subthalamic nucleus and external pallidum in basal ganglia circuitry (1995b) Brain Res Brain Res Rev 20: 128-54.

Parkin S, Aziz T, Gregory R, Bain P. Bilateral internal globus pallidus stimulation for the treatment of spasmodic torticollis (2001) Mov Disord 16: 489-93.

Pasquereau B, Nadjar A, Arkadir D, Bezard E, Goillandeau M, Bioulac B, et al. Shaping of motor responses by incentive values through the basal ganglia (2007) J Neurosci 27: 1176-83.

Pauletti G, Berardelli A, Cruccu G, Agostino R, Manfredi M. Blink reflex and the masseter inhibitory reflex in patients with dystonia (1993) *Mov Disord* 8: 495-500.

Peppe A, Pierantozzi M, Altibrandi MG, Giacomini P, Stefani A, Bassi A, et al. Bilateral GPi DBS is useful to reduce abnormal involuntary movements in advanced Parkinson's disease patients, but its action is related to modality and site of stimulation (2001) *Eur J Neurol* 8: 579-86.

Pessiglione M, Czernecki V, Pillon B, Dubois B, Schupbach M, Agid Y, et al. An effect of dopamine depletion on decision-making: the temporal coupling of deliberation and execution (2005a) *J Cogn Neurosci* 17: 1886-96.

Pessiglione M, Guehl D, Rolland AS, Francois C, Hirsch EC, Feger J, et al. Thalamic neuronal activity in dopamine-depleted primates: evidence for a loss of functional segregation within basal ganglia circuits (2005b) *J Neurosci* 25: 1523-31.

Pettigrew LC, Jankovic J. Hemidystonia: a report of 22 patients and a review of the literature (1985) *J Neurol Neurosurg Psychiatry* 48: 650-7.

Piercey MF. Pharmacology of pramipexole, a dopamine D3-preferring agonist useful in treating Parkinson's disease (1998) Clin Neuropharmacol 21: 141-51.

Piercey MF, Hoffmann WE, Smith MW, Hyslop DK. Inhibition of dopamine neuron firing by pramipexole, a dopamine D3 receptor-preferring agonist: comparison to other dopamine receptor agonists (1996) Eur J Pharmacol 312: 35-44.

Piercey MF, Hyslop DK, Hoffmann WE. Excitation of type II anterior caudate neurons by stimulation of dopamine D3 receptors (1997) Brain Res 762: 19-28.

Pinter MM, Pogarell O, Oertel WH. Efficacy, safety, and tolerance of the non-ergoline dopamine agonist pramipexole in the treatment of advanced Parkinson's disease: a double blind, placebo controlled, randomised, multicentre study (1999) J Neurol Neurosurg Psychiatry 66: 436-41.

Plaha P, Ben-Shlomo Y, Patel NK, Gill SS. Stimulation of the caudal zona incerta is superior to stimulation of the subthalamic nucleus in improving contralateral parkinsonism (2006) Brain 129: 1732-47.

Plaha P, Gill SS. Bilateral deep brain stimulation of the pedunculopontine nucleus for Parkinson's disease. *Neuroreport* (2005) 16: 1883-7.

Pogosyan A, Kuhn AA, Trottenberg T, Schneider GH, Kupsch A, Brown P. Elevations in local gamma activity are accompanied by changes in the firing rate and information coding capacity of neurons in the region of the subthalamic nucleus in Parkinson's disease (2006) *Exp Neurol* 202: 271-9.

Pollak P, Benabid AL, Limousin P, Benazzouz A, Hoffmann D, Le Bas JF, et al. Subthalamic nucleus stimulation alleviates akinesia and rigidity in parkinsonian patients (1996a) *Adv Neurol* 69: 591-4.

Pollak P, Benabid AL, Limousin P, Krack P. Treatment of Parkinson's disease. New surgical treatment strategies (1996b) *Eur Neurol* 36: 400-4.

Pool JL. Psychosurgery in older people (1954) *J Am Geriatr Soc* 2: 456-66.

Priori A, Ardolino G, Marceglia S, Mrakic-Sposta S, Locatelli M, Tamma F, et al. Low-frequency subthalamic oscillations increase after deep brain stimulation in Parkinson's disease. *Brain Res Bull* (2006) 71: 149-54.

Priori A, Berardelli A, Mercuri B, Manfredi M. Physiological effects produced by botulinum toxin treatment of upper limb dystonia. Changes in reciprocal inhibition between forearm muscles (1995) *Brain* 118 (Pt 3): 801-7.

Priori A, Foffani G, Pesenti A, Bianchi A, Chiesa V, Baselli G, et al.
Movement-related modulation of neural activity in human basal ganglia and its L-DOPA dependency: recordings from deep brain stimulation electrodes in patients with Parkinson's disease (2002) *Neurol Sci* 23 Suppl 2: S101-2.

Priori A, Foffani G, Pesenti A, Tamma F, Bianchi AM, Pellegrini M, et al.
Rhythm-specific pharmacological modulation of subthalamic activity in Parkinson's disease (2004) *Exp Neurol* 189: 369-79.

Quinn NP. Essential myoclonus and myoclonic dystonia (1996) *Mov Disord* 11: 119-24.

Rascol O, Lees AJ, Senard JM, Pirtosek Z, Brefel C, Montastruc JL, et al. A placebo-controlled study of ropinirole, a new D2 agonist, in the treatment of motor fluctuations of L-DOPA-treated parkinsonian patients (1996) *Adv Neurol* 69: 531-4.

Rattay F. The basic mechanism for the electrical stimulation of the nervous system (1999) *Neuroscience* 89: 335-46.

- Raz A, Feingold A, Zelanskaya V, Vaadia E, Bergman H. Neuronal synchronization of tonically active neurons in the striatum of normal and parkinsonian primates (1996) *J Neurophysiol* 76: 2083-8.
- Raz A, Frechter-Mazar V, Feingold A, Abeles M, Vaadia E, Bergman H. Activity of pallidal and striatal tonically active neurons is correlated in mptp-treated monkeys but not in normal monkeys (2001) *J Neurosci* 21: RC128.
- Raz A, Vaadia E, Bergman H. Firing patterns and correlations of spontaneous discharge of pallidal neurons in the normal and the tremulous 1-methyl-4-phenyl-1,2,3,6-tetrahydropyridine vervet model of parkinsonism (2000) *J Neurosci* 20: 8559-71.
- Rektor I, Sochurkova D, Bockova M. Intracerebral ERD/ERS in voluntary movement and in cognitive visuomotor task (2006) *Prog Brain Res* 159: 311-30.
- Richter EO, Davis KD, Hamani C, Hutchison WD, Dostrovsky JO, Lozano AM. Cingulotomy for psychiatric disease: microelectrode guidance, a callosal reference system for documenting lesion location, and clinical result (2004). *Neurosurgery* 54: 622-28; discussion 628-30.

Rivlin-Etzion M, Marmor O, Heimer G, Raz A, Nini A, Bergman H. Basal ganglia oscillations and pathophysiology of movement disorders (2006) *Curr Opin Neurobiol* 16: 629-37.

Rodriguez R, Kallenbach U, Singer W, Munk MH. Short- and long-term effects of cholinergic modulation on gamma oscillations and response synchronization in the visual cortex (2004) *J Neurosci* 24: 10369-78.

Rodriguez-Oroz MC, Rodriguez M, Guridi J, Mewes K, Chockkman V, Vitek J, et al. The subthalamic nucleus in Parkinson's disease: somatotopic organization and physiological characteristics (2001) *Brain* 124: 1777-90.

Rosenberg JR, Amjad AM, Breeze P, Brillinger DR, Halliday DM. The Fourier approach to the identification of functional coupling between neuronal spike trains (1989) *Prog Biophys Mol Biol* 53: 1-31.

Rothwell JC, Obeso JA, Day BL, Marsden CD. Pathophysiology of dystonias (1983) *Adv Neurol* 39: 851-63.

Rousseaux M, Krystkowiak P, Kozlowski O, Ozsancak C, Blond S, Destee A. Effects of subthalamic nucleus stimulation on parkinsonian dysarthria and speech intelligibility (2004) *J Neurol* 251: 327-34.

- Ruskin DN, Bergstrom DA, Tierney PL, Walters JR. Correlated multisecond oscillations in firing rate in the basal ganglia: modulation by dopamine and the subthalamic nucleus (2003) *Neuroscience* 117: 427-38.
- Sage JI, Duvoisin RC. Long-term efficacy of pergolide in patients with Parkinson's disease (1986) *Clin Neuropharmacol* 9: 160-4.
- Saint-Cyr JA, Hoque T, Pereira LC, Dostrovsky JO, Hutchison WD, Mikulis DJ, et al. Localization of clinically effective stimulating electrodes in the human subthalamic nucleus on magnetic resonance imaging (2002) *J Neurosurg* 97: 1152-66.
- Saint-Cyr JA, Trepanier LL, Kumar R, Lozano AM, Lang AE. Neuropsychological consequences of chronic bilateral stimulation of the subthalamic nucleus in Parkinson's disease (2000) *Brain* 123 (Pt 10): 2091-108.
- Salenius S, Avikainen S, Kaakkola S, Hari R, Brown P. Defective cortical drive to muscle in Parkinson's disease and its improvement with levodopa (2002) *Brain* 125: 491-500.
- Schneider S, Feifel E, Ott D, Schumacher M, Lucking CH, Deuschl G. Prolonged MRI T2 times of the lentiform nucleus in idiopathic spasmodic torticollis (1994) *Neurology* 44: 846-50.

Schultz W. Getting formal with dopamine and reward (2002) *Neuron* 36: 241-63.

Sharott A, Magill PJ, Bolam JP, Brown P. Directional analysis of coherent oscillatory field potentials in the cerebral cortex and basal ganglia of the rat (2005a) *J Physiol* 562: 951-63.

Sharott A, Magill PJ, Harnack D, Kupsch A, Meissner W, Brown P. Dopamine depletion increases the power and coherence of beta-oscillations in the cerebral cortex and subthalamic nucleus of the awake rat (2005b) *Eur J Neurosci* 21: 1413-22.

Shohamy D, Myers CE, Grossman S, Sage J, Gluck MA, Poldrack RA. Cortico-striatal contributions to feedback-based learning: converging data from neuroimaging and neuropsychology (2004) *Brain* 127: 851-9.

Shults CW. Lewy bodies (2006) *Proc Natl Acad Sci U S A* 103: 1661-8.

Siegfried J, Lippitz B. Bilateral chronic electrostimulation of ventroposterolateral pallidum: a new therapeutic approach for alleviating all parkinsonian symptoms (1994a) *Neurosurgery* 35: 1126-9; discussion 1129-30.

Siegfried J, Lippitz B. Chronic electrical stimulation of the VL-VPL complex and of the pallidum in the treatment of movement disorders: personal experience since 1982 (1994b) *Stereotact Funct Neurosurg* 62: 71-5.

Siegfried J, Wellis G. Chronic electrostimulation of ventroposterolateral pallidum: follow-up (1997) *Acta Neurochir Suppl* 68: 11-3.

Silberstein P, Kuhn AA, Kupsch A, Trottenberg T, Krauss JK, Wöhrle JC, et al. Patterning of globus pallidus local field potentials differs between Parkinson's disease and dystonia (2003) *Brain* 126: 2597-608.

Silberstein P, Oliviero A, Di Lazzaro V, Insola A, Mazzone P, Brown P. Oscillatory pallidal local field potential activity inversely correlates with limb dyskinesias in Parkinson's disease (2005a) *Exp Neurol* 194: 523-9.

Silberstein P, Pogosyan A, Kuhn AA, Hotton G, Tisch S, Kupsch A, et al. Cortico-cortical coupling in Parkinson's disease and its modulation by therapy (2005b) *Brain* 128: 1277-91.

Singer W. Neuronal representations, assemblies and temporal coherence (1993a) *Prog Brain Res* 95: 461-74.

Singer W. Synchronization of cortical activity and its putative role in information processing and learning (1993b) *Annu Rev Physiol* 55: 349-74.

Smith GS, Price JC, Lopresti BJ, Huang Y, Simpson N, Holt D, et al. Test-retest variability of serotonin 5-HT_{2A} receptor binding measured with positron emission tomography and [¹⁸F]altanserin in the human brain (1998a) *Synapse* 30: 380-92.

Smith GS, Schloesser R, Brodie JD, Dewey SL, Logan J, Vitkun SA, et al. Glutamate modulation of dopamine measured in vivo with positron emission tomography (PET) and ¹¹C-raclopride in normal human subjects (1998b) *Neuropsychopharmacology* 18: 18-25.

Smith MA, Shadmehr R. Intact ability to learn internal models of arm dynamics in Huntington's disease but not cerebellar degeneration (2005) *J Neurophysiol* 93: 2809-21.

Smith Y, Bevan MD, Shink E, Bolam JP. Microcircuitry of the direct and indirect pathways of the basal ganglia (1998c) *Neuroscience* 86: 353-87.

Smith Y, Shink E, Sidibe M. Neuronal circuitry and synaptic connectivity of the basal ganglia (1998d) *Neurosurg Clin N Am* 9: 203-22.

Sochurkova D, Rektor I. Event-related desynchronization/synchronization in the putamen. An SEEG case study (2003) *Exp Brain Res* 149: 401-4.

Speelman JD, Schuurman PR, de Bie RM, Bosch DA. Thalamic surgery and tremor (1998) *Mov Disord* 13 Suppl 3: 103-6.

Spillantini MG, Schmidt ML, Lee VM, Trojanowski JQ, Jakes R, Goedert M. Alpha-synuclein in Lewy bodies (1997) *Nature* 388: 839-40.

Starr PA, Turner RS, Rau G, Lindsey N, Heath S, Volz M, et al. Microelectrode-guided implantation of deep brain stimulators into the globus pallidus internus for dystonia: techniques, electrode locations, and outcomes (2004) *Neurosurg Focus* 17: E4.

Starr PA, Turner RS, Rau G, Lindsey N, Heath S, Volz M, et al. Microelectrode-guided implantation of deep brain stimulators into the globus pallidus internus for dystonia: techniques, electrode locations, and outcomes (2006) *J Neurosurg* 104: 488-501.

Stefani A, Lozano AM, Peppe A, Stanzione P, Galati S, Tropepi D, et al. Bilateral deep brain stimulation of the pedunculopontine and subthalamic nuclei in severe Parkinson's disease (2007) *Brain*

Stell R, Bronstein AM, Gresty M, Buckwell D, Marsden CD. Saccadic function in spasmodic torticollis (1990) *J Neurol Neurosurg Psychiatry* 53: 496-501.

Stell R, Bronstein AM, Marsden CD. Vestibulo-ocular abnormalities in spasmodic torticollis before and after botulinum toxin injections (1989) *J Neurol Neurosurg Psychiatry* 52: 57-62.

Stell R, Gresty M, Metcalfe T, Bronstein AM. Cervico-ocular function in patients with spasmodic torticollis (1991) *J Neurol Neurosurg Psychiatry* 54: 39-41.

Stern CD, Goodwin BC. Waves and periodic events during primitive streak formation in the chick (1977) *J Embryol Exp Morphol* 41: 15-22.

Stern EA, Jaeger D, Wilson CJ. Membrane potential synchrony of simultaneously recorded striatal spiny neurons in vivo (1998) *Nature* 394: 475-8.

Stern ER, Mangels JA. An electrophysiological investigation of preparatory attentional control in a spatial Stroop task (2006) *J Cogn Neurosci* 18: 1004-17.

Stover NP, Okun MS, Evatt ML, Raju DV, Bakay RA, Vitek JL. Stimulation of the subthalamic nucleus in a patient with Parkinson disease and essential tremor (2005) *Arch Neurol* 62: 141-3.

Suarez JI, Metman LV, Reich SG, Dougherty PM, Hallett M, Lenz FA.

Pallidotomy for hemiballismus: efficacy and characteristics of neuronal activity (1997) *Ann Neurol* 42: 807-11.

Sydow O, Thobois S, Alesch F, Speelman JD. Multicentre European study of thalamic stimulation in essential tremor: a six year follow up (2003) *J Neurol Neurosurg Psychiatry* 74: 1387-91.

Tai CH, Boraud T, Bezard E, Bioulac B, Gross C, Benazzouz A.

Electrophysiological and metabolic evidence that high-frequency stimulation of the subthalamic nucleus bridles neuronal activity in the subthalamic nucleus and the substantia nigra reticulata (2003) *Faseb J* 17: 1820-30.

Temperli P, Ghika J, Villemure JG, Burkhard PR, Bogousslavsky J, Vingerhoets FJ. How do parkinsonian signs return after discontinuation of subthalamic DBS? (2003) *Neurology* 60: 78-81.

Tijssen MA, Marsden JF, Brown P. Frequency analysis of EMG activity in patients with idiopathic torticollis (2000) *Brain* 123 (Pt 4): 677-86.

Tijssen MA, Munchau A, Marsden JF, Lees A, Bhatia KP, Brown P. Descending control of muscles in patients with cervical dystonia (2002) *Mov Disord* 17: 493-500.

Timmermann L, Wojtecki L, Gross J, Lehrke R, Voges J, Maarouf M, et al. Ten-Hertz stimulation of subthalamic nucleus deteriorates motor symptoms in Parkinson's disease (2004) *Mov Disord* 19: 1328-33.

Tinazzi M, Rosso T, Fiaschi A. Role of the somatosensory system in primary dystonia (2003) *Mov Disord* 18: 605-22.

Toda H, Hamani C, Lozano A. Deep brain stimulation in the treatment of dyskinesia and dystonia (2004) *Neurosurg Focus* 17: E2.

Tolosa E, Montserrat L, Bayes A. Blink reflex studies in focal dystonias: enhanced excitability of brainstem interneurons in cranial dystonia and spasmodic torticollis (1988) *Mov Disord* 3: 61-9.

Tremblay L, Filion M, Bedard PJ. Responses of pallidal neurons to striatal stimulation in monkeys with MPTP-induced parkinsonism (1989) *Brain Res* 498: 17-33.

Trottenberg T, Fogelson N, Kuhn AA, Kivi A, Kupsch A, Schneider GH, et al.

Subthalamic gamma activity in patients with Parkinson's disease (2006) *Exp Neurol* 200: 56-65.

Trottenberg T, Kupsch A, Schneider GH, Brown P, Kuhn AA.

Frequency-dependent distribution of local field potential activity within the subthalamic nucleus in Parkinson's disease (2007) *Exp Neurol*

Trottenberg T, Meissner W, Kabus C, Arnold G, Funk T, Einhaupl KM, et al.

Neurostimulation of the ventral intermediate thalamic nucleus in inherited myoclonus-dystonia syndrome (2001a) *Mov Disord* 16: 769-71.

Trottenberg T, Paul G, Meissner W, Maier-Hauff K, Taschner C, Kupsch A.

Pallidal and thalamic neurostimulation in severe tardive dystonia (2001b) *J Neurol Neurosurg Psychiatry* 70: 557-9.

Trottenberg T, Volkmann J, Deuschl G, Kuhn AA, Schneider GH, Muller J, et al.

Treatment of severe tardive dystonia with pallidal deep brain stimulation (2005) *Neurology* 64: 344-6.

Uhlhaas PJ, Linden DE, Singer W, Haenschel C, Lindner M, Maurer K, et al.

Dysfunctional long-range coordination of neural activity during Gestalt perception in schizophrenia (2006) *J Neurosci* 26: 8168-75.

Uhlhaas PJ, Singer W. Neural synchrony in brain disorders: relevance for cognitive dysfunctions and pathophysiology (2006) *Neuron* 52: 155-68.

Urbano FJ, Rosato-Siri MD, Uchitel OD. Calcium channels involved in neurotransmitter release at adult, neonatal and P/Q-type deficient neuromuscular junctions (Review) (2002) *Mol Membr Biol* 19: 293-300.

Vaillancourt DE, Prodoehl J, Verhagen Metman L, Bakay RA, Corcos DM. Effects of deep brain stimulation and medication on bradykinesia and muscle activation in Parkinson's disease (2004) *Brain* 127: 491-504.

Van der Kamp W, Rothwell JC, Thompson PD, Day BL, Marsden CD. The movement-related cortical potential is abnormal in patients with idiopathic torsion dystonia (1995) *Mov Disord* 10: 630-3.

van Manen J. Stereotaxic operations in cases of hereditary and intention tremor (1974) *Acta Neurochir (Wien)* Suppl 21: 49-55.

Vandewalle V, van der Linden C, Groenewegen HJ, Caemaert J. Stereotactic treatment of Gilles de la Tourette syndrome by high frequency stimulation of thalamus (1999) *Lancet* 353: 724.

Vidailhet M, Pollak P. Deep brain stimulation for dystonia: make the lame walk
(2005) *Ann Neurol* 57: 613-4.

Vidailhet M, Vercueil L, Houeto JL, Krystkowiak P, Benabid AL, Cornu P, et al.
Bilateral deep-brain stimulation of the globus pallidus in primary
generalized dystonia (2005) *N Engl J Med* 352: 459-67.

Vidailhet M, Vercueil L, Houeto JL, Krystkowiak P, Lagrange C, Yelnik J, et al.
Bilateral, pallidal, deep-brain stimulation in primary generalised dystonia: a
prospective 3 year follow-up study (2007) *Lancet Neurol* 6: 223-9.

Vitek JL. Surgery for dystonia (1998) *Neurosurg Clin N Am* 9: 345-66.

Vitek JL. Mechanisms of deep brain stimulation: excitation or inhibition (2002a)
Mov Disord 17 Suppl 3: S69-72.

Vitek JL. Pathophysiology of dystonia: a neuronal model (2002b) *Mov Disord* 17
Suppl 3: S49-62.

Vitek JL, Ashe J, DeLong MR, Kaneoke Y. Microstimulation of primate motor
thalamus: somatotopic organization and differential distribution of evoked
motor responses among subnuclei (1996) *J Neurophysiol* 75: 2486-95.

Vitek JL, Bakay RA. The role of pallidotomy in Parkinson's disease and dystonia
(1997) *Curr Opin Neurol* 10: 332-9.

Vitek JL, Bakay RA, Hashimoto T, Kaneoke Y, Mewes K, Zhang JY, et al.
Microelectrode-guided pallidotomy: technical approach and its application
in medically intractable Parkinson's disease. *J Neurosurg*(1998a) 88:
1027-43.

Vitek JL, Chockkan V, Zhang JY, Kaneoke Y, Evatt M, DeLong MR, et al.
Neuronal activity in the basal ganglia in patients with generalized dystonia
and hemiballismus (1999) *Ann Neurol* 46: 22-35.

Vitek JL, Giroux M. Physiology of hypokinetic and hyperkinetic movement
disorders: model for dyskinesia (2000) *Ann Neurol* 47: S131-40.

Vitek JL, Zhang J, Evatt M, Mewes K, DeLong MR, Hashimoto T, et al. GPi
pallidotomy for dystonia: clinical outcome and neuronal activity (1998b)
Adv Neurol 78: 211-9.

Volkman J, Benecke R. Deep brain stimulation for dystonia: patient selection and
evaluation (2002) *Mov Disord* 17 Suppl 3: S112-5.

Wang LY, Kaczmarek LK. High-frequency firing helps replenish the readily releasable pool of synaptic vesicles (1998) *Nature* 394: 384-8.

Wang S, Liu X, Yianni J, Green AL, Joint C, Stein JF, et al. Use of surface electromyography to assess and select patients with idiopathic dystonia for bilateral pallidal stimulation (2006) *J Neurosurg* 105: 21-5.

Weinberger M, Mahant N, Hutchison WD, Lozano AM, Moro E, Hodaie M, et al. Beta oscillatory activity in the subthalamic nucleus and its relation to dopaminergic response in Parkinson's disease (2006) *J Neurophysiol* 96: 3248-56.

Wennberg RA, Lozano AM. Intracranial volume conduction of cortical spikes and sleep potentials recorded with deep brain stimulating electrodes (2003) *Clin Neurophysiol* 114: 1403-18.

Wichmann T, Bergman H, DeLong MR. The primate subthalamic nucleus. I. Functional properties in intact animals (1994a) *J Neurophysiol* 72: 494-506.

Wichmann T, Bergman H, DeLong MR. The primate subthalamic nucleus. III. Changes in motor behavior and neuronal activity in the internal pallidum induced by subthalamic inactivation in the MPTP model of parkinsonism (1994b) *J Neurophysiol* 72: 521-30.

Wichmann TDM. Local inactivation of the sensorimotor territories of the internal segment of the globus pallidus and subthalamic nucleus alleviates motor signs in MPTP treated monkeys. In: Percheron G MJ, Feger J, editor, the basal ganglia IV: New ideas and data on structure and function (1994) New York: Plenum Press 357-64.

Williams D, Kuhn A, Kupsch A, Tijssen M, van Bruggen G, Speelman H, et al. The relationship between oscillatory activity and motor reaction time in the parkinsonian subthalamic nucleus (2005) Eur J Neurosci 21: 249-58.

Williams D, Kuhn A, Kupsch A, Tijssen M, van Bruggen G, Speelman H, et al. Behavioural cues are associated with modulations of synchronous oscillations in the human subthalamic nucleus (2003) Brain 126: 1975-85.

Williams D, Tijssen M, Van Bruggen G, Bosch A, Insola A, Di Lazzaro V, et al. Dopamine-dependent changes in the functional connectivity between basal ganglia and cerebral cortex in humans (2002) Brain 125: 1558-69.

Williams H, Mehta N. Changes in adult zebra finch song require a forebrain nucleus that is not necessary for song production (1999) J Neurobiol 39: 14-28.

Windels F, Bruet N, Poupard A, Feuerstein C, Bertrand A, Savasta M. Influence of the frequency parameter on extracellular glutamate and gamma-aminobutyric acid in substantia nigra and globus pallidus during electrical stimulation of subthalamic nucleus in rats (2003) *J Neurosci Res* 72: 259-67.

Wingeier B, Tchong T, Koop MM, Hill BC, Heit G, Bronte-Stewart HM. Intra-operative STN DBS attenuates the prominent beta rhythm in the STN in Parkinson's disease (2006) *Exp Neurol* 197: 244-51.

Yamada H, Fujimoto K, Yoshida M. Neuronal mechanism underlying dystonia induced by bicuculline injection into the putamen of the cat (1995) *Brain Res* 677: 333-6.

Yanagisawa N, Goto A. Dystonia musculorum deformans. Analysis with electromyography (1971) *J Neurol Sci* 13: 39-65.

Yelnik J, Damier P, Bejjani BP, Francois C, Gervais D, Dormont D, et al. Functional mapping of the human globus pallidus: contrasting effect of stimulation in the internal and external pallidum in Parkinson's disease (2000) *Neuroscience* 101: 77-87.

Yelnik J, Damier P, Demeret S, Gervais D, Bardinet E, Bejjani BP, et al.
 Localization of stimulating electrodes in patients with Parkinson disease by
 using a three-dimensional atlas-magnetic resonance imaging coregistration
 method (2003) J Neurosurg 99: 89-99.

Yelnik JD, P. Dormont, D. Francois, C. Tande D, Parain, C. Malandain, G.
 Ayache,N. Hirsch, E. Agid, Y. Delineation of the basal ganglia in MR
 images of patients by automatic registraiton of a multimodal atlas based on
 hstological and MR data (2003) In: 9th meeting of the Organization for the
 Human Brain Mapping, New York.

Yianni J, Bain P, Giladi N, Auca M, Gregory R, Joint C, et al. Globus pallidus
 internus deep brain stimulation for dystonic conditions: a prospective audit
 (2003a) Mov Disord 18: 436-42.

Yianni J, Bain PG, Gregory RP, Nandi D, Joint C, Scott RB, et al. Post-operative
 progress of dystonia patients following globus pallidus internus deep brain
 stimulation (2003b) Eur J Neurol 10: 239-47.

Yianni J, Wang SY, Liu X, Bain PG, Nandi D, Gregory R, et al. A dominant
 bursting electromyograph pattern in dystonic conditions predicts an early
 response to pallidal stimulation (2006) J Clin Neurosci 13: 738-46.

- Yoshida M. The neuronal mechanism underlying parkinsonism and dyskinesia: differential roles of the putamen and caudate nucleus (1991) *Neurosci Res* 12: 31-40.
- Zhang ZX, Roman GC. Worldwide occurrence of Parkinson's disease: an updated review (1993) *Neuroepidemiology* 12: 195-208.
- Zhuang P, Li Y, Hallett M. Neuronal activity in the basal ganglia and thalamus in patients with dystonia (2004) *Clin Neurophysiol* 115: 2542-57.
- Zimprich A, Grabowski M, Asmus F, Naumann M, Berg D, Bertram M, et al. Mutations in the gene encoding epsilon-sarcoglycan cause myoclonus-dystonia syndrome (2001) *Nat Genet* 29: 66-9.
- Zucker RS, Regehr WG. Short-term synaptic plasticity (2002) *Annu Rev Physiol* 64: 355-405.